Federal University of São Carlos

Graduate Program of Chemical Engineering

DOCTORAL THESIS

IMMOBILIZATION OF ENZYMES OF AGROINDUSTRIAL INTEREST ON HYDROXYAPATITE NANOPARTICLES: β-GLUCOSIDASE, XYLASE AND PHYTASE

Thamara Carvalho Coutinho

Doctoral thesis presented to the Graduate Program of Chemical Engineering at the Federal University of São Carlos as part of the requirements to obtain the title of Doctor in Chemical Engineering, area of concentration in Research and Development of Chemical Processes.

Supervisor: Cristiane Sanchez Farinas, PhD

São Carlos, SP, Brazil

March, 2020

Universidade Federal de São Carlos

Programa de Pós-graduação em Engenharia Química

TESE DE DOUTORADO

IMOBILIZAÇÃO DE ENZIMAS DE INTERESSE AGROINDUSTRIAL EM NANOPARTÍCULAS DE HIDROXIAPATITA: β-GLICOSIDASE, XILANASE E FITASE

Thamara Carvalho Coutinho

Tese de doutorado apresentada ao Programa de Pós-Graduação em Engenharia Química da Universidade Federal de São Carlos como parte dos requisitos necessários para a obtenção do título de Doutor em Engenharia Química, área de concentração em Pesquisa e Desenvolvimento de Processos Químicos.

Orientadora: Dra. Cristiane Sanchez Farinas

São Carlos, SP, Brasil

Março, 2020

MEMBROS DA BANCA EXAMINADORA DA DEFESA DE TESE DE THAMARA CARVALHO COUTINHO APRESENTADA AO PROGRAMA DE PÓS-GRADUAÇÃO EM ENGENHARIA QUÍMICA DA UNIVERSIDDE FEDERAL DE SÃO CARLOS, EM 10 DE MARÇO DE 2020.

BANCA EXAMINAFORA:

Cristiane Sanchez Farinas
Orientadora, EMBRAPA/UFSCar

Elaine Cristina Paris.
EMBRAPA

Marcel Otávio Cerri
UNESP

Willian Kopp
Kopp Technologies

Paulo Waldir Tardioli
UFSCar

Dedication

To God, for keeping my faith,

to my family, for the love and care.

''Temos a capacidade e a responsabilidade de escolher se nossas ações seguem um caminho virtuoso ou não.''

Dalai Lama

ACKNOWLEDGMENT

I thank God for keeping me in the faith.

To my parents, Helena Maria and Antônio Claret, and to all my family, for the unconditional love and the support in my choices.

To my life partner, Cassimiro, for understanding my absence and for all the support transmitted during this trajectory.

To my supervisor, Cristiane Farinas, PhD, for the guidance, for the patience and for the example of a professional that I will take throughout my career.

To friends made in São Carlos for friendship and moments of distraction.

To the laboratory colleagues of Embrapa Instrumentation for the daily help and encouragement to face the research challenges.

To Embrapa Instrumentation employees, especially to the laboratory technicians, for all the help, competence and dedication.

I thank Prof. Paulo Waldir Tardioli, PhD, from UFSCar and the Embrapa researcher Elaine Cristina Paris, PhD, for assisting the development of this research over the years.

To Embrapa Instrumentation, for providing the excellent structure for the development of this research, which took place mainly at the National Laboratory of Nanotechnology for Agribusiness (LNNA).

To UFSCar and the Department of Chemical Engineering for the opportunity to pursue the doctorate; to the professors of the Graduate Program in Chemical Engineering of UFSCar for their teachings and for adding so much knowledge and experience to my career.

To CAPES (Finance Code 001), CNPq and FAPESP for the financial support to carry out this research.

To all those who have somehow supported me in these four years!

AGRADECIMENTOS

Agradeço a Deus por manter-me na fé e ser meu guia em todos os momentos.

A toda minha família pelo amor e apoio em minhas escolhas, pelo aconchego de voltar pra minha cidade natal e compartilhar de momentos prazerosos.

Ao meu companheiro pelo incentivo, pela compreensão de minha ausência e por toda força transmitida durante essa trajetória.

A minha orientadora, Dra. Cristiane Farinas, por todos os ensinamentos, pela orientação, pela paciência e pelo exemplo de profissional que levarei por toda a minha carreira.

Aos amigos feitos em São Carlos pela amizade, pelo companheirismo e pelos momentos de descontração.

Aos colegas de laboratório da Embrapa Instrumentação pela troca de experiências dentro e fora do laboratório, pela ajuda e incentivo diário diante dos desafios da pesquisa.

A todos os técnicos dos laboratórios da Embrapa Instrumentação que nunca mediram esforços para ajudar, sempre com muita competência e dedicação.

Agradeço ao Prof. Dr. Paulo Waldir Tardioli da Ufscar e à pesquisadora da Embrapa Dra. Elaine Cristina Paris por acompanhar e auxiliar o desenvolvimento dessa pesquisa ao longo desses anos.

À Embrapa Instrumentação, por ceder a excelente estrutura física para o desenvolvimento desta pesquisa, que se deu principalmente no Laboratório Nacional de Nanotecnologia para o Agronegócio (LNNA).

À UFSCar e ao Departamento de Engenharia Química (Deq) pela oportunidade de realizar o doutorado; aos professores do Programa de Pós-Graduação em Engenharia Química pelos ensinamentos e por acrescentarem tantos conhecimentos e experiências à minha vida profissional .

À CAPES, CNPq e FAPESP pelo apoio financeiro para concretizar esta pesquisa.

A todos aqueles que de alguma forma me apoiaram nesses quatro anos!

LIST OF FIGURES AND TABLES

CHAPTER 1 - Structure of the Thesis, Literature Review and Objectives

CHAPTER 2 - β-glucosidase immobilization on hydroxyapatite nanoparticles

CHAPTER 3 - Phytase Immobilization on hydroxyapatite nanoparticles

SUPPLEMENTARY MATERIAL

CONTENTS

ABSTRACT

Industrial processes are increasingly requiring environmentally sustainable technologies and the use of enzymes is relevant due to the selectivity and specificity of these biocatalysts. However, the application of soluble enzymes in catalytic processes is often impracticable due to the high cost of these biocatalysts and the catalytic instability under severe physical-chemical process conditions. In this sense, the immobilization of enzymes guarantees the reuse of these biomolecules and often improves their stability. Among the supports used as immobilizing agents, nanoparticles have been increasingly studied due to the possibility of creating structures with high surface area to adsorb proteins and also to demonstrate low resistance to mass transfer, thus ensuring good accessibility of the catalyst to the substrate. Hydroxyapatite (HA) is a solid inorganic potential for immobilizing enzymes, since it is non-toxic, has good chemical and physical resistance, good ability to interact with proteins and can be synthesized in the form of nanoparticles; however, it has been little explored as a support for enzymatic immobilization. Given this context, the objective of this research was to evaluate the immobilization of the enzymes β-glucosidase, xylanase and phytase on hydroxyapatite nanoparticles (HA), as a strategy to improve the catalytic efficiency and stability of these enzymes. These enzymes have wide application in different sectors of the agribusiness, such as biofuels, food, animal feed and drugs. For this, HA nanoparticles were first characterized in order to understand their composition, size, morphology and surface area. Then, a systematic study of the immobilization of these enzymes in HA was carried out. The biochemical aspects of enzymatic immobilization were investigated, such as the physicochemical conditions of adsorption and desorption, that helps to understand the type of chemical interaction between support and enzyme. Changes in enzymatic activity profile, thermo-stability, conversion capacity during enzymatic hydrolysis and reuse of these biomolecules were also evaluated. The results obtained showed that the β-glucosidase, phytase and xylanase enzymes were efficiently immobilized on the HA nanoparticles using a simple and fast adsorption protocol, which occur mainly through coordination interactions between the Ca^{2+} sites of the HA with the carboxylic acids (COO^-) of the enzyme amino acids. The biochemical behavior of the enzymes in the presence of HA was evaluated under different physicochemical conditions of adsorption and desorption (pH and ionic strength), indicating a strong and highly stable interaction between enzymes and support, with immobilization yields close to 100% and recovered activities in the range of 70-100%. For β-glucosidase it was possible to recycle the immobilized enzyme and retain 70% of the initial activity during at least 10 hydrolysis cycles. For phytase, the immobilized enzyme showed broader activity profile as to pH and temperature, and higher stability at high temperatures than free enzyme, whose improvement in its properties suggested the potential of applying the immobilized form of phytase in animal feed. For xylanase, the immobilized enzyme demonstrated greater affinity for the HA support that was modified with Cu^{2+} ions, promoting chelation interaction with enzyme amino acids, generating derivatives with maintenance of their catalytic activity and with activity profile similar to that of the free enzyme. Finally, the three enzymes were immobilized on HA magnetic nanoparticles (synthesized with cobalt ferrite, $CoFe_2O_4$), demonstrating excellent recovery capacity from the reaction medium through the application of a magnetic field. The results obtained showed the potential of HA to act as a support for enzyme immobilization, creating derivatives with promising industrial applications, which can improve processes and make them more sustainable.

Keywords: immobilization, enzymes, nanoparticles, hydroxyapatite.

RESUMO

Processos industriais requerem cada vez mais a aplicação de tecnologias ambientalmente sustentáveis e o uso de enzimas se destaca devido à seletividade e especificidade desses biocatalisadores. Contudo, a aplicação de enzimas solúveis em processos catalíticos torna-se muitas vezes inviável devido ao alto custo desses biocatalisadores e a instabilidade catalítica em condições físico-químicas severas de processo. Nesse sentido, a imobilização de enzimas garante o reaproveitamento dessas biomoléculas e muitas vezes, o ganho de estabilidade. Dentre os suportes utilizados para imobilização de enzimas, as nanopartículas têm-se mostrado bastante atraentes devido à elevada área superficial específica e baixa resistência à transferência de massa, garantindo alta capacidade de imobilização enzimas e boa acessibilidade do substrato ao catalisador. A hidroxiapatita (HA) é um potencial sólido inorgânico para imobilização de enzimas, uma vez que não é tóxico, apresenta boa resistência química e física, boa capacidade de interação com proteínas e ainda pode ser sintetizada na forma de nanopartículas; contudo tem sido pouco explorada como suporte para imobilização enzimática. O objetivo deste projeto de doutorado foi avaliar a imobilização das enzimas β-glicosidase, xilanase e fitase em nanopartículas de HA, a fim de obter derivados mais interessantes para serem aplicados na indústria. Essas enzimas têm vasta aplicação em diferentes setores da agroindústria, como de biocombustíveis, de alimentos, de ração animal e de fármacos. Para isso, as nanopartículas de HA foram primeiramente caracterizadas com o objetivo de compreender sua composição, tamanho, morfologia e área de superfície. Em seguida, realizou-se um estudo sistemático da imobilização dessas enzimas em HA, avaliando os aspectos bioquímicos da imobilização, como as condições físico-químicas de adsorção e dessorção, que ajudaram a compreender o tipo de interação química entre suporte e enzima; alterações no perfil de atividade enzimática; melhora na estabilidade térmica; capacidade de hidrólise enzimática e reutilização dessas biomoléculas. Os resultados obtidos mostraram que as enzimas β-glicosidase, fitase e xilanase foram eficientemente imobilizadas nas nanopartículas de HA através de um protocolo de adsorção simples e rápido, principalmente através de interações de coordenação entre os sítios de Ca^{2+} da HA com os ácidos carboxílicos (COO^-) dos aminoácidos das enzimas. Foi avaliado o comportamento bioquímico das enzimas com a HA em diferentes condições físico-químicas de adsorção e dessorção (pH e força iônica), indicando uma interação forte e altamente estável entre enzimas e suporte, com rendimentos de imobilização próximos a 100% e atividades recuperadas na faixa de 70-100%. A β-glicosidase imobilizada em HA reteve até 70% de sua atividade catalítica após 10 ciclos de hidrólise, demonstrando alta capacidade de reuso. Já a fitase imobilizada apresentou maior atuação em ampla faixa de pH e temperatura, e maior termoestabilidade a 80 e 90 °C do que a enzima livre, demonstrando propriedades de interesse para aplicação em ração animal. A xilanase demonstrou maior afinidade pelo suporte de HA modificado com íons de Cu^{2+}, os quais promoveram quelação com aminoácidos da enzima, gerando derivados com manutenção de sua atividade catalítica e perfil de atividade semelhante ao da enzima livre. Por fim, as três enzimas foram imobilizadas em nanopartículas magnéticas de HA (sintetizadas com ferrita de cobalto, $CoFe_2O_4$), demonstrando excelente capacidade de recuperação desses biocatalisadores do meio reacional através da aplicação de um campo magnético. Os resultados obtidos mostraram o potencial da HA para atuar como suporte para imobilização de enzimas, gerando derivados enzimáticos com aplicações promissoras na indústria, que podem melhorar os processos e torná-los mais sustentáveis.

Palavras chave: imobilização, enzimas, nanopartículas, hidroxiapatita.

CHAPTER 1

"O que sabemos é uma gota, o que ignoramos é um oceano."
Isaac Newton

Structure of the Thesis, Literature Review and Objectives

1. Structure of the text

This thesis is divided into six chapters. This first one (Chapter 1) covers mainly concepts and important information that were studied during the development of this research, addressing literature review topics such as enzymatic immobilization, nanoparticles and the characteristics of hydroxyapatite and enzymes used in this work. It was sought to highlight issues and topics that were not explored in the subsequent chapters to avoid duplication of information. In the end of the Chapter 1 are presented the general and specific objectives of the research project.

The Chapters 2, 3, 4 and 5 were written in the form of scientific articles, which present the theoretical basis, the methodology adopted and the results obtained. The Chapters 2, 3 and 4 correspond to the research carried out on enzymatic immobilization on hydroxyapatite nanoparticles of the enzymes β-glucosidase, phytase and xylanase, respectively. Chapter 5 presents the research carried out on the immobilization of these three enzymes in magnetic hydroxyapatite nanoparticles. The introduction, methodology and some parts of the discussion of these chapters are inevitably somewhat similar since the scientific research of each one has many aspects in common. It is noteworthy that Chapters 2, 3 and 4 presented here are adapted versions of the scientific articles published in the journals: "International Journal of Biological Macromolecules" (Chapter 2 and Chapter 4) and "Applied Biochemistry and Biotechnology" (Chapter 3).

Chapter 6 presents an overview of the developed research, succinctly describing what has been done, follow of the general conclusions of the Thesis and the future perspectives on the research developed. The Supplementary Material includes extra tables and figures that complement the discussion of the results throughout the text. The Appendix 1 presents the authorizations granted by the journals to use the articles published in this thesis.

2. Literature Review: Immobilization of enzymes of agroindustrial interest on nanoparticles

2.1 Enzyme immobilization: what it is and why to use

Industrial processes are increasingly using enzymes in the conversion stages due to their high selectivity, high specificity, low toxicity, great performance under mild process conditions avoiding high energy costs, besides being biomolecules obtained by sustainable methods (Polaina and MacCabe, 2007). In this way, the use of biocatalysts allows rapid and efficient synthesis of green products, which are difficult to obtain using chemical/synthetic routes (Arhle, 2007). Despite the numerous advantages of enzymes, sometimes their use become impracticable due to the high cost of these biocatalysts and the high investment required to recovery them from reaction medium to be reused (Sheldon and van Pelt, 2013). In addition, the three-dimensional structure of these biomolecules can be irreversibly altered depending on the process conditions, such as extreme pH, ionic strength, temperature and pressure conditions (Ivry *et al.*, 2018). The immobilization of these biomolecules has been widely studied to circumvent these drawbacks (Alftren and Hobley, 2013; Liu *et al.*, 2015; Vaz *et al.*, 2016).

In general, the function of immobilization is to trap the enzymes inside or on the surface of the insoluble material while retaining its catalytic activity (Sheldon and van Pelt, 2013). Enzymatic immobilization aims to achieve two main objectives: the enzyme reuse and/or the improvement on enzyme stability. Once enzyme becomes insoluble after anchoring in a support, the product does not become contaminated by the residual presence of protein at the end of the process, decreasing the cost of product purification during the downstream step, which is usually the most expensive bioprocess step (Zydney, 2016). The immobilized enzyme may also to acquire a greater operational stability, being able to act under extreme and adverse conditions of industrial processes (Periyasamy *et al.*, 2016). This is probably due to the fact that the immobilized form of many enzymes mimics their natural mode in living cells, where most of them are linked to the cell cytoskeleton, membrane or organelles, ensuring greater robustness to the enzyme and greater resistance to changes in the environment (Hoarau *et al.*, 2017).

Still regarding the benefits of enzymatic immobilization, there are some cases in which the immobilized enzyme becomes more catalytically efficient than the free form, that are closely related to the stability and/or the conformational change that the protein acquires when binding to the support, making the active site more available for the biocatalysis (Mehta *et al.*, 2016). This may result in reduced reactor volume and/or shorter reaction time and consequently higher profitability to the bioprocess (Borges *et al.*, 2014; Sheldon and van Pelt, 2013). In some cases, enzyme immobilization allows to operate the reactor continuously, further generating profitability for the bioprocess (Gomez *et al.*, 2012).

2.2 Methods of enzyme immobilization

Enzymes may be immobilized on various supports by different methods, which can occur using chemical and/or physical interaction or using chemical reaction between support and protein, as illustrated in Fig. 1 (Sheldon and van Pelt, 2013). Interaction between enzyme and support means that molecules attract each other without breaking or forming new chemical bonds, that is also known as adsorption immobilization (Gregg, 1982). Enzyme immobilization by adsorption can occur by different types of interactions, which can be electrostatic, hydrophobic, Wan der Wals forces, hydrogen bonds, ionic bonds and even chelation (Jesionowski *et al.*, 2014).

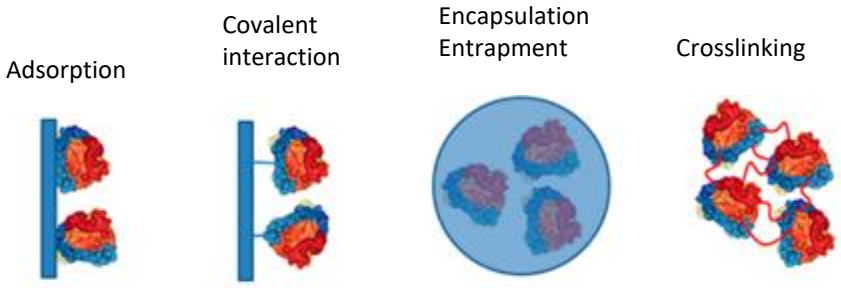

Fig. 1. Enzyme immobilization methods.

The main advantage of adsorption is the operational simplicity of the immobilization process, while the main disadvantage is the reversibility of interaction due to the low intensity of the forces between support and enzyme (Jesionowski *et al.*, 2014). Among the adsorption immobilization methods, the one by electrostatic interactions is most widely used, but it depends on the presence of charges on the surface of support and enzyme, being low resistant to high ionic forces of the reaction medium (Vieira *et al.*, 2011). Depending on the intensity of electrostatic interactions, they become ionic interactions. Regarding the chelation adsorption, highly stable coordination interactions are established between the amino acid residues, such as histidine imidazole functional group, glutamate and aspartate carboxylic acids, with chelated metal ions on the support surface, such as Cu^{2+}, Zn^{2+}, Fe^{2+}, Ca^{2+}, Co^{2+} (Bala *et al.*, 2007; Farinas *et al.*, 2007). Although these adsorption immobilization methods are reversible interactions that may cause enzyme leaching into the reaction medium, they may ensure maintenance of the enzyme's native structure during biocatalysis (Jesionowski *et al.*, 2014).

On the other hand, the immobilization method by chemical reaction refers to the covalent interactions between reactive groups of the support and the enzyme, being therefore, strong bonds that guarantee greater stability to the immobilization (Mohamad *et al.*, 2015). Enzymes immobilized on glyoxyl agarose supports can have a factor gain of stabilization in the order of 100 to 1000 times due to the formation of multi-punctional bonds, which ensure greater rigidity

of the enzyme structure compared to single point bind (Hoarau *et al.*, 2017). Enzyme functional groups that participate in support binding comprise amino acid side chains that are not involved in the catalytic activity, which might be lysine (ε-amino group), cysteine (thiol group) and aspartic and glutamic acids (carboxylic group) (Mohamad *et al.*, 2015). However, the stiffness generated in a covalent interaction may cause distortion of the enzyme's active site, reducing the advantages of this method of immobilization (Liu *et al.*, 2015).

Other immobilization method that have been increasingly studied are those that do not require interaction or chemical reaction between support and enzyme, such as gel and fiber microencapsulation, in which the enzyme is trapped three-dimensionally through a porous structure, maintaining its mobility and allowing the free passage of substrate and products (Javed *et al.*, 2016; Vandenberg *et al.*, 2011). In addition, enzymes can be immobilized by the method known as crosslinking enzyme aggregates (CLEA), which promotes crosslinking between groups not involved in enzyme catalysis using a crosslinking agent, usually glutaraldehyde, allowing the maintenance of biocatalyst activity (Sheldon, 2007). The CLEA method does not need any matrix to act as a support, since the crossing of the enzymes themselves confers the enzymatic immobilization (Periyasamy *et al.*, 2016).

2.3 Supports for enzyme immobilization

To understand the chemical and mechanical properties of the support is essential to assume the material effectiveness as an immobilizing agent. The support must have high surface area to allow immobilization of significant amounts of enzymes, which is often related to the matrix porosity (Barbosa *et al.*, 2013). In general, the support should be hydrophilic to allow good substrate diffusivity and should have low solubility to avoid product contamination (Puri *et al.*, 2013). The mechanical strength and thermal stability of the support are important factors that must be observed from the immobilization process step to the unit operations steps performed at the end of the process to obtain the bioproduct (Vaghari *et al.*, 2016).

Among the types of supports used to immobilize enzymes are the organic and inorganic supports. Examples of organic supports are the cellulose, agarose, chitosan, alginate, starch and polyacrylate polysaccharides. Mineral inorganic supports include silica, alumina, iron oxide, zeolite and hydroxyapatite (Mohamad *et al.*, 2015). Inorganic supports might be more interesting for the industry as they have good mechanical strength, thermal stability, resistance to organic solvents and degradation by microorganisms (Vaz *et al.*, 2016).

Some matrices have excellent physical properties to act as immobilizing agents, although do not have specific sites able to interact or to react with enzymes, being necessary to insert functional groups to improve the chemical characteristics of the matrix (Hoarau *et al.*, 2017). Such functional groups must have at least two reactive groups in the molecule, one that reacts

chemically with the support and another that interacts with the enzyme (Jesionowski *et al.*, 2014). Typical molecules that meet this condition are bifunctional carbonyl compounds, such as glutaraldehyde, which has five carbon chain and can also act as a spacer, allowing the substrate to access enzyme's active site (Agrawal *et al.*, 2016). Other compounds frequently used to modify supports are those that allow the insertion of amino groups such as silanized agents and agents such as ethylenediamine (EDA) and diethylaminoethyl (DEAE) (Xia *et al.*, 2016; Xie and Zang, 2017).

The use of magnetic particles is an important area of interest for enzymatic immobilization, which has been making significant progress in recent years in the development of new biocatalytic systems (Mukhopadhyay *et al.*, 2012; Kopp *et al.*, 2015). What differentiates these supports is the ease of recovery of the immobilized enzyme from the reaction medium by applying a magnetic field (Alftren and Hobley, 2013). One of the most widely used magnetic particles is magnetite (Fe_3O_4), due to its low toxicity and biocompatibility (Vaghari *et al.*, 2016). Another purely magnetic material is cobalt ferrite ($CoFe_2O_4$), which has excellent chemical stability, ease of synthesis and mechanical hardness, being a promising candidate for enzyme immobilization (Bohara *et al.*, 2016). These magnetic materials always tend to undergo aggregation because of their magnetic dipole-dipole attractions and their large surface area-to-volume ratio. For these reasons, magnetic materials are usually added to the inorganic material to form a magnetic composite or are coated with a polymeric organic material to generate attractive matrices to immobilize enzymes (Alftren and Hobley, 2013; Liu *et al.*, 2014).

2.3.1 Nanoparticles as support for enzyme immobilization

One of the main factors to achieve efficiency in the immobilization technique is the surface area of the material used, because materials with high surface area provide greater ability to immobilize enzymes (Sheldon and van Pelt, 2013). The use of nanoparticles as enzyme matrix have been increasingly studied due to the possibility of creating structures capable of retaining high enzymatic load per unit particle mass (Cipolatti *et al.*, 2014). This feature can result in reduced reactor volume, improving process cost (Vaz *et al.*, 2016). In addition, nanoparticles demonstrate low resistance to mass transfer, ensuring good substrate accessibility to the catalyst. This fact is very interesting for enzyme immobilization, since one of the drawbacks of conventional immobilization is the difficulty of diffusion of the substrate to the biocatalyst, especially in very porous substrates (Javed *et al.*, 2016).

Different types of materials have been synthesized as nanoparticles for enzyme immobilization, such as silica and chitosan, nanofibers of cellulose, nanotubes of carbon, iron oxide nanometals and nanocomposites based on the mixing of certain nanomaterials (Puri *et al.*, 2013). Surface modifications of these nanomaterials, such as silanization, carbodiimide

activation, crosslinking using glutaraldehyde, among others, can help in the binding of the enzyme to support by covalent interaction forming single or multi-point systems (Cipolatti *et al.*, 2014).

Nanoparticles are attractive for enzyme immobilization not only because of the larger surface area provided, but also because they are chemically stable materials, uniform in size and well dispersed in liquid media, being especially useful in large scale processes (Cipolatti *et al.*, 2014). However, it is noteworthy that there are specific disadvantages of using nanomaterials, represented mainly by health and environmental concerns and the difficulties of nanomaterial preparations such as aggregation, precipitation and thermodynamic stability (Puri *et al.*, 2013). In this work, it was used an inorganic nanomaterial with potential properties for the immobilization of enzymes, but which has been few explored for this purpose. The next topic will describe the general characteristics of hydroxyapatite nanoparticles.

2.4 Hydroxyapatite nanoparticles

Hydroxyapatite (HA) is a ceramic material with the chemical composition $Ca_{10}(PO_4)_6(OH)_2$ (Hench and Wilson, 1993). HA consists of calcium ions, phosphate groups in tetrahedral arrangements and hydroxyls, forming a hexagonal structure, as shown in Fig. 2 (Qi *et al.*, 2017). HA can be found in natural sources such as bovine bones, eggshells, shells and corals (Yelten *et al.*, 2012), but its main form of production is through chemical synthesis, which can be by dry chemical methods such as solid state reaction and combustion synthesis, and by wet chemical methods such as hydrolysis, hydrothermal processes, precipitation, synthesis sol-gel, among others (Sadat-Shojai *et al.*, 2013).

Sadat-Shojai *et al.* (2013) did a search and found that around 25% of the total 650 papers indexed over the period of 1999–2011 are solely connected to the conventional chemical precipitation method. Following chemical precipitation, combination methods and the hydrothermal process are the next most well-known methods of preparing HA, accounting for 16 and 14% of papers. To produce HA nanoparticles, chemical precipitation can be accomplished using various calcium and phosphatecontaining reagents, such as calcium hydroxide or calcium nitrate as the Ca^{2+} source and orthophosphoric acid or diammonium hydrogen phosphate as the PO_4^{3-} source. A typical procedure involves the dropwise addition of one reagent to another under continuous and gentle stirring, while the molar ratio of elements (Ca/P) is kept at stoichiometry according to its ratio in HAp (1.67).

The hydroxyapatite characteristics such as crystallinity, stoichiometry, structure, purity and particle size are closely related to its properties (Dorozhkin, 2010). The structure of HA admits substitution that can change the material characteristics such as solubility, crystallinity and ability to interact with proteins (Hench and Wilson, 1993). The Ca^{2+} ions of HA can be substituted on the surface of material by Cu^{2+} and Zn^{2+} ions, improving, for example, the adsorption capacity of

proteins with high histidine residues, which interact strongly with these metals (Farinas *et al.*, 2007). HA hydroxyls can be substituted by carbonates, fluorides and chlorides, changing the phase composition of the molecule (Hench and Wilson, 1993) and impacting interactions with proteins. HA nanoparticles modified with Mn^{2+} ions may confer more positive charges to interact with the BSA protein (bovine serum albumin), which has negative charges (Kojima *et al.*, 2018).

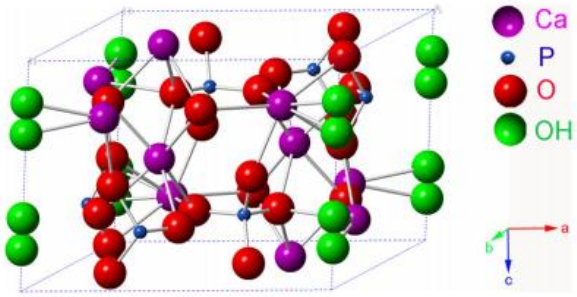

Fig. 2. Crystal structure of hydroxyapatite. Source: (Qi *et al.*, 2017)

Although HA solubility is directly related to characteristics such as size, structure and crystallinity, it is generally pH dependent, this is soluble in acidic solutions (forming precipitates), insoluble in basic solutions and poorly soluble in intermediate pH solutions (Dorozhkin, 2010). The solubilization phenomenon becomes more intense as pH decreases due to the increasing consumption of OH^- ions that are released during the solubilization of HA. Thus, the equilibrium reaction bellow is increasingly shifted to the right, increasing the solubilization phenomenon:

$$Ca_{10}(PO_4)_6(OH)_2 \rightleftharpoons 10\ Ca^{2+} + 6\ PO_4^{3-} + OH^-$$

Regarding the HA stoichiometry, the Ca/P ratio is generally 1.67, and particles synthesized with lower ratio are considered calcium deficient (Dorozhkin, 2010). Swain and Sarkar (2013) showed that needle-shaped HA nanoparticles have a higher Ca/P ratio to adsorb proteins than spherical and fibrous morphologies of the material.

HA nanoparticles are smaller than 100 nm in at least one direction (Mukhopadhyay *et al.*, 2012; Sadat-Shojai *et al.*, 2013) demonstrating high surface area for enzymatic immobilization. The Fig. 3 presents different morphologies that HA nanoparticles may present depending on the synthesis adopted. Swain and Sarkar (2013) obtained different HA formats from the precursors $(CH_3COO)_2Ca$ and KH_2PO_4, varying processing parameters such as temperature, pH and Ca/P ratio (Fig. 3a). On the other hand, Lin *et al.* (2011) obtained different morphologies of HA via hydrothermal treatment of a calcium solution using the precursor silicate (Fig. 3b), varying

preparation conditions such as phosphate solution type and chemical compositions of calcium silicate precursors.

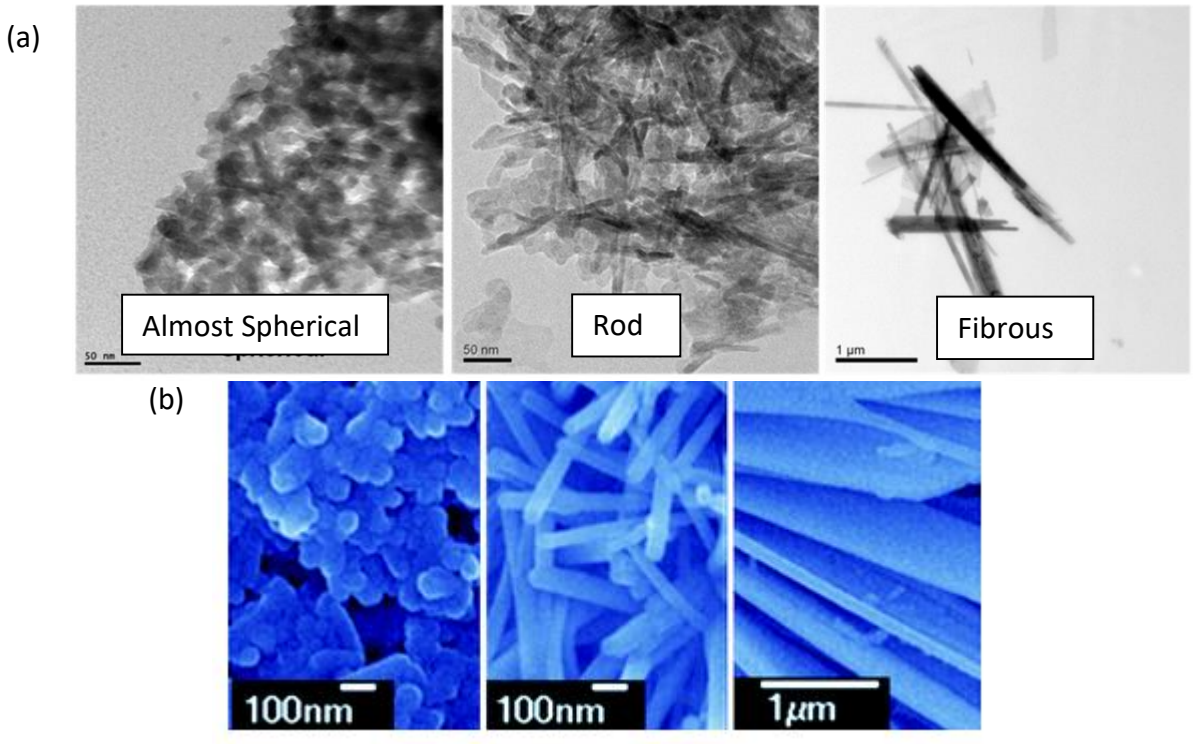

Fig. 3. Different morphologies of HA nanoparticles obtained by (a) Swain and Sarkar, (2013) and (b) Lin *et al.* (2011).

Research conducted to promote protein interaction with HA has investigated different morphologies of HA, as well as the effect of crystallinity, composition and surface structure such as porosity. Nagasaki *et al.* (2017) synthesized HA nanoparticles under mild conditions to avoid changes in their morphology, chemical composition and crystallinity, obtaining particles with controlled surface structures in order to analyze the adsorption behavior of proteins in different structures. They observed that to increase the porosity of HA nanoparticles did not affect bovine serum albumin (BSA) protein adsorption capacity, since the pores were much smaller (10 nm) than protein size (15 nm). Swain and Sarkar (2013) showed that the needle (or rod) shape of HA nanoparticles demonstrated larger surface area, ensuring the adsorption of 28 mg BSA/g support, while the spherical and fibrous shapes adsorbed 26.5 mg BSA/g. , and 25.7 mg/g support, respectively.

Most studies on protein adsorption on HA are restricted to health applications, mainly as orthopedic and dental materials, due to the biocompatibility and osteoconductivity of this compound (Nagasaki *et al.*, 2017). However, few studies have evaluated the potential of enzyme immobilization on these nanoparticles for various applications in industry. Ivic *et al.* (2016)

immobilized the lipase enzyme in HA nanoparticles by coordinating reaction of HA Ca^{2+} with the carboxylic acids of the enzymes. Xie and Zang (2017) immobilized lipase on Fe_3O_4 nanoparticles coated with HA, which were functionalized to perform covalent interactions, ensuring enzyme recovery by application of a magnetic field. Although still few explored as a support to immobilize enzymes, HA presents interesting characteristics and properties for this purpose, which will be investigated throughout this Thesis.

2.5 Enzymes of agroindustrial applications

Several industrial processes have become more sustainable and profitable with the use of enzymes as biocatalysts (Beg *et al.*, 2001; Cao *et al.*, 2007; Singhania *et al.*, 2013). This is due to the enzymes efficiency regarding chemical conversion, selectivity, specificity, low toxicity, better performance under mild process conditions and the renewable source of these biomolecules (microorganisms and plants) (Polaina and MacCabe, 2007).

The following items will describe the biochemical characteristics and applications of three enzymes of major application in different agroindustry sectors, β-glucosidase, xylanase and phytase, which had their immobilization feasibility on hydroxyapatite nanoparticles evaluated in this Thesis.

2.5.1 β-glucosidase enzyme

The β-glucosidases are enzymes present in many living organisms that catalyze specific hydrolysis of glycosidic bonds in oligosaccharides and disaccharides from the non-reducing end (Shewale, 1982). The hydrolysis product is glucose when the substrate is cellobiose (Singhania *et al.*, 2013), but also β-glucosidase may release some aglycones, such as aromatic aglycones when the substrates are isoflavone glycosides (Chen *et al.*, 2016) and monoterpene aglycones when the substrates are terpene glycosides (Maicas and Mateo, 2005). The action of β-glucosidase on these different substrates is illustrated in Fig. 4.

The physiological functions that β-glucosidase develops in its natural environments are very diverse and distributed among plants, animals and microorganisms, for example, in the catabolism of glycolipids in human tissue, in the pigmentation of plant cell walls, in the defense against pathogens in plants and in degradation of cellulose as a source of energy by fungi and bacteria (Narasimha *et al.*, 2016). Due to these varieties of functions, β-glucosidase has a wide application in industry and its commercial form is generally obtained from the cultivation of fungi, mainly *Aspergillus niger* (Lima *et al.*, 2013; Watanabe *et al.*, 1992). Thus, β-glucosidase has been obtained by different strains of *A. niger*, presenting molecular mass in the range of 65-240 kDa, isoelectric point (pI) in the range of 3.5-4.5, optimal pH between 4-6 and optimum temperature

between 50-65 ° C (Lima *et al.*, 2013; Narasimha *et al.*, 2016; Watanabe *et al.*, 1992; Yu *et al.*, 2004; Zhu *et al.*, 2010).

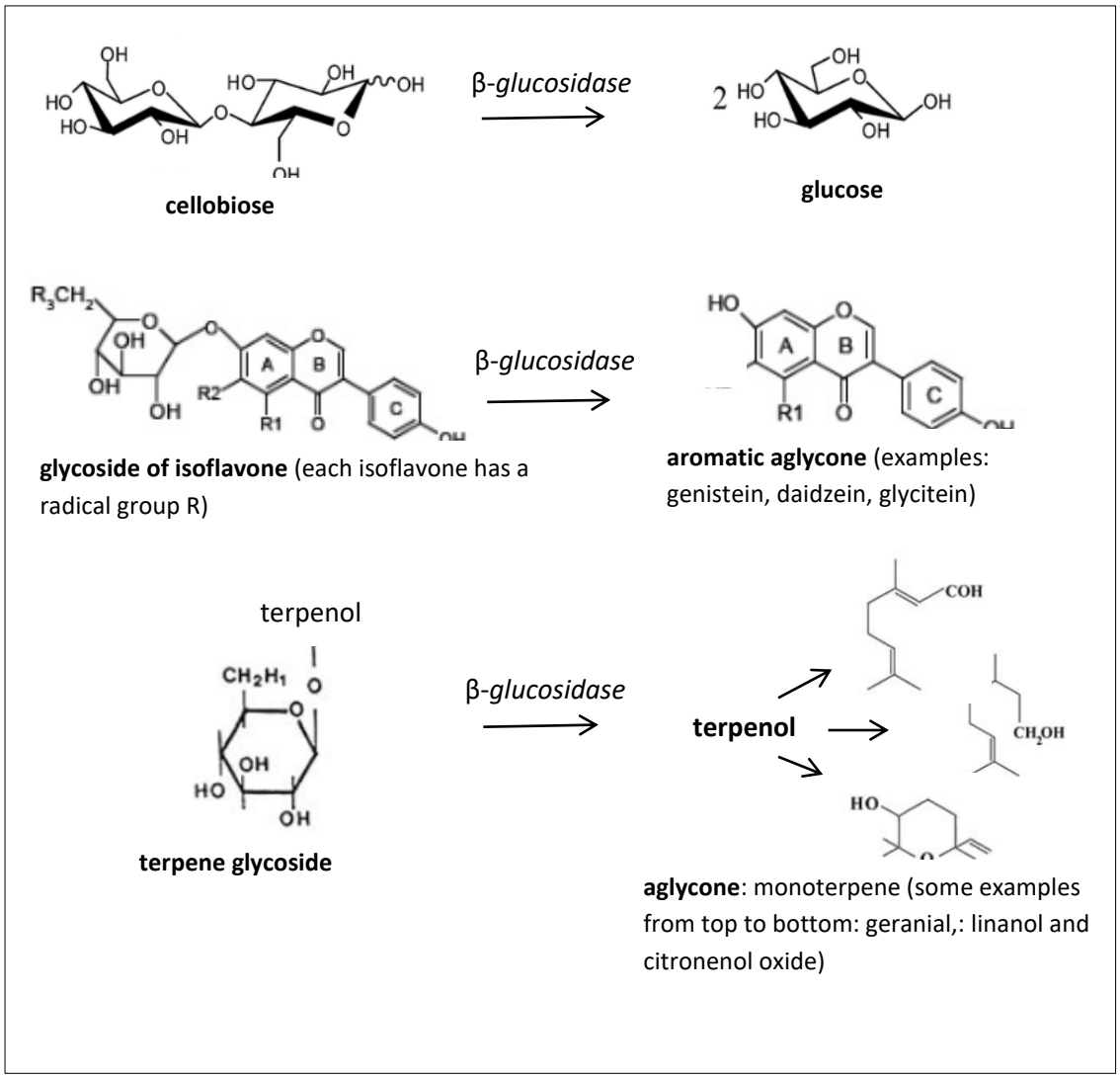

Fig. 4. Effect of β-glucosidase on its main substrates. For isoflavone and terpene, the other product released in hydrolysis is glucose (not shown in the figure).

In the agroindustry, β-glucosidase has been widely used in different sectors. In the beverage industry, it participates in the hydrolysis of glycosides that release aromatic constituents (such as monoterpenes), contributing to a natural flavor and improving the aroma in wines, teas and juices (Celik *et al.*, 2016). The Fig. 4 illustrates some of the various monoterpenes that can be released, such as geranial, diol, endiol, triol, netal, α-termineol, and others. It is worth mentioning that β-glucosidase participates in the last stage of release of these aromatic compounds, and other stages of hydrolysis are performed by glycosylases that act synergistically such as α-L-ramnosidase, α-L-arabinosidase and β-D-apiosidase (Maicas and Mateo, 2005; Zhu *et al.*, 2010).

The hydrolysis of isoflavones by β-glucosidases can originate molecules with an estrogenic effect that are applied in the pharmaceutical industry (Michlmayr and Kneifel, 2014; Chen *et al.*, 2016). This substrate (isoflavone) is found in agro-industrial co-product from soybean production, known as soybean molasse (Pham and Shah, 2009). Isoflavone glycosides belong to the subgroup of flavonoids that exhibit potential health benefits, including reduced cardiovascular disease, cancer prevention, protection against osteoporosis and antioxidant activities (Chen *et al.*, 2016).

Among the applications demonstrated for β-glucosidase, the main one is, together with other cellulases, in the conversion of lignocellulosic materials into simple sugars (Singhania *et al.*, 2013). Cellulases represent an enzymatic system with enzymes that act synergistically in the hydrolysis of specific regions of cellulose, the main polysaccharide found in the cell wall of vegetables, formed by glucose monomers (Lehninger, 2006). Among cellulases (endo-glucanase, cellobiohydrolase and β-glucosidase), β-glucosidase catalyzes the hydrolysis of cellobiose, one of the intermediates in the degradation of cellulose, generating glucose molecules (Shewale, 1982), as shown in Fig. 4.

The sugar released during the cellobiose hydrolysis can be used to obtain bioproducts and biofuels, according to the concept of biorefinery, being bioethanol one of the most important products of this route, which is obtained by fermenting the sugars generated in enzymatic hydrolysis (Beg *et al.*, 2001; Singhania *et al.*, 2017; Farinas *et al.*, 2018;). The catalytic action of β-glucosidase reduces the inhibition of endo-gluconase and cellobiohydrolase enzymes, caused by the accumulation of cellobiose, demonstrating the importance of β-glucosidase function (Alftren and Hobley, 2013; Javed *et al.*, 2016). Despite the specificity of β-glucosidase by β-D-glycosides, it can also hydrolyze other glycosides during the degradation of these lignocellulosic materials such as β-galactosides, α-galactosides, α-L-arabinosides, β-D-xylanosides (Zhang and Lynd, 2004).

Despite the range of applications of β-glucosidase in different agro-industrial processes, there is a considerable difficulty in recovering this enzyme from the reaction medium after biocatalysis. This limits its reuse and makes the process very expensive, due to the high cost of this biocatalyst (Klein-Marcuschamer *et al.*, 2012; Druzhinina and Kubicek, 2017). The β-glucosidase represents one of the most costly enzymes used in the process of obtaining cellulosic ethanol (Nghiem *et al.*, 2011). Therefore, the development of techniques for its immobilization allowing its reuse several times has been extensively researched in order to reduce the cost of cellulosic ethanol production (Vaz *et al.*, 2016). Other products obtained using β-glucosidase can also become more profitable after its immobilization (Maicas and Mateo, 2005; Michlmayr and Kneifel, 2014; Pham and Shah, 2009). For this reason, β-glucosidase has been immobilized in various materials by chemical and physical adsorption, encapsulation and covalent bonding (Vieira *et al.*, 2011; Gomez *et al.*, 2012; Borges *et al.*, 2014; Jorgensen and Pinelo, 2017). Different materials have been tested as a support for β-glucosidase, such as carbon nanotubes

coupled with chitosan (Celik *et al.*, 2016), magnetic nanospheres of Fe_3O_4 (Zhang *et al.*, 2015), silicon oxide nanoparticles (Agrawal *et al.*, 2016), agarose matrix (Vieira *et al.*, 2011), glyoxyl-agarose gel (Borges *et al.*, 2014), and others.

2.5.2 Xylanase enzyme

Xylanases are glycosyl hydrolases that perform the hydrolysis of the β-1,4-glycosidic bonds of the xylan polysaccharide (Schomburg and Schomburg, 2009). Xylan is a complex macromolecule that constitutes the group of hemicelluloses, appearing as the second largest proportion in the cell wall of vegetables (Lehninger, 2006). Xylan structure corresponds to β-1,4-xylopyranosyl molecules substituted by side chain residues, such as glucopyranosyl, methyl-gluco-pyranosyl, arabinofuranosyl, acetyl, feruloil (Polaina and MacCabe, 2007).

Due to the heterogeneous nature of xylan biopolymer, its degradation requires the synergistic action of different hydrolases (Polaina and MacCabe, 2007). The branching xylanases such as α-glucuronosidase, α-arabinosidase and acetyl xylan esterase are able to release the xylan side chains; the endoxylanases hydrolyze β-D-1,4-glycosidic bonds within xylan and finally, the β-xylosidase hydrolyzes xylobiose by releasing β-xylose from the non-reducing terminal (Schomburg and Schomburg, 2009). Fig. 5 shows the structure of xylan and the enzymes described above hydrolyzing the polysaccharide in specific regions.

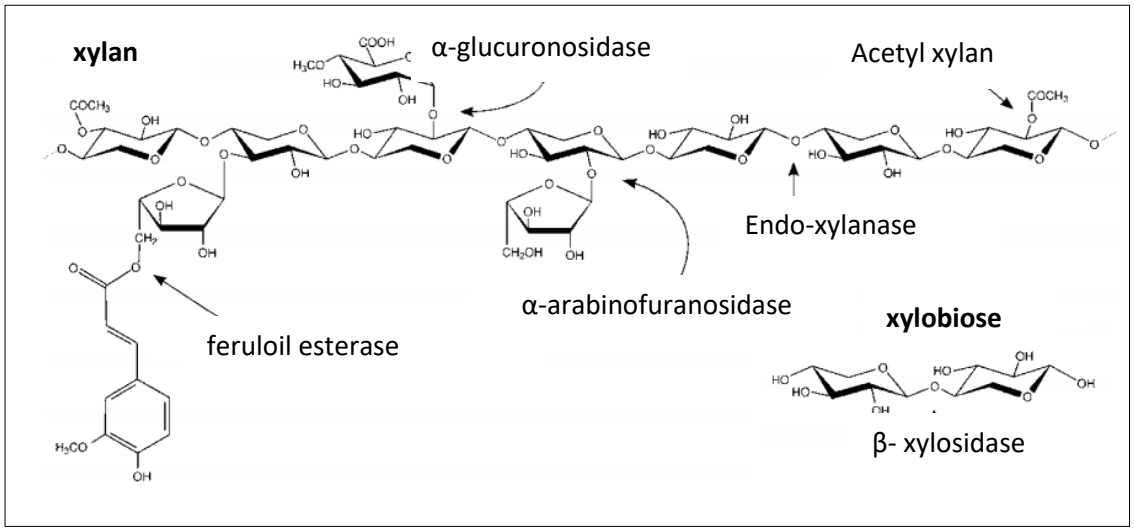

Fig. 5. Xylan structure and regions of action of xylanases. Source: modified from Polaine e MacCane (2007).

Xylan degradation is widespread among saprophytic microorganisms, including bacteria and fungi, which secrete xylanases into the extracellular medium in order to degrade the

polysaccharide (Linares-Pasten *et al.*, 2018). In this way, the cultivation of microorganisms (such as *Aspergillus, Trichoderma, Streptomyce*s, *Bacillu*s, among others) in the presence of xylan becomes the main source of obtaining these enzymes, although it is also found in the cell wall of plants (Kumar *et al.*, 2018).

The heterogeneity and complex nature of xylan resulted in a diversity of xylanases with different specificities (Linares-Pasten *et al.*, 2018). A system of classification was introduced in 1991 for glycosidic hydrolases, which is based on the comparison of primary structure of catalytic domains, grouping the enzymes into related families (Gilkes *et al.*, 1991). The classification comprises more than 100 families (GH1 to GH106), most of which differ in relation to the substrate specificity. Xylanases are generally classified into families of glycosylases GH10 and GH11, whose families include, respectively, xylanases with high molecular mass (> 30 kDa) and acid pI and xylanases with low molecular mass group (<30 kDa) and basic pI (Polaina and MacCabe, 2007). The GH10 family also includes other enzymes such as cellobiohydrolases (endo-β-1,4-xylanases and endo-β-1,4-xylanases), while the G11 family is monospecific and comprises only xylanases. In addition, each one of these 100 families includes many other xylanases with widely different physicochemical properties from these two groups. In addition, these others 100 families includes many different xylanases that presents physicochemical properties very different from these two groups (Linares-Pasten *et al.*, 2018).

Xylanases are often treated as an enzyme 'mix', especially when applied to the biotransformation of lignocellulosic materials (Beg *et al.*, 2001). This fact occur due to the synergism between the enzymes, since the degradation of the xylan ‘‘skeleton’’ often depends on the joint action of enzymes that are able to remove residues from its side chain (Polaina and MacCabe, 2007). One of the sectors with the greatest application of xylanases is in the release of fermentable sugars for ethanol production from lignocellulosic biomass, together with other enzymes such as cellulases, mannanases and glucanases (Beg *et al.*, 2001).

Another sector that depends on the action of these biocalatalysts is the pulp and cellulose industry, in which xylanase helps the bleaching step, increasing the extraction of lignin from the pulp by depolymerizing the hemicellulosic material associated with lignin (Woolridge, 2014). In the animal feed industry, xylanases are used as additives in the feeding of monogastric animals, acting on the enzymatic degradation of arabinoxylan, contributing to a better absorption of feed components (Norgaard *et al.*, 2016). In the beverage industry, such as juices and wines, xylanase is used together with pectinase as a clarifying agent for the final product (Shahrestani *et al.*, 2016). Another important market for xylanases is the production of xylooligosaccharides, that are xylan oligomers with nutraceutical properties, stimulating the growth of bifidobacteria in the human intestine (Beg *et al.*, 2001; Liu *et al.*, 2015).

Given the range of applications of xylanase in the industry, especially in the agro-industry, researchers are increasingly interested in finding techniques for immobilizing this enzyme in

order to increase its activity, stability and promote its reuse in the process (Kumar *et al.*, 2018). Spheres of sodium alginate were used as supports to immobilize xylanase by encapsulation, and thus, increase its stability over a wide range of pH and temperature (Jampala *et al.*, 2017). Glyoxyl-agarose gels was used to immobilize xylanase using covalent multi-interactions, allowing the coupling of the biocatalyst in a continuous reactor to optimize the production of xylooligosaccharides (Aragon *et al.*, 2013). Chitosan particles with glutaraldehyde were applied to immobilize xylanase and improve its pH stability in oligosaccharide degradation (Driss *et al.*, 2014). In addition, Fe_3O_4 magnetic nanoparticles coated with chitosan were prepared for the immobilization of xylanase isolated from *A. niger*, showing high activity recovered (AR = 87.5%) at high temperature (Liu *et al.*, 2014). In the same way, magnetic nanoparticles encapsulated in silica were used to immobilize xylanase with application in clarifying juices (Shahrestani *et al.*, 2016).

2.5.3 Phytase enzyme

The phytase enzyme, known as phospho-myoinositol hexaphosphate hydrolase, releases phosphate and myo-inositol residues from phytic acid or phytate (Fig. 6), the main chemical form of phosphorus found in vegetables (Polaina and MacCabe, 2007). Phytate is a common constituent of plant-derived foods and comprises 1% to 5% of the weight of legumes, oilseeds, cereals, pollen and nuts (Jain *et al.*, 2016).

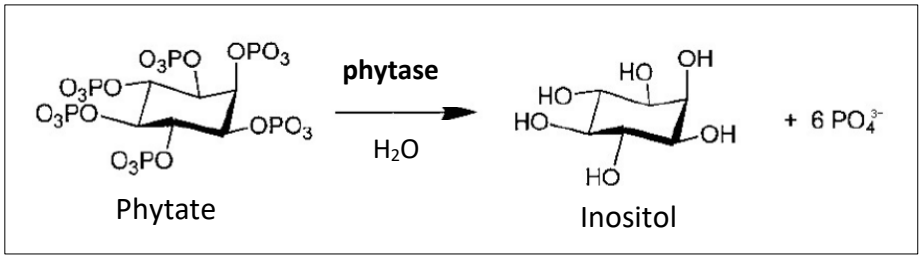

Fig. 6. Catalytic action of phytase on phytate, releasing phosphate ions.

The phytases can be derived from plants, animals and microorganisms; however, microbial sources (fungi and bacteria) are the most promising for obtaining this enzyme in industrial scale (Cao *et al.*, 2007; Vohra *et al.*, 2011; Jain *et al.*, 2016). Phytases obtained from bacteria differ from fungal phytases because their optimal pH varies from acid to alkaline, they are dependent on Ca^{2+} and are highly specific as to the substrate. They usually have a molecular mass from 37 to 55 kDa and optimum temperature from 40 to 70 ° C (Jain *et al.*, 2016). However, commercial phytases are usually obtained from genetically modified fungal sources (*Aspergillus*, *Penicillium* and *Thermomyces*); that are usually proteins of high molecular weight (mainly due to the fact that

they are glycosylated), having optimum pH around 5 and optimum temperature in the range of 55-80 ° C (Singh and Satyanarayana, 2015). In general, fungal phytases are more thermo-resistant and have a lower optimal pH range than bacterial phytases (Cao *et al.*, 2007).

The phytase enzyme is able to bioavailable the phosphorus from protein ingredients through the hydrolysis of phytate. For this reason, its main industrial application is as a food supplement for various animals, mainly in poultry, pork and fish diets (Jain *et al.*, 2016). This supplementation in animal feed with phytase is necessary because these animals are not able to synthesize this enzyme, making phytate an anti-nutritional compound. The anti-nutritional character of phytate is related to the fact that the compound forms complexes with metals and proteins, due to the negative charges of the phosphate groups (Vandenberg *et al.*, 2011). The formation of these complexes impede the absorption of essential trace elements, such as iron and zinc, as well as the absorption of essential amino acids (Singh and Satyanarayana, 2015). Another drawback related to the non-degradation of phytate is that when it becomes complex, it is eliminated as animal manure, contributing to the accumulation of phosphorus in the environment (Polaina and MacCabe, 2007). In this sense, the use of phytase as a food supplement reduces the excessive concentrations of phytate in the terrestrial and aquatic environments in which it is discarded, eliminating, for example, the eutrophication of rivers, lakes and reservoirs (Cao *et al.*, 2007).

In addition to acting in animal feed, phytase has also been increasingly studied for application in other areas within the agroindustry. One of them is to promote the growth of plants for agriculture, by supplementing the soil with the enzyme phytase, which will act on the bioavailability of phosphorus for these vegetables (Mezeli *et al.*, 2017). Another application of phytase is in the food industry, especially in baking. Phytase expression in bifidobacteria may allow, along with the fermentation of bread, the degradation of phytate. Phytate degradation in bread processing has become increasingly common in the manufacture of whole grain breads (Garcia-Mantrana *et al.*, 2016). Another promising application of phytase is in the synthesis of myo-inositol derivatives from agro-industrial residues rich in phytate, such as soybean meal (Quan *et al.*, 2003). These compounds are important in cell signaling pathways, being therefore molecules of great interest to the pharmaceutical industry.

In view of the wide range of action of phytase, the interest in its enzymatic immobilization will depend on its industrial application. In the feed industry, the gain in thermal stability of phytase after its immobilization can be very interesting, since during production the food is subjected to high temperatures (110 to 150 °C) during the pelletizing stage (Cho *et al.*, 2011; Dutta *et al.*, 2017). Cho *et al.* (2011) demonstrated an increase in the thermostability of phytase obtained from *Escherichia coli* after being immobilized on *Bacillus polyfermenticu* spores. They chose spores as supports because they are highly resistant to heat and solvents.

Other research has sought to assess the increase in the operational stability of phytase in immobilized form. These studies have shown the gain of phytase stability when immobilized on graphene oxide nanoparticles (Dutta *et al.*, 2017), in alginate hydrogels (Zhang and Xu, 2015), in chitosan magnetic nanoparticles (Onem and Nadaroglu, 2018) and even through the crossing of the enzyme by the CLEA method (Periyasamy, 2016).

On the other hand, studies like that of Trouillefou *et al.* (2015) have shown the application of phytase in immobilized form in soil supplementation for plant growth. In this work, phytase was immobilized on mesoporous silica, proving efficiency in delivering inorganic phosphorus to *Medicago truncatula* plants. Phytase immobilization can also be interesting to achieve a quick and effective quantitative determination of phytic acid, through the creation of new biosensors, since the conventional method is complicated and time-consuming (Taghavian *et al.*, 2015).

2.6 References

Agrawal, R., Verma, A., Satlewal, A., 2016. Application of nanoparticle-immobilized thermostable beta-glucosidase for improving the sugarcane juice properties. Innovative Food Science & Emerging Technologies 33, 472-482.

Alftren, J., Hobley, T., 2013. Covalent Immobilization of beta-Glucosidase on Magnetic Particles for Lignocellulose Hydrolysis. Applied Biochemistry and Biotechnology 169, 2076-2087.

Aragon, C.C., Santos, A.F., Ruiz-Matute, A.I., Corzo, N., Guisan, J.M., Monti, R., Mateo, C., 2013. Continuous production of xylooligosaccharides in a packed bed reactor with immobilized-stabilized biocatalysts of xylanase from Aspergillus versicolor. Journal of Molecular Catalysis B-Enzymatic 98, 8-14.

Arhle, W., 2007. Enzymes in Industry, Third ed. Wiley-VCH, The Netherlands.

Bala, T., Prasad, B., Sastry, M., Kahaly, M., Waghmare, U., 2007. Interaction of different metal ions with carboxylic acid group: A quantitative study. Journal of Physical Chemistry a 111, 6183-6190.

Barbosa, O., Torres, R., Ortiz, C., Berenguer-Murcia, A., Rodrigues, R.C., Fernandez-Lafuente, R., 2013. Heterofunctional Supports in Enzyme Immobilization: From Traditional Immobilization Protocols to Opportunities in Tuning Enzyme Properties. Biomacromolecules 14, 2433-2462.

Beg, Q.K., Kapoor, M., Mahajan, L., Hoondal, G.S., 2001. Microbial xylanases and their industrial applications: a review. Applied Microbiology and Biotechnology 56, 326-338.

Bohara, R.A., Thorat, N.D., Pawar, S.H., 2016. Immobilization of cellulase on functionalized cobalt ferrite nanoparticles. Korean Journal of Chemical Engineering 33, 216-222.

Borges, D., Baraldo, A., Farinas, C., Giordano, R., Tardioli, P., 2014. Enhanced saccharification of sugarcane bagasse using soluble cellulase supplemented with immobilized beta-glucosidase. Bioresource Technology 167, 206-213.

Cao, L., Wang, W.M., Yang, C.T., Yang, Y., Diana, J., Yakupitiyage, A., Luo, Z., Li, D.P., 2007. Application of microbial phytase in fish feed. Enzyme and Microbial Technology 40, 497-507.

Celik, A., Dincer, A., Aydemir, T., 2016. Characterization of beta-glucosidase immobilized on chitosan-multiwalled carbon nanotubes (MWCNTS) and their application on tea extracts for aroma enhancement. International Journal of Biological Macromolecules 89, 406-414.

Chen, K.I., Yao, Y.J., Chen, H.J., Lo, Y.C., Yu, R.C., Cheng, K.C., 2016. Hydrolysis of isoflavone in black soy milk using cellulose bead as enzyme immobilizer. Journal of Food and Drug Analysis 24, 788-795.

Cho, E.A., Kim, E.J., Pan, J.G., 2011. Adsorption immobilization of Escherichia coli phytase on probiotic Bacillus polyfermenticus spores. Enzyme and Microbial Technology 49, 66-71.

Cipolatti, E., Silva, M., Klein, M., Feddern, V., Feltes, M., Oliveira, J., Ninow, J., de Oliveira, D., 2014. Current status and trends in enzymatic nanoimmobilization. Journal of Molecular Catalysis B-Enzymatic 99, 56-67.

Dorozhkin, S.V., 2010. Amorphous calcium (ortho)phosphates. Acta Biomaterialia 6, 4457-4475.

Driss, D., Zouari-Ellouzi, S., Chaari, F., Kallel, F., Ghazala, I., Bouaziz, F., Ghorbel, R., Chaabouni, S.E., 2014. Production and in vitro evaluation of xylooligosaccharides generated from corncobs using immobilized Penicillium occitanis xylanase. Journal of Molecular Catalysis B-Enzymatic 102, 146-153.

Druzhinina, I., Kubicek, C., 2017. Genetic engineering of Trichoderma reesei cellulases and their production. Microbial Biotechnology 10, 1485-1499.

Dutta, N., Raj, D., Biswas, N., Mallick, M., Omesh, S., 2017. Nanoparticle assisted activity optimization and characterization of a bacterial phytase immobilized on single layer graphene oxide. Biocatalysis and Agricultural Biotechnology 9, 240-247.

Farinas, C., Reis, P., Ferraz, H., Salim, V., Alves, T., 2007. Adsorption of myoglobin onto hydroxyapatite modified with metal ions. Adsorption Science & Technology 25, 717-727.

Farinas, C.S., Marconcini, J.M., Mattoso, L.H.C., 2018. Enzymatic Conversion of Sugarcane Lignocellulosic Biomass as a Platform for the Production of Ethanol, Enzymes and Nanocellulose. Journal of Renewable Materials 6, 203-216.

Garcia-Mantrana, I., Yebra, M.J., Haros, M., Monedero, V., 2016. Expression of bifidobacterial phytases in Lactobacillus casei and their application in a food model of whole-grain sourdough bread. International Journal of Food Microbiology 216, 18-24.

Gilkes, N.R., Henrissat, B., Kilburn, D.G., Miller, R.C., Warren, R.A.J., 1991. Domains in microbial beta-1,4-glycanases - sequence conservation, function, and enzyme families. Microbiological Reviews 55, 303-315.

Gomez, J., Romero, M., Fernandez, T., Diez, E., 2012. Immobilization of beta-glucosidase in fixed bed reactor and evaluation of the enzymatic activity. Bioprocess and Biosystems Engineering 35, 1399-1405.

Gregg, S.J.S., K. S. W., 1982. *Adsorption, Surface Area and Porosity*. Academic Press,, London.

Hench, L.L., Wilson, J., 1993. An introduction to bioceramics, First ed. World Scientific, Singapore.

Hoarau, M., Badieyan, S., Marsh, E., 2017. Immobilized enzymes: understanding enzyme - surface interactions at the molecular level. Organic & Biomolecular Chemistry 15, 9539-9551.

Ivic, J., Velickovic, D., Dimitrijevic, A., Bezbradica, D., Dragacevic, V., Jankulovic, M., Milosavic, N., 2016. Design of biocompatible immobilized Candida rugosa lipase with potential application in food industry. Journal of the Science of Food and Agriculture 96, 4281-4287.

Ivry, S.L., Meyer, N.O., Winter, M.B., Bohn, M.F., Knudsen, G.M., O'Donoghue, A.J., Craik, C.S., 2018. Global substrate specificity profiling of post-translational modifying enzymes. Protein Science 27, 584-594.

Jain, J., Sapna, Singh, B., 2016. Characteristics and biotechnological applications of bacterial phytases. Process Biochemistry 51, 159-169.

Jampala, P., Preethi, M., Ramanujam, S., Harish, B.S., Uppuluri, K.B., Anbazhagan, V., 2017. Immobilization of levan-xylanase nanohybrid on an alginate bead improves xylanase stability at wide pH and temperature. International Journal of Biological Macromolecules 95, 843-849.

Javed, M., Buthe, A., Rashid, M., Wang, P., 2016. Cost-efficient entrapment of beta-glucosidase in nanoscale latex and silicone polymeric thin films for use as stable biocatalysts. Food Chemistry 190, 1078-1085.

Jesionowski, T., Zdarta, J., Krajewska, B., 2014. Enzyme immobilization by adsorption: a review. Adsorption-Journal of the International Adsorption Society 20, 801-821.

Jorgensen, H., Pinelo, M., 2017. Enzyme recycling in lignocellulosic biorefineries. Biofuels Bioproducts & Biorefining-Biofpr 11, 150-167.

Klein-Marcuschamer, D., Oleskowicz-Popiel, P., Simmons, B., Blanch, H., 2012. The challenge of enzyme cost in the production of lignocellulosic biofuels. Biotechnology and Bioengineering 109, 1083-1087.

Kojima, S., Nagata, F., Kugimiya, S., Kato, K., 2018. Synthesis of peptide-containing calcium phosphate nanoparticles exhibiting highly selective adsorption of various proteins. Applied Surface Science 458, 438-445.

Kopp, W., Silva, F.A., Lima, L.N., Masunaga, S.H., Tardioli, P.W., Giordano, R.C., Araujo-Moreira, F.M., Giordano, R.L.C., 2015. Synthesis and characterization of robust magnetic carriers for bioprocess applications. Materials Science and Engineering B-Advanced Functional Solid-State Materials 193, 217-228.

Kumar, V., Dangi, A.K., Shukla, P., 2018. Engineering Thermostable Microbial Xylanases Toward its Industrial Applications. Molecular Biotechnology 60, 226-235.

Lehninger, A.L., 2006. Princípios de Bioquímica, Fourth ed, São Paulo.

Lima, M., Oliveira-Neto, M., Kadowaki, M., Rosseto, F., Prates, E., Squina, F., Leme, A., Skaf, M., Polikarpov, I., 2013. Aspergillus niger beta-Glucosidase Has a Cellulase-like Tadpole Molecular Shape Insights into glycoside hydrolase family 3 (gh3) beta-glucosidase structure and function. Journal of Biological Chemistry 288, 32991-33005.

Lin, K.L., Chang, J., Liu, X.G., Chen, L., Zhou, Y.L., 2011. Synthesis of element-substituted hydroxyapatite with controllable morphology and chemical composition using calcium silicate as precursor. Crystengcomm 13, 4850-4855.

Linares-Pasten, J.A., Aronsson, A., Karlsson, E.N., 2018. Structural Considerations on the Use of Endo-Xylanases for the Production of prebiotic Xylooligosaccharides from Biomass. Current Protein & Peptide Science 19, 48-67.

Liu, M.Q., Dai, X.J., Guan, R.F., Xu, X., 2014. Immobilization of Aspergillus niger xylanase A on Fe3O4-coated chitosan magnetic nanoparticles for xylooligosaccharide preparation. Catalysis Communications 55, 6-10.

Liu, M.Q., Huo, W.K., Xu, X., Jin, D.F., 2015. An immobilized bifunctional xylanase on carbon-coated chitosan nanoparticles with a potential application in xylan-rich biomass bioconversion. Journal of Molecular Catalysis B-Enzymatic 120, 119-126.

Maicas, S., Mateo, J., 2005. Hydrolysis of terpenyl glycosides in grape juice and other fruit juices: a review. Applied Microbiology and Biotechnology 67, 322-335.

Mehta, J., Bhardwaj, N., Bhardwaj, S.K., Kim, K.H., Deep, A., 2016. Recent advances in enzyme immobilization techniques: Metal-organic frameworks as novel substrates. Coordination Chemistry Reviews 322, 30-40.

Mezeli, M.M., Menezes-Blackburn, D., George, T.S., Giles, C.D., Neilson, R., Haygarth, P.M., 2017. Effect of citrate on Aspergillus niger phytase adsorption and catalytic activity in soil. Geoderma 305, 346-353.

Michlmayr, H., Kneifel, W., 2014. beta-Glucosidase activities of lactic acid bacteria: mechanisms, impact on fermented food and human health. Fems Microbiology Letters 352, 1-10.

Mohamad, N., Marzuki, N., Buang, N., Huyop, F., Wahab, R., 2015. An overview of technologies for immobilization of enzymes and surface analysis techniques for immobilized enzymes. Biotechnology & Biotechnological Equipment 29, 205-220.

Mukhopadhyay, A., Dasgupta, A., Chattopadhyay, D., Chakrabarti, K., 2012. Improvement of thermostability and activity of pectate lyase in the presence of hydroxyapatite nanoparticles. Bioresource Technology 116, 348-354.

Nagasaki, T., Nagata, F., Sakurai, M., Kato, K., 2017. Effects of pore distribution of hydroxyapatite particles on their protein adsorption behavior. Journal of Asian Ceramic Societies 5, 88-93.

Narasimha, G., Sridevi, A., Ramanjaneyulu, G., Reddy, B., 2016. Purification and Characterization of beta-Glucosidase from Aspergillus niger. International Journal of Food Properties 19, 652-661.

Nghiem, N., Ramirez, E., McAloon, A., Yee, W., Johnston, D., Hicks, K., 2011. Economic analysis of fuel ethanol production from winter hulled barley by the EDGE (Enhanced Dry Grind Enzymatic) process. Bioresource Technology 102, 6696-6701.

Norgaard, J.V., Pedersen, T.F., Blaabjerg, K., Knudsen, K.E.B., Laerke, H.N., 2016. Xylanase supplementation to rye diets for growing pigs. Journal of Animal Science 94, 91-94.

Onem, H., Nadaroglu, H., 2018. Immobilization of Purified Phytase Enzyme from Tirmit (Lactarius volemus) on Coated Chitosan with Iron Nanoparticles and Investigation of Its Usability in Cereal Industry. Iranian Journal of Science and Technology Transaction a-Science 42, 1063-1075.

Periyasamy, K., Santhalembi, L., Mortha, G., Aurousseau, M., Subramanian, S., 2016. Carrier-free co-immobilization of xylanase, cellulase and beta-1,3-glucanase as combined cross-linked enzyme aggregates (combi-CLEAs) for one-pot saccharification of sugarcane bagasse. Rsc Advances 6, 32849-32857.

Pham, T., Shah, N., 2009. Hydrolysis of isoflavone glycosides in soy milk by beta-galactosidase and beta-glucosidase. Journal of Food Biochemistry 33, 38-60.

Polaina, J., MacCabe, A.P., 2007. Industrial enzymes: Structure, function and application, First ed. Springer, Dordrecht.

Puri, M., Barrow, C., Verma, M., 2013. Enzyme immobilization on nanomaterials for biofuel production. Trends in Biotechnology 31, 215-216.

Qi, M.L., He, K., Huang, Z.N., Shahbazian-Yassar, R., Xiao, G.Y., Lu, Y.P., Shokuhfar, T., 2017. Hydroxyapatite Fibers: A Review of Synthesis Methods. Jom 69, 1354-1360.

Quan, C.S., Fan, S.D., Ohta, Y., 2003. Immobilization of Candida krusei cells producing phytase in alginate gel beads: an application of the preparation of myo-inositol phosphates. Applied Microbiology and Biotechnology 62, 41-47.

Sadat-Shojai, M., Khorasani, M., Dinpanah-Khoshdargi, E., Jamshidi, A., 2013. Synthesis methods for nanosized hydroxyapatite with diverse structures. Acta Biomaterialia 9, 7591-7621.

Schomburg, D., Schomburg, I., 2009. Springer Handbook of Enzymes, Second ed. Springer, New York.

Shahrestani, H., Taheri-Kafrani, A., Soozanipour, A., Tavakoli, O., 2016. Enzymatic clarification of fruit juices using xylanase immobilized on 1,3,5-triazine-functionalized silica-encapsulated magnetic nanoparticles. Biochemical Engineering Journal 109, 51-58.

Sheldon, R., van Pelt, S., 2013. Enzyme immobilisation in biocatalysis: why, what and how. Chemical Society Reviews 42, 6223-6235.

Sheldon, R.A., 2007. Cross-linked enzyme aggregates (CLEA (R) s): stable and recyclable biocatalysts. Biochemical Society Transactions 35, 1583-1587.

Shewale, J., 1982. Beta-glucosidase - its role in cellulase synthesis and hydrolysis of cellulose. International Journal of Biochemistry 14, 435-443.

Singh, B., Satyanarayana, T., 2015. Fungal phytases: characteristics and amelioration of nutritional quality and growth of non-ruminants. Journal of Animal Physiology and Animal Nutrition 99, 646-660.

Singhania, R., Patel, A., Pandey, A., Ganansounou, E., 2017. Genetic modification: A tool for enhancing beta-glucosidase production for biofuel application. Bioresource Technology 245, 1352-1361.

Singhania, R., Patel, A., Sukumaran, R., Larroche, C., Pandey, A., 2013. Role and significance of beta-glucosidases in the hydrolysis of cellulose for bioethanol production. Bioresource Technology 127, 500-507.

Swain, S.K., Sarkar, D., 2013. Study of BSA protein adsorption/release on hydroxyapatite nanoparticles. Applied Surface Science 286, 99-103.

Taghavian, H., Ranaei-Siadat, S.O., Kalaee, M.R., Mazinani, S., Ranaei-Siadat, S.E., Harati, J., 2015. Optimizing the Activity of Immobilized Phytase on Starch Blended Polyacrylamide Nanofibers-Nanomembranes by Response Surface Methodology. Fibers and Polymers 16, 1048-1056.

Trouillefou, C.M., Le Cadre, E., Cacciaguerra, T., Cunin, F., Plassard, C., Belamie, E., 2015. Protected activity of a phytase immobilized in mesoporous silica with benefits to plant phosphorus nutrition. Journal of Sol-Gel Science and Technology 74, 55-65.

Vaghari, H., Jafarizadeh-Malmiri, H., Mohammadlou, M., Berenjian, A., Anarjan, N., Jafari, N., Nasiri, S., 2016. Application of magnetic nanoparticles in smart enzyme immobilization. Biotechnology Letters 38, 223-233.

Vandenberg, G.W., Scott, S.L., Sarker, P.K., Dallaire, V., de la Noue, J., 2011. Encapsulation of microbial phytase: Effects on phosphorus bioavailability in rainbow trout (Oncorhynchus mykiss). Animal Feed Science and Technology 169, 230-243.

Vaz, R., Moreira, L., Ferreira, E., 2016. An overview of holocellulose-degrading enzyme immobilization for use in bioethanol production. Journal of Molecular Catalysis B-Enzymatic 133, 127-135.

Vieira, M., Vieira, A., Zanin, G., Tardioli, P., Mateo, C., Guisan, J., 2011. beta-Glucosidase immobilized and stabilized on agarose matrix functionalized with distinct reactive groups. Journal of Molecular Catalysis B-Enzymatic 69, 47-53.

Vohra, A., Kaur, P., Satyanarayana, T., 2011. Production, characteristics and applications of the cell-bound phytase of Pichia anomala. Antonie Van Leeuwenhoek International Journal of General and Molecular Microbiology 99, 51-55.

Watanabe, T., Sato, T., Yoshioka, S., Koshijima, T., Kuwahara, M., 1992. Purification and properties of aspergillus-niger beta-glucosidase. European Journal of Biochemistry 209, 651-659.

Woolridge, E.M., 2014. Mixed Enzyme Systems for Delignification of Lignocellulosic Biomass. Catalysts 4, 1-35.

Xia, T.T., Liu, C.Z., Hu, J.H., Guo, C., 2016. Improved performance of immobilized laccase on amine-functioned magnetic Fe3O4 nanoparticles modified with polyethylenimine. Chemical Engineering Journal 295, 201-206.

Xie, W., Zang, X., 2017. Covalent immobilization of lipase onto aminopropyl-functionalized hydroxyapatite-encapsulated-gamma-Fe2O3 nanoparticles: A magnetic biocatalyst for interesterification of soybean oil. Food Chemistry 227, 397-403.

Yelten, A., Yilmaz, S., Oktar, F.N., 2012. Sol-gel derived alumina-hydroxyapatite-tricalcium phosphate porous composite powders. Ceramics International 38, 2659-2665.

Yu, X., Gao, Y.H., Chen, Z.F., 2004. Purification and characterization of an extracellular beta-glucosidase with high transglucosylation activity and stability from Aspergillus niger no. 5.1. Applied Biochemistry and Biotechnology 119, 229-240.

Zhang, W., Qiu, J., Feng, H., Zang, L., Sakai, E., 2015. Increase in stability of cellulase immobilized on functionalized magnetic nanospheres. Journal of Magnetism and Magnetic Materials 375, 117-123.

Zhang, W.Z., Xu, F., 2015. Hierarchical Composites Promoting Immobilization and Stabilization of Phytase via Transesterification/Silification of Modulated Alginate Hydrogels. ACS Sustainable Chemistry & Engineering 3, 2694-2703.

Zhang, Y.H.P., Lynd, L.R., 2004. Toward an aggregated understanding of enzymatic hydrolysis of cellulose: Noncomplexed cellulase systems. Biotechnology and Bioengineering 88, 797-824.

Zhu, F.M., Du, B., Gao, H.S., Liu, C.J., Li, J., 2010. Purification and Characterization of an Intracellular beta-Glucosidase from the Protoplast Fusant of Aspergillus oryzae and Aspergillus niger. Applied Biochemistry and Microbiology 46, 626-632.

Zydney, A.L., 2016. Continuous downstream processing for high value biological products: A Review. Biotechnology and Bioengineering 113, 465-475.

3. Objectives

The objective of this PhD Thesis was to evaluate the immobilization of β-glucosidase, phytase and xylanase enzymes onto hydroxyapatite (HA) nanoparticles aiming to obtain derivatives with enhanced catalytic properties such as activity, operational stability and reusability. This work aimed to develop enzymatic immobilization protocols of these enzymes on HA with the purpose of being utilized in the future in specific agro-industrial processes. The specific objectives were:

i) To investigate the morphological and structural characteristics of hydroxyapatite using Microscopy (FEG-SEM), X-ray diffraction (XRD), nitrogen adsorption/desorption isotherms (BET), zeta potential and infrared spectroscopy (FT-IR) techniques, in order to understand the possible modes of enzyme/support interaction.

ii) To investigate the ideal physicochemical conditions of enzymatic adsorption such as pH, temperature, ionic strength and time.

iii) To conduct a desorption study of derivatives obtained with potential desorbing agents in order to investigate the chemical interaction between enzyme and support.

iv) To evaluate if there were changes in the enzyme activity profile after being immobilized (within a determined range of pH and temperature).

v) To investigate the thermal stability of the obtained derivative obtained (when this was one of the objectives of immobilizing the enzyme).

vi) To investigate the biocatalyst reuse capacity in repeated hydrolysis cycles (when this was one of the objectives of immobilizing the enzyme).

vii) To synthesize composites of hydroxyapatite with ferrite cobalt (HA:$CoFe_2O_4$) to act as magnetic matrix for β-glucosidase, phytase and xylanase immobilization. The aim was to facilitate the enzyme recovery from the reaction medium by magnetic field application.

CHAPTER 2

β-glucosidase immobilization on hydroxyapatite nanoparticles

This chapter is an adapted version of the article "Nanoimmobilization of β-glucosidase onto hydroxyapatite" published in 2018 in the International Journal of Biological Macromolecules, volume 119, pages 1042-1051.

Graphical Abstract

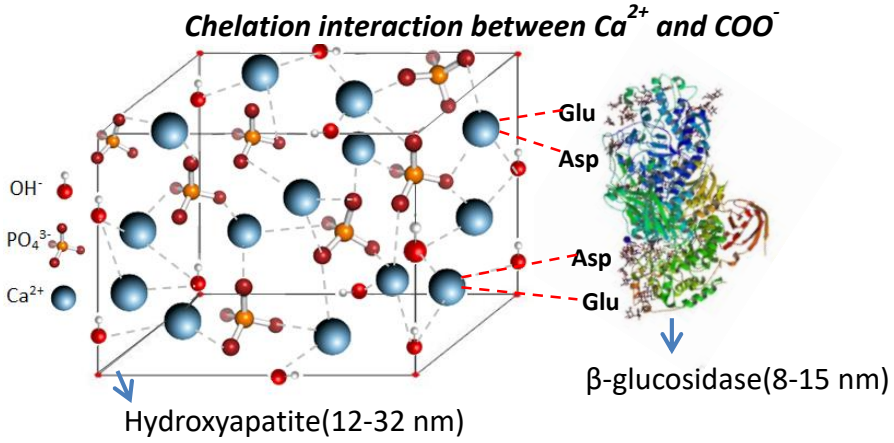

Abstract

β-Glucosidase is an enzyme of great industrial interest that is used in biorefineries and in the pharmaceutical, food, and beverage sectors, among others. These industrial processes would benefit from the use of immobilized enzyme systems that allow several reuses of the enzyme. A promising inorganic and nontoxic material for such application is hydroxyapatite (HA), which can be synthesized at nanometric scale, hence providing good accessibility of the substrate to the catalyst. Here, we carried out a systematic study to evaluate the feasibility of immobilizing β-glucosidase on HA nanoparticles. The immobilization process was highly effective over wide ranges of pH and ionic strength, resulting in immobilization yields and recovered activities up to 90%. Investigation of the type of interaction between β-glucosidase and HA (using FT-IR, zeta potential measurements, and desorption tests with different salts) indicated the formation of coordination bonds between Ca^{2+} sites of HA and COO^- of amino acids. Even after 10 cycles of reuse, the immobilized β-glucosidase retained about 70% of its initial activity, demonstrating the operational stability of the immobilized enzyme. The results showed that β-glucosidase could be efficiently immobilized on HA nanoparticles by means of a very simple adsorption protocol, offering a promising strategy for performing repeated enzymatic hydrolysis reactions.

Keywords: Immobilization; nanoparticles, β-glucosidase, hydroxyapatite; adsorption.

1. Introduction

The β-glucosidase enzyme catalyzes the specific hydrolysis of β-D-1,4-glycosidic bonds in oligosaccharides, disaccharides, and conjugated glycosides (Shewale, 1982; Langston *et al.*, 2006), consequently finding many applications in different industrial sectors. In the lignocellulosic biomass conversion process, β-glucosidase acts together with other specialized cellulase enzymes in the hydrolysis of cellulose to glucose, which can be used to obtain biofuels and other bioproducts, according to the biorefinery concept (Liguori *et al.*, 2016; Farinas *et al.*, 2018). β-Glucosidase plays a key role in these biomass-to-sugar platforms, releasing glucose from cellobiose and preventing inhibition of the enzymes endoglucanase and cellobiohydrolase (Singhania *et al.*, 2013; Pereira *et al.*, 2015). β-Glucosidase enzymes are also important in the food and beverage sectors, where they are used to enhance the quality of wines, teas, and juices (Maicas and Mateo, 2005; Celik *et al.*, 2016;). In the pharmaceutical sector, β-glucosidase is employed for the hydrolysis of isoflavone glycosides, found in soybean agro-industrial residues, generating aglycone molecules that have estrogenic properties (Chang *et al.*, 2013; Chen *et al.*, 2016). Therefore, finding an effective strategy to allow the recovery of β-glucosidase for reuse would be of great interest to these industrial sectors, given the high cost of the enzyme (Klein-Marcuschamer *et al.*, 2012; Druzhinina and Kubicek, 2017).

The development of immobilization techniques for β-glucosidase offers a potential way to enable its reuse several times (Vaz *et al.*, 2016). The aim of immobilization is to trap the enzyme within or on the surface of an insoluble material with retention of its catalytic activity (Hoarau *et al.*, 2017). The immobilization strategy also enables continuous operation, improves the stability of the biocatalyst, and allows use of a smaller reactor volume (Sheldon and van Pelt, 2013). The feasibility of immobilizing β-glucosidase enzymes on different supports has been previously demonstrated using physical and ionic adsorption, encapsulation and covalent attachment (Vieira *et al.*, 2011; Gomez *et al.*, 2012; Borges *et al.*, 2014;; Jorgensen and Pinelo, 2017). However, it remains a challenge to find a support that presents the specific characteristics required for high enzyme immobilization efficiency and the robustness to endure different process conditions, at a competitive cost.

Typically, the support should have a high surface area to allow immobilization of significant amounts of enzymes, hydrophilicity to ensure good diffusivity of the substrate, and low solubility in order to avoid product contamination (Puri *et al.*, 2013). The mechanical resistance and thermal stability of the support are important throughout the entire process, from immobilization of the biocatalyst to enzyme recovery (Vaghari *et al.*, 2016). Another important parameter to be evaluated in an immobilization process is the diffusivity of the substrate towards the catalyst. Materials synthesized at the nanometric scale have demonstrated low resistance to mass transfer, ensuring good accessibility of the substrate to the catalyst (Cipolatti *et al.*, 2014).

The main advantage of using nanoparticles as supports to immobilize enzymes is their high surface area, which allows higher enzymatic loading per unit mass of particles (Javed *et al.*, 2016). Previous studies have reported the immobilization of β-glucosidase on nanomaterials such as chitosan-multiwalled carbon nanotubes (Celik *et al.*, 2016), magnetic Fe_3O_4 nanospheres functionalized with amino-silane (Zhang *et al.*, 2015) , nanoscale polymeric materials including polyurethane, latex and silicone (Javed *et al.*, 2016), and silicon oxide nanoparticles (Agrawal *et al.*, 2016). However, in these previous studies, the immobilization of enzymes usually required chemical modifications of the support and/or the enzyme, such as activation with glyoxyl groups for covalent attachment, crosslinking with glutaraldehyde, amination of the enzyme or of the support side groups for ionic adsorption, or insertion of a spacer arm, among others. Therefore, finding a nanomaterial for enzyme immobilization that does not require any additional chemical modification procedures would contribute to process viability, from both the technical and economic standpoints.

A promising inorganic solid for the immobilization of enzymes is hydroxyapatite (HA), a nontoxic material that can be synthesized as nanoparticles (Andre *et al.*, 2012; Mukhopadhyay *et al.*, 2012). The adsorption of proteins onto HA has been demonstrated for various applications such as separation of proteins by chromatography (Farinas *et al.*, 2007; Yang *et al.*, 2015), bone regeneration in biomedicine (Chen *et al.*, 2018; Tohamy *et al.*, 2018) and drug delivery in the pharmaceutical industry (Kollath *et al.*, 2015). The hydroxyapatite structure includes phosphate and calcium groups that are available for ionic adsorption involving protein side groups (Wang *et al.*, 2012). The calcium ions present in HA can also undergo chelation reactions with carboxylic acid groups present in the amino acids of enzymes, resulting in highly stable interactions for immobilization (Ivic *et al.*, 2016a). Recent studies have reported the immobilization of lipase enzymes on HA nanoparticles (Ivic *et al.*, 2016b; Xie and Zang, 2017) . However, to the best of our knowledge, there have been no reports of the use of HA nanoparticles for immobilization of β-glucosidase enzymes. Given the vast range of industrial applications of this biocatalyst and the interesting properties of HA, which has still been little explored as a support for immobilization of enzymes, the development of a simple protocol for the immobilization of β-glucosidase onto HA could be of potential interest to several industrial sectors.

Here, a systematic study of immobilization of the β-glucosidase enzyme onto HA nanoparticles was carried out. The support was first characterized in terms of particle size using microscopy (FEG-SEM), structure using X-ray diffraction (XRD), and specific surface area using nitrogen adsorption/desorption isotherms (BET method). The biocatalyst was then immobilized on HA under different conditions of pH and ionic strength, in order to find the conditions that resulted in the best immobilization yield and recovered activity. The efficiency of the immobilized β-glucosidase derivative was evaluated in terms of cellobiose hydrolysis and the reusability of the biocatalyst. The nature of the chemical interaction between the support and the enzyme was

investigated using zeta potential measurements, desorption tests, and acquisition of FT-IR spectra. The aim was to obtain a simple and effective immobilization method to ensure high catalytic activity and reusability of β-glucosidase in different industrial applications.

2. Materials and Methods

2.1 Materials

The β-glucosidase enzyme (specified as 22118) was donated by Novozymes (Denmark). The hydroxyapatite nanoparticles and the cellobiose substrate were purchased from Sigma-Aldrich (St. Louis, US). All other reagents were analytical grade.

2.2 Characterization of the hydroxyapatite support

The FEG-SEM (field emission gun-scanning electron microscopy) technique was used to analyze the morphology of the hydroxyapatite particles. A surface of a metallic disc (stub) was coated with graphite and the sample was dispersed over it. The sample was analyzed using a JEOL Model JSM-6701F microscope operated at 2.0 kV, with 1.0 nm resolution. The histogram was constructed considering the sizes of 100 different particles. The specific surface area (SSA) was determined by means of nitrogen isotherms, according to the Brunauer, Emmett, and Teller (BET) method, employing a surface area analyzer (ASAP 2020, Micromeritics).

The crystallinity of the hydroxyapatite particles was investigated using X-ray diffraction (XRD) measurements performed with a Shimadzu Model 6000 X-ray diffractometer. The diffractograms were recorded in the diffraction range (2Θ) 20-70º, with a scanning speed of 1º min^{-1}, using a Cu-Kα incident beam (λ=0.1546 nm). Functional group analyses of the HA particles with and without enzyme were performed by Fourier transform infrared spectroscopy (FT-IR), using a Bruker Vertex 70 instrument. The samples were mixed with pre-dried FT-IR-grade KBr, followed by pressing into disks. The measurements were carried out in transmission mode, in the mid-infrared range (400-4000 cm^{-1}), at a resolution of 4 cm^{-1} (32 scans).

2.3 Immobilization of β-glucosidase on the hydroxyapatite nanoparticles

The immobilization solution was prepared with hydroxyapatite at a concentration of 0.1 g mL^{-1}, using an appropriate buffer for the pH and ionic strength described for each specific assay. The protein content of the commercial enzymatic solution was determined colorimetrically (at 562 nm) using a BCA protein assay kit (Pierce), with bovine serum albumin as a protein standard. The capacity of the support was evaluated using enzyme loadings ranging from 10 to 50 mg protein g^{-1} support.

The enzyme-support adsorption was carried out in 5 mL tubes, with gentle stirring for 1 h at 25 °C. The course of the immobilization was monitored by measuring (in triplicate) the enzyme

activity in the supernatant obtained by centrifugation at 8000 rpm for 2 min. The activity was also determined for the control (soluble enzyme). The derivative (immobilized enzyme) was washed three times with the same buffer used for immobilization, in order to remove proteins that did not adsorb on the support. The activity of the final derivative (A_{DE}) was measured in triplicate. The results were presented in terms of the immobilization parameters, which were calculated from the averages of the activity measurements.

2.3.1 Calculation of immobilization parameters

The percentage of immobilization yield (*IY*) was calculated using the equation:

$$IY\ (\%) = 1 - {}^{A_{F,S}}\!/_{A_{F,C}} \times 100\ ,$$

where $A_{F,S}$ (IU mL^{-1}) and $A_{F,C}$ (IU mL^{-1}) are the final activities of the supernatant and the control (free enzyme), respectively. The activity that was offered to the support (A_{Of}) was calculated using the equation:

$$A_{Of}\left(\frac{IU}{g\ support}\right) = \frac{A_{FE} \times volume\ of\ enzyme\ offered\ (in\ mL)}{mass\ of\ support\ (in\ g)}\ ,$$

where A_{FE} (IU mL^{-1}) is the activity of the free enzyme. The theoretically immobilized activity (A_{TI}, in IU g^{-1} support) was obtained as the product of the activity offered to the support (A_{Of}) and IY × 100^{-1}. The recovered activity (*RA*) of the immobilized enzyme was calculated as follows:

$$RA\ (\%) = {}^{A_{DE}}\!/_{A_{TI}} \times 100,$$

where A_{DE} is the activity of the derivative (IU g^{-1} support).

2.4 Enzymatic activity assays

The enzymatic activities of the soluble and immobilized β-glucosidase were determined as described by Ghose (1987), with measurement of the concentration of glucose produced using cellobiose as substrate. Equal volumes of enzymatic solution (or suspension, in the case of the immobilized enzyme) and cellobiose solution (15 mM, prepared using 50 mM sodium acetate buffer at pH 4.8) were allowed to react for 20 min, at 50 °C, under stirring. The reaction was quenched using thermal inactivation of the enzyme by placing the vials in boiling water for 5 min. The product of the reaction was measured using a GOD-POD enzymatic assay kit (Doles, Brazil). One unit of enzyme activity (IU) represented the amount of enzyme required to release 1 μmol of glucose per minute into the reaction mixture. All the activity measurements were performed in triplicate, with calculation of the immobilization parameters as means ± standard deviation.

2.5 Effect of pH and ionic strength on the immobilization procedure

In order to find the ideal conditions for the immobilization procedure, adsorption assays were performed at different pHs and ionic strengths, with an enzyme loading of 10 mg protein g^{-}

[1] support. The enzyme was immobilized at pH 4 and 5 using sodium acetate buffer and at pH 6, 7, and 8 using sodium phosphate buffer, with the ionic strength set at 20 mM in all the assays. In order to evaluate the effect of ionic strength, enzyme immobilization was carried out at the optimum pH, with different concentrations of sodium chloride (20, 50, 100, 200, 400, 800, and 1600 mM). The ideal pH and ionic strength for immobilization were considered to be those that resulted in the highest values for immobilization yield (IY) and recovered activity (RA).

2.6 Effect of pH and temperature on enzyme activity

The activity of the β-glucosidase immobilized under the best adsorption conditions was evaluated at different temperatures and pH values. The effects of temperature on the activities of free and immobilized β-glucosidase were investigated at 30, 40, 45, 50, 55, 60, and 70 °C, at pH 4.8 (using 50 mM sodium acetate buffer). In order to determine if there was any difference between the free and immobilized enzymes in terms of the activation energy (*Ea*) required for the hydrolysis, the *Ea* values for both forms of enzyme were calculated using Arrhenius plots (Tardioli *et al.*, 2006). The effects of pH on the activities of free and immobilized β-glucosidase were evaluated in the pH range 4-8, using sodium acetate buffer for pH 4 and 5 and sodium phosphate buffer for pH 6, 7, and 8 (all at 50 mM and 50 °C). The highest activity obtained in the temperature or pH ranges was designated as 100% and the activities at all the remaining temperatures and pHs were calculated as the activity (in %) relative to that highest activity.

2.7 Zeta potentials of enzyme and support (with and without enzyme)

The zeta potentials of the free enzyme and the support with and without immobilized enzyme were measured using a Zetasizer 200 system (Malvern Instruments). A mass of 0.001 g (transformed into volume for the enzyme, according to the measured protein concentration) of sample was placed in 100 mL of Milli-Q water. The pH was adjusted using 0.05-0.2 M HCl or KOH and the mobilities were measured as a function of pH in the range 2-10. The data represent the averages of three runs per sample (50 cycles per run). The isoelectric point (pI) was identified as the point crossing the x-axis, where the zeta potential was zero.

2.8 Enzyme desorption assays

The immobilized enzyme was inserted into solutions of varying ionic strength (all at pH 4) prepared using different sodium salts: sodium chloride, sodium citrate, and sodium acetate. Firstly, the supernatant from the suspension, obtained by centrifugation at 8000 rpm for 2 min, was discarded and the same volume of each ionic solution was added to give the following concentrations: 50, 100, 200, 300, 400mM. The suspension was gently stirred for 40 min and desorption from the HA support was monitored by measuring (in triplicate) the enzyme activity in the supernatant. The highest activity, designated as 100%, corresponded to the activity of the

whole immobilized enzyme, while the activities in the supernatants with different ionic strengths were calculated as the desorbed activity (%) relative to that highest activity.

2.9 Hydrolysis of cellobiose

The efficiency of immobilized β-glucosidase was evaluated in terms of cellobiose hydrolysis and was compared to soluble β-glucosidase. Cellobiose (30 g L^{-1}) was hydrolyzed in 50 mM sodium acetate buffer (pH 4.8) at 50 °C (in an incubator), under agitation, using soluble and immobilized β-glucosidase at an enzyme loading of 40 U g^{-1} cellobiose (8.2 mg protein g^{-1} support). The reaction took place in 10 ml falcon tubes. The release of glucose was quantified using a GOD-POD glucose oxidase enzymatic assay kit (Doles, Brazil) during the course of the reaction, until stabilization. The experiment was performed in duplicate and the results were presented as mean ± standard deviation.

3.10 Reusability of the immobilized enzyme

The reusability of immobilized β-glucosidase was studied in assays performed in 15 mL Falcon tubes, under the hydrolysis assay conditions described above, adopting an enzyme loading of 40 U g^{-1} cellobiose (8.2 mg protein g^{-1} support). After each cycle of 12 h of reaction, the derivative was separated by centrifugation (8000 rpm for 5 min) and was then re-suspended in the fresh substrate. The glucose concentration measured in the first cycle corresponded to 100%, while the concentrations of the sugar in the nine remaining cycles were calculated as the glucose production (%) relative to that first cycle. The experiment was performed in duplicate and the results were presented as mean ± standard deviation.

4. Results and Discussion

3.1 Physicochemical characterization of the hydroxyapatite

Hydroxyapatite nanoparticles have potential applications in various different biochemical processes, although their use as a support for the immobilization of enzymes remains little explored. The HA nanoparticles used for immobilization of β-glucosidase were characterized in terms of the following parameters: crystallinity (by XRD), size (by FEG-SEM), and specific surface area (SSA, by the BET method). The X-ray diffraction (XRD) analyses were performed in order to identify the phases present in the HA structure (Fig. S1, Supplementary Material). Comparison of the diffractogram with the Joint Committee on Powder Diffraction Standards (JCPDS) card number 3701-089-4405 confirmed the presence of the characteristic peaks of HA (Table S1, Supplementary Material), which possesses a hexagonal crystalline structure (Farinas *et al.*, 2007; Andre *et al.*, 2012).

The FEG-SEM images (Fig. 1) revealed needle-shaped particles of size 12-32 nm (considering the diameter). As can be seen in Fig. 1, the HA nanoparticles tended to agglomerate, indicating that they were held together by fairly weak forces (Puvvada *et al.*, 2010; Sadat-Shojai *et al.*, 2013). Nevertheless, previous studies have shown that the binding of proteins to the nanoparticles can destabilize these forces and alter particle agglomeration (Allouni *et al.*, 2009; Muller *et al.*, 2014).

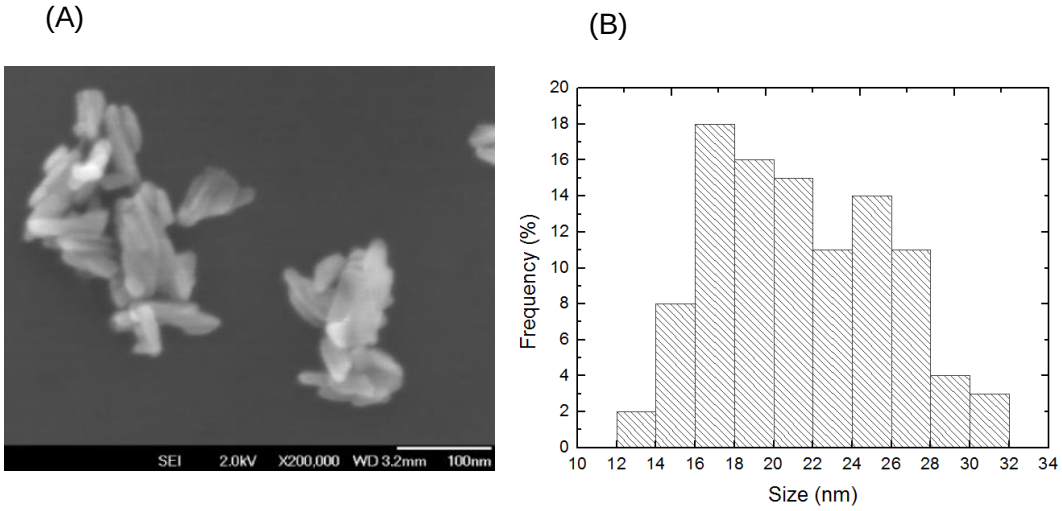

Fig. 1. (A) FEG-SEM images of hydroxyapatite nanoparticles. (B) Histogram of the particle size distribution.

The measured SSA of the HA, obtained using the N_2 adsorption/desorption (BET) method, was 58.2 m^2 g^{-1}. This value included the internal (pore) and external areas of the particles, with the external area normally being much smaller than the internal area (Gregg, 1982). The β-glucosidase from *A. niger* used in this work (obtained from Novozymes) was previously characterized by Lima *et al.* (2013) as presenting a "tadpole" molecular shape showed in a 3D structural model, with a molecular weight of about 116 kDa, a maximum diameter of 15 nm, and a gyration radius (R_g, a global measure of the size of the molecular complex) of about 4.1 nm. Therefore, considering the dimensions and morphologies of the enzyme and the HA support, it could be assumed that the enzyme would be preferentially immobilized on the external surfaces of the HA nanoparticles, thus reducing intra-particle mass transfer limitations.

3.2. Evaluation of immobilization conditions

In order to evaluate whether the β-glucosidase enzyme was able to adsorb onto the HA nanoparticles, an initial test was performed in which the immobilization profile was monitored during a total period of 60 min, using an enzymatic loading of 10 mg protein g^{-1} support in 20

mM sodium acetate buffer at pH 4 (Fig. 2). The enzyme was efficiently immobilized on the HA nanoparticles, with immobilization yield (IY) of 90% and almost total recovered activity (RA). After 5 min of incubation, about 87% of the β-glucosidase had bound to the HA matrix, indicating high binding affinity of the enzyme towards the HA nanoparticles. The IY stabilized after 10 min of reaction, so an incubation time of 60 min was adopted in the following set of experiments, since that period would allow sufficient time to achieve β-glucosidase immobilization.

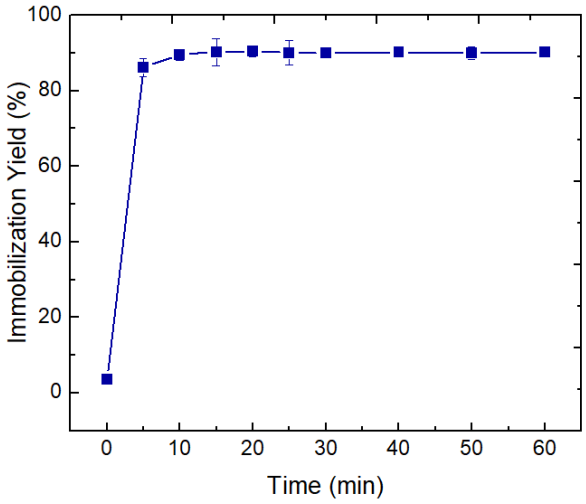

Fig. 2. Course of immobilization of β-glucosidase onto HA nanoparticles at 25 °C and pH 4 (in 20 mM sodium acetate buffer), using an enzymatic loading of 10 mg protein g^{-1} support.

In the next step of the study, the effects of pH and ionic strength on the immobilization process were evaluated. For this set of experiments, the enzymatic activity assays were always performed at the standard conditions of 50 mM sodium acetate buffer at pH 4.8, 50 °C. Around 87% of the β-glucosidase offered to the support was able to bind to it in the wide pH 4-8 range evaluated (Fig. 3A). The ideal immobilization pH was considered to be pH 4, because the biocatalyst showed the best ability to perform its function after immobilization at this pH, with RA of 90% indicating that 90% of the bound enzyme molecules were readily available for substrate transformation. Interestingly, the ideal immobilization condition (pH 4) coincided with the optimal condition for β-glucosidase activity (Fig. 4A, discussed below), indicating that the enzyme could bind to the support in its best conformation for acting as a biocatalyst. This represented a major advantage of the immobilization procedure employed here.

Although the enzyme was demonstrated to be able to remain adsorbed on the carrier over a wide range of pH, the RA decreased as the immobilization pH was increased above pH 4. In other words, the enzyme immobilized at pH 8 (as well as at pH 5, 6, and 7) did not have the same activity as the enzyme that was immobilized at pH 4. This suggested that the multiple interactions

between the enzyme and the support (discussed below) became more intense as the enzyme charges became more negative, due to the higher pH, which may have caused distortion in the enzyme, resulting in decreased RA. Another finding that supported this hypothesis was that the free enzyme (control), which was also kept for 1 h at each of these pH values, maintained its stability and showed no drop in activity (data not shown).

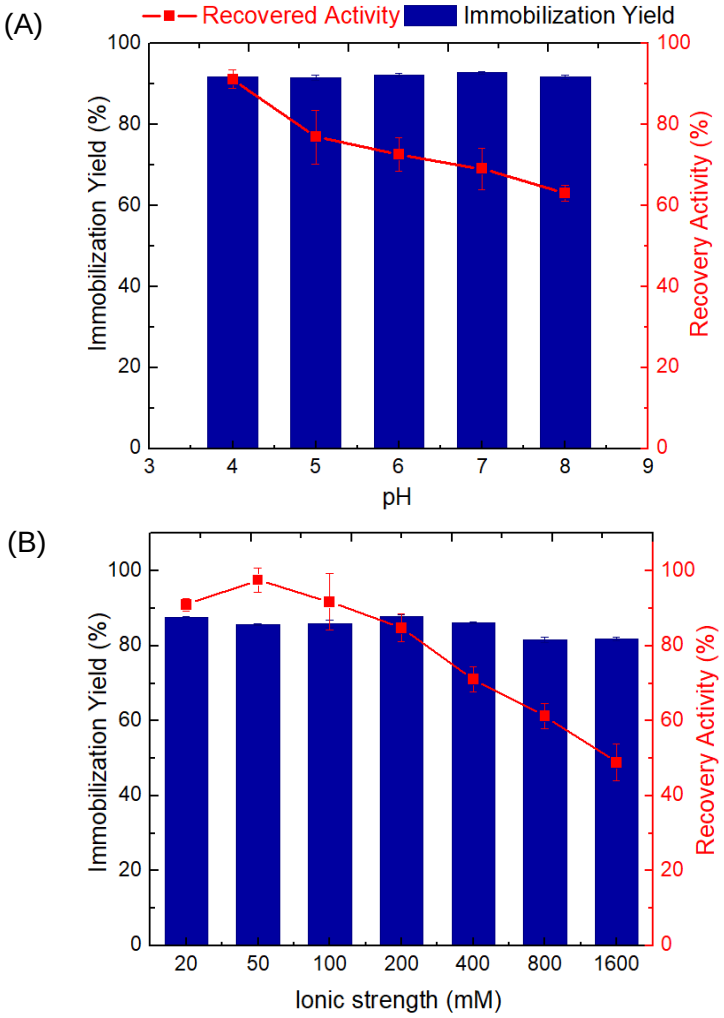

Fig. 3. Effects of (A) pH (at ionic strength of 20 mM) and (B) ionic strength (at pH 4) on the immobilization of β-glucosidase onto HA nanoparticles during 1 h at 25 °C. The immobilization yields and recovered activities were calculated from averages of triplicates.

Evaluation of the effect of ionic strength on the immobilization of β-glucosidase on HA showed that there was no change in immobilization yield (~87%) with increase of the salt concentration (Fig. 3B). The ideal ionic strength for the immobilization was considered to be up to 50 mM, since RA decreased when higher ionic strengths were used during the immobilization. This behavior suggested that the enzyme became inactivated at high ionic strength. However, the activity of the free enzyme was also measured in the presence of high ionic concentrations (data

not shown), with no inactivation being observed. A possible explanation for the reduction in RA of the derivative when immobilized under high ionic strength conditions was immobilization of the enzyme on the support surface by other types of interactions. For example, hydrophobic adsorption involving areas of the protein with high concentrations of external hydrophobic groups (Barbosa *et al.*, 2013) would probably make the enzyme active sites unavailable for participation in bioconversion. Therefore, an ionic strength of 20 mM was selected for use in the subsequent immobilization experiments.

Nevertheless, it is important to note that despite the reduction of RA observed with the increase of the ionic strength and pH applied in the immobilization procedure, the enzyme retained approximately 50% of its activity even under the most extreme conditions of immobilization (namely pH 4, 1600 mM NaCl and pH 8, 20 mM NaCl). These severe immobilization conditions were also evaluated simultaneously (pH 8, 1600 mM NaCl) and resulted in IY of 85% and RA of 50% (data not shown). These findings further support the high affinity of β-glucosidase for the support (without any chemical modification) even under possible adverse industrial conditions.

3.3 Effect of pH and temperature on β-glucosidase activity

A set of enzymatic reaction experiments was carried out at different pH values and temperatures, in order to determine the activity profiles of the β-glucosidase before and after the immobilization process, which was performed for 1 h at 25 °C, pH 4, in 20 mM sodium acetate buffer. The results (Fig. 4) showed that the profiles for pH and temperature were the same for the free and immobilized enzymes, within the ranges evaluated, with optimal activity at pH 4 and 60 °C in both cases. These interesting results suggest that the enzyme was not significantly affected when immobilized on the HA nanoparticles.

Differences in pH and temperature activity profiles commonly occur when an enzyme is immobilized, depending on the immobilization method used. Concerning the pH activity profile, the electrostatic potential of the microenvironment of enzymes immobilized within a porous support that contains ionized functional groups (such as negatively or positively charged exchange resins) can affect the local concentration of H^+, which in turn influences the observed pH activity profile of the immobilized enzyme (Randolph *et al.*, 1987). This effect was reported by Celik *et al.* (2016) for the covalent immobilization of β-glucosidase on chitosan-multiwalled carbon nanotubes, with the optimal pH shifting from pH 6 (for the free enzyme) to pH 5 (after immobilization). Das *et al.* (2014) also reported a shift in the optimum pH (from pH 4.5 to 6.5) after the immobilization of β-glucosidase by entrapment in alginate beads.

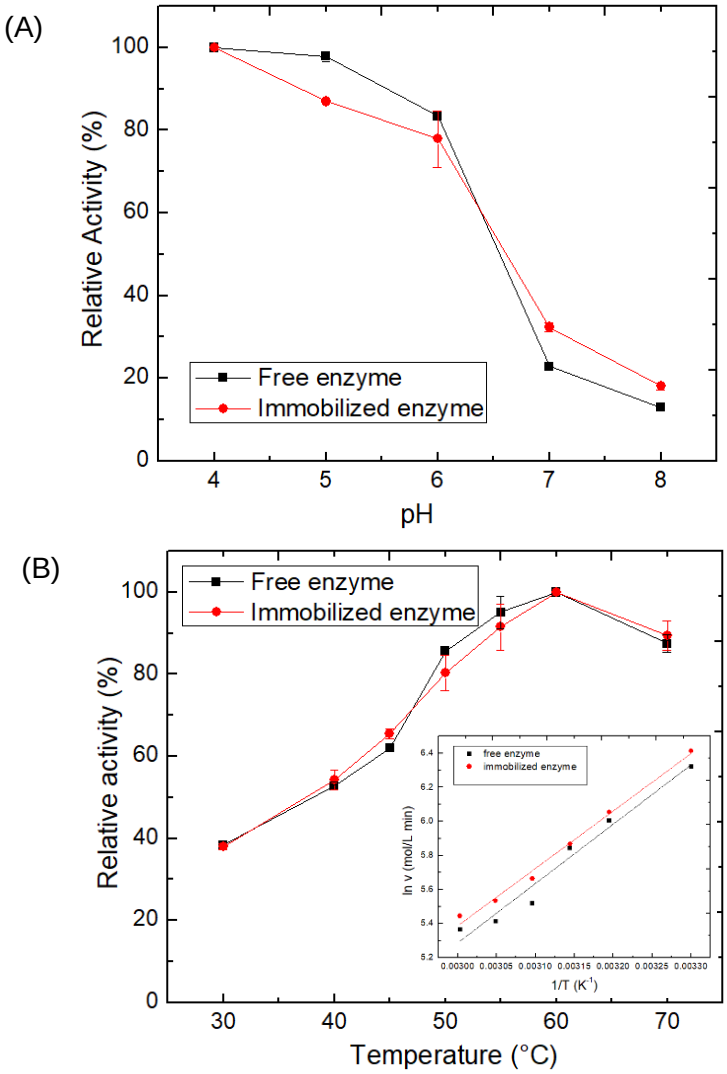

Fig. 4. Activity profiles according to (A) pH and (B) temperature for free and immobilized β-glucosidase. Relative activity calculated from averages of triplicates. Enzyme immobilized for 1 h at 25 °C and pH 4 (in 20 mM sodium acetate buffer).

In the case of the temperature activity profile, the immobilization did not alter the activation energy (*Ea*) of the enzyme for cellobiose hydrolysis, as determined from the Arrhenius plot (Fig. 4B), with values of 28.94 kJ/mol for the free enzyme and 28.02 kJ/mol for the immobilized enzyme. The similarity of the *Ea* values suggested that the limiting step for biocatalysis was the same for the free and immobilized enzyme. In other words, the energy required to reach the transition state of the substrate at the active site of the enzyme was the same for both free and immobilized enzyme. This finding was in agreement with previous work by Karboune *et al.* (2005), who obtained similar *Ea* values for free and immobilized epoxide hydrolase (35.4 and

38.8 kJ/mol, respectively) when ionic adsorption was used for the immobilization. These results suggest that enzyme immobilization by adsorption does not usually have any major impact on the activity profile, within a certain temperature range.

3.4 Investigation of the type of interaction between β-glucosidase and HA

The adsorption method of enzyme immobilization has the advantages of being inexpensive and chemically simple, since no reagents are required and the process involves only a minimum number of steps (Mohamad *et al.*, 2015). Additionally, the enzyme is less likely to be denatured during the immobilization process, compared with other methods such as covalent binding. The possible binding forces that can be involved in adsorption of β-glucosidase onto HA are ionic bonds and/or coordinate bonds, together with possible contributions from weaker interactions such as hydrogen bonds and Van der Waal's forces. The hydroxyapatite structure includes phosphate, hydroxyl, and calcium groups that are available for ionic interactions with the charged side groups of proteins (Kollath *et al.*, 2015). However, this type of interaction was unlikely to have predominated, because the enzyme was able to interact chemically with the support, even under high ionic strength conditions (Fig. 3B). Therefore, further experiments were carried out in order to investigate the nature of the interaction between the β-glucosidase enzyme and the HA.

3.4.1 Characterization of the derivative by FT-IR

FT-IR spectroscopy was used to investigate the surface functional groups present on the hydroxyapatite structure and the binding of β-glucosidase onto HA. The FT-IR spectra of hydroxyapatite with and without immobilized β-glucosidase are shown in Fig. 5A, with indication of the absorption bands corresponding to the hydroxyl and phosphate groups (Wu *et al.*, 2010) present in the hydroxyapatite molecule ($Ca_{10}(PO_4)_6(OH)_2$). The expanded FT-IR spectra (Fig. 5B) showed characteristic bands at 1549 cm^{-1}, attributed to absorbance by the amino groups of the enzyme. The intensities of the amino bands increased according to the amount of immobilized enzyme (from 4 to 16%), whereas no band in this region was observed for hydroxyapatite alone. In addition, the FT-IR spectra showed a strong band at 1650 cm^{-1}, corresponding to symmetrical C=O stretching absorption, indicating the presence of an essential bond in the carboxylic acids of amino acids. These results reflected the successful immobilization of β-glucosidase onto the HA nanoparticles. Agrawal *et al.* (2016) also confirmed the immobilization of β-glucosidase (onto SiO_2 nanoparticles) by the analysis of FT-IR spectra, with the presence of bands at 1550 and 1650 cm^{-1} attributed to N-H and C=O stretching vibrations, respectively.

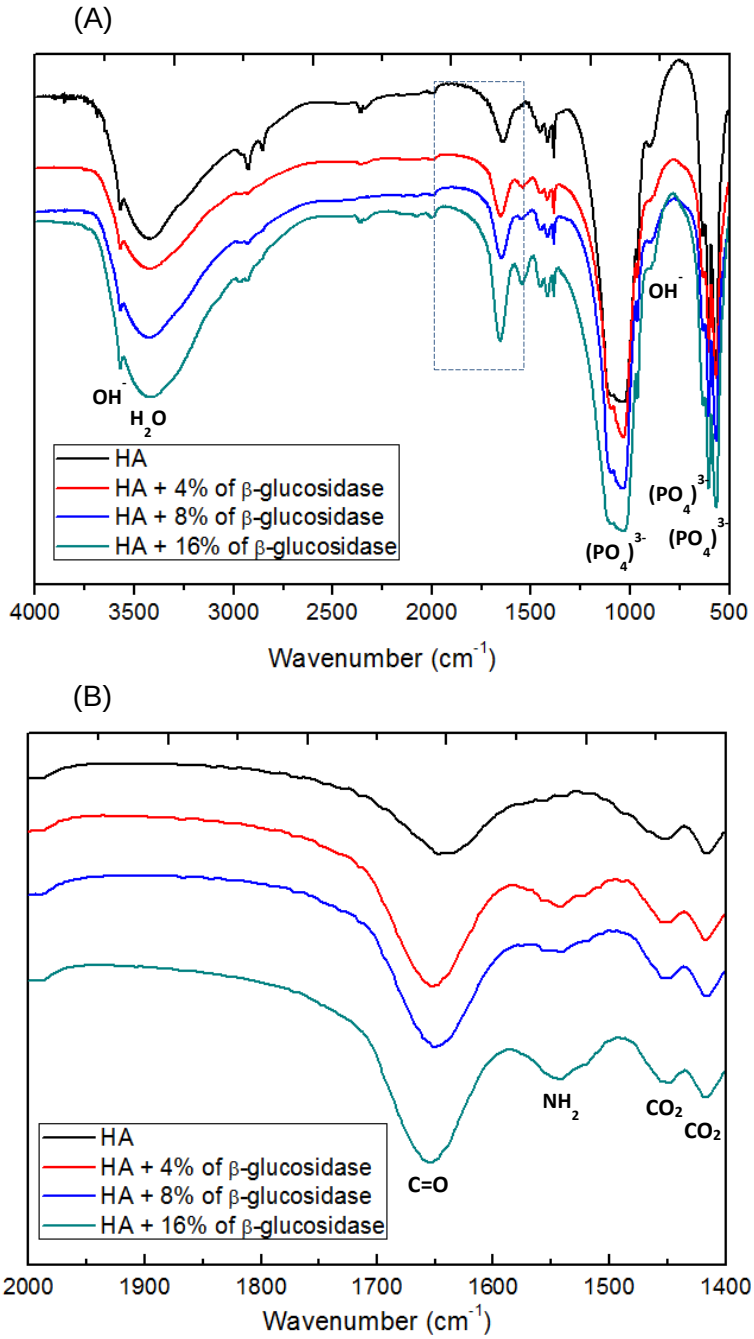

Fig. 5. FT-IR spectra of hydroxyapatite (HA) with and without immobilized β-glucosidase, showing (A) the entire region, indicating the functional groups of HA, and (B) the region containing functional groups of the enzyme.

Although much less intense, the absorption band at 1650 cm^{-1} was also observed in the spectrum of hydroxyapatite without the enzyme, possibly corresponding to the presence of atmospheric CO_2 in the nanoparticles. Similarly, bands at 1421 and 1458 cm^{-1} corresponded to the presence of C=O in the nanoparticles (Rehman and Bonfield, 1997) and could also indicate

the absorption of CO_2 from the air by the nanoparticles, since the signals did not increase when the concentration of β-glucosidase in the support was increased from 4 to 16%. The band corresponding to the C=O bond (1650 cm^{-1}) of the amino acids became slightly more intense as the enzyme concentration increased. The fact that the intensity of this band (1650 cm^{-1}) did not increase more strongly suggested that some of the carboxylic acids of the amino acid residues of the enzyme could have interacted with the support, hence providing further evidence of the immobilization of β-glucosidase on HA.

3.4.2 Characterization of the derivative using zeta potential measurements

The surface charges of the free enzyme and the support with and without enzyme were investigated using zeta potential determinations (Fig. 6). The HA nanoparticles showed negative potentials in the pH range 2-10, which decreased as the pH increased, with an isoelectric point of 2.3. The variations in zeta potential are probably caused by differences in the surface conditions of the particles, as well as interactions involving other particles and ions in the solution (Puvvada *et al.*, 2010). For this reason, the nanoparticles containing immobilized enzyme had the zeta potential measured. They showed a potential slightly more negative than nanoparticles alone (although presented the same isoelectric point). This finding was suggestive of interaction of the enzyme with the positive Ca^{2+} sites of the support. However, it is important to note that the loading of enzyme on the carrier (1%) was probably too small to cause a greater change in the potential, with only some of the positive charges of the support being neutralized by the enzyme.

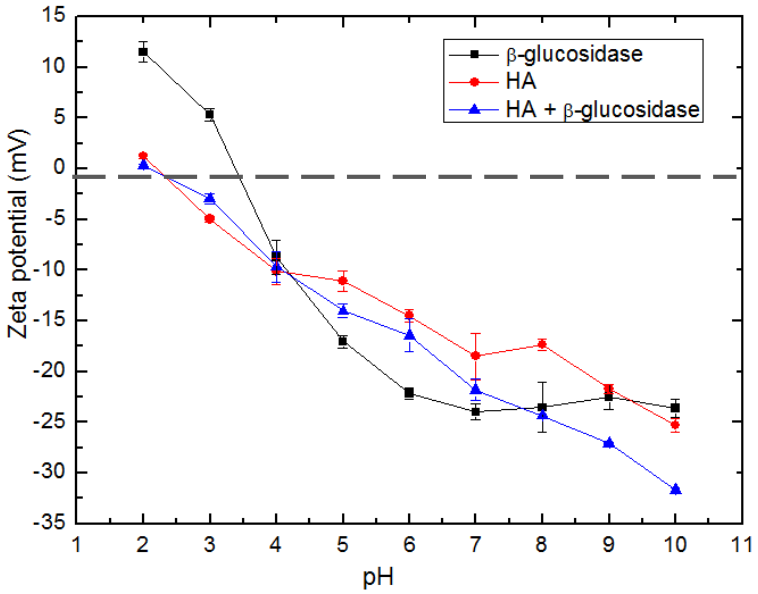

Fig. 6. Zeta potentials of β-glucosidase and the HA support (with and without enzyme).

It can be seen from Fig. 6 that at pH 4 (the pH used for immobilization) the enzyme and the hydroxyapatite had the same potential (approximately -10 mV). The negative charges of β-glucosidase derived from the deprotonated carboxylic acids would repel the negative charges of the support (phosphate and hydroxyl groups), hence inhibiting ionic interactions in the immobilization process. At the same time, the repulsion between the charges did not prevent binding of the enzyme to the support by means of other types of interactions.

3.4.3 Evaluation of enzyme desorption from the support

Unless covalent interaction occurs, some types of reversible chemical bonding between the enzyme and the support may be undone in the presence of substances (such as ions or complexation agents) that are able to compete with the enzyme for the active sites of the support (Jesionowski *et al.*, 2014). In this step of the study, desorption was performed with different sodium salts to evaluate the detachment of β-glucosidase from the HA nanoparticles. As can be seen in Fig. 7, solutions of sodium chloride and sodium acetate were unable to desorb the enzyme from the carrier, even at high concentrations (up to 400 mM). These observations were indicative of the non-prevalence of ionic interactions that could be undone in the presence of these salts at high concentrations. In contrast, Vieira *et al.* (2011) found that an ionic strength of 200 mM (NaCl) was sufficient to desorb all the β-glucosidase ionically adsorbed on a polyethylenimine-agarose support. The strong physical adsorption of the β-glucosidase enzyme onto HA has important industrial implications, since the enzyme might not easily leach from the support under the reaction conditions.

In contrast to the desorption tests with sodium chloride and sodium acetate, the enzyme was not resistant to even low concentrations of sodium citrate, with relative desorbed activity values reaching 100% for almost the entire salt concentration range (Fig. 7). Considering that the citrate salt has three carboxylic acid moieties, while sodium acetate has only one, this finding provided strong evidence that the COO^- site of the enzyme was crucial for interaction with the HA nanoparticles. The influence of these carboxylic acids could be attributed to the attraction of the polar groups to the Ca^{2+} ions of the HA nanoparticles, resulting in a type of coordination reaction. The Ca^{2+} ions act as hard acids that coordinate stably with hard bases such as the oxygen atoms of carboxylic acids (Bresolin *et al.*, 2009).

The β-glucosidase enzyme exhibits more negative amino acid residues, as demonstrated by the zeta potential of the enzyme, than positive residues such as lysine (Borges *et al.*, 2014; Vieira *et al.*, 2011). These negative groups correspond mainly to aspartate and glutamate, accounting for 12.8% and 9.9% of the total enzyme, respectively whereas lysine contributes only 3.8% (Yu *et al.*, 2004). Therefore, the immobilization method employed here was favored by the high presence of deprotonated carboxylic acids (COO^-) on the surface of the enzyme, which were available to interact with the Ca^{2+} ions of the support.

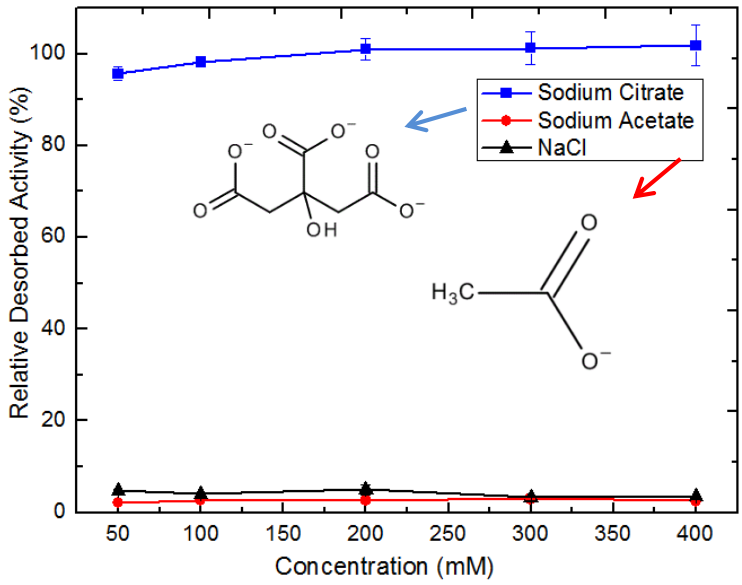

Fig. 7. Profiles of desorption of β-glucosidase from the HA support for suspensions placed in contact with different salt solutions for 40 min. The enzyme was immobilized at pH 4 (in 20 mM sodium acetate buffer).

Ivic *et al.* (2016a) demonstrated the same interaction during immobilization of lipase on hydroxyapatite. One of the experiments performed by them to prove this interaction force was analogous to the desorption test used here. However, they attempted to immobilize (and not to desorb) the enzyme with a high concentration of chelating citrate ions, which masked the available Ca^{2+} of HA by interacting with the metals by means of coordination bonds. This experiment resulted in an IY for lipase on HA that was much lower than the immobilization process performed without chelating citrate. Another similarity found in the two studies was a rapid immobilization time, with 90% IY obtained in 10 min in the present work (Fig. 2), while Ivic *et al.* (2016b) achieved 70% IY in 10 min. These results showed that the coordination bonds between COO^- and Ca^{2+} led to high binding affinity of the enzyme to the HA matrix.

Proteins can be adsorbed by coordination bonds established with the remaining sites of the chelated metal ions on the surface of a matrix. This type of chemical interaction has been widely used for protein purification using the method known as immobilized metal ion affinity chromatography (IMAC) (Farinas *et al.*, 2007; Bresolin *et al.*, 2009). In the present study, the Ca^{2+} metal ion was not chelated by a complexing agent, because the metal was already part of the crystal structure of hydroxyapatite. The high stability of the complex formed could be the result of formation of a ring structure, resembling a chelation reaction. Other forces can also be involved, such as electrostatic forces between charged groups, van der Waals forces, and

hydrogen bonds with OH^- groups of hydroxyapatite, although it is difficult to determine their relative contributions (Bresolin *et al.*, 2009).

3.5 Effect of enzymatic loading on immobilization efficiency

Considering the high immobilization yield (90%) obtained for the initial enzymatic load offered (10 mg protein g^{-1} support), investigation was made of the effect on immobilization efficiency of using an enzyme loading up to 5-fold higher. The IY remained high for all the loads offered (Table 1), indicating a linear increase in the concentration of immobilized enzyme. However, the recovered activity decreased with increase of the immobilized enzyme concentration (data not showed), which could be explained by greater diffusional limitation as more enzyme molecules were immobilized adjacent to each other, consequently blocking the active sites of the enzyme.

Table 1. Immobilization parameters obtained using different β-glucosidase loadings offered to the HA support.

Parameters	Enzyme offered (mg protein g^{-1} support)				
	10	20	30	40	50
IY (%)	90 ± 0	90 ± 0	87 ± 1	82 ± 2	65 ± 5
Enzyme immobilized (mg protein g^{-1} support)	9.0 ± 0	18.0 ± 0	26.1 ± 0.3	32.8 ± 0.7	32.5 ± 2.5

Zhang *et al.* (2015) immobilized 120 mg β-glucosidase g^{-1} support (functionalized magnetic nanospheres) and obtained RA of 87%. Although the results were promising, the IY was only 14%, so 86% of the enzyme offered during the immobilization process would need to be re-immobilized, so as not to be lost. Others studies of immobilization of β-glucosidase on different nanoparticles have used lower enzyme loadings. For example, Celik *et al.* (2016) obtained 27% IY with a loading of 20 mg enzyme g^{-1} support (chitosan-multiwalled carbon nanotubes), with 5.4 mg protein g^{-1} support being covalently attached to the support. Javed *et al.* (2016) obtained an entrapment efficiency of around 2 mg protein g^{-1} support for β-glucosidase immobilized in latex silicone and polyurethane matrices. Therefore, when compared to other nanometric materials, the surface area of the HA nanostructures was able to retain a substantial enzymatic loading per unit mass, highlighting its potential as a support for enzyme immobilization by a very simple adsorption method.

3.6 Hydrolysis of cellobiose substrate

β-Glucosidase is a key enzyme in the conversion of lignocellulosic biomass into soluble sugars, participating in the last step of cellulose hydrolysis by converting cellobiose into glucose (Zhang *et al.*, 2006). In order to evaluate the efficiency of conversion achieved using β-glucosidase immobilized on HA in such a reaction, the enzymatic suspension was used to catalyze the hydrolysis of cellobiose, with determination of the glucose released (Fig. 8). Hydrolysis was also performed using free β-glucosidase, as a control for the purposes of comparison. The two forms of the enzyme presented similar hydrolysis profiles, with glucose released of around 190 and 175 μmol mL^{-1} obtained for the free and immobilized enzyme, respectively. These results were consistent with the results shown in Fig. 3, since in a hypothetical application the immobilized enzyme would provide 90% of the conversion capacity of the free enzyme.

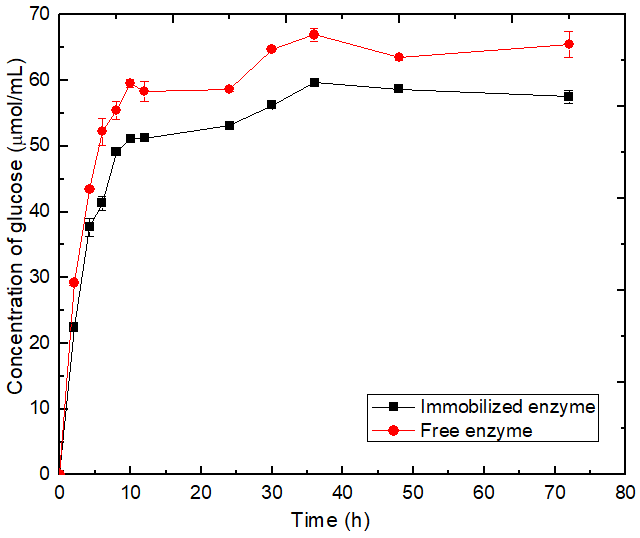

Fig. 8. Kinetics of glucose production by the free and immobilized enzyme. The reaction was performed with an enzyme loading of 40 U g^{-1} cellobiose, at 50 °C and pH 4.8.

Borges *et al.* (2014) performed the hydrolysis of cellobiose with β-glucosidase immobilized by ionic adsorption on polyacrylic resin (BG-PC) and by covalent interaction in glyoxyl agarose gel (BG-GA) under the same conditions (pH 4.8. 50 °C) but with a larger enzymatic loading (56 U g^{-1} cellobiose). Cellobiose conversions of around 97% and 90% were obtained using BG-PC and BG-GA, respectively, compared to use of the free enzyme. However, to obtain these results it was necessary several experimental procedures to chemically activate the support and/or modify the enzyme surface by amination. We can conclude that the great advantage of the method proposed in this work is that in addition to the high values obtained for the immobilization efficiency and enzymatic activity, it employs a very simple procedure for the

adsorption of β-glucosidase, with no requirement for chemical modifications of the support or the enzyme, together with a short adsorption time (less than 1 h).

3.7 Reusability of the immobilized enzyme

The reusability of immobilized β-glucosidase is an important consideration for industrial applications. The relative glucose production of the immobilized enzyme remained high up to the 10th hydrolysis cycle, when the value was around 70% of the initial production (Fig. 9). The decrease observed in the hydrolysis rate in the second cycle could possibly have been due to the mass loss of smaller particles after the first centrifugation cycle.

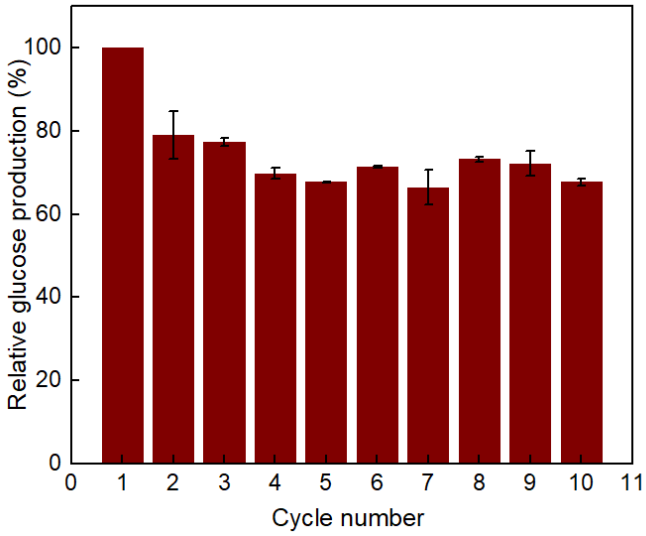

Fig. 9. Reusability of β-glucosidase immobilized at pH 4 (in 20 mM sodium acetate buffer). Each cycle of cellobiose hydrolysis was performed for 12 h at pH 4.8 and 50 °C, with an enzymatic loading of 40 U g^{-1} cellobiose.

In order to confirm the operational stability of the immobilized β-glucosidase under the process conditions, an additional stability assay was performed at pH 4.8 and 50 °C, in 50 mM sodium acetate buffer, measuring the activities of the derivative and the free enzyme every 2 h during a total period of 12 h. The results were in agreement with the recycling data, since no loss of enzyme activity was observed after 12 h, compared to the free enzyme (data not shown), indicating that the catalytic state of the β-glucosidase was maintained under process conditions.

Similar results (high residual activity after 10 or more cycles) have been obtained for β-glucosidase immobilized on other supports, but only when covalent binding was used (Agrawal *et al.*, 2016; Celik *et al.*, 2016; Javed *et al.*, 2016). The present findings demonstrated that the β-glucosidase/HA complex formed by means of coordination reactions was as stable as those

obtained employing strong chemical bonds, with the advantage of requiring only a very simple adsorption protocol.

4. Conclusions

The results of this work showed that β-glucosidase could be efficiently immobilized onto hydroxyapatite nanoparticles in a single adsorption step. The enzyme adsorption was accomplished by coordination bonds between remaining Ca^{2+} sites of HA and COO^- of amino acids. The immobilization process resulted in high-affinity interaction between the enzyme and the support over wide ranges of pH and ionic strength, with high enzyme binding capacity (around 32 mg protein g^{-1} support). The optimal immobilization conditions favorably resembled the optimal enzyme activity conditions, resulting in immobilization yield and recovered activity values of 90%. Furthermore, it was possible to recycle the immobilized β-glucosidase and retain 70% of the initial activity during at least 10 hydrolysis cycles. Therefore, the β-glucosidase was successfully immobilized on HA nanoparticles using a very simple adsorption protocol, showing excellent potential for applications in various industrial sectors.

5. References

Agrawal, R., Verma, A., Satlewal, A., 2016. Application of nanoparticle-immobilized thermostable beta-glucosidase for improving the sugarcane juice properties. Innovative Food Science & Emerging Technologies 33, 472-482.

Allouni, Z.E., Cimpan, M.R., Hol, P.J., Skodvin, T., Gjerdet, N.R., 2009. Agglomeration and sedimentation of TiO2 nanoparticles in cell culture medium. Colloids and Surfaces B-Biointerfaces 68, 83-87.

Andre, R., Paris, E., Gurgel, M., Rosa, I., Paiva-Santos, C., Li, M., Varela, J., Longo, E., 2012. Structural evolution of Eu-doped hydroxyapatite nanorods monitored by photoluminescence emission. Journal of Alloys and Compounds 531, 50-54.

Barbosa, O., Torres, R., Ortiz, C., Berenguer-Murcia, A., Rodrigues, R.C., Fernandez-Lafuente, R., 2013. Heterofunctional Supports in Enzyme Immobilization: From Traditional Immobilization Protocols to Opportunities in Tuning Enzyme Properties. Biomacromolecules 14, 2433-2462.

Borges, D., Baraldo, A., Farinas, C., Giordano, R., Tardioli, P., 2014. Enhanced saccharification of sugarcane bagasse using soluble cellulase supplemented with immobilized beta-glucosidase. Bioresource Technology 167, 206-213.

Bresolin, I., Miranda, E., Bueno, S., 2009. Immobilized metal-ion affinity chromatography (imac) of biomolecules: fundamental aspects and technological applications. Quimica Nova 32, 1288-1296.

Celik, A., Dincer, A., Aydemir, T., 2016. Characterization of beta-glucosidase immobilized on chitosan-multiwalled carbon nanotubes (MWCNTS) and their application on tea extracts for aroma enhancement. International Journal of Biological Macromolecules 89, 406-414.

Chang, J., Lee, Y.S., Fang, S.J., Park, D.J., Choi, Y.L., 2013. Hydrolysis of isoflavone glycoside by immobilization of beta-glucosidase on a chitosan-carbon in two-phase system. International Journal of Biological Macromolecules 61, 465-470.

Chen, K.I., Yao, Y.J., Chen, H.J., Lo, Y.C., Yu, R.C., Cheng, K.C., 2016. Hydrolysis of isoflavone in black soy milk using cellulose bead as enzyme immobilizer. Journal of Food and Drug Analysis 24, 788-795.

Chen, Q., Cao, L., Wang, J., Zhao, H., Lin, H., Fan, Z., Dong, J., 2018. Improved cell adhesion and osteogenesis using a PLTGA (poly L-lactide, 1,3-trimethylene carbonate, and glycolide) terpolymer by gelatin-assisted hydroxyapatite immobilization for bone regeneration. Journal of Materials Chemistry B 6, 301-311.

Cipolatti, E., Silva, M., Klein, M., Feddern, V., Feltes, M., Oliveira, J., Ninow, J., de Oliveira, D., 2014. Current status and trends in enzymatic nanoimmobilization. Journal of Molecular Catalysis B-Enzymatic 99, 56-67.

Das, A., Jana, A., Paul, T., Halder, S., Ghosh, K., Maity, C., Das Mohapatra, P., Pati, B., Mondal, K., 2014. Thermodynamics and kinetic properties of halostable endoglucanase from Aspergillus fumigatus ABK9. Journal of Basic Microbiology 54, S142-S151.

Druzhinina, I., Kubicek, C., 2017. Genetic engineering of Trichoderma reesei cellulases and their production. Microbial Biotechnology 10, 1485-1499.

Farinas, C., Reis, P., Ferraz, H., Salim, V., Alves, T., 2007. Adsorption of myoglobin onto hydroxyapatite modified with metal ions. Adsorption Science & Technology 25, 717-727.

Farinas, C.S., Marconcini, J.M., Mattoso, L.H.C., 2018. Enzymatic Conversion of Sugarcane Lignocellulosic Biomass as a Platform for the Production of Ethanol, Enzymes and Nanocellulose. Journal of Renewable Materials 6, 203-216.

Ghose, T., 1987. Measurement of cellulase activities. Pure and Applied Chemistry 59, 257-268.

Gomez, J., Romero, M., Fernandez, T., Diez, E., 2012. Immobilization of beta-glucosidase in fixed bed reactor and evaluation of the enzymatic activity. Bioprocess and Biosystems Engineering 35, 1399-1405.

Gregg, S.J.S., K. S. W., 1982. *Adsorption, Surface Area and Porosity*. Academic Press,, London.

Hoarau, M., Badieyan, S., Marsh, E., 2017. Immobilized enzymes: understanding enzyme - surface interactions at the molecular level. Organic & Biomolecular Chemistry 15, 9539-9551.

Ivic, J., Dimitrijevic, A., Milosavic, N., Bezbradica, D., Drakulic, B., Jankulovic, M., Pavlovic, M., Rogniaux, H., Velickovic, D., 2016a. Assessment of the interacting mechanism between Candida rugosa lipases and hydroxyapatite and identification of the hydroxyapatite-binding sequence through proteomics and molecular modelling. Rsc Advances 6, 34818-34824.

Ivic, J., Velickovic, D., Dimitrijevic, A., Bezbradica, D., Dragacevic, V., Jankulovic, M., Milosavic, N., 2016b. Design of biocompatible immobilized Candida rugosa lipase with potential application in food industry. Journal of the Science of Food and Agriculture 96, 4281-4287.

Javed, M., Buthe, A., Rashid, M., Wang, P., 2016. Cost-efficient entrapment of beta-glucosidase in nanoscale latex and silicone polymeric thin films for use as stable biocatalysts. Food Chemistry 190, 1078-1085.

Jesionowski, T., Zdarta, J., Krajewska, B., 2014. Enzyme immobilization by adsorption: a review. Adsorption-Journal of the International Adsorption Society 20, 801-821.

Jorgensen, H., Pinelo, M., 2017. Enzyme recycling in lignocellulosic biorefineries. Biofuels Bioproducts & Biorefining-Biofpr 11, 150-167.

Karboune, S., Archelas, A., Furstoss, R., Baratti, J., 2005. Immobilization of epoxide hydrolase from Aspergillus niger onto DEAE-cellulose: enzymatic properties and application for the enantioselective resolution of a racemic epoxide. Journal of Molecular Catalysis B-Enzymatic 32, 175-183.

Klein-Marcuschamer, D., Oleskowicz-Popiel, P., Simmons, B., Blanch, H., 2012. The challenge of enzyme cost in the production of lignocellulosic biofuels. Biotechnology and Bioengineering 109, 1083-1087.

Kollath, V., Van den Broeck, F., Feher, K., Martins, J., Luyten, J., Traina, K., Mullens, S., Cloots, R., 2015. A Modular Approach To Study Protein Adsorption on Surface Modified Hydroxyapatite. Chemistry-a European Journal 21, 10497-10505.

Langston, J., Sheehy, N., Xu, F., 2006. Substrate specificity of Aspergillus oryzae family 3 beta-glucosidase. Biochimica Et Biophysica Acta-Proteins and Proteomics 1764, 972-978.

Liguori, R., Ventorino, V., Pepe, O., Faraco, V., 2016. Bioreactors for lignocellulose conversion into fermentable sugars for production of high added value products. Applied Microbiology and Biotechnology 100, 597-611.

Lima, M., Oliveira-Neto, M., Kadowaki, M., Rosseto, F., Prates, E., Squina, F., Leme, A., Skaf, M., Polikarpov, I., 2013. Aspergillus niger beta-Glucosidase Has a Cellulase-like Tadpole Molecular Shape Insights into glycoside hydrolase family 3 (gh3) beta-glucosidase structure and function. Journal of Biological Chemistry 288, 32991-33005.

Maicas, S., Mateo, J., 2005. Hydrolysis of terpenyl glycosides in grape juice and other fruit juices: a review. Applied Microbiology and Biotechnology 67, 322-335.

Mohamad, N., Marzuki, N., Buang, N., Huyop, F., Wahab, R., 2015. An overview of technologies for immobilization of enzymes and surface analysis techniques for immobilized enzymes. Biotechnology & Biotechnological Equipment 29, 205-220.

Mukhopadhyay, A., Dasgupta, A., Chattopadhyay, D., Chakrabarti, K., 2012. Improvement of thermostability and activity of pectate lyase in the presence of hydroxyapatite nanoparticles. Bioresource Technology 116, 348-354.

Muller, K.H., Motskin, M., Philpott, A.J., Routh, A.F., Shanahan, C.M., Duer, M.J., Skepper, J.N., 2014. The effect of particle agglomeration on the formation of a surface-connected compartment induced by hydroxyapatite nanoparticles in human monocyte-derived macrophages. Biomaterials 35, 1074-1088.

Pereira, S.C., Maehara, L., Machado, C.M.M., Farinas, C.S., 2015. 2G ethanol from the whole sugarcane lignocellulosic biomass. Biotechnology for Biofuels 8, 16.

Puri, M., Barrow, C., Verma, M., 2013. Enzyme immobilization on nanomaterials for biofuel production. Trends in Biotechnology 31, 215-216.

Puvvada, N., Panigrahi, P., Pathak, A., 2010. Room temperature synthesis of highly hemocompatible hydroxyapatite, study of their physical properties and spectroscopic correlation of particle size. Nanoscale 2, 2631-2638.

Randolph, T.W., Skerker, P.S., Blanch, H.W., Prausnitz, J.M., Clark, D.S., 1987. Effect of enzyme and substrate conformation on enzymatic-activity in a supercriticial fluid - kinetic and electron-spin-resonance studies. Abstracts of Papers of the American Chemical Society 194, 24-MBTD.

Rehman, I., Bonfield, W., 1997. Characterization of hydroxyapatite and carbonated apatite by photo acoustic FTIR spectroscopy. Journal of Materials Science-Materials in Medicine 8, 1-4.

Sadat-Shojai, M., Khorasani, M., Dinpanah-Khoshdargi, E., Jamshidi, A., 2013. Synthesis methods for nanosized hydroxyapatite with diverse structures. Acta Biomaterialia 9, 7591-7621.

Sheldon, R., van Pelt, S., 2013. Enzyme immobilisation in biocatalysis: why, what and how. Chemical Society Reviews 42, 6223-6235.

Shewale, J., 1982. Beta-glucosidase - its role in cellulase synthesis and hydrolysis of cellulose. International Journal of Biochemistry 14, 435-443.

Singhania, R., Patel, A., Sukumaran, R., Larroche, C., Pandey, A., 2013. Role and significance of beta-glucosidases in the hydrolysis of cellulose for bioethanol production. Bioresource Technology 127, 500-507.

Tardioli, P.W., Zanin, G.M., de Moraes, F.F., 2006. Characterization of Thermoanaerobacter cyclomaltodextrin glucanotransferase immobilized on glyoxyl-agarose. Enzyme and Microbial Technology 39, 1270-1278.

Tohamy, K.M., Mabrouk, M., Soliman, I.E., Beherei, H.H., Aboelnasr, M.A., 2018. Novel alginate/hydroxyethyl cellulose/hydroxyapatite composite scaffold for bone regeneration: In vitro cell viability and proliferation of human mesenchymal stem cells. International Journal of Biological Macromolecules 112, 448-460.

Vaghari, H., Jafarizadeh-Malmiri, H., Mohammadlou, M., Berenjian, A., Anarjan, N., Jafari, N., Nasiri, S., 2016. Application of magnetic nanoparticles in smart enzyme immobilization. Biotechnology Letters 38, 223-233.

Vaz, R., Moreira, L., Ferreira, E., 2016. An overview of holocellulose-degrading enzyme immobilization for use in bioethanol production. Journal of Molecular Catalysis B-Enzymatic 133, 127-135.

Vieira, M., Vieira, A., Zanin, G., Tardioli, P., Mateo, C., Guisan, J., 2011. beta-Glucosidase immobilized and stabilized on agarose matrix functionalized with distinct reactive groups. Journal of Molecular Catalysis B-Enzymatic 69, 47-53.

Wang, K., Zhou, C., Hong, Y., Zhang, X., 2012. A review of protein adsorption on bioceramics. Interface Focus 2, 259-277.

Wu, C., Huang, S., Tseng, T., Rao, Q., Lin, H., 2010. FT-IR and XRD investigations on sintered fluoridated hydroxyapatite composites. Journal of Molecular Structure 979, 72-76.

Xie, W., Zang, X., 2017. Covalent immobilization of lipase onto aminopropyl-functionalized hydroxyapatite-encapsulated-gamma-Fe2O3 nanoparticles: A magnetic biocatalyst for interesterification of soybean oil. Food Chemistry 227, 397-403.

Yang, G., Wei, Z., Sun, W., Cui, F., Wang, D., Yu, S., Zhou, Q., 2015. Purification and enzymatic characterization of membrane-bound D-gluconate dehydrogenase from Arthrobacter globiformis. Journal of Molecular Catalysis B-Enzymatic 113, 14-22.

Yu, X., Gao, Y.H., Chen, Z.F., 2004. Purification and characterization of an extracellular beta-glucosidase with high transglucosylation activity and stability from Aspergillus niger no. 5.1. Applied Biochemistry and Biotechnology 119, 229-240.

Zhang, W., Qiu, J., Feng, H., Zang, L., Sakai, E., 2015. Increase in stability of cellulase immobilized on functionalized magnetic nanospheres. Journal of Magnetism and Magnetic Materials 375, 117-123.

Zhang, Y., Himmel, M., Mielenz, J., 2006. Outlook for cellulase improvement: Screening and selection strategies. Biotechnology Advances 24, 452-481.

CHAPTER 3

Phytase Immobilization on hydroxyapatite nanoparticles

This chapter is an adapted version of the article "Phytase Immobilization on Hydroxyapatite Nanoparticles Improves Its Properties for Use in Animal" published in 2019 in the journal Applied Biochemistry and Biotechnology, volume 190, pages 270-292.

Graphical Abstract

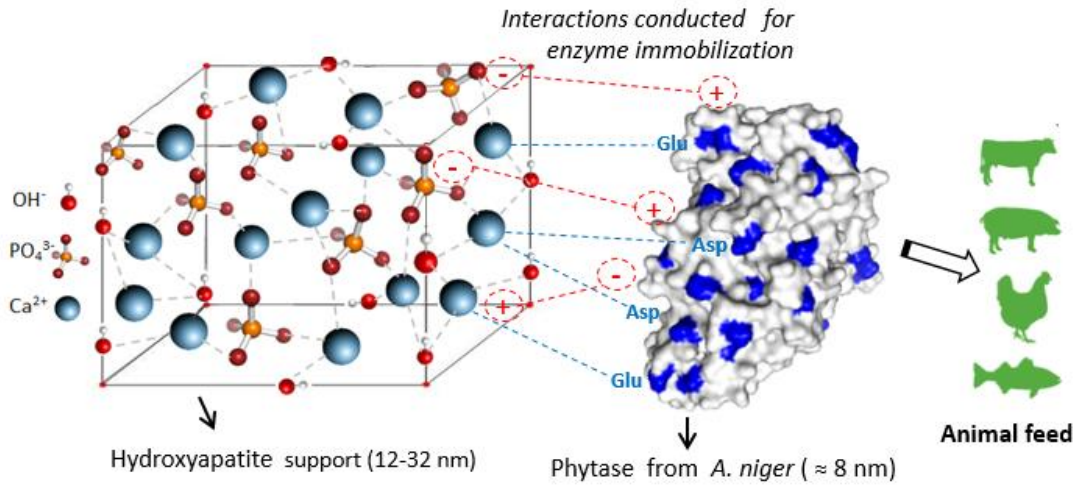

Abstract

The enzyme phytase has important applications in animal feed, because it favors the bioavailability of phosphorus present in phytate, an antinutritional compound widely found associated with plant proteins. However, for feed applications, the phytase must withstand high temperatures during the feed pelleting process, as well as the gastrointestinal conditions of the animal. This work evaluates the feasibility of immobilizing phytase on hydroxyapatite (HA) nanoparticles, in order to improve the properties of the enzyme for use in animal feed. HA is a material with excellent physicochemical characteristics for enzyme immobilization and it can also act as an inorganic source of phosphorus and calcium in animal feed. The strong affinity of the phytase for the support resulted in rapid adsorption (within 10 min, at 25 °C), with total immobilization yield and recovered activity greater than 100%. After immobilization, the phytase showed a broader activity profile in terms of pH and temperature, together with considerably higher thermoresistance at 80 and 90 °C. The results indicated that the adsorption of phytase involved coordination bonds between Ca^{2+} sites of the HA and COO^- of amino acids of the enzyme, complemented by electrostatic interactions between the charged groups of the enzyme and the support. As a proof of concept, it was shown that the phytase immobilized on HA presented behavior analogous to that of the free enzyme when passing through simulated gastrointestinal conditions of fish, demonstrating good resistance to acidic conditions and resistance to proteolysis. Furthermore, immobilized phytase showed similar kinetics of phosphorus release as the free enzyme, with 61% conversion of the phytate present in soybean meal, an ingredient widely used in animal feed. The findings showed that phytase immobilized onto HA presents suitable properties and has great potential for use in animal feed.

Keywords: Phytase, hydroxyapatite, immobilization, animal feed, enzyme.

1. Introduction

The enzyme phytase, also known as myo-inositol hexaphosphate phosphohydrolase, is specialized in releasing phosphate residues and myo-inositol from phytate (inositol hexakisphosphate), the main chemical form of phosphorus found in plants (Konietzny and Greiner, 2002). Several studies have investigated the application of phytase in areas such as agriculture (Trouillefou *et al.*, 2015), the food industry (Garcia-Mantrana *et al.*, 2016), and the pharmaceutical sector (Quan *et al.*, 2003). However, the most important industrial application of phytase is as a feed supplement for animals including poultry, pigs, and fish, which present very low levels of phytase in their gastrointestinal tracts (Jain *et al.*, 2016). The plant proteins used as ingredients in animal feed, such as those derived from crops of soybean, wheat, corn, and rice, are rich in phytate, which is considered an antinutritional factor (Viveros *et al.*, 2000). Phytate is a highly negative compound due to the presence of six phosphate groups, enabling it to form complexes with proteins, amino acids, and metals, hence compromising metabolism and the absorption of essential trace elements such as iron, zinc, and calcium (Cheryan, 1980). For these reasons, simple-stomached animals need phytase enzyme supplementation to prevent the deleterious effects of phytate and to improve phosphorus absorption. Associated with these effects, the enzyme can help to reduce the excessive concentrations of phosphorus in soils and the aquatic environment that contribute to the eutrophication of reservoirs (Cao *et al.*, 2007).

The predominant source of commercial phytase is from microorganisms, especially fungi genetically modified such as a strain of *Aspergillus niger* (Natuphos®), *Aspergillus oryzae* (Ronozyme®) and *Pichia pastoris* (Optiphos®) (Aquilina *et al.*, 2016; Rychen *et al.*, 2017a; Rychen *et al.*, 2017b). In the last two decades, several studies have shown the benefits provided to different animals by supplementing feed with the phytase enzyme (Cao *et al.*, 2007; Pontoppidan *et al.*, 2007). However, for use in feed, phytate-degrading enzymes must meet certain criteria, including high specific activity, broad pH stability, resistance to proteolysis, and good stability during storage, feed pelleting, and passage through the digestive tract (Konietzny and Greiner, 2002; Nielsen *et al.*, 2015). Among these criteria, the thermal instability of phytase is particularly problematic in commercial feeds, given that a large proportion of compound diets are currently extruded during the pelletizing process, which involves high temperature, pressure, and shear forces, consequently reducing the phytase activity (Cian *et al.*, 2018).

Approaches used to improve the thermal stability of phytase include identifying new thermoresistant phytases from different microbial sources (Zhang *et al.*, 2010), producing recombinant phytase using genetically modified micro-organisms (Ranjan *et al.*, 2015), promoting molecular changes by introducing substitute amino acid into the phytase molecule (Ushasree *et al.*, 2015), as well as immobilizing non-thermoresistant phytases using insoluble supports (Zhang and Xu, 2015; Harati *et al.*, 2017). The immobilization technique provides

greater resistance to denaturation when enzyme is exposed to high temperatures and may also improve the stability of phytase in gastric media with acidic pH and avoid degradation by proteases. Previous studies have reported the immobilization of phytase using various methods and supports, based on covalent interaction (Dutta *et al.*, 2017; Harati *et al.*, 2017), electrostatic adsorption (Cho *et al.*, 2011), crosslinked enzyme aggregates (CLEA) (Tirunagari *et al.*, 2018), and encapsulation (Zhang and Xu, 2015). However, most of these immobilization methods require chemical modifications of the support and/or the enzyme, as well as laborious procedures. Therefore, it remains a challenge to find a support that presents the specific characteristics required for efficient phytase immobilization using a simple and rapid method. Furthermore, the support should be nontoxic and be able to be incorporated into animal feed at a competitive cost.

Hydroxyapatite (HA) is an inorganic solid material with excellent physico-chemical properties for enzyme immobilization (Yewle *et al.*, 2012). It is a nontoxic calcium phosphate salt with the chemical composition $Ca_{10}(PO_4)_6(OH)_2$, which can be synthesized in the form of nanoparticles (Qi *et al.*, 2017). Nanomaterials provide a high surface area for enzymatic loading and low resistance for mass transfer of the substrate to the catalyst (Cipolatti *et al.*, 2014). The adsorption of proteins on HA nanoparticles has been investigated in different areas, especially in medicine, mainly due to interactions involving the phosphate and calcium groups of the HA, which are available for ionic adsorption involving the charged side groups of proteins (Farinas *et al.*, 2007; Lee *et al.*, 2012; Yewle *et al.*, 2012; Kollath *et al.*, 2015). The potential of HA nanoparticles as a support for enzyme immobilization is beginning to be exploited, with studies showing that besides ionic adsorption, HA can present covalent interactions after amino-functionalization, as well as chelation reactions involving carboxylic acid groups present in the amino acids of enzymes (Xie and Zang, 2017; Coutinho *et al.*, 2018). Recent reports have shown that chelation reactions between the calcium ions present in HA and the carboxylic acid groups of enzymes occur rapidly, resulting in highly stable and promising interactions for enzyme immobilization (Ivic *et al.*, 2016a; Coutinho *et al.*, 2018). Moreover, given the chemical composition of HA, its use as an enzyme support could also be considered as a source of Ca and P for animal nutrition. However, to the best of our knowledge, there have been no previous studies concerning the use of HA for the immobilization of phytase.

Therefore, the aim of the present work was to investigate the feasibility of immobilizing phytase on hydroxyapatite nanoparticles for use in animal feed. The binding of the enzyme to the support was analyzed by Fourier transform infrared (FT-IR) spectroscopy. The biochemical behavior of the interaction between the enzyme and the support was evaluated by varying the physicochemical conditions of immobilization and desorption of the enzyme. This systematic study enabled elucidation of the type of chemical interaction between phytase and HA. Evaluation was also made of the characteristics of the immobilized phytase, such as the pH and temperature of maximum activity, as well as its thermostability. The gastrointestinal conditions of fish were

simulated *in vitro*, in order to investigate the effect on the immobilized phytase. Finally, the immobilized phytase was applied in the hydrolysis of soybean meal, a component widely used in animal feed.

2. Materials and Methods

2.1 Materials

The phytase enzyme (Natuphos®) used in this work was produced commercially by a genetically modified strain of *Aspergillus niger* (Rychen *et al.*, 2017a) and was kindly donated by BASF S/A (Mount Olive, USA). The hydroxyapatite (HA) nanoparticles and the phytic acid sodium salt substrate were purchased from Sigma-Aldrich (St. Louis, USA). All other reagents were analytical grade.

2.2 Immobilization of phytase onto hydroxyapatite

Stock solutions of the phytase enzyme were prepared at a concentration of 0.1 g mL^{-1}, using the same pH, ionic strength, and buffer employed for each immobilization process. The enzyme solution was centrifuged for 10 min at 8000 rpm, in order to remove the solids present, mainly starch at about 82% (w/w) (Rychen *et al.*, 2017a). The protein content of the supernatant was determined colorimetrically at 595 nm, using the method of Bradford (1976), with bovine serum albumin as a protein standard. The hydroxyapatite suspension was prepared at a concentration of 0.05 g mL^{-1}, using an appropriate buffer for the pH and ionic strength described for each specific assay. The enzyme-support adsorption was carried out in 10 mL tubes, with an enzymatic loading of 5 mg protein g^{-1} support, under gentle rotary stirring for 1 h at 25 °C.

At the end of the immobilization process, the derivative (suspension of immobilized enzyme) was centrifuged for 2 min at 8000 rpm and the protein concentration in the supernatant was measured by the Bradford method. The protein concentration was also determined for the control (free enzyme). The immobilized enzyme was washed two times with the same buffer used for immobilization, in order to remove proteins that had not adsorbed on the support, which had the content determined. The enzymatic activity of the final derivative (A_{DE}) was measured in duplicate, as described in Section 2.3. The results were presented in terms of the immobilization parameters, which were calculated from the averages of the protein concentration and enzymatic activity measurements.

2.2.1 Calculation of immobilization parameters

The percentage immobilization yield (*IY*) was calculated using the equation:

$$IY\ (\%) = 1 - \frac{[P_{supernatant1}] + [P_{supernatant2}]}{[P_{control}]} \times 100\ ,$$

where $P_{supernatant1}$ and $P_{supernatant2}$ (mg mL^{-1}) are the protein concentrations for supernatant 1 (obtained after the first wash) and supernatant 2 (obtained after the second wash), respectively, and $P_{control}$ (mg mL^{-1}) is the protein concentration for the control (soluble enzyme). The enzymatic activity that was offered to the support (A_{Of}) was calculated using the equation:

$$A_{Of}\left(\frac{IU}{g\ support}\right) = \frac{A_{soluble\ enzyme} \times volume\ of\ enzyme\ offered\ (in\ mL)}{mass\ of\ support\ (in\ g)},$$

where $A_{soluble\ enzyme}$ (IU mL^{-1}) is the activity of the free enzyme. The theoretically immobilized activity (A_{TI}, in IU g^{-1} support) was obtained as the product of the activity offered to the support (A_{Of}) and IY × 100^{-1}. The recovered activity (*RA*) of the immobilized enzyme was calculated as follows:

$$RA\ (\%) = {}^{A_{DE}}/_{A_{TI}} \times 100,$$

where A_{DE} is the activity of the derivative (IU g^{-1} support).

2.3 Enzymatic activity assays

The enzymatic activities of the soluble and immobilized phytase were determined as described by Harland and Harland (1980), with modifications, by measuring the concentration of phosphorus released from the phytate substrate. The reaction consisted of mixing 50 µL of the suspension of immobilized phytase in 2.5 mL of the substrate solution (2.5 mM phytic acid sodium salt prepared in 100 mM sodium acetate buffer, at pH 5). The reaction mixture was allowed to react for 15 min at 37 °C, under rotary stirring, being that under these conditions the release of P from phytate was linear with time. The reaction was quenched by adding 200 µL of trichloroacetic acid (10%) to 400 µL of reaction mixture. The phosphorus released in the reaction was determined colorimetrically at 660 nm, after reaction for 30 s of a mixture of 200 µL of distilled water and 500 µL of Taussky reagent (Taussky and Shorr, 1953) in test tubes. One unit of enzymatic activity (IU) represented the amount of enzyme required to release 1 µmol of phosphorus per minute into the reaction mixture. The immobilization parameters were calculated as means ± standard deviations, with all the activity measurements performed in duplicate.

2.4 Characterization of the derivative by FT-IR

The enzyme functional groups involved in the binding to the HA support were analyzed by Fourier transform infrared spectroscopy (FTIR), using a Bruker Vertex 70 instrument. The samples (1 mg) were mixed with pre-dried FTIR-grade KBr (100 mg), followed by pressing into disks. The measurements were carried out in transmission mode, in the mid-infrared range (400-4000 cm^{-1}), at a resolution of 4 cm^{-1} (32 scans).

2.5 Effect of pH and ionic strength on the immobilization procedure

Selection of the conditions for the immobilization procedure employed adsorption assays at different pH values and ionic strengths, with an enzyme loading of 5 mg protein g^{-1} support and HA concentration of 0.05 mg mL^{-1}. In order to evaluate the effect of pH, the enzyme was immobilized at pH 4 and 5, using sodium acetate buffer, and at pH 6, 7, and 8, using sodium phosphate buffer, with the ionic strength set at 20 mM in all the assays. In order to evaluate the effect of ionic strength, enzyme adsorption was carried out at the selected pH value, in the presence of different concentrations of sodium chloride (20, 50, 100, 200, 400, and 800 mM). The experiments were performed in duplicate. The best pH and ionic strength for immobilization were considered to be the conditions that resulted in the highest values for immobilization yield (IY) and recovered activity (RA).

2.6 Effect of different salts on enzyme desorption

The ability of the immobilized phytase to be released from the support was evaluated by incubating the derivative in solutions of different sodium salts (chloride, acetate, and citrate) at increasing concentrations (50, 100, 200, 400, and 800 mM). A suspension of immobilized phytase was centrifuged at 8000 rpm for 2 min, after which the supernatant was discarded. An equal volume of ionic solution was added to the precipitate (derivative), followed by gentle stirring for 40 min. The protein concentration in the supernatant was then measured (in duplicate), using the Bradford method. The desorption assays were performed in duplicate at each ionic strength. The protein immobilized onto the HA was designated as 100%, while the protein contents obtained in the supernatants with different ionic strengths were calculated as the percentage of desorbed enzyme (%), relative to the immobilized protein.

2.7 Effect of pH and temperature on enzyme activity

The effect of pH on the activity of phytase (free and immobilized) was evaluated in the pH range 2-8, using glycine-HCl buffer (for pH 2, 2.5, and 3), sodium acetate buffer (for pH 4 and 5), sodium phosphate buffer (for pH 6), and Tris-HCl buffer (for pH 7 and 8), all at 100 mM and 37 °C. The effect of temperature on the activity of free and immobilized phytase was investigated at 20, 30, 40, 50, 55, and 60 °C, at pH 5 (using 100 mM sodium acetate buffer). The experiment was performed in duplicate. The activation energy (*Ea*) required for the hydrolysis was calculated for both forms of the enzyme, using Arrhenius plots (Tardioli *et al.*, 2006). The highest activity obtained in the temperature or pH ranges employed was designated as 100%, while the activities at all the remaining temperatures and pHs were calculated as the activity ($R_{lt}A$, in %) relative to that highest activity.

2.8 Thermostability of immobilized phytase

The thermostabilities of the free and immobilized phytase were determined by incubation for 3 h at temperatures of 60, 70, 80, and 90 °C, in 20 mM sodium acetate buffer (pH 5). At 15 min intervals, samples were withdrawn for determination of thermal denaturation by means of enzymatic activity measurements. The phytase activity was measured (in duplicate) at 37 °C and pH 5.0, as described in Section 2.3. Two replicates of each treatment were performed. The activity obtained at time zero was designated as 100% and the activities at all the remaining times were calculated as the activity (in %) relative to that highest activity. The two-parameter deactivation model developed by Sadana and Henley (1987) was fitted to the experimental data, in order to describe the deactivation kinetics. The expression describing the non-first order kinetic model is as follows:

$$Ract = (1 - \alpha) \times e^{-kt} + \alpha,$$

where *Ract* is the relative activity (ranging from 0 to 1), *t* is the time (in min), *k* is the deactivation rate coefficient (min^{-1}), and α is the ratio between the specific activities of the enzyme final state, E_f, and the enzyme initial state, E_0. The parameter α describes the level of enzymatic stabilization, while the parameter *k* describes the process of enzymatic deactivation. The two parameters were estimated using the Levenberg-Marquardt method of iterative convergence, at a 0.95 confidence level. The enzyme half-life ($t_{1/2}$) was then calculated using the fitted model.

2.9 *In vitro* simulation of gastric pH conditions of fish and proteolysis resistance

In order to mimic the conditions of the stomach and intestine of fishes, acidic and neutral solutions were employed in the assays, respectively. An adaptation of the methodology described by Rodriguez *et al.* (2018) was utilized to simulate the acid secretion of fishes. Firstly, 200 µL aliquots of free or immobilized phytase (at pH 5) were exposed to an abrupt pH drop, simulating the stomach conditions. The samples were immersed during 1 h in 2 mL of acid solutions with pH 3, 2.5, and 2, prepared using 100 mM glycine-HCl buffer. After acidic incubation, 500 µL of each sample were placed in 3 mL of 100 mM Tris-HCl buffer (pH 7) and incubated for a further 1 h, simulating the intestinal conditions. All the incubations were performed at 28 °C, which is the body temperature of some commercial fishes, such as the Nile tilapia (Moriarty, 1973). The control consisted of enzymes not exposed to acidic conditions, which were incubated for 2 h at pH 7 (100 mM Tris-HCl). The experiment was performed in duplicate. Finally, the phytase activity was assayed as described in Section 2.3, but using reaction conditions reflecting the environment of the intestines of some fishes (28 °C and pH 7).

The resistance of phytase to proteolysis was assessed as described by Zhang *et al.* (2010), with modifications. Pepsin hydrolysis occurred under simulated stomach conditions (glycine-HCl buffer, pH 2.5, 28 °C), while trypsin hydrolysis occurred under simulated intestinal conditions (Tris-HCl buffer, pH 7, 28 °C). The phytase:protease ratios evaluated were 2:1 and 10:1, with the

free and immobilized enzymes being incubated with the proteases for 2 h. The residual phytase activity was determined using the phytase assay described in Section 2.3.

2.10 Hydrolysis of soybean meal

Soybean meal, which is rich in phytate and is widely used in fish feed, was employed as the substrate for evaluation of the efficiency of conversion by the free and immobilized phytase. Soybean meal solutions (100 g L^{-1}), prepared in 100 mM sodium acetate buffer (pH 5), were hydrolyzed at 55 °C, under 30 rpm stirring, using the soluble and immobilized phytase at an enzyme loading of 25 U g^{-1} soybean meal (57 µg enzyme g^{-1} soybean meal). The phosphorus released during the course of the reaction was quantified as described in Section 2.3, until stabilization. The control consisted of phosphorus released by soybean meal without the presence of enzyme. The experiment was performed in duplicate and the results were presented as means ± standard deviations.

3. Results and Discussion

3.1 Immobilization of phytase onto HA nanoparticles

The immobilization of phytase onto HA was initially performed using an enzymatic loading of 5 mg protein g^{-1} support, with an immobilization solution prepared using 20 mM sodium acetate buffer (pH 5). All the enzyme was immobilized onto the HA nanoparticles (IY close to 100%) after only 10 min of reaction, indicating a high binding affinity of phytase towards the HA matrix (Fig. 1). A similar enzymatic loading (6.3 mg protein g^{-1} support) was obtained by Trouillefou *et al.* (2015) for the immobilization of *A. niger* phytase on mesoporous silica, although the adsorption was conducted for 10 h. This preliminary result demonstrated that phytase was efficiently immobilized onto hydroxyapatite nanoparticles by means of a very simple and fast adsorption protocol.

The HA nanoparticles used in this work were needle-shaped particles with a size range of 12-32 nm and surface area of 58.2 m^2 g^{-1} (Coutinho *et al.*, 2018) (FEG-SEM images are shown in the Fig.S2 of Supplementary Material). The deglycosylated phytase had a molecular weight of 48-52 kDa and unit cell dimensions (length in nm) of a = 7.1, b = 8.7, and c = 8.2 (Kostrewa *et al.*, 1997; Oakley, 2010). The cations exposed (Ca^{2+}) on the inorganic matrix will be able to establish ionic adsorption with negatively charged proteins, as well as chelation with the carboxylic acid side chains of Asp and Glu residues abundant on the phytase surface (Kostrewa *et al.*, 1997; Oakley, 2010), as illustrated in Fig. 2.

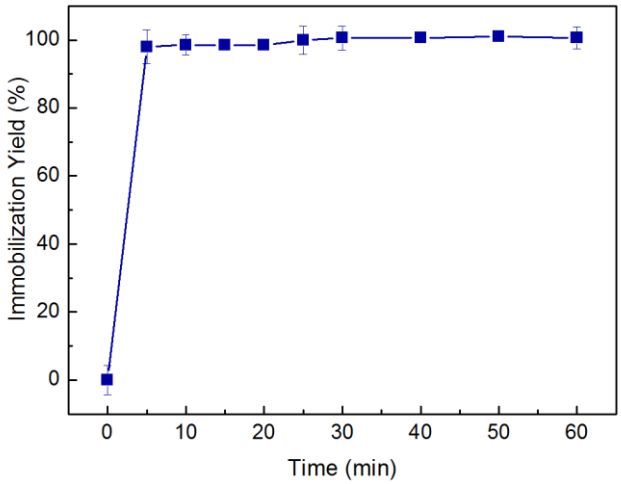

Fig. 1. Time course of immobilization of phytase onto HA nanoparticles at 25 °C and pH 5 (in 20 mM sodium acetate buffer), using an enzymatic loading of 5 mg protein g^{-1} support.

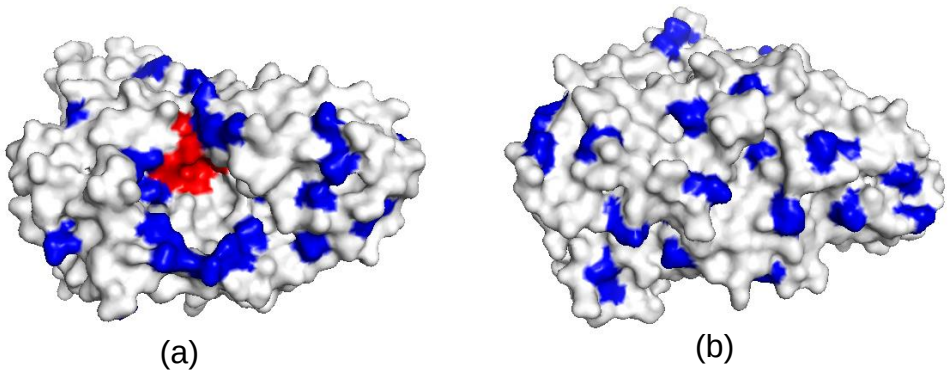

Fig. 2. Three-dimensional structure of *Aspergillus niger* phytase, constructed using the PyMOL program (PyMOL Molecular Graphics System; Version 2.1.0; Schrodinger, LLC.). The 3K4P structure from PDB has two chains in total (A and B). Here, only the chain surface mode is shown, where (a) is the active site side and (b) is the reverse side of the active site. Asp and Glu residues are highlighted in blue. Residues involved in the catalytic process (Arg58, His59, Arg62, Arg142, His338, and Asp339) are highlighted in red.

Furthermore, due to the particle size and surface area of the support, enzyme molecules were most likely to bind on the external surfaces of the HA nanoparticles, which would also contribute to minimizing diffusional limitations of the substrate during biocatalysis. Such diffusional limitation of substrate and products is commonly found for porous supports, as observed by Vandenberg *et al.* (2011) after encapsulation of phytase (Natuphos) using sodium alginate. The encapsulated phytase showed a reduction of its ability to release phosphorus (P) in the feeding of rainbow trout (*Oncorhynchus mykiss*), because the enzyme remained trapped within

the microcapsules in the gastric region of the fish intestine, resulting in reduced interaction between the enzyme and phytate. Therefore, the use of a support that minimizes problems with diffusional limitations, such as hydroxyapatite, is of great interest for immobilization of phytase.

The presence of surface functional groups and the binding of phytase onto hydroxyapatite were investigated by FT-IR spectroscopy. The spectra obtained for hydroxyapatite with and without immobilized phytase are illustrated in Fig. 3. Table 1 lists the absorption bands corresponding to the hydroxyl and phosphate groups present in the molecules of hydroxyapatite ($Ca_{10}(PO_4)_6(OH)_2$) (Wu *et al.*, 2010). The bands at 3572 and 3445 cm^{-1} could be attributed to OH^- groups of hydroxyapatite or to the vibration of water molecules adsorbed on the surface of sample (Wu *et al.*, 2010). Both of these bands became more intense with the presence of enzyme, due to the hydroxyl groups of amino acid residues such as serine, threonine, and tyrosine (Kumar *et al.*, 2016).

Table 1. Characteristic FT-IR bands for different functional groups present in the HA and the HA with immobilized phytase.

Functional group	Hydroxyapatite	Phytase enzyme
	Wavenumber (cm^{-1})	
$(PO_4)^{3-}$	1110; 1036; 962; 612; 574; 473	–
OH^-	3572; 3445; 646	3572; 3445
–CH	–	2869; 2953; 2934
C=O	1421; 1468; 1650	1421; 1468; 1650
N–H	–	1549

The vibrational bands observed at 2953, 2934, and 2869 cm^{-1} in the spectra for HA with enzyme (Fig. 3b) could be attributed to stretching of –CH associated with the side chains of amino acid residues, such as the alkane side chain of lysine (Kollath *et al.*, 2015; Swain and Sarkar, 2013). In Fig. 3c, the spectra show bands at 1650, 1421, and 1458 cm^{-1} for both forms of the HA support (with and without enzyme). These bands correspond to C=O stretching vibrations and might indicate the absorption of atmospheric CO_2 by the HA nanoparticles (Rehman and Bonfield, 1997) or the presence of a second $CaCO_3$ phase (Cipreste *et al.*, 2016). The spectrum for the support with immobilized enzyme showed greater intensity of the band at 1650 cm^{-1}, due

to C=O stretching vibration of amino acid residues such as asparagine and glutamine that possess amide functional groups (Kojima *et al.*, 2018). In addition, the greater intensities of bands at 1421 and 1458 cm^{-1} were due to the carboxylic acids of amino acid residues such as aspartate and glutamate (Agrawal *et al.*, 2016). A specific band at 1549 cm^{-1} in the spectrum for HA with immobilized phytase could be attributed to absorbance by the amino groups of the enzyme, as previously observed in the immobilization of β-glucosidase on HA nanoparticles (Coutinho *et al.*, 2018). These results indicate the successful immobilization of phytase onto the HA nanoparticles.

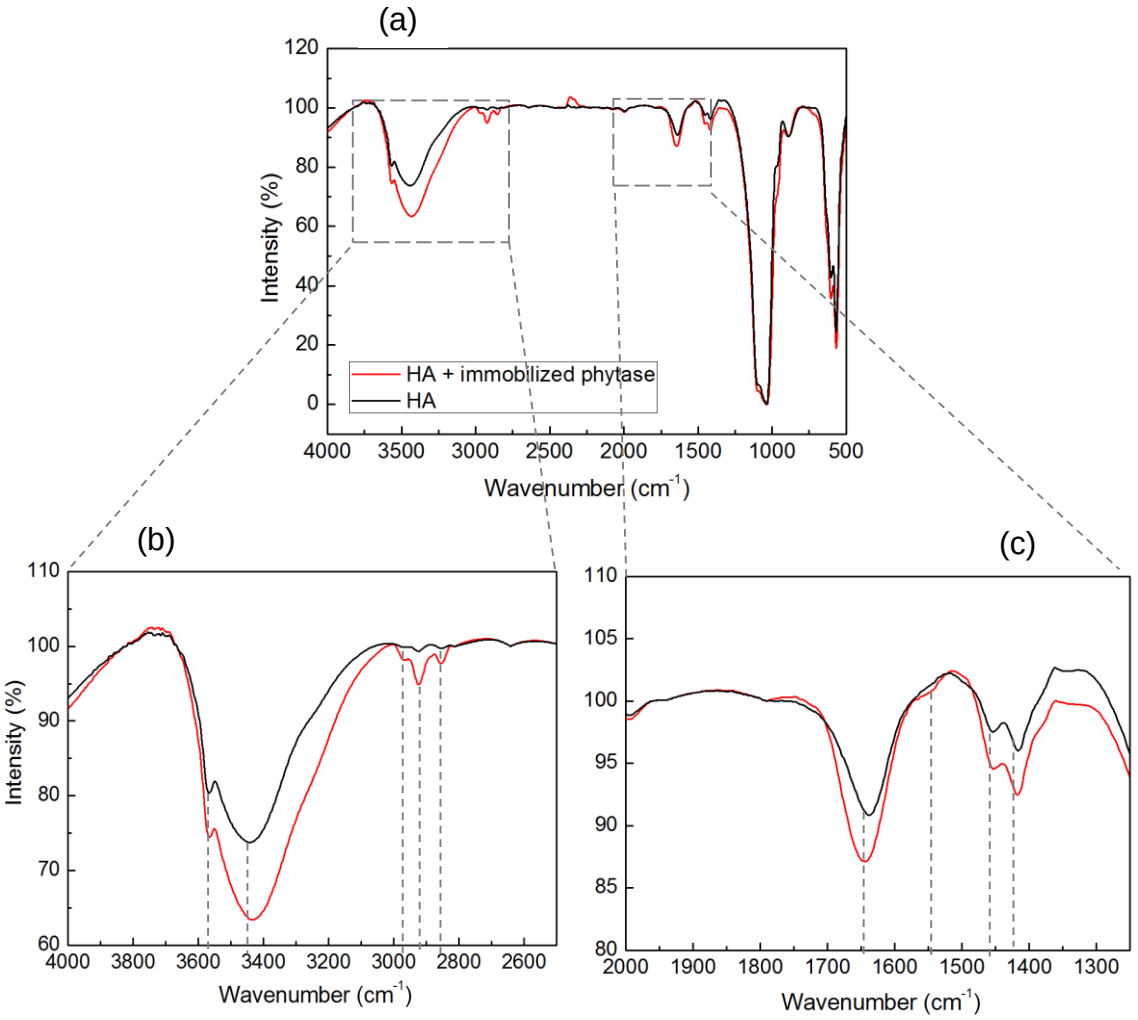

Fig. 3. FT-IR spectra of hydroxyapatite (HA) with and without immobilized phytase, showing (a) the entire region, indicating the functional groups of HA, and (b) (c) the region containing the functional groups of the enzyme. The enzyme loading was 5 mg protein g^{-1} support (0.5%).

3.2 Effect of pH and ionic strength on immobilization

Evaluation was made of the effect of pH and ionic strength on the immobilization yield (IY) and recovered activity (RA) of the phytase on the HA (Fig. 4).

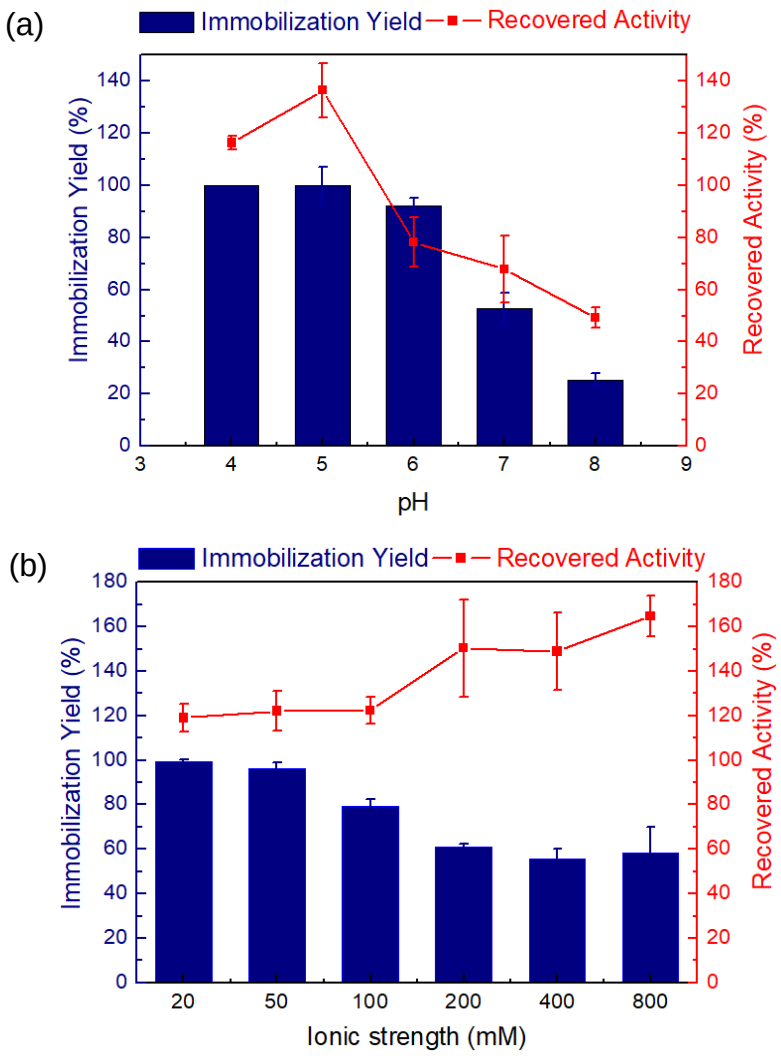

Fig. 4. Effects of (a) pH (at ionic strength of 20 mM) and (b) ionic strength (at pH 5) on the immobilization of phytase onto HA nanoparticles during 1 h at 25 °C. The immobilization yields and recovered activities were calculated from averages of duplicates.

Higher IY and RA were achieved at pH 5 (Fig. 4a), while decreases of these parameters were observed when pH above 6 was used during the immobilization process. An increase of pH causes deprotonation of some of the charged amino acid residues of the enzyme, with the protein consequently becoming increasingly negative. Phytase from *A. niger* (Natuphos®) has an isoelectric point (pI) of 4.5 (Ullah and Gibson, 1987), so the enzyme has predominantly negative charges at pH above 4.5. Hydroxyapatite has negative charges (in the pH 4-8 range evaluated), which become even more negative with increasing pH, as demonstrated by zeta potential analysis (Coutinho *et al.*, 2018). Therefore, the less acidic immobilization conditions generated repellency between the enzyme and the support, due to the negative charges of both, as reflected by the lower IY values obtained at pH 7 and 8. Swain and Sarkar (2013) adsorbed the BSA protein on HA

nanoparticles, as a model protein for the study of drug delivery. The BSA protein has pI 4.75 and it was released under the alkaline conditions of the organism (pH 7.4), indicating the low affinity of the enzyme for the HA matrix, under alkaline conditions.

Another interesting observation was that the enzyme adsorbed onto the support under less acidic conditions presented lower RA values, compared to the enzyme immobilized at more acidic pH. For example, at pH 8, the IY was 24% and the RA was 47% (Fig. 4a). A possible explanation for this is related to the different ways in which the enzyme could bind to the support at less acidic pH. For instance, the amino acid His59 is located at the active site of the phytase, in a favorable position to perform nucleophilic attack on the scissile phosphorous of phytate during the biocatalysis (Kostrewa *et al.*, 1997; Oakley, 2010). However, histidine side chains have pKR of 6.04, becoming deprotonated at pH 7 and 8 used for immobilization. Although determination of enzyme activity was performed under standard conditions (pH 5, 100 mM, and 37 °C), the conformation in which the enzyme bound to the support at pH 6, 7, and 8 may have prevented re-protonation of the His59 at the active site during the reaction at pH 5. It may even have caused distortion of the active site of the enzyme, consequently reducing the catalytic activity.

Evaluation of the effect of ionic strength on the immobilization of phytase on HA showed that the IY values decreased with increasing ionic strength (Fig. 4b). Nevertheless, at the highest ionic strength tested (800 mM), it was possible to immobilize around 60% of the enzyme offered to the support. The decrease of the IY with increasing ionic strength used in the immobilization indicated that electrostatic interactions contributed to the adsorption of the enzyme on the support. This showed that in the presence of a high ionic concentration in the adsorption solution, the enzyme and/or the HA nanoparticles preferentially interacted with the ions in solution, rather than with each other.

Although the IY decreased with increasing immobilization ionic strength, it was observed that the RA became higher at high ionic strengths, evidencing that the presence of a salt (NaCl) in the immobilization environment favored the activity of the enzyme. In other words, the presence of Na^+ ions remaining from the immobilization process could have stimulated phytase to degrade phytate. Many studies have evaluated the effect of metal ions on phytase activity, demonstrating both positive and deleterious effects of metals on the activities of different phytases (Rao *et al.*, 2009). Therefore, evaluation was made of the effects of the metals Na^+, Ca^{2+}, Zn^{2+}, Mg^{2+}, Mn^{2+}, and K^+ on the activities of the free and immobilized phytase (Table 2).

The objective was to investigate whether the presence of Na^+ in the reaction medium contributed to the activity of the enzyme, in order to explain the higher RA values obtained using higher ionic strengths (Fig. 4b), as well as to determine whether other metals might have a positive effect on phytase biocatalysis. The cations Na^+, Ca^{2+}, Mg^{2+}, and Mn^{2+}, at concentrations of 1 and 5 mM, favored the activity of phytase in both free and immobilized forms (Table 2). The results obtained for the effect of Na^+ corroborated the RA results shown in Fig. 4b, evidencing the

positive effect on enzyme activity of Na^+ remaining from the immobilization process. Besides demonstrating the contribution of Na^+ in the biocatalysis of phytase, the results indicated that the presence of other metals (Ca^{2+}, Mg^{2+}, and Mn^{2+}) in the reaction medium also favored enzyme activity. On the other hand, the presence of Zn^{2+} was highly deleterious to phytase, probably due to the low solubility of the product of complexation of this metal with phytate (Konietzny and Greiner, 2002), as reported previously by Soni *et al.* (2010) for phytase from *A. niger*.

Table 2. Effects of different metals, at concentrations of 1 and 5 mM, on the activities of the free and immobilized phytase.

Metal	Relative activity (%)	
	1 mM	5 mM
Free phytase		
None	100.0	100.0
K^+	88.9 ± 5.3	95.9 ± 13.1
Na^+	140.8 ± 13.7	137.8 ± 12.7
Mg^{2+}	140.9 ± 12.9	182.9 ± 18.4
Mn^{2+}	186.2 ± 10.7	202.2 ± 13.5
Ca^{2+}	209.1 ± 1.14	157.3 ± 9.8
Zn^{2+}	0.0	2.0 ± 0.0
Immobilized phytase		
None	100.0	100.0
K^+	100.0 ± 7.6	129.7 ± 16.7
Na^+	138.4 ± 2.7	178.4 ± 23.4
Mg^{2+}	161.9 ± 36.6	165.1 ± 21.6
Mn^{2+}	229.5 ± 50.9	206.7 ± 25.6
Ca^{2+}	151.6 ± 17.6	230.8 ± 33.3
Zn^{2+}	2.0 ± 0.0	0.0

Considering the immobilization pH and ionic strength conditions that were evaluated, the best conditions for adsorption of phytase on HA were pH 5 and ionic strength of 20 mM, which resulted in IY of 100% and RA greater than 100%. These conditions presented a higher enzymatic activity of derivative (2086 ± 41 IU × g^{-1} support) compared to the other conditions (for instance, at pH 5, 800 mM, the RA was 160%, but the enzymatic activity was 1324 ± 25 IU × g^{-1}). For these reasons and also in order to favor attraction between the enzyme and the support due to ionic interactions, an ionic strength of 20 mM was adopted in the adsorption protocol used in the following steps.

Regarding the improvement in phytase performance after the immobilization onto HA, two hypotheses could explain this fact. The first is that after being immobilized, the enzyme acquired a conformation that made its active site more available for phytate biotransformation. The second hypothesis is that in addition to acting as a support, the nanoparticles provided a source of calcium cofactor for the enzyme, since it has been shown that Ca^{2+} ions improve phytate conversion (Table 2). Studies have demonstrated that the use of HA in nanoparticle form (in the concentration range 2-10 µg/mL) as a calcium cofactor increased the thermostability and activity of enzymes such as cellulase and xylanase (Dutta *et al.*, 2014), as well as pectate lyase (Mukhopadhyay *et al.*, 2012). Other work reported a 2.4-fold increase in phytase activity when magnesium nanoparticles were added to the reaction mixture (Dutta *et al.*, 2017). These interesting observations about the effect of nanoparticles as sources of cofactors on enzyme activity support the notion that the increase in phytase activity following immobilization on HA could be closely related to the source of the calcium cofactor for the active site of the enzyme.

3.2.1 Desorption studies

Desorption of the enzyme from the support in the presence of certain substances can provide evidence about the type of interaction that occurs between the protein and the support, when covalent interactions are not present. Therefore, different sodium salts were tested as potential desorbing agents, in order to improve understanding of the mechanism of the phytase-HA interaction (Fig. 5).

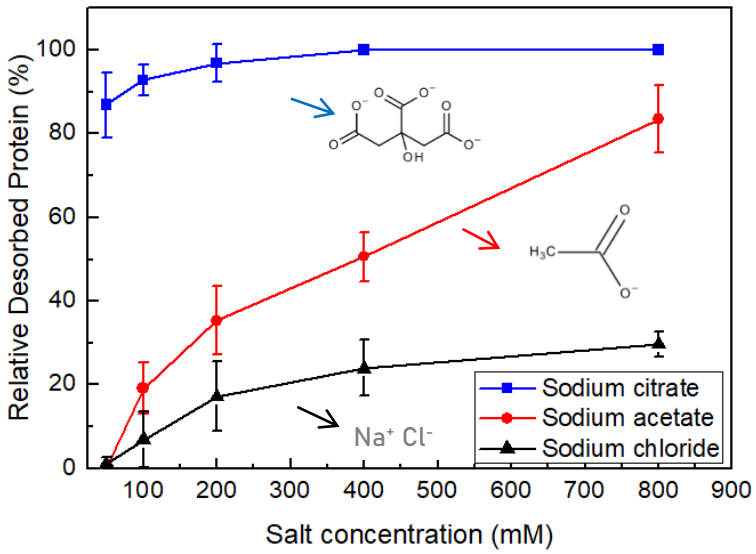

Fig. 5. Profiles of desorption of phytase from the HA support for suspensions placed in contact with different salt solutions for 40 min. The enzyme was immobilized at pH 5 (in 20 mM sodium acetate buffer). The relative desorbed activities were calculated from averages of duplicates.

For the sodium chloride and sodium acetate salts, desorption of the enzyme was dependent on the salt concentration in the medium, with the higher concentration (800 mM) of NaCl resulting in 30% removal of the enzyme from the support, while 800 mM of sodium acetate removed 84% of the enzyme. These results indicated that only high concentrations of these ions in solution were able to disrupt the ionic interactions that contributed to the binding of the enzyme to the support. It should also be noted that the effect of sodium acetate as a desorbing agent was greater than that of sodium chloride, probably due to the higher affinity of the support for the COO^- group of sodium acetate. This effect became more evident when 87% of the immobilized enzyme was leached from the HA using the lower concentration of the sodium citrate salt (50 mM), which possesses three carboxylic acid groups and was able to completely release the enzyme from the support.

The desorption results indicated the high affinity of the HA support for the COO^- groups, suggesting that the enzyme and the support interacted by means of metal coordination bonding between Ca^+ on the HA and the deprotonated carboxylic acid groups (COO^-) of the phytase amino acids. Other studies have evaluated the adsorption of amino acids and proteins on HA matrices for a variety of purposes, including drug delivery, chromatography columns, and bone regeneration. The main proposed interactions were electrostatic, due to the charged PO_4^{3-} and Ca^{2+} sites of the inorganic matrix (Lee *et al.*, 2012; Swain and Sarkar, 2013; Kollath *et al.*, 2015). At the same time, recent research has shown that in addition to ionic interactions, the acidic amino acids, such as glutamic and aspartic acids, may form coordination bonds with the exposed Ca^+ cations of HA in a bridging structure (Ivic *et al.*, 2016a; Lagazzo *et al.*, 2017; Coutinho *et al.*, 2018). As demonstrated in the present work, these studies also showed that citrate salts are retarding agents for the coordination between Ca^+ and COO^-.

The enzymes lipase and β-glucosidase that were previously immobilized onto HA by coordination interactions showed strong affinity with the support, which was attributed to the short time (less than 10 min) required for stabilization of the protein concentration in the supernatant during the immobilization process (Ivic *et al.*, 2016b; Coutinho *et al.*, 2018;). A very short immobilization time was also demonstrated for phytase (Fig. 1), evidencing the potential of the immobilization method proposed here. Despite the strong evidence of coordination interactions, other forces were probably involved in the phytase/HA interaction, especially electrostatic forces between charged groups, as demonstrated in the adsorption and desorption experiments. In addition, van der Waals forces and hydrogen bonds with hydroxyl groups of hydroxyapatite could have contributed to maintaining the stability of the enzyme attached to the support. It is important to note that the observed desorption behavior was for enzymes that were immobilized at pH 5 (using 20 mM acetate buffer), so the entire interpretation of the type of interaction was valid for these physicochemical adsorption conditions. Phytases immobilized on

HA nanoparticles using different pH, buffers, and ionic strength could present different chemical and/or physical interactions.

3.3 Effect of pH and temperature on enzyme activity

Evaluation was made of the effect of pH and temperature on the activity of the free and immobilized phytase (Fig. 6). The derivative was obtained under the best immobilization conditions identified (pH 5 and 20 mM sodium acetate).

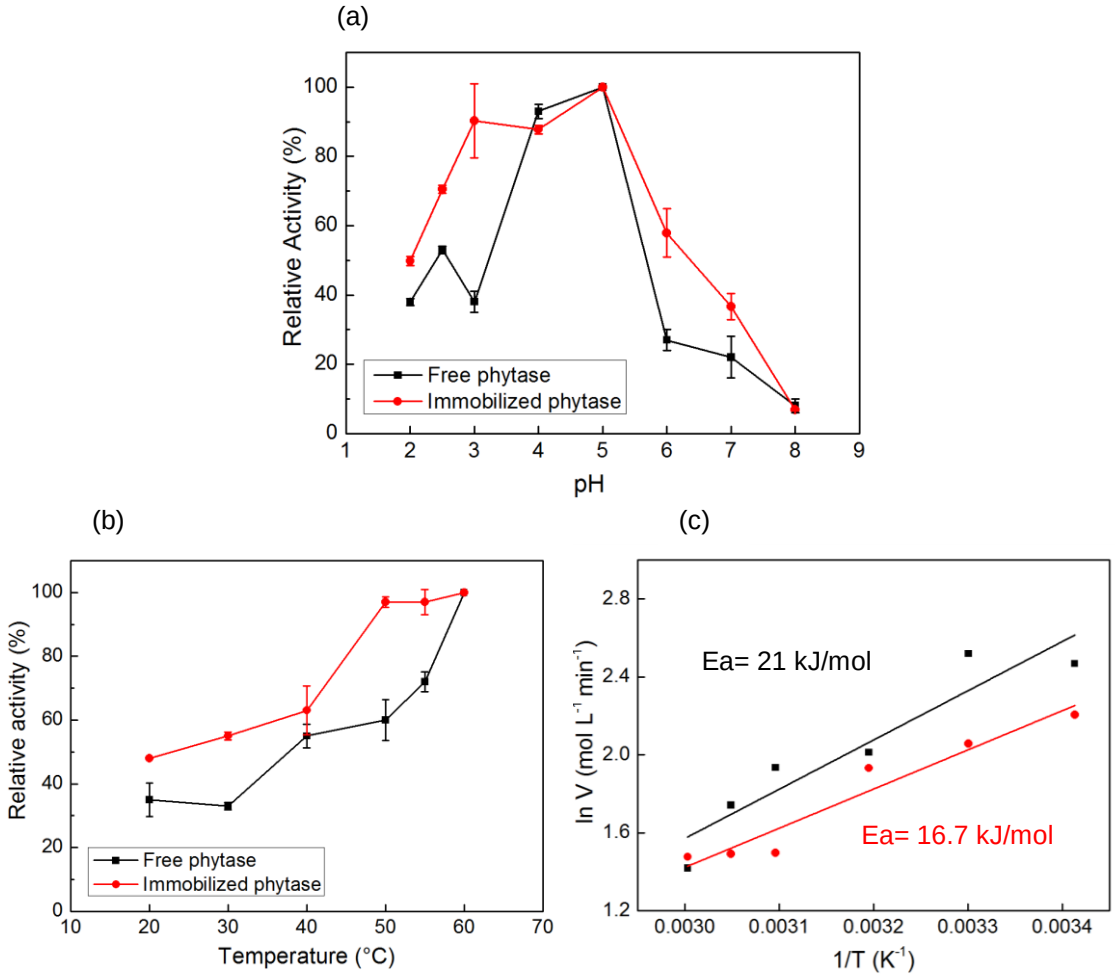

Fig. 6. Activity profiles according to (a) pH and (b) temperature for the free and immobilized phytase. The relative activities were calculated from averages of duplicates. The enzyme was immobilized for 1 h at 25 °C and pH 5 (in 20 mM sodium acetate buffer). (c) Arrhenius plots for calculating the activation energies (*Ea*) of the two forms of the enzyme.

The results showed somewhat broader pH and temperature profiles for the immobilized phytase, although the optimum pH (pH 5) (Fig. 6a) and temperature (60 °C) (Fig. 6b) values were very close for both enzyme forms. The optimum temperature (50-60 °C) and the two distinctive optimum pH values (pH 2.5 and 5-5.5) obtained for the free enzyme (Fig. 6a) are characteristic of the phytase from *A. niger* (Oakley, 2010; Ullah and Gibson, 1987). The lower activity values at pH 7 and 8 could have been because in this pH range, water molecules are tightly bound at positions equivalent to the oxygen atoms of the phosphate groups of phytate. The water molecules mimic the substrate/product and prevent substrate binding (Oakley, 2010), hence reducing the enzyme activity.

The optimal condition for phytase activity coincided with the best immobilization pH (pH 5, as shown in Fig. 4a), which represented a major advantage of the immobilization procedure employed here, since the enzyme could bind to the support in its best conformation for acting as a biocatalyst. It is interesting to note that the immobilized enzyme showed increases in relative activity from 40 to 90% at pH 3, and from 23 to 38% at pH 7, both being conditions that could be encountered by the enzyme in the gastrointestinal tracts of animals (Dersjant-Li *et al.*, 2015). The improvement in the activity of the immobilized enzyme at different reaction pH values could be explained by the immobilization method employed. The electrostatic potential of the microenvironment of enzymes immobilized on HA (which contains the ionized functional groups Ca^{+} and PO_4^{3-}) can affect the local concentration of H^{+}, influencing the behavior of the enzyme under different pH conditions.

The activity profiles at different temperatures showed that the immobilized phytase retained more activity throughout the tested temperature range, compared to free phytase (Fig. 6b). The increase in relative activity at different temperatures for the immobilized enzyme became more evident from the decrease in the activation energy (*Ea*) from 21 kJ/mol (for the free enzyme) to 16 kJ/mol (for the immobilized phytase) (Fig. 6c). In previous work, Dutta *et al.* (2017) observed a decrease from 24.3 kJ/mol to 9.7 kJ/mol for the *Ea* of *B. subtilis* phytase after immobilization on graphene oxide (GO) in the presence of Mg nanoparticles. It was reported that factors contributing to the decrease in *Ea* were covalent interactions by glutaraldehyde crosslinking during the immobilization process, as well as the presence of Mg nanoparticles that acted as cofactors for the enzyme. The findings of this earlier study and the present work indicated that the energy required to reach the transition state of the phytate at the active site of phytase could become lower for the immobilized enzyme, suggesting that changes in the conformational state of the enzyme after immobilization facilitated the reaction pathway. Furthermore, the presence of cofactors such as calcium and magnesium could have contributed to the decreased activation energy for biocatalysis.

3.4 Thermostability of the enzyme

The thermal stability of phytases is crucially important in animal feed applications, where the feed briefly reaches processing temperatures of 85–90°C during the step in which the enzymes are normally incorporated into the grains, prior to pelletization (Rao *et al.*, 2009). In order to investigate whether there was any improvement in the thermostability of the phytase after being immobilized onto the HA nanoparticles, the free and immobilized enzymes were kept at temperatures of 60, 70, 80, and 90 °C for 3 h, with periodic measurements of the activity under standard conditions (pH 5, 37 °C).

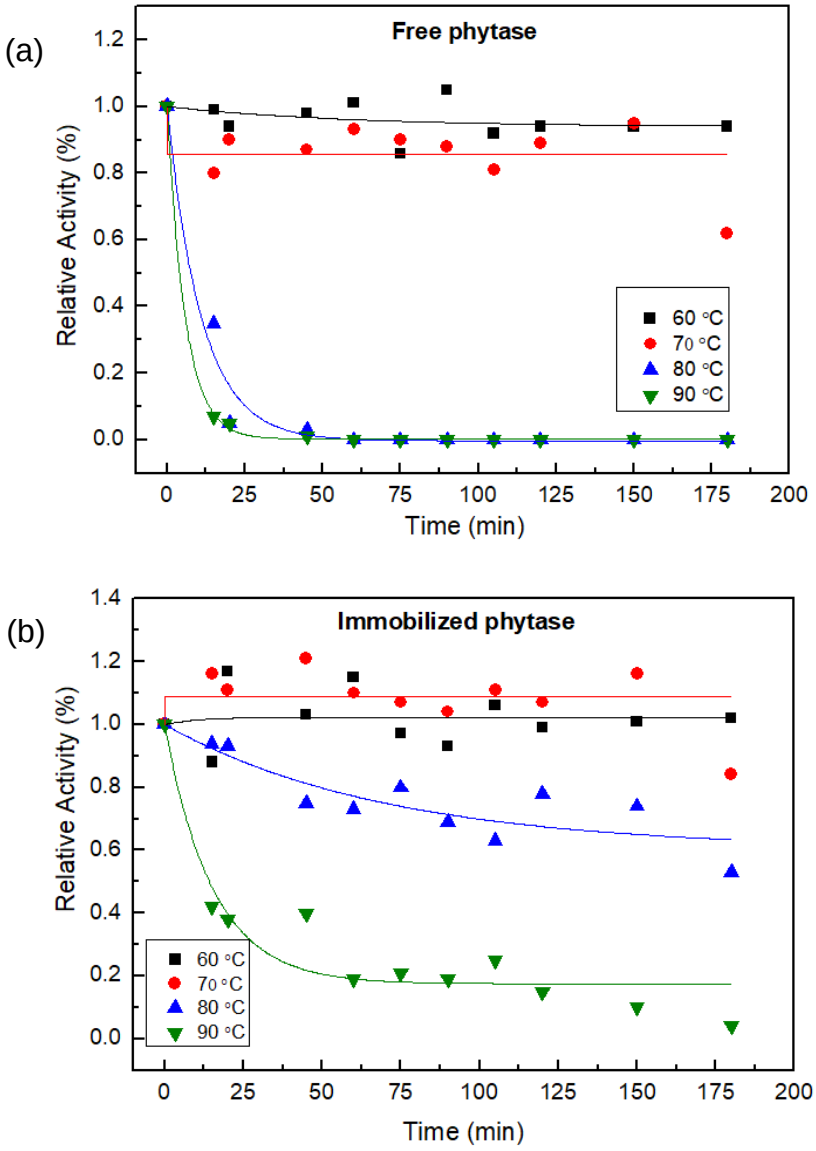

Fig. 7. Comparison of the thermostabilities of the free (a) and immobilized (b) phytase. The residual phytase activities were measured during incubation (in duplicate) at different temperatures. The experimental data were fitted using the model proposed by Sadana and Henley (1987).

As shown in Fig. 7, both the free and immobilized phytase proved to be stable at 60 and 70 °C, although the free enzyme showed a small decrease of relative activity after 3 h. Differently, at 80 and 90 °C, the denaturation process was irreversible for the soluble enzyme, since the free enzyme completely lost activity in 20 min. On the other hand, the immobilized phytase retained almost 60% of its activity after 3 h at 80 °C, while about 40% was retained after 20 min at 90 °C. It was likely that the coordination reaction between the carboxylic acid groups of the enzyme and the Ca^{2+} on the surface of the support (as well as the other ionic forces stabilizing the immobilization process) resulted in greater rigidity of the phytase 3-D structure. This acted to preserve the disulfide bridges that play a crucial role in the folding of phytase from *A. niger* (Ullah *et al.*, 2008), leading to a dramatic increase in operational stability at elevated temperatures. The gain of stability is also related to the fact that enzyme did not release from the support at all evaluated temperatures even after 3 h of experiments (data not shown, experiment performed by protein measurement in the supernatant).

At the highest temperature evaluated (90 °C), the immobilized enzyme showed a 3.6-fold increase in half-life ($t_{1/2}$), from 4 min for the free enzyme to 14.2 min for the immobilized enzyme. The proposed mathematical model did not allow calculation of the half-life of the immobilized enzyme for the 80 °C stability test, because the relative activity of the enzyme remained constant and higher than 50% over the 3 h evaluated, indicating a substantial improvement in the thermostability of the enzyme at this temperature. Zhang and Xu (2015) prepared a composite of phytase (from *E. coli*) immobilized on modulated alginate hydrogels by Fe^{3+} cross-linked sodium alginate/propylene glycol alginate-xanthan gum. They also reported an increase in the half-life at 80 °C, from 0.2 min for free phytase to 11.3 min for the immobilized enzyme.

These findings show that different methods of phytase immobilization can provide clear thermal stabilization of the enzyme (Tirunagari *et al.*, 2018; Zhang *et al.*, 2010; Zhang and Xu, 2015). However, some immobilization methods are laborious, because they require many chemical steps and long reaction times. The enzymatic method proposed here for the immobilization of phytase onto HA is extremely simple and fast (10 min of adsorption), compared to other techniques that have been studied. The phytase enzyme used in this work showed considerable thermal resistance at 60 and 70 °C, in its soluble form. Nevertheless, the increased thermal stability at 80 and 90 °C, after immobilization on the HA nanoparticles, would appear to justify the application of this system in animal feed, especially when the pelletizing step is performed at high temperatures.

3.5 *In vitro* simulation of the gastrointestinal conditions of fish

In addition to being resistant to high temperatures during the pelletizing step of feed processing, the phytase enzyme must be resistant to the extremely acidic conditions found in the gastrointestinal tracts of most animals (Dersjant-Li *et al.*, 2015). For instance, in fishes the feed

needs to pass through stomach conditions before reaching the intestine, where the enzyme will perform the hydrolysis of phytate (Rodriguez *et al.*, 2018). Therefore, evaluation was made of the effects of the acidic stomach environment on the integrity of phytase, either free or immobilized on HA. Both forms of phytase were kept for 1 h at pH 2, 2.5, and 3 (glycine-HCL buffer), followed by 1 h at alkaline pH (Tris-HCl buffer, pH 7) simulating the microenvironment of the intestine, at which the activity of the enzyme was measured. As shown in Fig. 8, the free and immobilized forms of the enzyme retained about 77% activity after being subjected to the severe conditions of the fish stomach, suggesting that the immobilization of phytase did not cause any major harm to the action of the protein, under the conditions simulating the fish organism.

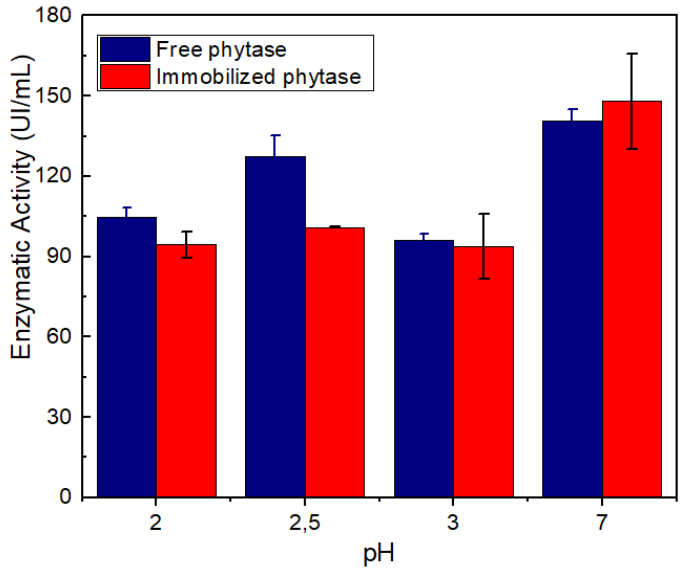

Fig. 8. Enzymatic activity results for the free and immobilized enzyme kept (in duplicate) for 1 h at acid pH (100 mM glycine-HCL buffer) and then for another 1 h at alkaline pH (100 mM tris-HCl buffer). The control consisted of enzyme kept for 2 h at pH 7 and 28 °C. The activity was measured at alkaline pH simulating the intestinal conditions under which the enzyme would act.

This experiment was considered very important in order to confirm that the enzyme would be active when reaching the fish intestine. It should be noted that the acidic conditions of the stomach can cause phytase to be desorbed from the nanoparticles of HA. Desorption tests performed at pH 2 and 3 (using 100 mM Tris-HCl buffer) showed that 70% of the immobilized enzyme was released from the support (data not shown). However, the fact that the enzyme could be released from the support under acidic conditions would not have any effect on its performance in the degradation of phytate, since the free form was shown to be no more efficient than the insoluble form.

In the case of phytate degradation by pigs, the main site of phytase activity is in the stomach, although a small percentage of the digestion may also occur in the upper part of the

small intestine (Dersjant-Li *et al.*, 2015). In the pig's stomach, the pH increases to 5 with feeding, after which it gradually decreases to pH 2.5-3. According to Pontoppidan *et al.* (2007), a simulation of phytase performance in the pig's stomach would require 30 min at pH 5, then 30 min at pH 4, and finally 30 min at pH 3, all at the body temperature of the pig (39 °C). The results obtained for the activity profile of phytase at different pH values (Fig. 6a) indicated that this simulation would lead to similar performances of the free and immobilized phytase at pH 4 and 5, but better performance of the immobilized enzyme at pH 3, compared to the free enzyme.

In addition to its stability at different pH values, the application of phytase as an animal feed additive is critically dependent on its stability towards protease digestion. Zhang and Xu (2015) and Tirunagari *et al.* (2018) showed that immobilization of phytase from bacteria by different techniques (encapsulation and CLEA, respectively) resulted in greater resistance to proteolysis, compared to the free enzyme. In order to investigate the resistance to proteolysis of the two forms of phytase, evaluation was made of the degradation of phytase by pepsin and trypsin, using phytase:protease ratios of 2:1 and 10:1. Pepsin hydrolysis occurred under simulated stomach conditions, using glycine-HCl buffer at pH 2.5 and 28 °C, while trypsin hydrolysis occurred under the simulated intestinal conditions, using Tris-HCl buffer at pH 7 and 28 °C. The data obtained showed that for both phytase:protease ratios evaluated, there was no reduction in activity of either form of the enzyme after 2 h of incubation (data not shown). The results indicated that the immobilization of phytase did not affect its resistance to proteolysis and that the enzyme was not degraded under simulated gastrointestinal conditions.

3.6 Hydrolysis of soybean meal

Soybean meal is the most important protein source used in animal *feed*, especially fish feed (Hardy, 2010). This protein ingredient is phytate-rich, so it is an important storage form of P, while at the same time it is an antinutritional factor that reduces the availability of nutrients and minerals (Cao *et al.*, 2007). The phytase enzyme present in animal feed should be able to hydrolyze the phytate present in soybean meal. Therefore, investigation was made of the hydrolysis of soybean meal by the free and immobilized phytase, with the released P content being measured until it stabilized. The hydrolysis conditions were a soybean concentration of 10% (w/v), enzymatic loading of 25 U g^{-1} soybean, pH 5, and 55 °C.

The two forms of phytase (free and immobilized) showed the same performance during the hydrolysis, which stabilized after 50 min, when 61% conversion was reached (Fig. 9). Celem and Onal (2009) evaluated the hydrolysis of soybean milk by phytase immobilized on a glyoxyl-activated Sepabead EC-EP polymer. The enzyme used was isolated from soybean meal and presented characteristics similar to those of the phytase used in this study (optimum temperature of 60 °C and optimum pH 5). Conversions of 92.5 and 98% were obtained for the immobilized and free phytase, respectively, after 7 h of hydrolysis at 60 °C. The higher conversion achieved

could have been related to higher bioavailability of phytate in soybean milk than in soybean meal associated with the longer reaction time used. In the present study, the two forms of the enzyme (free and immobilized) showed the same performance in soybean meal hydrolysis, indicating that phytase immobilized on HA was effective in the degradation of phytate present in the soybean meal and has potential for application in animal feed.

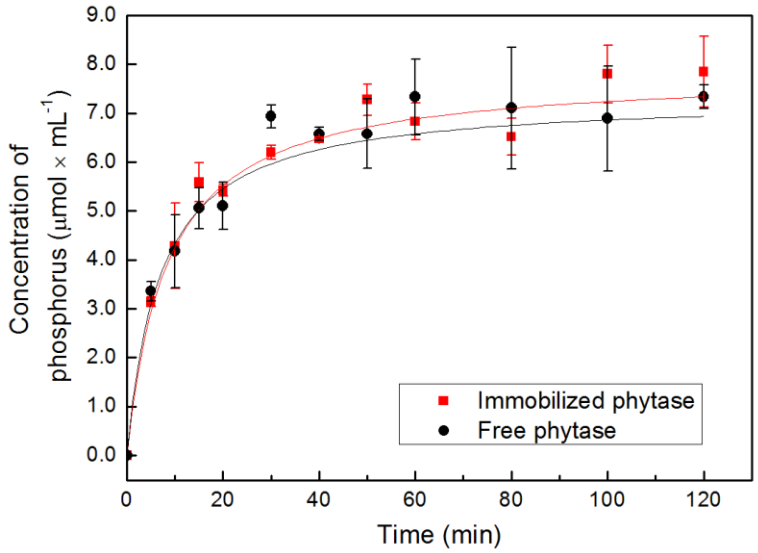

Fig. 9. Kinetics of phosphorus release from soybean meal by the free and immobilized enzyme. The reaction was performed with an enzyme loading of 25 U g^{-1} soybean meal, at 55 °C and pH 5.

4. Conclusion

The phytase enzyme was efficiently immobilized onto hydroxyapatite nanoparticles by means of a very simple and fast adsorption protocol resulting in a derivative with properties suitable for application in animal feed. The results showed a strong and stable interaction between enzyme and support, indicating the formation of coordination bonds between Ca^{2+} sites of HA and COO^- of amino acid residues of the enzyme, besides the ionic bindings. The immobilized phytase showed broader activity profile as to pH and temperature, and higher stability at high temperatures than free enzyme. The improvement in the properties of immobilized phytase in HA suggest the potential of applying the immobilized form of phytase in animal feed, since the enzyme will be more resistant to the high temperatures during the process of pelletizing the feed and will be as active as the soluble enzyme in the gastrointestinal conditions of monogastric animals. Furthermore, the hydroxyapatite might also act as an inorganic source of phosphorus and calcium for animal feed.

5. References

Agrawal, R., Verma, A., Satlewal, A., 2016. Application of nanoparticle-immobilized thermostable beta-glucosidase for improving the sugarcane juice properties. Innovative Food Science & Emerging Technologies 33, 472-482.

Aquilina, G., Azimonti, G., Bampidis, V., Bastos, M.D., Bories, G., Chesson, A., Cocconcelli, P.S., Flachowsky, G., Gropp, J., Kolar, B., Kouba, M., Puente, S.L., Lopez-Alonso, M., Mantovani, A., Mayo, B., Ramos, F., Rychen, G., Saarela, M., Villa, R.E., Wallace, R.J., Wester, P., Additives, E.P., Prod Subst Used Animal Feed, F., 2016. Safety and efficacy of Ronozyme (R) HiPhos (6-phytase) as a feed additive for sows and fish. Efsa Journal 14, 10.

Bradford, M.M., 1976. Rapid and sensitive method for quantitation of microgram quantities of protein utilizing principle of protein-dye binding. Analytical Biochemistry 72, 248-254.

Cao, L., Wang, W.M., Yang, C.T., Yang, Y., Diana, J., Yakupitiyage, A., Luo, Z., Li, D.P., 2007. Application of microbial phytase in fish feed. Enzyme and Microbial Technology 40, 497-507.

Celem, E.B., Onal, S., 2009. Immobilization of phytase on epoxy-activated Sepabead EC-EP for the hydrolysis of soymilk phytate. Journal of Molecular Catalysis B-Enzymatic 61, 150-156.

Cheryan, M., 1980. Phytic acid interactions in food systems. Crc Critical Reviews in Food Science and Nutrition 13, 297-335.

Cho, E.A., Kim, E.J., Pan, J.G., 2011. Adsorption immobilization of Escherichia coli phytase on probiotic Bacillus polyfermenticus spores. Enzyme and Microbial Technology 49, 66-71.

Cian, R.E., Bacchetta, C., Cazenave, J., Drago, S.R., 2018. Extruded fish feed with high residual phytase activity and low mineral leaching increased P-mesopotamicus mineral retention. Animal Feed Science and Technology 240, 78-87.

Cipolatti, E., Silva, M., Klein, M., Feddern, V., Feltes, M., Oliveira, J., Ninow, J., de Oliveira, D., 2014. Current status and trends in enzymatic nanoimmobilization. Journal of Molecular Catalysis B-Enzymatic 99, 56-67.

Cipreste, M.F., Gonzalez, I., Martins, T.M.D., Goes, A.M., Macedo, W.A.D., de Sousa, E.M.B., 2016. Attaching folic acid on hydroxyapatite nanorod surfaces: an investigation of the HA-FA interaction. Rsc Advances 6, 11.

Coutinho, T.C., Rojas, M.J., Tardioli, P.W., Paris, E.C., Farinas, C.S., 2018. Nanoimmobilization of beta-glucosidase onto hydroxyapatite. International Journal of Biological Macromolecules 119, 1042-1051.

Dersjant-Li, Y., Awati, A., Schulze, H., Partridge, G., 2015. Phytase in non-ruminant animal nutrition: a critical review on phytase activities in the gastrointestinal tract and influencing factors. Journal of the Science of Food and Agriculture 95, 878-896.

Dutta, N., Mukhopadhyay, A., Dasgupta, A.K., Chakrabarti, K., 2014. Improved production of reducing sugars from rice husk and rice straw using bacterial cellulase and xylanase activated with hydroxyapatite nanoparticles. Bioresource Technology 153, 269-277.

Dutta, N., Raj, D., Biswas, N., Mallick, M., Omesh, S., 2017. Nanoparticle assisted activity optimization and characterization of a bacterial phytase immobilized on single layer graphene oxide. Biocatalysis and Agricultural Biotechnology 9, 240-247.

Farinas, C., Reis, P., Ferraz, H., Salim, V., Alves, T., 2007. Adsorption of myoglobin onto hydroxyapatite modified with metal ions. Adsorption Science & Technology 25, 717-727.

Garcia-Mantrana, I., Yebra, M.J., Haros, M., Monedero, V., 2016. Expression of bifidobacterial phytases in Lactobacillus casei and their application in a food model of whole-grain sourdough bread. International Journal of Food Microbiology 216, 18-24.

Harati, J., Siadat, S.O.R., Taghavian, H., Kaboli, S., Khorshidi, S., 2017. Improvement in biochemical characteristics of glycosylated phytase through immobilization on nanofibers. Biocatalysis and Agricultural Biotechnology 12, 96-103.

Hardy, R.W., 2010. Utilization of plant proteins in fish diets: effects of global demand and supplies of fishmeal. Aquaculture Research 41, 770-776.

Harland, B.F., Harland, J., 1980. Fermentative reduction of phytate in rye, white, and whole wheat breads. Cereal Chemistry 57, 226-229.

Ivic, J., Dimitrijevic, A., Milosavic, N., Bezbradica, D., Drakulic, B., Jankulovic, M., Pavlovic, M., Rogniaux, H., Velickovic, D., 2016a. Assessment of the interacting mechanism between Candida rugosa lipases and hydroxyapatite and identification of the hydroxyapatite-binding sequence through proteomics and molecular modelling. Rsc Advances 6, 34818-34824.

Ivic, J., Velickovic, D., Dimitrijevic, A., Bezbradica, D., Dragacevic, V., Jankulovic, M., Milosavic, N., 2016b. Design of biocompatible immobilized Candida rugosa lipase with potential application in food industry. Journal of the Science of Food and Agriculture 96, 4281-4287.

Jain, J., Sapna, Singh, B., 2016. Characteristics and biotechnological applications of bacterial phytases. Process Biochemistry 51, 159-169.

Kojima, S., Nagata, F., Kugimiya, S., Kato, K., 2018. Synthesis of peptide-containing calcium phosphate nanoparticles exhibiting highly selective adsorption of various proteins. Applied Surface Science 458, 438-445.

Kollath, V., Van den Broeck, F., Feher, K., Martins, J., Luyten, J., Traina, K., Mullens, S., Cloots, R., 2015. A Modular Approach To Study Protein Adsorption on Surface Modified Hydroxyapatite. Chemistry-a European Journal 21, 10497-10505.

Konietzny, U., Greiner, R., 2002. Molecular and catalytic properties of phytate-degrading enzymes (phytases). International Journal of Food Science and Technology 37, 791-812.

Kostrewa, D., Leitch, F.G., Darcy, A., Broger, C., Mitchell, D., vanLoon, A., 1997. Crystal structure of phytase from Aspergillus ficuum at 2.5 angstrom resolution. Nature Structural Biology 4, 185-190.

Kumar, S., Sharma, J.G., Maji, S., Malhotra, B.D., 2016. A biocompatible serine functionalized nanostructured zirconia based biosensing platform for non-invasive oral cancer detection. Rsc Advances 6, 10.

Lagazzo, A., Barberis, F., Carbone, C., Ramis, G., Finocchio, E., 2017. Molecular level interactions in brushite-aminoacids composites. Materials Science & Engineering C-Materials for Biological Applications 70, 721-727.

Lee, W.H., Loo, C.Y., Van, K.L., Zavgorodniy, A.V., Rohanizadeh, R., 2012. Modulating protein adsorption onto hydroxyapatite particles using different amino acid treatments. Journal of the Royal Society Interface 9, 918-927.

Moriarty, D.J., 1973. Physiology of digestion of blue-green-algae in cichlid fish, tilapia-nilotica. Journal of Zoology 171, 25-39.

Mukhopadhyay, A., Dasgupta, A., Chattopadhyay, D., Chakrabarti, K., 2012. Improvement of thermostability and activity of pectate lyase in the presence of hydroxyapatite nanoparticles. Bioresource Technology 116, 348-354.

Nielsen, A.V.F., Nyffenegger, C., Meyer, A.S., 2015. Performance of Microbial Phytases for Gastric Inositol Phosphate Degradation. Journal of Agricultural and Food Chemistry 63, 943-950.

Oakley, A.J., 2010. The structure of Aspergillus niger phytase PhyA in complex with a phytate mimetic. Biochemical and Biophysical Research Communications 397, 745-749.

Pontoppidan, K., Pettersson, D., Sandberg, A.S., 2007. Peniophora lycii phytase is stabile and degrades phytate and solubilises minerals in vitro during simulation of gastrointestinal digestion in the pig. Journal of the Science of Food and Agriculture 87, 2700-2708.

Qi, M.L., He, K., Huang, Z.N., Shahbazian-Yassar, R., Xiao, G.Y., Lu, Y.P., Shokuhfar, T., 2017. Hydroxyapatite Fibers: A Review of Synthesis Methods. Jom 69, 1354-1360.

Quan, C.S., Fan, S.D., Ohta, Y., 2003. Immobilization of Candida krusei cells producing phytase in alginate gel beads: an application of the preparation of myo-inositol phosphates. Applied Microbiology and Biotechnology 62, 41-47.

Ranjan, B., Singh, B., Satyanarayana, T., 2015. Characteristics of Recombinant Phytase (rSt-Phy) of the Thermophilic mold Sporotrichum thermophile and its applicability in dephytinizing foods. Applied Biochemistry and Biotechnology 177, 1753-1766.

Rao, D., Rao, K.V., Reddy, T.P., Reddy, V.D., 2009. Molecular characterization, physicochemical properties, known and potential applications of phytases: An overview. Critical Reviews in Biotechnology 29, 182-198.

Rehman, I., Bonfield, W., 1997. Characterization of hydroxyapatite and carbonated apatite by photo acoustic FTIR spectroscopy. Journal of Materials Science-Materials in Medicine 8, 1-4.

Rodriguez, Y.E., Laitano, M.V., Pereira, N.A., Lopez-Zavala, A.A., Haran, N.S., Fernandez-Gimenez, A.V., 2018. Exogenous enzymes in aquaculture: Alginate and alginate-bentonite microcapsules for the intestinal delivery of shrimp proteases to Nile tilapia. Aquaculture 490, 35-43.

Rychen, G., Aquilina, G., Azimonti, G., Bampidis, V., Bastos, M.D., Bories, G., Chesson, A., Flachowsky, G., Gropp, J., Kolar, B., Kouba, M., Lopez-Alonso, M., Puente, S.L., Mantovani, A., Mayo, B., Ramos, F., Saarela, M., Villa, R.E., Wallace, R.J., Wester, P., Brantom, P., Dierick, N.A., Glandorf, B., Herman, L., Karenlampi, S., Aguilera, J., Anguita, M., Cocconcelli, P.S., Subst, E.P.A.P., 2017a. Safety and efficacy of Natuphos (R) E (6-phytase) as a feed additive for avian and porcine species. Efsa Journal 15, 3.

Rychen, G., Aquilina, G., Azimonti, G., Bampidis, V., de Lourdes Bastos, M., Bories, G., Chesson, A., Cocconcelli, P.S., Flachowsky, G., Gropp, J., Kolar, B., Kouba, M., Alonso, M.L., Puente, S.L., Mantovani, A., Mayo, B., Ramos, F., Saarela, M., Villa, R.E., Wallace, R.J., Wester, P., Brantom, P., Dierick, N.A., Anguita, M., Efsa Panel, A., Prod, 2017b. Safety and efficacy of OPTIPHOS (R) (6-phytase) as a feed additive for finfish. Efsa Journal 15, 10.

Sadana, A., Henley, J.P., 1987. Single-step unimolecular non-1st-order enzyme deactivation kinetics. Biotechnology and Bioengineering 30, 717-723.

Soni, S.K., Magdum, A., Khire, J.M., 2010. Purification and characterization of two distinct acidic phytases with broad pH stability from Aspergillus niger NCIM 563. World Journal of Microbiology & Biotechnology 26, 2009-2018.

Swain, S.K., Sarkar, D., 2013. Study of BSA protein adsorption/release on hydroxyapatite nanoparticles. Applied Surface Science 286, 99-103.

Tardioli, P.W., Zanin, G.M., de Moraes, F.F., 2006. Characterization of Thermoanaerobacter cyclomaltodextrin glucanotransferase immobilized on glyoxyl-agarose. Enzyme and Microbial Technology 39, 1270-1278.

Taussky, H.H., Shorr, E., 1953. A microcolorimetric method for the determination of inorganic phosphorus. Journal of Biological Chemistry 202, 675-685.

Tirunagari, H., Basetty, S., Rode, H.B., Fadnavis, N.W., 2018. Crosslinked enzyme aggregates (CLEA) of phytase with soymilk proteins. Journal of Biotechnology 282, 67-69.

Trouillefou, C.M., Le Cadre, E., Cacciaguerra, T., Cunin, F., Plassard, C., Belamie, E., 2015. Protected activity of a phytase immobilized in mesoporous silica with benefits to plant phosphorus nutrition. Journal of Sol-Gel Science and Technology 74, 55-65.

Ullah, A.H.J., Gibson, D.M., 1987. Extracellular phytase (ec 3.1.3.8) from aspergillus-ficuum nrrl 3135 - purification and characterization. Preparative Biochemistry 17, 63-91.

Ullah, A.H.J., Sethumadhavan, K., Mullaney, E.J., 2008. Unfolding and refolding of Aspergillus niger PhyB phytase: Role of disulfide bridges. Journal of Agricultural and Food Chemistry 56, 8179-8183.

Ushasree, M.V., Vidya, J., Pandey, A., 2015. Replacement P212H Altered the pH-Temperature Profile of Phytase from Aspergillus niger NII 08121. Applied Biochemistry and Biotechnology 175, 3084-3092.

Vandenberg, G.W., Scott, S.L., Sarker, P.K., Dallaire, V., de la Noue, J., 2011. Encapsulation of microbial phytase: Effects on phosphorus bioavailability in rainbow trout (Oncorhynchus mykiss). Animal Feed Science and Technology 169, 230-243.

Viveros, A., Centeno, C., Brenes, A., Canales, R., Lozano, A., 2000. Phytase and acid phosphatase activities in plant feedstuffs. Journal of Agricultural and Food Chemistry 48, 4009-4013.

Wu, C., Huang, S., Tseng, T., Rao, Q., Lin, H., 2010. FT-IR and XRD investigations on sintered fluoridated hydroxyapatite composites. Journal of Molecular Structure 979, 72-76.

Xie, W., Zang, X., 2017. Covalent immobilization of lipase onto aminopropyl-functionalized hydroxyapatite-encapsulated-gamma-Fe2O3 nanoparticles: A magnetic biocatalyst for interesterification of soybean oil. Food Chemistry 227, 397-403.

Yewle, J.N., Wei, Y.N., Puleo, D.A., Daunert, S., Bachas, L.G., 2012. Oriented Immobilization of Proteins on Hydroxyapatite Surface Using Bifunctional Bisphosphonates as Linkers. Biomacromolecules 13, 1742-1749.

Zhang, G.Q., Dong, X.F., Wang, Z.H., Zhang, Q., Wang, H.X., Tong, J.M., 2010. Purification, characterization, and cloning of a novel phytase with low pH optimum and strong proteolysis resistance from Aspergillus ficuum NTG-23. Bioresource Technology 101, 4125-4131.

Zhang, W.Z., Xu, F., 2015. Hierarchical Composites Promoting Immobilization and Stabilization of Phytase via Transesterification/Silification of Modulated Alginate Hydrogels. ACS Sustainable Chemistry & Engineering 3, 2694-2703.

CHAPTER 4

Xylanase Immobilization on hydroxyapatite nanoparticles modified with metal ions

This chapter is an adapted version of the article "Hydroxyapatite nanoparticles modified with metal ions for xylanase immobilization" published in 2020 in the International Journal of Biological Macromolecules, volume 150, pages 344-354.

Graphical Abstract

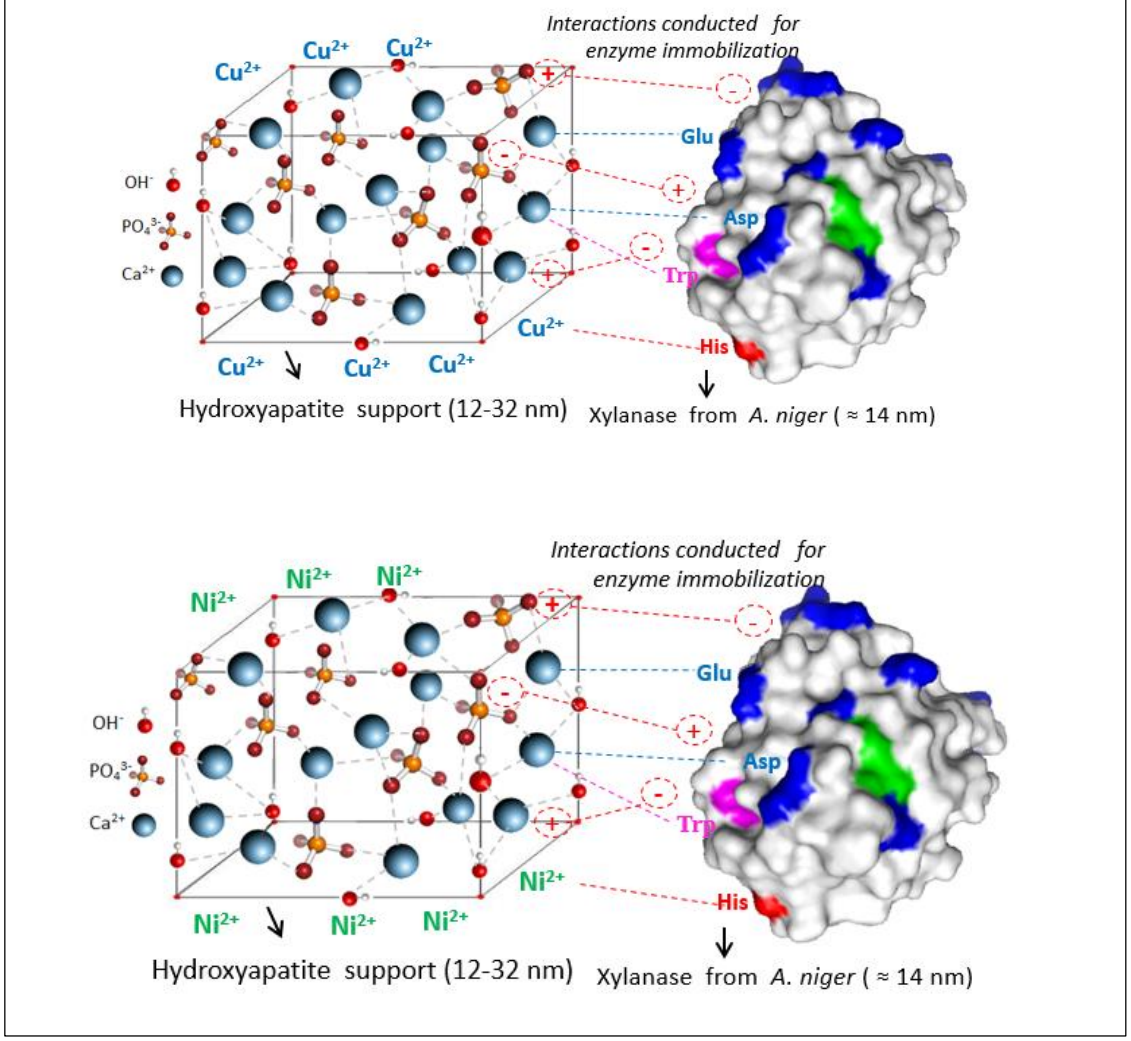

Abstract

Hydroxyapatite (HA) nanoparticles are promising materials for enzyme immobilization, since they provide a high specific surface area for enzyme loading and can also be modified with metal ions (HA-Me^{2+}) to enable interaction with proteins. The adsorption of proteins on HA-Me^{2+} has been explored for purification purposes, while the use of this material as a support for the immobilization of enzymes remains to be further investigated. Xylanase is an enzyme of considerable industrial interest, being used in the biofuel, pharmaceutical, pulp, and food & beverage sectors, among others. The immobilization of xylanase can enable recovery of the enzyme after biocatalysis, so that it can be reused several times, hence reducing the costs of industrial processes. Here, a systematic study was performed of the immobilization of xylanase on HA nanoparticles modified with metal ions (Cu^{2+} and Ni^{2+}). A simple, fast, and efficient immobilization protocol was established using statistical experimental design as a tool, generating derivatives by interactions involving complexation of metals of the support with electron donor groups of the enzyme. The affinity towards xylanase was higher for the HA-Cu^{2+} support, compared to HA and HA-Ni^{2+}. The pH and temperature profiles for the immobilized enzyme activity remained the same as for the soluble enzyme, indicating that the xylanase did not undergo major changes in its conformational state after immobilization. The HA-Cu^{2+} support was the most effective in reuse assays, retaining up to 80% activity in the second cycle. The results showed that xylanase could be immobilized on HA nanoparticles modified with Cu^{2+} and Ni^{2+} metal ions, using a simple and effective method, indicating the promising potential of the system for applications in different industrial processes.

Keywords: Hydroxyapatite, xylanase, immobilization, metal ions, nanoparticles.

1. Introduction

Hydroxyapatite (HA) is a ceramic material with the chemical composition $Ca_{10}(PO_4)_6(OH)_2$ and a hexagonal structure. HA can be used as a matrix for protein adsorption, mainly due to electrostatic interactions of the phosphate and calcium groups of HA with charged side groups of proteins (Kollath *et al.*, 2015). However, the potential of these nanoparticles to act as enzyme matrix can be more explored if they were modified with metals, such as copper, zinc, and nickel, which can be attached to the surface of HA, improving the protein adsorption capacity by means of complexation interactions (Hench and Wilson, 1993; Farinas *et al.*, 2007). The interaction of proteins with metal ions has been utilized in the immobilized metal affinity chromatography (IMAC) technique, employed for protein purification (Gutierrez *et al.*, 2007), but the chemical principle of this technique could also be used for enzyme immobilization, with the aim of reusing the biocatalyst in industrial processes. The complexation reaction is based on the selective interaction of metal ions (Cu^{2+}, Zn^{2+}, Ni^{2+}, or Co^{2+}) on the solid support with electron donor groups of proteins, especially amino acids such as histidine, cysteine, tryptophan, and arginine, which possess strong electron donor groups in their side chains (Kumar *et al.*, 1998; Bresolin *et al.*, 2009;).

Enzyme immobilization has two main objectives, namely the reuse of the biocatalyst, retaining its catalytic activity, and/or improvement of enzyme stability under adverse process conditions (Vaghari *et al.*, 2016). Since the enzyme becomes insoluble after being anchored on a support, the product is not contaminated by residual enzyme at the end of the process, hence reducing the cost of bioproduct purification during the downstream step, which is usually the most expensive bioprocess step (Zydney, 2016). The use of nanometric structures as matrices for enzyme immobilization provides a high surface area capable of retaining a high enzyme loading (Cipolatti *et al.*, 2014). Nanoparticles also allow good access of the substrate to the catalyst, due to the low resistance to mass transfer of these nanostructures (Javed *et al.*, 2016).

Hydroxyapatite is an inorganic solid that can be synthesized as nanoparticles (Andre *et al.*, 2012), with the additional advantages of being nontoxic and presenting excellent physical and chemical properties when used as a support for enzyme immobilization. Recent studies have evaluated the potential of enzyme immobilization on HA for applications in industry. The lipase enzyme was immobilized on HA nanoparticles for use in the food industry (Ivic *et al.*, 2016b), as well as on Fe_3O_4 nanoparticles functionalized to perform covalent interactions and coated with HA, enabling recovery of the enzyme by application of a magnetic field (Xie and Zang, 2017). The β-glucosidase enzyme was immobilized on HA nanoparticles, obtaining derivatives with various applications in agroindustry (Coutinho *et al.*, 2018). Coutinho *et al.* (2019) immobilized phytase on HA nanoparticles for application in the animal feed industry. Despite these recent studies, the potential of HA as matrix for enzymes for applications in industry remains to be further investigated.

Xylanases are glycosyl hydrolases that hydrolyze the β-1,4-glycosidic bonds of the xylan polysaccharide (Schomburg and Schomburg, 2009). Due to the heterogeneous nature of this biopolymer, xylan degradation requires the synergistic action of different hydrolases including exoxylanases (α-glucuronosidase, α-arabinosidase, and acetyl xylan esterase), endoxylanases, and β-xylosidase (Beg *et al.*, 2001; Farinas *et al.*, 2010). For these reasons, xylanase is considered to be an enzymatic mixture, having many applications in different industrial sectors. In biorefineries, xylanase acts together with other specialized cellulases, mannanases, and glucanases in the conversion of lignocellulosic biomass to obtain biofuels and other bioproducts (Beg *et al.*, 2001). In the beverage industry, xylanase is used together with pectinases as a clarifying agent (Shahrestani *et al.*, 2016). In the animal feed industry, xylanase is used as a feed additive, acting in the enzymatic degradation of arabinoxylan (Norgaard *et al.*, 2016). In the paper industry, xylanase assists the bleaching step, increasing pulp lignin extraction by the depolymerization of hemicellulosic material (Woolridge, 2014). In the pharmaceutical industry, xylanase is employed for the production of xylooligosaccharides that have nutraceutical properties (Liu *et al.*, 2015). Given the range of applications of xylanase in industry, and especially in agro-industry, researchers have become increasingly interested in finding techniques for the immobilization of this enzyme, in order to increase its activity and stability, as well as to enable its reuse in the processes (Aragon *et al.*, 2013; Driss *et al.*, 2014; Jampala *et al.*, 2017). To the best of our knowledge, there have been no reports of the use of HA nanoparticles for the immobilization of xylanase.

Here, a systematic study was performed of the immobilization of xylanase on HA nanoparticles modified with the metals Cu^{2+} and Ni^{2+} (HA-Me^{2+}). The amounts of Cu and Ni attached to the HA structure were elucidated by determining the concentrations of these metals in the supernatants by flame atomic absorption spectrometry (FAAS). The chemical compositions of the supports were characterized using energy dispersive X-ray spectroscopy (EDS) and their crystallinity was investigated using X-ray diffraction (XRD). A full factorial design was used as a statistical tool to select the best conditions of pH and ionic strength used in the immobilization process. Adsorption curves were constructed to evaluate the enzyme loadings of the supports. The biochemical behavior of the immobilized xylanase was evaluated considering the changes in the activity profile at different pHs and temperatures, the degree of leaching from the supports using different desorbing agents, and the thermal stability of the enzyme. The efficiency of the immobilized xylanase was evaluated in the hydrolysis of xylan, and the ability to reuse the biocatalyst was assessed. The aim was to obtain a simple and effective immobilization method that ensured high catalytic activity and the ability to reuse xylanase in different industrial applications.

2. Material and Methods

2.1 Material

The xylanase enzyme (NS22083) was donated by Novozymes (Bagsvaerd, Denmark). The hydroxyapatite (HA) nanoparticles and the xylan substrate were purchased from Sigma-Aldrich (St. Louis, MO, USA). The HA nanoparticles were needle-shaped particles with a size range of 12-32 nm and surface area of 58.2 $m^2 g^{-1}$ (Coutinho *et al.*, 2018). All other reagents were analytical grade.

2.2 Preparation and characterization of the hydroxyapatite supports (HA-Me^{2+})

Quantities of 0.5 g of hydroxyapatite were placed in Falcon tubes, together with 10 mL volumes of 50 mM $CuSO_4$ and $NiSO_4$ solutions. The suspensions were agitated end-over-end for 60 min, at room temperature, followed by centrifugation at 8000 *g* for 5 min. The resulting HA-Me^{2+} was washed twice with distilled water, followed by equilibration in 20 mM sodium acetate buffer (pH 5). The crystallinity of the HA-Me^{2+} particles was investigated using X-ray diffraction (XRD) measurements performed with a Shimadzu Model 6000 instrument. The diffractograms were recorded in the 2Θ range 20-70º, at a scanning rate of 1º min^{-1}, using a Cu Kα incident beam (λ = 0.1546 nm). The energy dispersive X-ray spectroscopy (EDS) technique was used for qualitative analysis of the chemical composition of the hydroxyapatite particles (HA-Me^{2+}). For this, the surface of a metallic disc (stub) was coated with graphite and the sample was dispersed over it. The sample was analyzed (in duplicate) using a JEOL Model JSM-6510 scanning electron microscope operated at 15 kV, with 10 nm resolution. The elemental Cu and Ni concentrations in the first and second supernatants (after washing the support) were determined by FAAS, using a PinAAcle 900T instrument (PerkinElmer) operated with an air-acetylene flame (with air and acetylene flow rates of 10.0 and 2.5 L min^{-1}, respectively). Cu and Ni were measured (in triplicate) at wavelengths of 324.7 and 232.0 nm, respectively.

2.3 Experimental design for the immobilization of xylanase on HA-Me^{2+}

A full factorial design was used to evaluate the effects of two variables, namely pH (4-8) and ionic strength (60-300 mM NaCl), in the process of immobilization of xylanase on the hydroxyapatite supports (HA, HA-Cu^{2+}, and HA-Ni^{2+}). The experimental design selected was a central composite rotational design (CCRD) comprising eleven runs, corresponding to four cube points, four axial points, and three replicates at the central point. The factors and levels (independent variables) investigated are shown in Table 1. The dependent variables (responses) were the immobilization yield (IY) and the activity of the derivative (A_{DE}). The main statistical method used to analyze the experimental data was analysis of variance (ANOVA), performed with Statistica v. 7.0 software.

The enzyme-support adsorption process was carried out in 2 mL tubes, with an enzymatic loading of 5 mg protein g^{-1} support and HA-Me^{2+} at a concentration of 0.05 g mL^{-1}, under gentle rotary stirring for 1 h, at 25 °C. At the end of the immobilization process, the derivative obtained was washed two times with the same buffer used for immobilization (with centrifugation for 2 min at 8000 rpm). The protein contents of the supernatants were quantified by the Bradford method (Bradford, 1976), in order to determine the immobilization yield (IY), calculated as follows:

$$IY\ (\%) = 1 - \frac{[P_{supernatant1}] + [P_{supernatant2}]}{[P_{control}]} \times 100 \qquad \text{(Eq. 1)}$$

where $P_{supernatant1}$ and $P_{supernatant2}$ (mg mL^{-1}) are the protein concentrations for supernatant 1 (obtained after the first wash) and supernatant 2 (obtained after the second wash), respectively, and $P_{control}$ (mg mL^{-1}) is the protein concentration for the control (soluble enzyme). The enzymatic activity of the final derivative (A_{DE}) was measured (in duplicate) as described in Section 2.4.

2.4 Enzymatic activity assays

The enzymatic activities of the soluble and immobilized xylanase were determined as described previously (Bailey *et al.*, 1992), by incubating 100 μL of enzymatic solution (or suspension, in the case of the immobilized enzyme) and 900 μL of the xylan substrate solution (1% m/v, prepared using 50 mM sodium acetate buffer at pH 5). The reaction was allowed to proceed for 5 min, at 50 °C, under stirring, after which it was quenched using thermal inactivation of the enzyme by placing the vials in boiling water for 5 min. Reducing sugar (xylose) released in the assays was measured according to the DNS method (Miller, 1959). One unit of enzyme activity (IU) represented the amount of enzyme required to release 1 μmol of glucose per minute into the reaction mixture. All the protein and activity measurements were performed in duplicate, with calculation of the immobilization parameters (IY and A_{DE}) as means ± standard deviations. All subsequent experiments were performed under the established optimum immobilization conditions.

2.5 Desorption studies

The ability of the immobilized xylanase to be released from the supports (HA, HA-Cu^{2+} and HA-Ni^{2+}**)** was evaluated by incubating the derivative in solutions of sodium chloride, sodium citrate and imidazole at increasing concentrations (50, 100, 200, 400, and 800 mM), all at pH 5. A suspension of immobilized phytase was centrifuged at 8000 rpm for 2 min, after which the supernatant was discarded. An equal volume of the desorbing agent solution was added to the precipitate (derivative), followed by gentle stirring for 40 min. The protein concentration in the supernatant was then measured (in duplicate), using the Bradford method (Bradford, 1976). Desorption assays were performed in duplicate at each ionic strength. The protein immobilized

on the HA was designated as 100%, while the protein contents obtained in the supernatants with different ionic strengths were calculated as the percentage of desorbed enzyme (%), relative to the immobilized protein.

2.6 Enzymatic loading and adsorption isotherms

The adsorption capacities of the supports (HA, HA-Cu^{2+}, and HA-Ni^{2+}) were evaluated using enzyme loadings ranging from 5 to 80 mg protein g^{-1} support in the immobilization process. Adsorption isotherms were then constructed by plotting the amount of xylanase adsorbed by the HA matrix (Q_e, in mg protein g^{-1} support) as a function of the concentration of unbound protein (C_e, in mg protein at equilibrium mL^{-1}). The Langmuir isotherm model (Eq. 2) was used to describe the experimental data:

$$Q_e = \frac{Q_m K_L C_e}{1 + K_L C_e} \quad \text{(Eq. 2)}$$

where $1/K_L$ is the affinity constant (mg mL^{-1}) and Q_m is the adsorption corresponding to complete surface coverage (mg g^{-1}), which were both determined by nonlinear regression of the experimental data.

2.7 Effects of pH and temperature on enzyme activity

The effect of pH on the activity of xylanase (free and immobilized on HA, HA-Cu^{2+}**,** and HA-Ni^{2+}) was evaluated in the pH range 3-8, using glycine-HCl buffer (for pH 3), sodium acetate buffer (for pH 4, 5, and 6), and sodium phosphate buffer (for pH 7 and 8), all at 100 mM and 50 °C. The effect of temperature on the activities of the free and immobilized xylanase was investigated at 30, 40, 50, 60, and 70 °C, at pH 5 (using 100 mM sodium acetate buffer). The experiment was performed in duplicate. The highest activity obtained in the temperature or pH ranges employed was designated as 100%, while the activities at all the remaining temperatures and pHs were calculated as the activity ($R_{lt}A$, in %) relative to that highest activity.

2.8 Enzyme thermostability

The thermostabilities of the free and immobilized (on HA, HA-Cu^{2+}, and HA-Ni^{2+}) xylanase were determined by incubation for 2 h at temperatures of 60, 70, and 90 °C, in 20 mM sodium acetate buffer (pH 5). At 15 min intervals, samples were withdrawn for determination of thermal denaturation by means of enzymatic activity measurements. The xylanase activity was measured (in duplicate) at 50 °C and pH 5.0, as described in Section 2.4. Two replicates of each treatment were performed. The activity obtained at time zero was designated as 100% and the activities at all the remaining times were calculated as the activity (in %) relative to that highest activity.

2.9 Hydrolysis of xylan and reusability of the immobilized enzyme

The efficiency of the immobilized xylanase (on HA, HA-Cu^{2+}, and HA-Ni^{2+}) was evaluated in terms of xylan hydrolysis and was compared to the use of soluble xylanase. The xylan substrate (20 g L^{-1}) was hydrolyzed in 100 mM sodium acetate buffer (pH 5) at 50 °C, under agitation, using the soluble and immobilized xylanase at an enzyme loading of 60 IU g^{-1} xylan. The release of xylose during the course of the reaction was quantified using the DNS method, until stabilization. The experiment was performed in duplicate and the results were presented as mean ± standard deviation.

The reusability of the immobilized xylanase (on HA, HA-Cu^{2+}, and HA-Ni^{2+}) was studied in assays performed in 2 mL tubes, under the hydrolysis assay conditions described above. After each 30 min reaction cycle, the enzymatic material was separated by centrifugation (8000 rpm for 5 min) and was then resuspended in the fresh substrate. The xylose concentration measured in the first cycle corresponded to 100%, while the concentrations of the sugar in the nine remaining cycles were calculated as the xylose production (%) relative to that first cycle. The experiment was performed in duplicate and the results were presented as mean ± standard deviation.

3. Results and Discussion

3.1 Characterization of the hydroxyapatite supports

The final colors of the HA powders, after contact with the copper and nickel salt solutions, were from white to blue and light green, respectively. Elemental analysis by energy dispersive spectroscopy (EDS) at different locations of the samples was used to confirm that the metals had been inserted into the HA structure. The EDS spectra showed the presence of the expected major elements in the structure of hydroxyapatite ($Ca_5(PO_4)_3(OH)$), including Ca, P, and O, together with minor elements such as Mg, K, Al, and Si. Peaks for Cu and Ni in the HA-Cu^{2+} and HA-Ni^{2+} spectra, respectively, confirmed that the metals had been inserted into the HA structure (Fig. S3, Supplementary Material). The amounts of Cu and Ni inserted were obtained by measuring the concentrations of these metals in the supernatants by FAAS. The initial Cu and Ni concentrations were 3.79 ± 0.096 and 3.60 ± 0.099 g L^{-1}, respectively, while the final concentrations were 1.19 ± 0.090 and 2.61 ± 0.104 g L^{-1}, respectively. These values indicated that 68% of the Cu initially present in the HA suspension was transferred to the matrix, resulting in 52.2 mg Cu g^{-1} HA, while 27% of the Ni initially present was transferred to the matrix, resulting in 19.8 mg Ni g^{-1} HA. The higher amount of Cu transferred to the HA surface, compared to Ni, was in agreement with the enzyme immobilization results (discussed below).

X-ray diffraction (XRD) analyses were performed in order to identify the phases present in the HA structure (Fig. 1). Comparison of the diffractograms with the Joint Committee on Powder Diffraction Standards (JCPDS) card number 3701-089-4405 confirmed the presence of the

characteristic peaks of HA (Table S1, Supplementary Material), which presents a hexagonal crystalline structure.

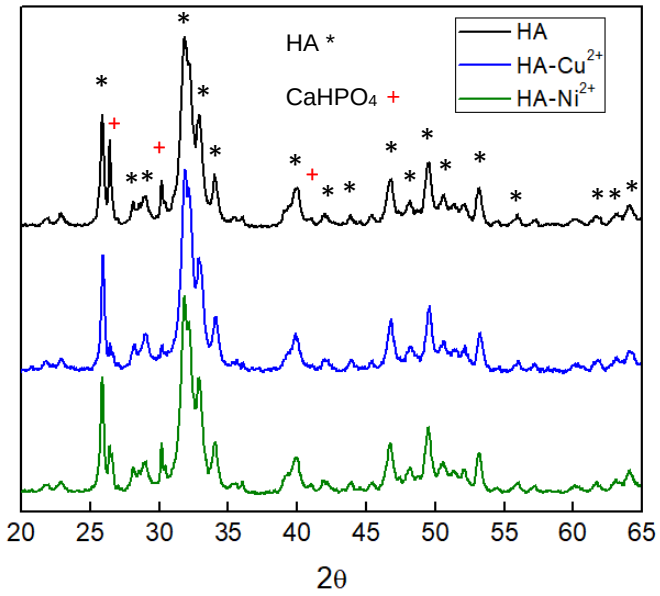

Fig. 1. X-ray diffractograms of the hydroxyapatite supports (HA, HA-Cu^{2+}, and HA-Ni^{2+}).

The main conclusion of the XRD analysis was that the metal ions that were incorporated into the surface structure of HA did not significantly affected the structure or creating any new segregated phases. The diffractograms for the HA-Cu^{2+} and HA-Ni^{2+} supports showed decreased intensities of peaks related to $CaHPO_4$ (known to be a contaminant phase of commercial HA), which was probably due to the solubilization of calcium phosphate during the support modification procedure.

3.2 Immobilization of xylanase on HA, HA-Cu^{2+}, and HA-Ni^{2+}

A full 2^2 factorial design was used as a statistical tool to investigate the effects of pH and ionic strength on the adsorption of xylanase on the pure hydroxyapatite nanoparticles and the nanoparticles modified with the metals (HA-Me^{2+}), in order to establish the ideal physicochemical conditions during the immobilization process. Table 1 shows the experimental conditions and the results for the adsorption of xylanase at an initial enzyme loading of 5 mg protein g^{-1} support, which was performed for 60 min. The highest immobilization yields (IY) and activities of the derivatives (A_{DER}) were obtained at pH 5.5. Immobilization on HA-Cu^{2+} showed the highest IY values, for all pH and ionic strength conditions, while immobilization on HA-Ni^{2+} showed the lowest IY and A_{DER} values. The correlation coefficients (R) and p-values obtained in the ANOVA analysis (Table 2) showed that the predictive capabilities of the models were satisfactory, enabling them to be used to construct the adsorption curves by fixing the ionic strength in the model

equation and then calculating the adsorption capacity by varying the pH. The model coefficients for the construction of these curves are shown in Table S2 (Supplementary Material).

Table 1. Experimental design (CCRD).

	Independent variable		Response variable					
			IY (%)			IU/g support		
Run	pH	NaCl (mM)	HA	HA-Cu^{2+}	HA-Ni^{2+}	HA	HA-Cu^{2+}	HA-Ni^{2+}
1	5.5	100	73.2	86.5	60.7	276	228	258
2	5.5	300	69.1	85.1	43.0	255	203	187
3	7.5	100	13.7	22.9	1.2	80	41	1
4	7.5	300	17.4	28.0	3.2	48	49	10
5	5.0	200	59.5	95.0	50.7	206	208	201
6	8.0	200	14.0	23.0	4.8	53	51	43
7	6.5	60	34.4	46.3	20.0	92	115	90
8	6.5	340	31.2	42.5	12.3	112	62	53
9	6.5	200	27.3	42.4	7.1	114	70	52
10	6.5	200	27.4	41.9	8.5	112	81	53
11	6.5	200	27.0	41.3	7.9	113	72	53

Table 2. ANOVA results.

	IY		IU/g support	
Support	R	p (≤0.1)	R	p (≤0.1)
HA	0.89	0.000132	0.82	0.000862
HA-Cu^{2+}	0.95	0.000005	0.91	0.000009
HA-Ni^{2+}	0.91	0.000092	0.86	0.000351

As shown in Fig. 2, there was a greater effect of pH, compared to ionic strength, in the process of immobilization of xylanase on HA-Me^{2+}. For all the supports, there was a significant (at the 90% confidence level) negative linear effect of pH on the two immobilization parameters (IY and A_{DER}), indicating that an increase in pH would lead to decreased xylanase immobilization, especially in the case of HA-Cu^{2+}, for which the values of the pH effects were higher. On the other hand, the interaction effects of pH and ionic strength were not statistically significant (in other words, the effects of these variables could be interpreted separately). Increase of the pH causes deprotonation of some of the charged amino acid residues of the enzyme, so the protein becomes increasingly negative. Hydroxyapatite has negative charges (in the pH 4-8 range

evaluated) and becomes even more negative with increasing pH, as demonstrated by zeta potential analysis (Coutinho *et al.*, 2018). Due to the negative charges of both enzyme and support, the less acidic immobilization conditions led to electrostatic repulsion between them, as reflected by the lower IY and consequently lower A_{DER}.

Charge repulsion between support and protein has been observed for the adsorption on HA of other proteins, such as BSA (Swain and Sarkar, 2013) and the phytase enzyme (Coutinho *et al.* 2019). These proteins have isoelectric points (pI) of 4.75 and 4.5, respectively, becoming negatively charged at pH above the pI, so they are not adsorbed on HA nanoparticles under alkaline conditions. Determination of the zeta potential of xylanase (using a Zetasizer 200 system), as a function of pH in the range 2-10, indicated that the enzyme used in this work presented pI of 3-4, associated with the xylanase groups with acid pI. This characteristic of xylanase evidenced that the decrease of IY at more alkaline pH was probably due to electrostatic repulsion between the negatively charged support and the enzyme.

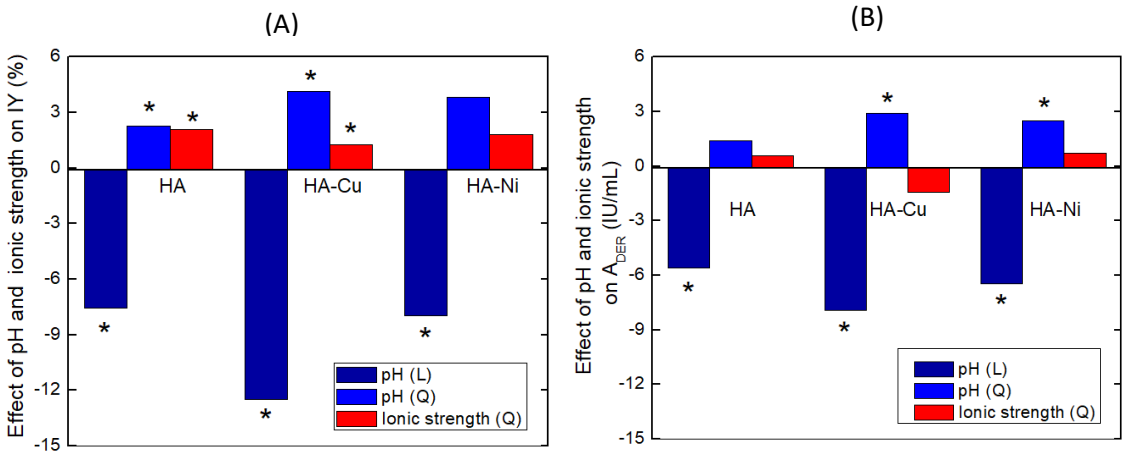

Fig. 2. Effects of pH and ionic strength on (A) IY and (B) A_{DER} for xylanase immobilization on HA, HA-Cu^{2+}, and HA-Ni^{2+}. Immobilization conditions: 5 mg protein/g support, 0.05 g support/mL, 1 h, 25 °C.

The linear effect of ionic strength in the process of immobilization of xylanase on HA-Me^{2+} was not significant. However, this interpretation was limited to the range of ionic strength evaluated (concentrations of 60-300 mM NaCl added to 20 mM acetate buffer). In an attempt to improve the immobilization parameters, adsorption experiments were performed with decrease of the NaCl concentration from 100 to 20 mM, fixing the pH at 5.5. This resulted in increases of IY from 61 to 79%, from 72 to 84%, and from 83 to 96% for the HA-Ni^{2+}, HA, and HA-Cu^{2+} supports, respectively. Therefore, the optimized conditions for xylanase immobilization on the HA-Me^{2+} supports were pH 5.5 (20 mM acetate sodium buffer) and 20 mM NaCl. The improvement in IY with decreased ionic strength suggested that electrostatic interactions could

have contributed to the process of adsorption of the enzyme on the support, since ionic adsorption on charged supports is favored using low ionic strength media.

The enzyme/support interaction experiments performed to establish the physicochemical conditions for the immobilization were conducted during periods of 60 min. The adsorption kinetics was investigated in order to determine the time taken for the immobilization process to stabilize, which showed that the protein concentration in the supernatant stabilized after only 30 min (Fig. 3).

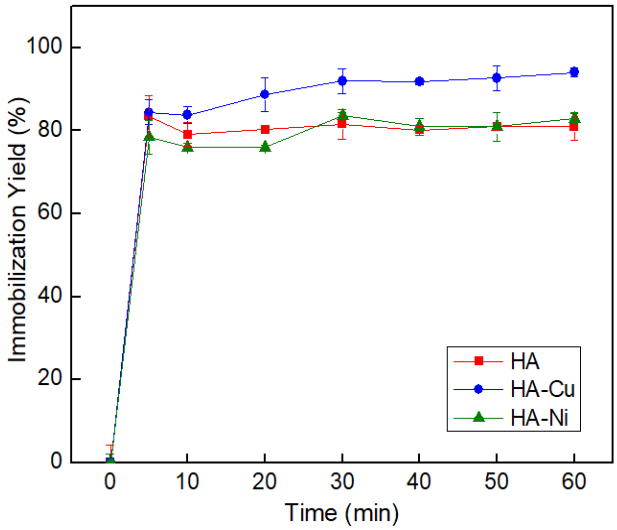

Fig. 3. Time course of immobilization of xylanase on HA, HA-Cu^{2+}, and HA-Ni^{2+} nanoparticles at 25 °C and pH 5.5 (in 20 mM sodium acetate buffer), using an enzymatic loading of 5 mg protein/g support and a support concentration of 0.05 g/mL.

This rapid stabilization of the adsorption kinetics demonstrated that there was strong attraction between xylanase and the HA supports tested. The fast adsorption (within 10 min) and strong attraction of enzymes on the HA support has recently been observed for the immobilization of lipase, β-glucosidase, and phytase, demonstrating the coordination of nucleophiles of the enzyme (negatively charged or neutral side-chains of amino acid residues containing at least one non-shared electron pair) to the central Ca^{2+} ion on the HA surface (Ivic *et al.*, 2016a; Coutinho *et al.*, 2018; Coutinho *et al.*, 2019). In order to understand the types of interactions that could have contributed to the immobilization of xylanase on the HA supports (pure and modified with Cu and Ni), desorption experiments were performed with potential desorbing agents, as described below.

3.3 Desorption studies

The results of the desorption experiments showed that for the three derivatives, xylanase desorption was highest in the presence of sodium citrate solution, followed by imidazole solution and sodium chlorite solution (Fig. 4).

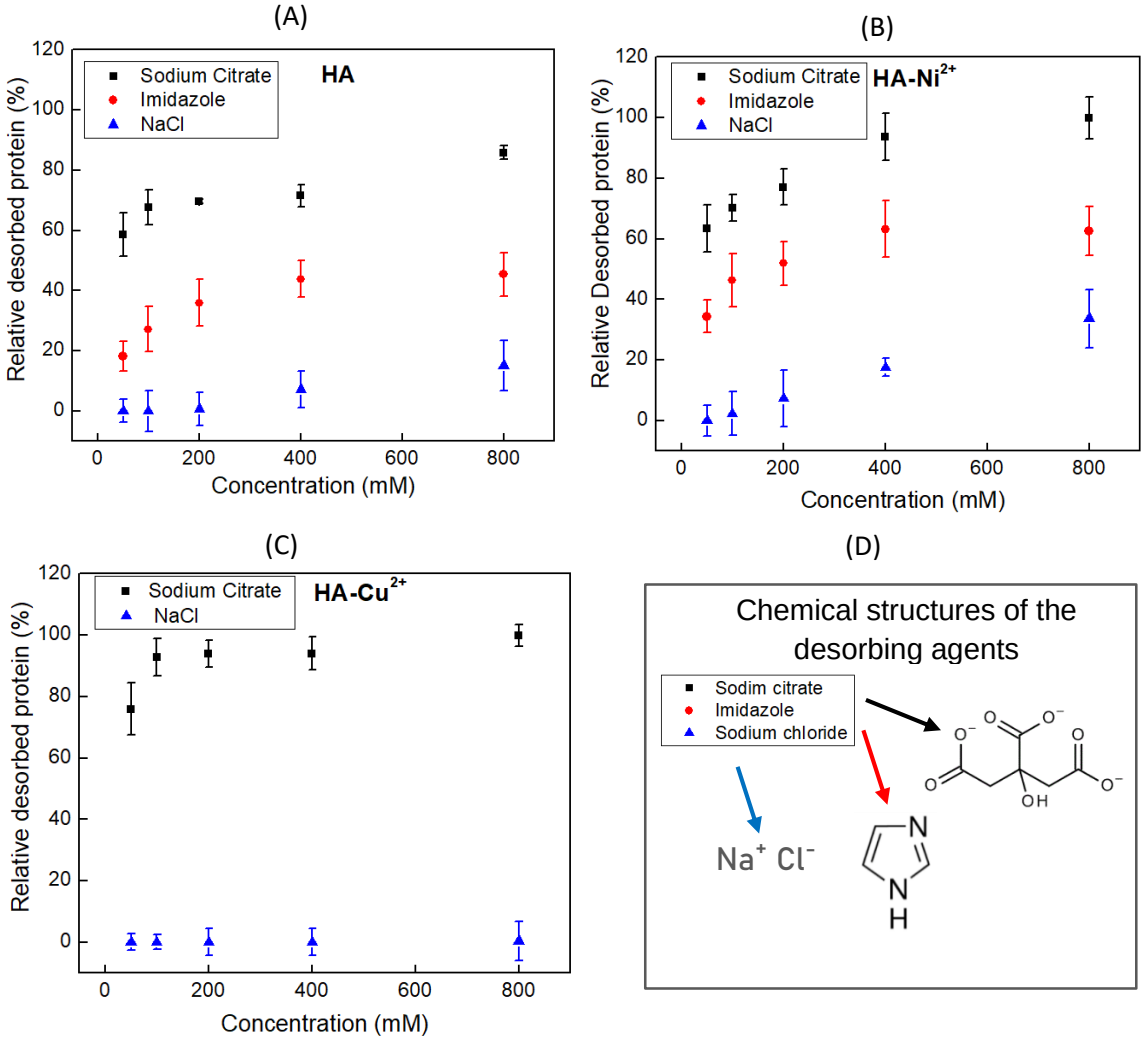

Fig. 4. Profiles of desorption of xylanase from the (A) HA, (B) HA-Cu^{2+}, and (C) HA-Ni^{2+} supports incubated in different solutions (all at pH 5) for 40 min. The enzyme was immobilized at pH 5.5 (20 mM), using an enzymatic loading of 5 mg protein/g support and a support concentration of 0.05 g/mL.

The sodium citrate salt acted as a strong desorption agent, almost completely leaching the enzyme from the supports, even at low salt concentrations. The ability of this salt to act as a desorbing agent was probably due to the higher affinity of the support for the COO^- groups abundant in the solution, compared to COO^- of the enzyme, leading to leaching of the enzyme from the HA-Me^{2+}. The xylanase used in this work was of fungal origin and mainly contained

endoxylanases (according to the manufacturer, Novozymes). In order to evaluate the surface amino acids of the xylanase studied, the 3D surfaces of two model endoxylanases from *Trichoderma reesei* and *Aspergillus niger* were obtained from the Protein Data Bank (PDB) . The 3D surfaces (Fig. 5) showed that both xylanases mainly presented the amino acids glutamate and aspartate in their surface structures, resulting in the presence of many carboxylate groups on the surface.

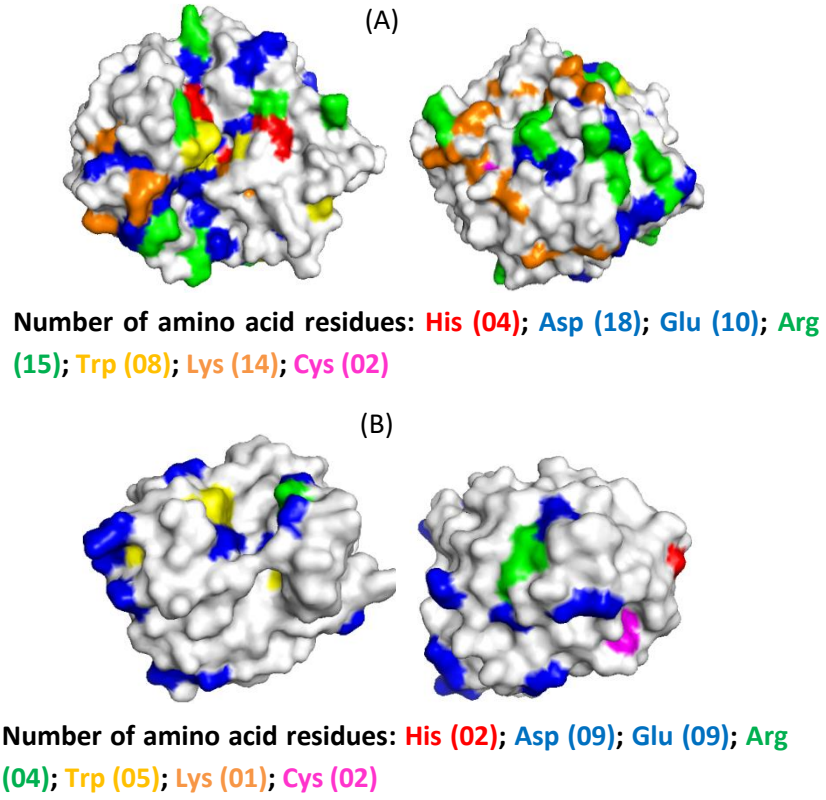

Fig. 5. 3D surfaces of endoxylanases from (A) *Trichoderma reesei* (Protein Data Bank, code 4XV0) and (B) *Aspergillus niger* (Protein Data Bank, code 6QE8), both constructed using the PyMOL Molecular Graphics System, Version 2.3.3 Schrödinger, LLC. The model structures of the xylanases show both faces, with colors representing the amino acid residues, as follows: red – His; blue – Glu and Asp; green – Arg; yellow – Trp; orange – Lys; magenta – Cys.

This feature, together with the results of desorption using sodium citrate, provided strong evidence that coordination between divalent cations on the HA structure and carboxylate groups on the enzyme surface was the predominant phenomenon in the chemical immobilization process. It could be inferred from the desorption curves that the affinity between the metal cations present on the supports and the carboxylate groups in solution followed the order $Cu^{2+} > Ni^{2+} > Ca^{2+}$, since desorption increased in this order. It has been reported previously that Cu^{2+} is more selective

than Ni^{2+} for chelation with COO^-, due to the smaller atomic radius of Cu^{2+}, which implies a higher force between the nucleus and the electrosphere (Bresolin *et al.*, 2009).

In the same way, in the presence of the imidazole agent, the behaviors observed for xylanase desorption from the supports (HA, HA-Ni^{2+}, and HA-Cu^{2+}) differed from each other. Incubation in the presence of 800 mM imidazole resulted in 60% release of the immobilized enzyme from the HA-Ni^{2+} support, while only 40% release was observed from the HA support, under the same conditions. This indicated that the HA-Ni^{2+} support had greater attraction for the imidazole groups present in solution, compared to the HA support, with the imidazole forming more stable chelates with Ni^{2+} than with Ca^{2+} (Bresolin *et al.*, 2009). In the case of xylanase desorption from the HA-Cu^{2+} support, it was not possible to construct the desorption curves, due to a change in the color of the supernatant, from transparent to intense blue, after incubation of the immobilized enzyme in the imidazole solution, making it unfeasible to quantify the protein in the supernatant using the Bradford method. This suggested that it was not only xylanase that was released from the HA-Cu^{2+} support, but also Cu^{2+}, by chelation with the imidazole rings. These results indicated that coordination interactions between the metal ions on the supports and the imidazole nitrogen of histidine residues on the enzyme surface may have contributed to the immobilization process, which was most pronounced for HA-Cu^{2+}, followed by HA-Ni^{2+} and HA.

In previous work, this type of interaction was observed for the adsorption of myoglobin on a hydroxyapatite matrix modified with Cu^{2+}, Zn^{2+}, and Ni^{2}, with the affinity following the order: $Cu^{2+} > Zn^{2+} > Ni^{2+}$ (Farinas *et al.*, 2007). Although the desorption results indicated the possible occurrence of interactions between the metals and amino acid residues (His) containing imidazole, this type of interaction probably did not prevail in the anchoring of the enzyme on the support, due to the presence of few histidine amino acid residues on the xylanase surface, as shown in Fig. 5. In the case of the HA-Cu^{2+} support, for example, four molecules of ammonium (in the imidazole *ring)* on the enzyme surface would be required for complexing with Cu^{2+}, due to its coordination number of 4 (Arnold, 1991). In addition, the amino acid residues (His) capable of complexing with cations should be close in the protein structure, in order to be able to form coordinate bonds (Gutierrez *et al.*, 2007).

Similar low desorption of xylanase from the HA and HA-Ni^{2+} supports was observed in the presence of sodium chloride, while no protein was desorbed from HA-Cu^{2+}, even at high sodium chloride concentrations (up to 800 mM). These results suggested that coupling of the enzyme to HA-Me^{2+} was influenced by ionic interactions, which were probably more pronounced for HA and HA-Ni^{2+}, compared to HA-Cu^{2+}. Although electrostatic interactions contributed to anchoring of the enzyme to the support, a general conclusion of the desorption experiments was that the immobilization of xylanase on the HA-Me^{2+} supports was probably mainly due to coordination interactions between metal ions on the support surface (Ca^{2+}, Cu^{2+}, and Ni^{2+}) and electron pair donors on the enzyme surface, such as carboxylate (from Glu and Asp, which are abundant on the

xylanase surface, as shown in Fig. 5) (Arnold, 1991; Gutierrez *et al.*, 2007; Bresolin *et al.*, 2009). Other amino acids with groups containing electron pairs available for coordination bonds may interact with metals, such as the amino acids His, Arg, Trp, and Lys (Kumar *et al.*, 1998), which are also present on the xylanase surface, but in smaller proportions than Glu and Asp (Fig. 5). In addition, other weaker links may have contributed to binding of the enzyme to the supports, such as van der Waals forces and hydrogen bonds (Johnson and Arnold, 1995).

3.4 Enzymatic loading and adsorption isotherms

Adsorption isotherms were constructed in order to establish the maximum adsorption capacity of each support, as well as to identify any differences in the affinity of the xylanase for the different HA-Me^{2+} supports. The Langmuir adsorption model fitted to the experimental data indicated that the adsorption occurred as a monolayer, without interaction among the adsorbed enzymes. The equilibrium values for the affinity constant ($1/K_L$) and maximum adsorption capacity (Q_m) are shown in Fig. 6.

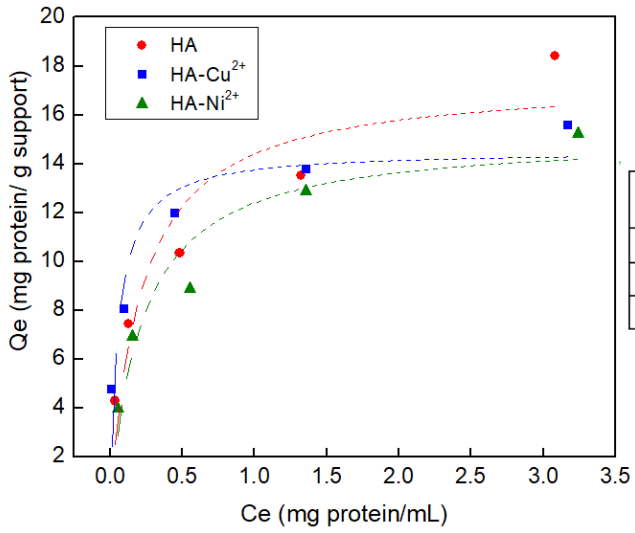

Support	$1/K_L$ (mg mL^{-1})	Q_m (mg P g^{-1} support)	R^2
HA	0.219	17.45 ± 2.1	0.84
HA-Cu^{2+}	0.057	14.52 ± 1.2	0.84
HA-Ni^{2+}	0.222	15.15 ± 1.4	0.89

Fig. 6. Profiles for the adsorption of xylanase on HA, HA-Cu^{2+}, and HA-Ni^{2+}. The dashed lines represent Langmuir isotherms fitted to the experimental data. Immobilization conditions: pH 5.5, 20 mM, 0.05 g support/mL, 1 h, 25 °C.

Although the adsorption curves were quite similar, the affinity constants showed that the xylanase had greater affinity for the HA-Cu^{2+}. On the other hand, the maximum adsorption capacities of the supports did not differ significantly (considering the standard deviations), with a maximum protein loading of around 17 mg protein g^{-1} support. The immobilization yield (IY) decreased with increase of the enzymatic loading provided for immobilization (data not shown), such that attainment of the maximum adsorption capacity (14-17 mg protein g^{-1} support) required the provision of 80 mg protein g^{-1} support in the immobilization process. For this reason, in order

to define the best enzymatic loading for use in the immobilization protocol, the final activity of the derivative (A_{DER}) was evaluated. A loading of 20 mg protein g^{-1} support resulted in the highest A_{DER} values for the three supports evaluated (Table 3), suggesting that mass transfer delays could have limited the reaction rate for the other higher-loaded derivatives.

Table 3. Activities of the derivatives (A_{DER}) obtained using different enzymatic loadings in the xylanase immobilization procedure.

		Enzymatic loading (mg protein g^{-1} support)				
		5	10	**20**	40	80
A_{DER} (IU g^{-1} support)	HA	302	421	**522**	479	486
	HA-Cu^{2+}	358	438	**475**	461	378
	HA-Ni^{2+}	359	361	**448**	416	389

3.5 Activity profiles and thermostability

Evaluation was made of the effects of pH and temperature on the activity of the xylanase, either free or immobilized on HA, HA-Ni^{2+}, and HA-Cu^{2+}. The pH profiles for the free and immobilized enzymes were similar, although some differences can be highlighted (Fig. 7A).

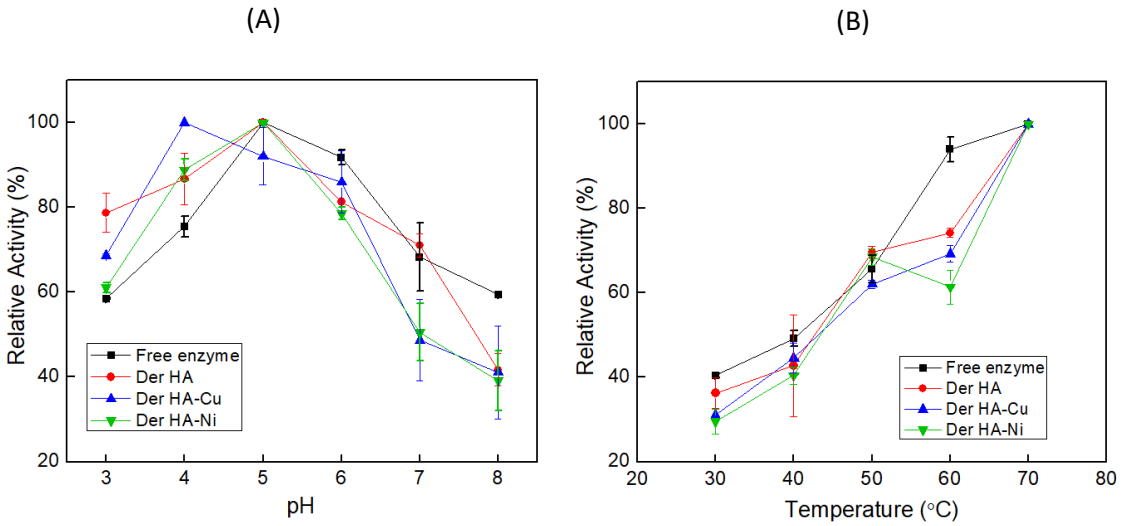

Fig. 7. Profiles of the activities of xylanase, free and immobilized on HA, HA-Cu^{2+}, and HA-Ni^{2+}, at different (A) pHs and (B) temperatures. In the legend, "Der" is an abbreviation of Derivative.

The enzymes immobilized on the HA supports showed higher relative activity (RA) at acidic pH (3 and 4), compared to the free enzyme. Therefore, under the most acidic hydrolysis conditions, the immobilized xylanase presented higher performance than the free xylanase. The

improved activities of the immobilized enzymes at different reaction pH values could be explained by the immobilization method employed. The electrostatic potential of the microenvironment of enzymes immobilized on HA (which contains ionized species such as Ca^{2+}, Ni^{2+}, Cu^{2+}, and PO_4^{3-}) can affect the local concentration of H^+, influencing the behavior of the enzyme under different pH conditions. On the other hand, at more alkaline pH (7 and 8), the free enzyme was more effective than the enzymes immobilized on the supports, with the exception of the xylanase immobilized on HA, which presented the same action as the free enzyme, at pH 7. There was no change in the optimal pH of the enzyme after its immobilization on HA and HA-Ni^{2+}, while for the enzyme immobilized on HA-Cu^{2+}, the optimum pH changed from 5 to 4.

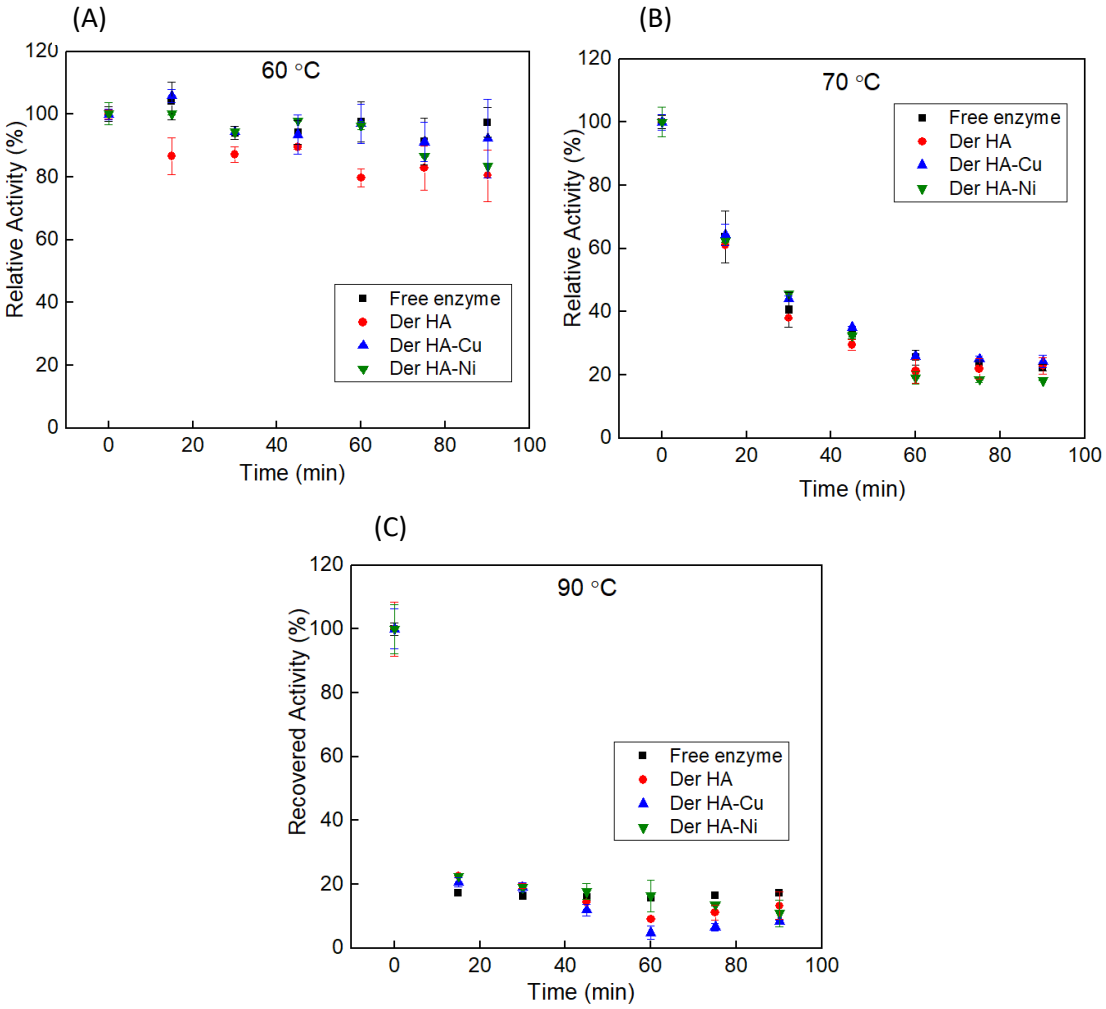

Fig. 8. Thermal inactivation profiles of xylanase, free and immobilized on HA, HA-Cu^{2+}, and HA-Ni^{2+}, at (A) 60, (B) 70, and (C) 90 ºC. In the legend, "Der" is an abbreviation of Derivative.

The temperature profiles obtained for the free and immobilized enzymes were similar, with maximum activities reached at 70 °C, in the temperature range evaluated (Fig. 7B). The similarities of the profiles of both pH and temperature for the free and immobilized enzymes suggested that there were no significant conformational changes in the enzyme structure that

affected the enzymatic activity. Similar findings were reported previously for the immobilization of β-glucosidase on HA nanoparticles, in the pH and temperature ranges evaluated (Coutinho *et al.*, 2018).

Immobilization of the enzyme on the different supports did not alter the xylanase thermal deactivation profile. The free and immobilized enzymes retained, on average, 90% of their initial activities after 90 min at 60 °C, while they retained around 20 and 10% after 90 min at 70 and 90 °C, respectively (Fig. 8). Higher thermostability of immobilized enzymes has been reported previously, notably for enzymes covalently linked to the supports (Borges *et al.*, 2014; Mendes *et al.*, 2013; Pal and Khanum, 2011). However, a high degree of stabilization is not expected when an enzyme is physically or ionically adsorbed on a solid support, due to the reversibility of the enzyme-support bonds, and the three-dimensional structure of the native enzyme is almost always preserved (Jesionowski *et al.*, 2014).

3.6 Hydrolysis of xylan and reuse assays

The performance of the biocatalysts (free and immobilized xylanases) were evaluated in the hydrolysis of xylan, by monitoring xylose released into the reaction medium. The free and immobilized enzymes presented similar hydrolysis profiles, yielding a xylose concentration of around 26 μmol mL^{-1} after reaction for 3 h (Fig. 9A). These findings showed that under the conditions evaluated, there was no diffusional delay for the reactions catalyzed by the xylanases immobilized on the HA supports. The metal ions (Ca^{2+}, Cu^{2+}, or Ni^{2+}) present on the HA surface did not appear to affect the reaction kinetics, neither activating nor inhibiting the enzyme.

The reusability of the immobilized xylanases is an important consideration for industrial applications. The HA-Cu^{2+} catalyst showed the best performance in the reuse assays, retaining up to 80% of the original activity in the second cycle. For all the supports, a decrease in xylan hydrolysis was observed at each cycle, up to the fifth cycle (Fig. 9B), after which the hydrolysis remained constant for the next 4 cycles (data not shown). The results revealed that in all the cycles, the xylanase immobilized on HA-Cu^{2+} provided higher xylose yields, compared to the other derivatives. The higher stability of this derivative in the reuse assays could be related to the previous findings that greater insertion of Cu than Ni in the HA support (Section 3.1) resulted in a higher immobilization yield (Section 3.2), with higher affinity of the enzyme for HA-Cu^{2+} than for the HA and HA-Ni^{2+} supports (Section 3.4). Use of the hydroxyapatite support modified with Cu resulted in the formation of chelates with xylanase that were more stable (Section 3.3) and able to complex more effectively with proteins (Farinas *et al.*, 2007; Gutierrez *et al.*, 2007). For this reason, the xylanase/HA-Cu^{2+} derivative showed the greatest potential for use in future studies.

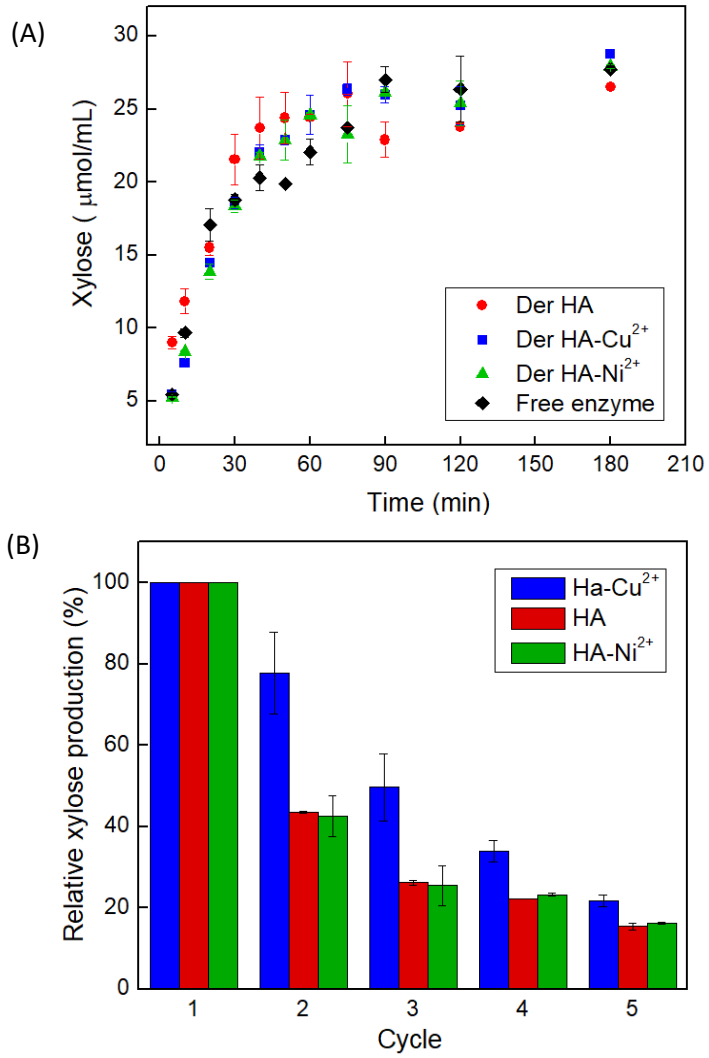

Fig. 9. (A) Xylan hydrolysis by xylanase, free and immobilized on HA, HA-Cu^{2+}, and HA-Ni^{2+}. Reaction conditions: 60 U/g xylan, 20 g xylan/L, 50 °C. (B) Reuse of immobilized xylanase in the hydrolysis of xylan, under the same conditions.

4. Conclusions

Hydroxyapatite nanoparticles, used pure or modified with metal ions (Cu^{2+} and Ni^{2+}), were shown to be potential supports for immobilization of the xylanase enzyme. A simple, fast, and efficient immobilization protocol was developed using experimental design, generating derivatives by coordination interactions between metal ions on the support surface and electron donor groups on the enzyme surface. The activity profiles at different pH and temperature for the immobilized enzyme remained the same as for the soluble enzyme, indicating that the xylanase did not undergo major changes in its conformational state after immobilization. The affinity constant values obtained from adsorption isotherms indicated that xylanase showed higher affinity for the HA-Cu^{2+} support compared to HA and HA-Ni^{2+}. This fact became even more evident in the recycling experiments, in which the derivative of HA-Cu^{2+} showed the best results,

resulting in a promising derivative for applications of industrial interest, such as in the biofuel, pharmaceutical, pulp, and food & beverage sectors.

5. References

Andre, R., Paris, E., Gurgel, M., Rosa, I., Paiva-Santos, C., Li, M., Varela, J., Longo, E., 2012. Structural evolution of Eu-doped hydroxyapatite nanorods monitored by photoluminescence emission. Journal of Alloys and Compounds 531, 50-54.

Aragon, C.C., Santos, A.F., Ruiz-Matute, A.I., Corzo, N., Guisan, J.M., Monti, R., Mateo, C., 2013. Continuous production of xylooligosaccharides in a packed bed reactor with immobilized-stabilized biocatalysts of xylanase from Aspergillus versicolor. Journal of Molecular Catalysis B-Enzymatic 98, 8-14.

Arnold, F.H., 1991. Metal-affinity separations - a new dimension in protein processing. Bio-Technology 9, 151-156.

Bailey, M.J., Biely, P., Poutanen, K., 1992. Interlaboratory testing of methods for assay of xylanase activity. Journal of Biotechnology 23, 257-270.

Beg, Q.K., Kapoor, M., Mahajan, L., Hoondal, G.S., 2001. Microbial xylanases and their industrial applications: a review. Applied Microbiology and Biotechnology 56, 326-338.

Borges, D., Baraldo, A., Farinas, C., Giordano, R., Tardioli, P., 2014. Enhanced saccharification of sugarcane bagasse using soluble cellulase supplemented with immobilized beta-glucosidase. Bioresource Technology 167, 206-213.

Bradford, M.M., 1976. Rapid and sensitive method for quantitation of microgram quantities of protein utilizing principle of protein-dye binding. Analytical Biochemistry 72, 248-254.

Bresolin, I., Miranda, E., Bueno, S., 2009. Immobilized metal-ion affinity chromatography (imac) of biomolecules: fundamental aspects and technological applications. Quimica Nova 32, 1288-1296.

Cipolatti, E., Silva, M., Klein, M., Feddern, V., Feltes, M., Oliveira, J., Ninow, J., de Oliveira, D., 2014. Current status and trends in enzymatic nanoimmobilization. Journal of Molecular Catalysis B-Enzymatic 99, 56-67.

Coutinho, T.C., Rojas, M.J., Tardioli, P.W., Paris, E.C., Farinas, C.S., 2018. Nanoimmobilization of beta-glucosidase onto hydroxyapatite. International Journal of Biological Macromolecules 119, 1042-1051.

Coutinho, T.C., Tardioli, P.W., Farinas, C.S., Phytase Immobilization on Hydroxyapatite Nanoparticles Improves Its Properties for Use in Animal (2019). Applied Biochemistry and Biotechnology, 2.

Driss, D., Zouari-Ellouzi, S., Chaari, F., Kallel, F., Ghazala, I., Bouaziz, F., Ghorbel, R., Chaabouni, S.E., 2014. Production and in vitro evaluation of xylooligosaccharides generated from corncobs using immobilized Penicillium occitanis xylanase. Journal of Molecular Catalysis B-Enzymatic 102, 146-153.

Farinas, C., Loyo, M., Baraldo, A., Tardioli, P., Neto, V., Couri, S., 2010. Finding stable cellulase and xylanase evaluation of the synergistic effect of pH and temperature. New Biotechnology 27, 810-815.

Farinas, C., Reis, P., Ferraz, H., Salim, V., Alves, T., 2007. Adsorption of myoglobin onto hydroxyapatite modified with metal ions. Adsorption Science & Technology 25, 717-727.

Gutierrez, R., del Valle, E.M.M., Galan, M.A., 2007. Immobilized metal-ion affinity chromatography: Status and trends. Separation and Purification Reviews 36, 71-111.

HENCH, L.L., WILSON, J., 1993. An introduction to bioceramics, First ed. World Scientific, Singapore.

Ivic, J., Dimitrijevic, A., Milosavic, N., Bezbradica, D., Drakulic, B., Jankulovic, M., Pavlovic, M., Rogniaux, H., Velickovic, D., 2016a. Assessment of the interacting mechanism between Candida rugosa lipases and hydroxyapatite and identification of the hydroxyapatite-binding sequence through proteomics and molecular modelling. Rsc Advances 6, 34818-34824.

Ivic, J., Velickovic, D., Dimitrijevic, A., Bezbradica, D., Dragacevic, V., Jankulovic, M., Milosavic, N., 2016b. Design of biocompatible immobilized Candida rugosa lipase with potential application in food industry. Journal of the Science of Food and Agriculture 96, 4281-4287.

Jampala, P., Preethi, M., Ramanujam, S., Harish, B.S., Uppuluri, K.B., Anbazhagan, V., 2017. Immobilization of levan-xylanase nanohybrid on an alginate bead improves xylanase stability at wide pH and temperature. International Journal of Biological Macromolecules 95, 843-849.

Javed, M., Buthe, A., Rashid, M., Wang, P., 2016. Cost-efficient entrapment of beta-glucosidase in nanoscale latex and silicone polymeric thin films for use as stable biocatalysts. Food Chemistry 190, 1078-1085.

Jesionowski, T., Zdarta, J., Krajewska, B., 2014. Enzyme immobilization by adsorption: a review. Adsorption-Journal of the International Adsorption Society 20, 801-821.

Johnson, R.D., Arnold, F.H., 1995. Multipoint binding and heterogeneity in immobilized metal affinity-chromatography. Biotechnology and Bioengineering 48, 437-443.

Kollath, V., Van den Broeck, F., Feher, K., Martins, J., Luyten, J., Traina, K., Mullens, S., Cloots, R., 2015. A Modular Approach To Study Protein Adsorption on Surface Modified Hydroxyapatite. Chemistry-a European Journal 21, 10497-10505.

Kumar, A., Galaev, I.Y., Mattiasson, B., 1998. Metal chelate affinity precipitation: a new approach to protein purification. Bioseparation 7, 185-194.

Liu, M.Q., Huo, W.K., Xu, X., Jin, D.F., 2015. An immobilized bifunctional xylanase on carbon-coated chitosan nanoparticles with a potential application in xylan-rich biomass bioconversion. Journal of Molecular Catalysis B-Enzymatic 120, 119-126.

Mendes, A.A., de Castro, H.F., Andrade, G.S.S., Tardioli, P.W., Giordano, R.D.C., 2013. Preparation and application of epoxy-chitosan/alginate support in the immobilization of microbial lipases by covalent attachment. Reactive & Functional Polymers 73, 160-167.

Miller, G.L., 1959. Use of dinitrosalicylic acid reagent for determination of reducing sugar. Analytical Chemistry 31, 426-428.

Norgaard, J.V., Pedersen, T.F., Blaabjerg, K., Knudsen, K.E.B., Laerke, H.N., 2016. Xylanase supplementation to rye diets for growing pigs. Journal of Animal Science 94, 91-94.

Pal, A., Khanum, F., 2011. Covalent immobilization of xylanase on glutaraldehyde activated alginate beads using response surface methodology: Characterization of immobilized enzyme. Process Biochemistry 46, 1315-1322.

Protein Data Bank. Available on https://www.rcsb.org/. Accessed in 10/october/2019.

Sadat-Shojai, M., Khorasani, M., Dinpanah-Khoshdargi, E., Jamshidi, A., 2013. Synthesis methods for nanosized hydroxyapatite with diverse structures. Acta Biomaterialia 9, 7591-7621.

Schomburg, D., Schomburg, I., 2009. Springer Handbook of Enzymes, Second ed. Springer, New York.

Shahrestani, H., Taheri-Kafrani, A., Soozanipour, A., Tavakoli, O., 2016. Enzymatic clarification of fruit juices using xylanase immobilized on 1,3,5-triazine-functionalized silica-encapsulated magnetic nanoparticles. Biochemical Engineering Journal 109, 51-58.

Swain, S.K., Sarkar, D., 2013. Study of BSA protein adsorption/release on hydroxyapatite nanoparticles. Applied Surface Science 286, 99-103.

Vaghari, H., Jafarizadeh-Malmiri, H., Mohammadlou, M., Berenjian, A., Anarjan, N., Jafari, N., Nasiri, S., 2016. Application of magnetic nanoparticles in smart enzyme immobilization. Biotechnology Letters 38, 223-233.

Woolridge, E.M., 2014. Mixed Enzyme Systems for Delignification of Lignocellulosic Biomass. Catalysts 4, 1-35.

Xie, W., Zang, X., 2017. Covalent immobilization of lipase onto aminopropyl-functionalized hydroxyapatite-encapsulated-gamma-Fe2O3 nanoparticles: A magnetic biocatalyst for interesterification of soybean oil. Food Chemistry 227, 397-403.

Yelten, A., Yilmaz, S., Oktar, F.N., 2012. Sol-gel derived alumina-hydroxyapatite-tricalcium phosphate porous composite powders. Ceramics International 38, 2659-2665.

Zydney, A.L., 2016. Continuous downstream processing for high value biological products: A Review. Biotechnology and Bioengineering 113, 465-475.

CHAPTER 5

Article in preparation:

Hydroxyapatite magnetic nanoparticles (HA:$CoFe_2O_4$) for enzymes immobilization: β-glucosidase, phytase and xylanase

Graphical Abstract

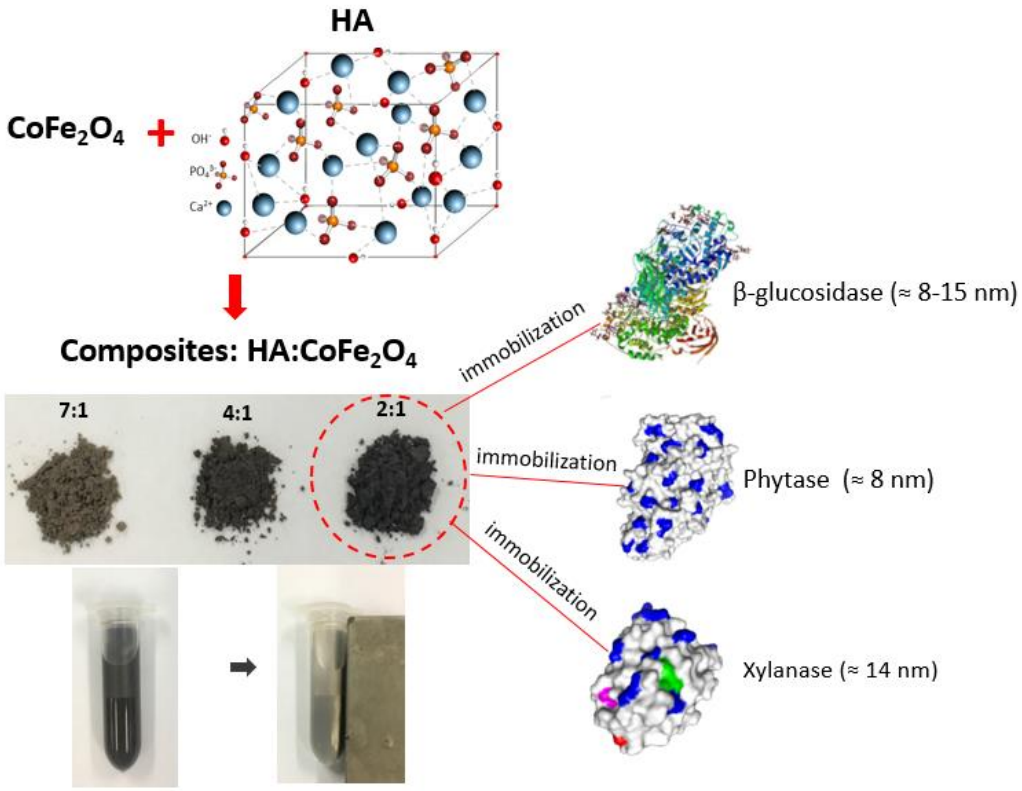

Abstract

The development of new biocatalytic systems using magnetic particles has been increasing in recent years, since this type of material can be fast recovered from the reaction medium by applying an external magnetic field. Hydroxyapatite (HA) is a ceramic material that can be employed for the preparation of magnetic composites for enzyme immobilization thanks to its good chemical properties and to its great ability to interact with proteins. Cobalt ferrite ($CoFe_2O_4$) is a material purely magnetic that has excellent chemical stability, ease of synthesis and mechanical hardness, however is still few used to compose magnetic materials. In this work the HA:$CoFe_2O_4$ composite was synthetized with different HA and $CoFe_2O_4$ proportions by the coprecipitation method in order to obtain an effective matrix for enzyme immobilization. The enzymes utilized were β-glucosidase, phytase and xylanase, which are widely used in the biofuel, pharmaceutical and food & beverage industrial sectors, among others. The results demonstrated that for phytase and xylanase, the composite with the highest cobalt ferrite content (2:1) showed higher immobilization yield (IY) and higher final derivative activity (A_{DER}) than the other composites; while β-glucosidase showed similar and high values of IY and A_{DER} for the three composites evaluated. For these reasons, the composite 2:1 was chosen as a matrix for these enzymes, favoring their recovery step from the medium reaction. The derivatives were obtained by means of a very simple and fast adsorption protocol, resulting in the formation of coordination bonds between HA:$CoFe_2O_4$ and enzymes, complemented by ionic bindings. The enzymes immobilized could be easily recovered from the medium reaction by applying a magnetic field and then be reused, demonstrating promising applications of industrial interest.

Key-words: enzymes, immobilization, magnetic nanoparticles, hydroxyapatite, cobalt ferrite.

1. Introduction

The use of magnetic particles is an important area of interest for enzyme immobilization, which has made significant progress in recent years in the development of new biocatalytic systems (Alftren and Hobley, 2013; Liu *et al.*, 2014; Kopp *et al.*, 2015;; Xia *et al.*, 2016; Garcia Embid *et al.*, 2018). The use of magnetic supports allows the biocatalyst to be recovered from the reaction medium more rapidly by applying an external magnetic field than using other techniques such as filtration and centrifugation (Vaghari *et al.*, 2016). In addition, the catalytic reaction can be readily stop by taking out the enzyme from the solution. The nanomaterials, as magnetic nanoparticles, have unique properties due the large surface area-to-volume ratio and reactivity, being applied in various fields as catalysis and adsorption process for example, however they tend to undergo aggregation because of their magnetic dipole-dipole attractions (Xie and Zang, 2017). Therefore, the incorporation of magnetic nanoparticles into inert materials can form a composite matrix, in which both materials are merged and effectively prevent material aggregation, improving the chemical stability (Netto *et al.*, 2013).

Hydroxyapatite (HA) is an important inorganic material with the formula $Ca_{10}(PO_4)_6(OH)_2$ that can potentially be employed for the preparation of magnetic composites thanks to its good physicochemical stability, non-toxicity and ease of further surface modification (Hench and Wilson, 1993; Foroughi *et al.*, 2015;; Qi *et al.*, 2017). Besides that, HA has great ability to interact with proteins, mainly due to electrostatic interactions of the phosphate and calcium groups of HA with charged side groups of proteins and also due to chelation of calcium groups of HA with electron donor groups of proteins (Gagnon, 2009). For these reasons HA has been investigated as a matrix for protein adsorption which has been utilized in different areas, such as separation of proteins by chromatography (Farinas *et al.*, 2007; Kojima *et al.*, 2018), bone regeneration in biomedicine (Tohamy *et al.*, 2018) and drug delivery in the pharmaceutical industry (Kollath *et al.*, 2015).

The potential of HA nanoparticles as a support for enzyme immobilization is beginning to be explored (Yewle *et al.*, 2012; Ivic *et al.*, 2016; Xie and Zang, 2017). Our recent reports have demonstrated the immobilization of important enzymes with different applications in industry (β-glucosidase, phytase and xylanase) in pure HA through a single adsorption step (Coutinho *et al.*, 2018; Coutinho *et al.*, 2019*;* Coutinho *et al.*, 2020). These enzymes are used in the biofuel, pharmaceutical, pulp, and food & beverage sectors, among others (Polizeli *et al.*, 2005; Graebin *et al.*, 2016; Jain *et al.*, 2016). The results have shown that chelation reactions between the metals ions present in HA and the carboxylic acid groups of enzymes occur rapidly, resulting in highly stable and promising interactions for enzyme immobilization. For β-glucosidase it was possible to recycle the derivative and retain 70% of the initial activity during at least 10 hydrolysis cycles (Coutinho *et al.*, 2018). For phytase, the derivative showed broader activity profile as to pH and temperature, and higher stability at high temperatures than free enzyme, demonstrating potential

applications in animal feed (Coutinho *et al.* 2019). For xylanase, the enzyme showed higher affinity for the HA support modified with cupper, resulting in a promising derivative for applications of industrial interest (Coutinho *et al.*, 2020). Despite these excellent results, the recoverability of these biocatalysts could be improved by the use of a magnetic support.

Most of studies on the immobilization of enzyme using magnetic supports reported in literature has utilized iron oxide (Fe_3O_4) nanoparticles, due to the low toxicity and biocompatibility of the material, being other ferrites still few explored for this application (Netto *et al.*, 2013; Liu *et al.*, 2014; Zhang *et al.*, 2015). In this sense, another material purely magnetic is cobalt ferrite ($CoFe_2O_4$), which has excellent chemical stability, ease of synthesis and mechanical hardness, being a promising candidate for enzyme immobilization (Bohara *et al.*, 2016). Moreover, its transition metal ions, Co^{2+} and Fe^{2+}, could chelate electron donor atoms including O, N and S from proteins, contributing to the immobilization process (Wang *et al.*, 2019). There are some recent reports in the literature on the synthesis of the HA composite with cobalt ferrite using the microemulsion method (Foroughi *et al.*, 2015), the chronoamperometry technique (Abdel-Hamid *et al.*, 2017), the microwave assisted wet precipitation method (Sangeetha *et al.*, 2019) and the hydrothermal process (Karthickraja *et al.*, 2019). However, these works have synthesized the composite for different applications, which do not include enzyme immobilization in order to recovery the enzyme in industrial biocatalysis processes.

The aim of this work was to synthesize the composites of hydroxyapatite and cobalt ferrite by the coprecipitation method, using different proportions of HA and $CoFe_2O_4$, in order to immobilize the enzymes β-glucosidase, phytase and xylanase. The distribution of elements in nanocomposites obtained (HA:$CoFe_2O_4$) was investigated by field emission gun-scanning electron microscopy (SEM-EDS) technique, the crystallinity was investigated using X-ray diffraction (XRD) and the specific surface area was investigated using nitrogen adsorption/desorption isotherms (BET method). The biochemical behavior of the immobilized enzymes on HA:$CoFe_2O_4$ was evaluated considering the changes in the activity profile at different pHs and temperatures, the degree of leaching from the supports using different desorbing agents and the thermal stability of the enzyme. The efficiency of the immobilized enzymes was evaluated in the hydrolysis of the specifics substrates, and the ability to reuse the biocatalyst was assessed. The aim was to investigate the improvement in the properties of the derivatives and to enable their recovery and reuse through magnetic field application.

2. Material and Methods

2.1 Material

The β-glucosidase (NS22118) and xylanase (NS22083) enzymes was donated by Novozymes (Denmark); the phytase enzyme (Natuphos®) was produced commercially by a

genetically modified strain of *Aspergillus niger* (Rychen *et al.*, 2017) and was kindly donated by BASF S/A (Mount Olive, USA). The cellobiose, xylan and phytate substrates as well as hydroxyapatite were purchased from Sigma-Aldrich (St. Louis, MO, USA). The HA nanoparticles were needle-shaped particles with a size range of 12-32 nm and surface area of 58.2 m^2 g^{-1} (Coutinho *et al.*, 2018). All other reagents were analytical grade.

2.2 Preparation of the magnetic hydroxyapatite supports (HA-$CoFe_2O_4$)

The synthesis of cobalt ferrite nanoparticles ($CoFe_2O_4$) was perfomed by the coprecipitation method. Initially were prepared two solutions of iron (III) (0.40 mol L^{-1}), and cobalt (II) (0.20 mol L^{-1}) by salts solubilization, ferrite nitrate and cobalt nitrate, under magnetic stirring. After completed the solubilization and homogeneization it was added sodium hydroxide (NaOH) 3.00 mol L^{-1} until the formation of black precipitate. Subsequently, the solution containing the precipitate was washed to a pH equivalent to 7 and centrifugated (10,000 rpm for 10 min and 15 °C) by Branonan – Digital Sonifier ultrassom. At the end, the precipitate was dried in a circulation oven at 50 °C for 24 h and thermally treated for 4 h at 300 °C and 700 °C for 3 h. To obtain the HA:$CoFe_2O_4$ nanocomposite, the proportions os 2:1, 4:1 and 7:1 (w/w) were used. After accomplished the co-precipitation stage on the iron and cobalt salts, HA was added and disperse together in proportion proper. Subsequetly, the steps of the procedure were similar to that described above.

2.3 Characterization of the magnetic hydroxyapatite supports (HA-$CoFe_2O_4$)

The FEG-SEM (field emission gun-scanning electron microscopy) technique was used to analyze the morphology of the composites nanoparticles. A surface of a metallic disc (stub) was coated with graphite and the sample was dispersed over it. The sample was analyzed using a JEOL Model JSM-6701F microscope operated at 2.0 kV, with 1.0 nm resolution. The energy dispersive X-ray spectroscopy (EDS) technique was used for qualitative analysis of the chemical composition of the composite particles. For this, the surface of a metallic disc (stub) was coated with graphite and the sample was dispersed over it. The sample was analyzed (in duplicate) using a JEOL Model JSM-6510 scanning electron microscope operated at 15 kV, with 10 nm resolution.

The crystallinity of the hydroxyapatite, the cobalt ferrite and the composites HA-$CoFe_2O_4$ was investigated using X-ray diffraction (XRD) measurements performed with a Shimadzu Model 6000 instrument. The diffractograms were recorded in the 2Θ range 20-70º, at a scanning rate of 1º min^{-1}, using a Cu Kα incident beam (λ = 0.1546 nm). The specific surface area (SSA) was determined by means of nitrogen isotherms, according to the Brunauer, Emmett, and Teller (BET) method, employing a surface area analyzer (ASAP 2020, Micromeritics). The zeta potentials of the composites were measured using a Zetasizer 200 system (Malvern Instruments).

A mass of 0.001 g of sample was placed in 100 mL of acetate buffer, 10 mM (with Milli-Q water). The data represent the averages of three runs per sample (50 cycles per run).

2.4 Immobilization of β-glucosidase, xylanase and phytase on composites of (HA-$CoFe_2O_4$)

The β-glucosidase, phytase and xylanase enzymes were immobilized on the HA:$CoFe_2O_4$ composites with different proportions (2:1, 4:1 and 7:1). The enzyme-support adsorption was carried out in 2 mL tubes, using support concentration of 0.05 g mL^{-1} at acetate buffer pH 5, 20 mM, with an enzymatic loading of 5 mg protein g^{-1} support, under gentle rotary stirring for 1 h at 25 °C. At the end of the immobilization process, the derivative (suspension of immobilized enzyme) was centrifuged for 2 min at 8000 rpm and the protein concentration in the supernatant was measured by the Bradford method. The protein concentration was also determined for the control (free enzyme). The immobilized enzyme was washed two times with the same buffer used for immobilization, in order to remove proteins that had not adsorbed on the support, which had the content determined. The enzymatic activity of the final derivative (A_{DE}) was measured in duplicate, as described in Section 2.5. The results were presented in terms of the immobilization parameters (IY, RA and A_{DE}), described in Section 2.4.1).

2.4.1 Calculation of immobilization parameters

The percentage immobilization yield (*IY*) was calculated using the equation:

$$IY(\%) = 1 - \frac{[P_{supernatant1}]+[P_{supernatant2}]}{[P_{control}]} \times 100,$$

where $P_{supernatant1}$ and $P_{supernatant2}$ (mg mL^{-1}) are the protein concentrations for supernatant 1 (obtained after the first wash) and supernatant 2 (obtained after the second wash), respectively, and $P_{control}$ (mg mL^{-1}) is the protein concentration for the control (soluble enzyme). The enzymatic activity that was offered to the support (A_{Of}) was calculated using the equation:

$$A_{of}\left(\frac{IU}{g\ support}\right) = \frac{A_{solubleenzyme} \times volume\ of\ enzyme\ offered\ (in\ mL)}{mass\ of\ support\ (in\ g)},$$

where $A_{soluble\ enzyme}$ (IU mL^{-1}) is the activity of the free enzyme. The theoretically immobilized activity (A_{TI}, in IU g^{-1} support) was obtained as the product of the activity offered to the support (A_{Of}) and IY × 100^{-1}. The recovered activity (*RA*) of the immobilized enzyme was calculated as follows:

$$RA(\%) = {A_{DE}}\Big/{A_{of}} \times 100,$$

where A_{DE} is the activity of the derivative (IU g^{-1} support).

2.5 Enzymatic activity assays

The enzymatic activities of the soluble and immobilized β-glucosidase were determined as described by (Ghose, 1987), measuring the concentration of glucose produced using cellobiose as substrate. Equal volumes of enzymatic solution (or suspension, in the case of the immobilized enzyme) and cellobiose solution (15 mM, prepared using 50 mM sodium acetate buffer at pH 4.8) were allowed to react for 20 min, at 50 °C, under stirring. The reaction was quenched using thermal inactivation of the enzyme by placing the vials in boiling water for 5 min. The product of the reaction was measured using a GOD-POD enzymatic assay kit (Doles, Brazil).

The enzymatic activities of the soluble and immobilized phytase were determined as described by Harland and Harland (1980) with modifications, by measuring the concentration of phosphorus released from the phytate substrate. The reaction consisted of mixing 50 μL of the enzymatic solution (or suspension, in the case of the immobilized enzyme) in 2.5 mL of the substrate solution (2.5 mM phytic acid sodium salt prepared in 100 mM sodium acetate buffer, at pH 5). The reaction mixture was allowed to react for 15 min at 37 °C, under rotary stirring. The reaction was quenched by adding 200 μL of trichloroacetic acid (10%) to 400 μL of reaction mixture. The phosphorus released in the reaction was determined colorimetrically at 660 nm, after reaction for 30 s of a mixture of 200 μL of distilled water and 500 μL of Taussky reagent (Taussky and Shorr, 1953) in test tubes.

The enzymatic activities of the soluble and immobilized xylanase were determined as described previously (Bailey *et al.*, 1992), by incubating 100 μL of enzymatic solution (or suspension, in the case of the immobilized enzyme) and 900 μL of the xylan substrate solution (1% m/v, prepared using 50 mM sodium acetate buffer at pH 5). The reaction was allowed to proceed for 5 min, at 50 °C, under stirring, after which it was quenched using thermal inactivation of the enzyme by placing the vials in boiling water for 5 min. Reducing sugar (xylose) released in the assays was measured according to the DNS method (Miller, 1959).

For the three enzymes, one unit of enzymatic activity (IU) represented the amount of enzyme required to release 1 μmol of glucose/phosphorus/xylose per minute into the reaction mixture. All the activity measurements were performed in duplicate, with calculation of the immobilization parameters as means ± standard deviation.

2.6 Enzymatic loading

The adsorption capacities of the supports HA:$CoFe_2O_4$ (in the proportion 2:1) was evaluated using enzyme loadings ranging from 5 to 80 mg protein g^{-1} support in the immobilization process. The derivatives obtained (β-glucosidase, phytase and xylanase immobilized) were washed two times with the same buffer used for immobilization, in order to remove proteins that had not adsorbed on the support. The protein concentration in the two

supernatants was measured by the Bradford method for the calculation of Immobilization Yield (IY).

2.7 Desorption experiments

The ability of the immobilized enzymes to be released from the support was evaluated by incubating the derivative in solutions of different sodium salts (chloride and citrate) at increasing concentrations (50, 100, 200, 400, and 800 mM). A suspension of immobilized enzyme was centrifuged at 8000 rpm for 2 min, after which the supernatant was discarded. An equal volume of ionic solution was added to the precipitate (derivative), followed by gentle stirring for 40 min. The protein concentration in the supernatant was then measured (in duplicate), using the Bradford method. The desorption assays were performed in duplicate at each ionic strength. The protein immobilized onto the HA:$CoFe_2O_4$ was designated as 100%, while the protein contents obtained in the supernatants with different ionic strengths were calculated as the percentage of desorbed enzyme (%), relative to the immobilized protein.

2.8 Effects of pH and temperature on enzymes activities

The effect of pH on the activity of β-glucosidase, phytase and xylanase (free and immobilized on HA:$CoFe_2O_4$ in the proportion 2:1) was evaluated in the pH range 3-8, using glycine-HCl buffer (for pH 3), sodium acetate buffer (for pH 4, 5, and 6), and sodium phosphate buffer (for pH 7 and 8), at 100 mM and 50 °C for β-glucosidase and xylanase and 100 mM, 37°C for phytase. The effect of temperature on the activities of the free and immobilized enzymes was investigated at 30, 40, 50, 60, and 70 °C, at pH 5 (using 100 mM sodium acetate buffer). The experiment was performed in duplicate. The highest activity obtained in the temperature or pH ranges employed was designated as 100%, while the activities at all the remaining temperatures and pHs were calculated as the activity (in %) relative to that highest activity.

2.9 Enzyme thermostability

The thermostabilities of the free and immobilized enzymes were determined by incubation for 2 h at temperatures of 70 and 90 °C, in 20 mM sodium acetate buffer (pH 5). At 30 min intervals, samples were withdrawn for determination of thermal denaturation by means of enzymatic activity measurements. The enzymes activities were measured (in duplicate) as described in Section 2.4. The activity obtained at time zero was designated as 100% and the activities at all the remaining times were calculated as the activity (in %) relative to that highest activity.

2.10 Hydrolysis of substrates and reusability of the immobilized enzymes

The efficiency of the immobilized enzymes (on HA:$CoFe_2O_4$ in the proportion 2:1) was evaluated in terms of cellobiose, phytate and xylan hydrolysis and was compared to the use of soluble enzymes. Cellobiose in the concentration of 15 g L^{-1} was hydrolyzed in 100 mM sodium acetate buffer (pH 5) at 50 °C, under agitation, using the soluble and immobilized β-glucosidase at an enzyme loading of 40 IU g^{-1} cellobiose. Xylan in the concentration of 15 g L^{-1} was hydrolyzed in 100 mM sodium acetate buffer (pH 5) at 50 °C, under agitation, using the soluble and immobilized xylanase at an enzyme loading of 40 IU g^{-1} xylan. Phytate in the concentration of 30 g L^{-1} was hydrolyzed in 100 mM sodium acetate buffer (pH 5) at 37 °C, under agitation, using the soluble and immobilized phytase at an enzyme loading of 150 IU g^{-1} phytate. The release of glucose, phosphorus and xylose during the course of the reaction was quantified according to the 2.5 section, until stabilization. The experiments were performed in duplicate and the results were presented as mean ± standard deviation.

The reusability of the immobilized enzymes was studied in assays performed in 2 mL tubes, under the hydrolysis assay conditions described above. After each 2 h reaction cycle for β-glucosidase and xylanase and 1 h reaction cycle for phytase, the enzymatic material was separated by two different ways: by centrifugation (8000 rpm for 5 min) and by the application of a magnetic field. Then the enzymatic material was resuspended in the fresh substrate to start the new cycle. The product concentration measured in the first cycle corresponded to 100%, while the concentrations in the remaining cycles were calculated as the product production (%) relative to that first cycle. The experiment was performed in duplicate and the results were presented as mean ± standard deviation.

3. Results and discussion

3.1 Characterization of the magnetic supports

The magnetic hydroxyapatite nanoparticles (HA:$CoFe_2O_4$ at proportions 2:1, 4:1 and 7:1) were successfully prepared as can be seen in the characterization analysis of XDR and SEM-EDS (Fig. 1). The XRD spectra for HA:$CoFe_2O_4$ composites (2:1, 4:1 and 7:1) reveals that the hydroxyapatite phases, JCPDS card n° 9-0432, were kept after composite formation (Fig. 1a). Except the $CaHPO_4$ phase identified by peak at 2θ 26.4, 30.2 and 41.0° (a contaminant phase of commercial HA), that is highly soluble and probably has solubilized during the synthesis of the composites. The phases of cobalt ferrite crystal, JCPDS card n° 22-1086, were also kept after composite formation. Therefore, the XDR spectra results suggests that the hexagonal crystalline structure of HA was unchanged during the process of composites formation.

Due to the magnetic character attributed to the nanocomposites, they tend to agglomerate, which were observed in the FEG images (Fig. S4 of Supplementary Material). In order to confirm that the cobalt ferrite were inserted into the HA structure, the energy dispersive spectroscopy

(EDS) technique was used, that allows an elemental analysis on different microscopic sections of the samples. The SEM-EDS images revealed the homogeneous distribution of the elements P, Ca, O, Co and Fe throughout the material (Fig. 1b). This indicates that cobalt ferrite was incorporated homogeneously in the HA, attributing a similar magnetic character between the nanoparticles. The final appearance of the composites formed was of brown powders, becoming darker according to the higher cobalt ferrite content in their composition, which demonstrated superior dispersibility in aqueous media (Fig. 1c).

The recovery of magnetic supports from aqueous media by applying a magnetic field for 30 seconds was evaluated followed by drying and mass weighed. As expected, the greater mass loss occurred for the lowest magnetic support, although mass loss has been practically negligible for the three magnetic supports tested, being 0.17, 0.37 and 0.57% for the composite 2:1, 4:1 and 7:1, respectively. These results indicate the excellent recoverability of the magnetic supports from an aqueous solution.

The surface charges of supports were evaluated (at the same pH used in the immobilization process, pH 5) using zeta potential determinations. The values were very close and negative for the three composites (Table 1). These results corroborate the fact that visually the composites demonstrated similar dispersibility in aqueous medium. That is, the way the negatively charged nanoparticles repel each other is very similar between the composites, resulting in equal distribution of these nanocomposites in aqueous medium. Considering the surface area of HA of 58.2 m^2/g and for cobalt ferrite of 8.4 m^2/g, the surface area of the magnetic composites were smaller than that of pure HA, as expected (Table 1). The HA:$CoFe_2O_4$ (2:1) support presented the highest surface area among the three composites, which is a very interesting result for enzyme immobilization, because besides offering greater surface area for protein adsorption between the composites, it is also the support with the greatest magnetic character to facilitate the recovery of the biocatalyst from the reaction medium.

The surface area of the derivatives decreased after enzyme immobilization, indicating that the enzymes bind externally to the surface of the support, altering its surface area. The reduction in surface area was more pronounced for the derivative with β-glucosidase, corroborating the immobilization results that showed that β-glucosidase demonstrated the highest immobilization yield between the enzymes, that is, more β-glucosidase enzymes were adsorbed on the support than phytase and xylanase, thus causing a more pronounced blockage in the surface area. Xie and Zang (2017) also noted a decrease in the surface area of HA magnetic support after lipase immobilization, the phenomenon of which was attributed to the blocking of pores of HA-Fe_2O_3 nanoparticles amino-functionalized by using 3-aminopropyltriethoxysiane in order to obtain covalent interaction.

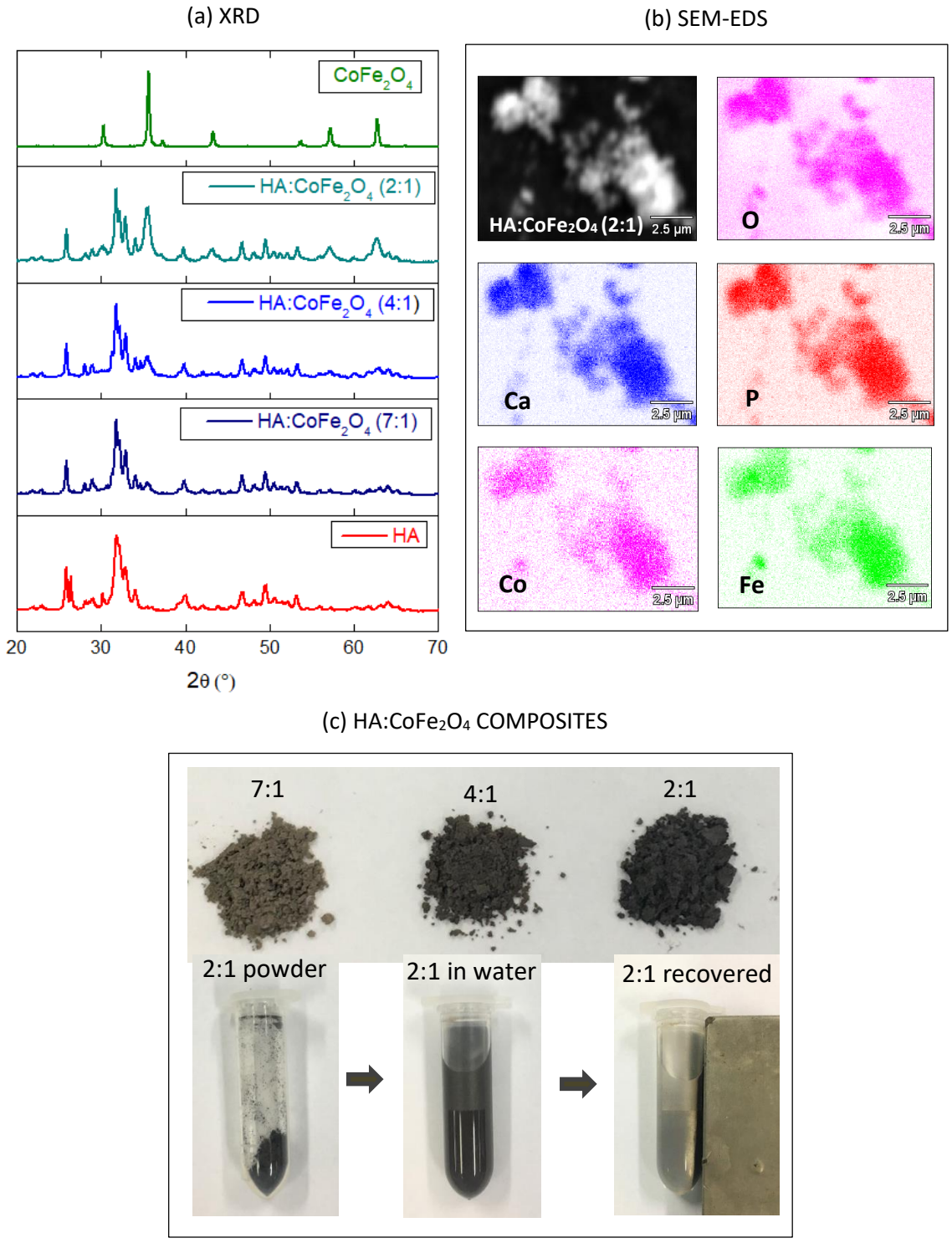

Fig. 1. Characterization of supports using (A) Energy dispersive X-ray spectroscop (SEM-EDS) and (B) XRD spectra. (C) Illustrations of the composites obtained and their recovery using a magnetic field.

Table 1- Surface Area (BET) and Zeta potential of supports before and after enzyme immobilization.

Support	Surface area (m^2/g)	Zeta Potential in pH 5
HA	58.2	-
HA:$CoFe_2O_4$ (2:1)	27.7	-12.7 ± 1.1
HA:$CoFe_2O_4$ (4:1)	19.2	-10.6 ± 0.7
HA:$CoFe_2O_4$ (7:1)	20.8	-13.3 ± 1.6
HA:$CoFe_2O_4$ (2:1) + β-glucosidase	18.64	-
HA:$CoFe_2O_4$ (2:1) + xylanase	20.75	-
HA:$CoFe_2O_4$ (2:1) + phytase	17.74	-
$CoFe_2O_4$	8.49	-

3.2 Evaluation of enzymes immobilization on HA:$CoFe_2O_4$ composites

The enzymes β-glucosidase, phytase and xylanase were immobilized on the three HA:$CoFe_2O_4$ composites with the proportions of 2:1, 4:1 and 7:1. The immobilization conditions were selected according to the results for the immobilization of these same enzymes in pure HA, demonstrated in our previous work as pH 5, 20 mM, 1 h, 25 °C (Coutinho *et al.*, 2018; Coutinho *et al.* 2019; Coutinho *et al.* 2020). Among the three enzymes immobilized on magnetic hydroxyapatite nanoparticles, β-glucosidase presented the best results related to the immobilization parameters, once it reached almost total adsorption in all evaluated supports and Recovery Activity (RA) in the range of 80%, meaning that after anchoring the enzyme to the support, it retained 80% of its free-form activity (Fig. 2a).

These results were very similar to those obtained for β-glucosidase immobilization on pure HA (Coutinho *et al.*, 2018), in which they obtained an immobilization yield (IY) of about 90% and RA of about 80%. These similarities indicate that the insertion of different proportions of cobalt ferrite in the structure of HA did not change the HA ability of immobilization, on the contrary, the $CoFe_2O_4$ was also a source of enzyme adsorption. In order to verify that, an experiment of immobilization of β-glucosidade on $CoFe_2O_4$ was performed (at the same conditions used in the immobilization on composites) to confirm if enzyme would interact with the magnetic component pure, resulting in a IY of 69.9 ± 0,1% and RA of 78 ± 11%. It can thus be suggested that the metals (Co^{2+} and Fe^{2+}) of cobalt ferrite (pure or in composite form) may interact electrostatically or by chelation with the negative amino acids of the enzyme. In the work of Wang *et al.* (2019), they used Co^{2+} nanoparticles to chelated lipase by affinity immobilization, indicating the potential of this metal to form metal-chelated with proteins.

Regarding the immobilization parameters for phytase and xylanase on magnetic hydroxyapatite nanoparticles (Fig. 2b and 2c), it was observed an increase in IY with the increase of $CoFe_2O_4$ content in the support. The highest IY obtained for 2:1 support could be attributed to the fact that it is the support with the largest surface area (Table 1). However, this behavior did

not occur with β-glucosidase, indicating that the type of interaction between this enzyme and support does not depend on $CoFe_2O_4$ content as observed with phytase and xylanase.

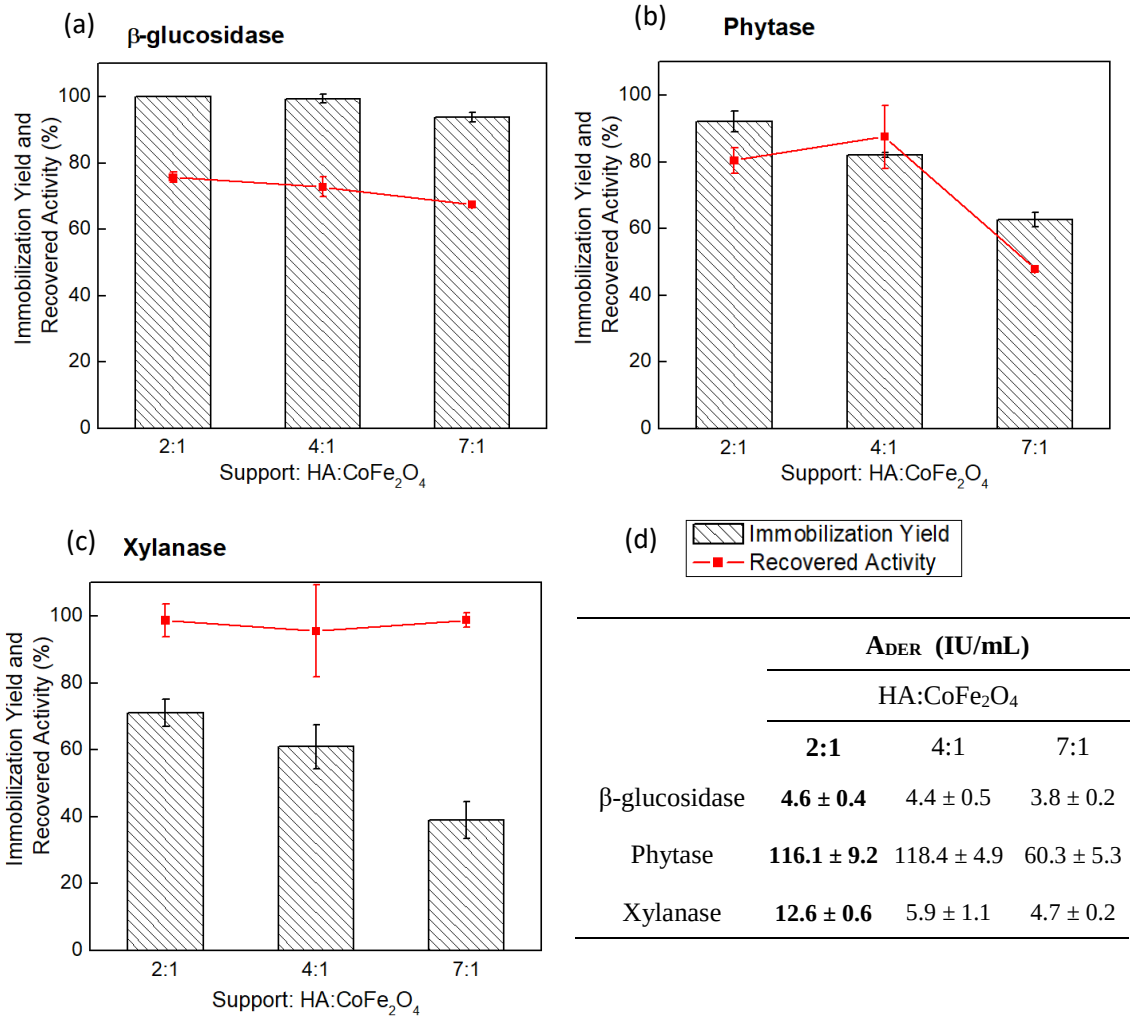

	A_{DER} (IU/mL)		
	HA:$CoFe_2O_4$		
	2:1	4:1	7:1
β-glucosidase	**4.6 ± 0.4**	4.4 ± 0.5	3.8 ± 0.2
Phytase	**116.1 ± 9.2**	118.4 ± 4.9	60.3 ± 5.3
Xylanase	**12.6 ± 0.6**	5.9 ± 1.1	4.7 ± 0.2

Fig. 2. Results of immobilization parameters of β-glucosidase (A), phytase (B) and xylanase (C) immobilized on HA:$CoFe_2O_4$ supports with different proportions (2:1, 4:1 and 7:1). The table shows the A_{DER} in IU/mL. The immobilization conditions were pH 5, 20 mM, during 1 h under agitation, u
sing support concentration of 0.05 g/mL and enzymatic loading of 5 mg protein/g support.

Regarding the RA results for phytase immobilized on HA:$CoFe_2O_4$ supports, it was observed values below 100%, differently of the ones observed by Coutinho *et al.* (2019) when phytase was immobilized on pure HA. They found RA values higher than 100%, indicating an improvement in phytase catalytic activity after being immobilized in pure HA. This behavior may not have been observed in the phytase immobilization on HA:$CoFe_2O_4$ because of the way the elements were distributed in the formation of composite, which might have interfered in the adsorption process of phytase on it. It is possible that the arrangement of the elements in the

composite structure do not allow the enzyme to have the active site conformation more favored to the biocatalysis, and/or do not allow the HA to act as a cofactor (Ca^{2+} source). These both phenomena were discussed by Coutinho *et al.* (2019) about the improvement on phytase activity after enzyme being adsorbed on HA pure.

Although β-glucosidase and phytase demonstrated RA below 100%, xylanase showed RA values close to 100%, indicating that the enzyme showed no change in enzymatic activity after its anchorage in the HA:$CoFe_2O_4$ support. According to this data, we can infer that the active site of xylanase remained fully available for biocatalysis after immobilization on the magnetic support. The enzyme adsorption experiments on the three composites with different HA and $CoFe_2O_4$ proportions were carried out to choose the one that was most efficient to act as a matrix of these enzymes. Since the HA:$CoFe_2O_4$ support (2:1) presented the highest IY values and also the highest enzymatic activity values for the three enzymes (shown in Fig. 2d), it was chosen for the following steps. Besides, the 2:1 composite has the highest magnetic content, thus favoring the enzyme recovery step from the reaction medium and consequently the enzyme reuse.

The adsorption of the three enzymes on the HA:$CoFe_2O_4$ support (2:1) showed to be very fast, especially for β-glucosidase that had all enzymes offered to the support (5 mg protein/g support) immobilized in just five minutes (Fig. 3). Considering that β-glucosidase also interacts with the composite metals Co^{2+} and Fe^{2+}, the results show that this interaction may occurs rapidly within the first 5 minutes.

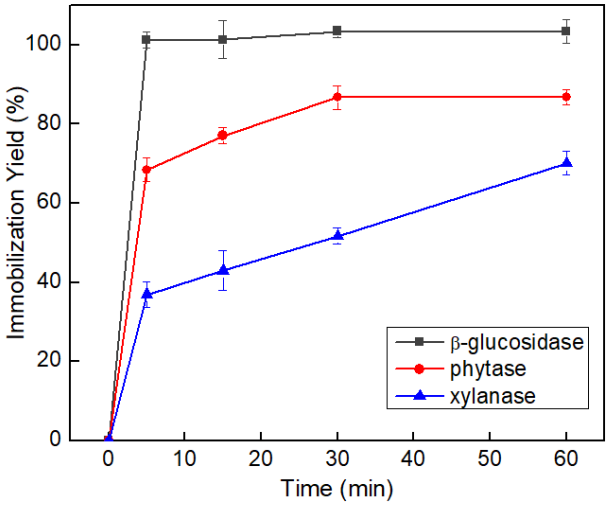

Fig. 3. Time course of immobilization of β-glucosidase, phytase and xylanase onto HA:$CoFe_2O_4$ (2:1) nanoparticles at 25 °C, pH 5.0 (in 20 mM sodium acetate buffer), using an enzymatic loading of 5 mg protein/g support and support concentration of 0.05 g/mL.

Regarding the enzymatic loading, for the three enzymes, the largest amount of protein adsorbed to each biocatalyst was 14.7 mg protein/g support for β-glucosidase, followed by 6.9 mg protein/g support for xylanase and 4.5 mg protein/g support for phytase. This order of adsorption capacity was also obtained during the immobilization of these enzymes in pure HA (β glucosidase> xylanase> phytase), although the adsorption capacity on HA has been higher, 32, 15 and 6 mg protein/g support, respectively (Coutinho *et al.*, 2018; Coutinho *et al.*, 2019; Coutinho *et al.*, 2020). The decrease in adsorption capacity of enzymes on composite in relation to pure HA is probably due to the decrease in surface area of composite compared with the surface area of HA (Table 1).

3.3 Desorption experiments

The desorption study of enzymes from the support (HA:$CoFe_2O_4$, 2:1) in the presence of potential desorbing agents can help to elucidate the type of interaction that occurs between the protein and the support. Therefore, chloride sodium and citrate sodium salts were tested as desorbing agents, in order to improve understanding of the mechanism of the enzyme-support interaction. The results showed that for the three derivatives, desorption was more expressive in the presence of citrate sodium solution than with sodium chlorite solution (Fig. 4). The ability of this salt to act as a desorbing agent is probably due to the higher affinity of the support for the COO^- groups abundant in solution than for the COO^- groups of enzyme, causing enzyme leaching from the HA:$CoFe_2O_4$ even under low salt concentrations. This observation is indicative that prevailing interactions are coordination bonds between remaining Ca^{2+}, Co^{2+} and Fe^{2+} sites of composite and COO^- of amino acids such as Glu and Asp.

Since β-glucosidase remained bound to the support even in the presence of high concentrations of sodium chloride, the electrostatic interactions between support and enzyme were not considered relevant to the immobilization process, on the contrary of complexation interactions between metals of support and carboxylic acids of enzyme, which can be considered prevalent in the adsorption process. These carboxylic acids belong to the Glu and Asp groups, which are abundant on the surface of the enzyme, according to Yu *et al.* (2004). These results demonstrate that the biochemical behavior of β-glucosidase immobilized on the composite is very similar to that one observed on pure HA (Coutinho *et al.*, 2018). Moreover, the strong desorption of the enzyme even in the presence of low concentrations of citrate salt (Fig. 4a) reveals that there is a strong affinity between enzyme and support, which corroborates with the rapid adsorption of the enzyme to the support shown in Fig. 3.

The phytase and xylanase desorption from the composite using sodium citrate was less expressive than β-glucosidase desorption, probably because they have less amino acid content containing carboxylic acids on the surface, such as Glu and Asp, than β-glucosidase (Fig. 5) (Yu

et al., 2004; Oakley, 2010; Coutinho *et al.*, 2020). This result indicates that interaction of metals chelation with the carboxylic acids (COO^-) of the enzymes is not so predominant for phytase and xylanase as it is for β-glucosidase. It can be indicative that other amino acids besides Glu and Asp containing electron pair donor on xylanase and phytase, such as His, Arg, Trp and Lys, were performing chelation interactions with the metals present in the composite, such as Ca^{2+}, Fe^{2+} and Co^{2+}. The Fig. 5 illustrates the three-dimensional structure of phytase and xylanase, highlighting the amino acid residues capable of chelating with the metals of the composite. Studies of Kumar *et al.* (1998) and Bresolin *et al.* (2009) described that metals ions such as Cu^{2+}, Zn^{2+}, Ni^{2+} and Co^{2+} are able to complex selectively with electron donor groups of proteins, such as histidine (His), cysteine (Cys), tryptophan (Try), and arginine (Arg) amino acids.

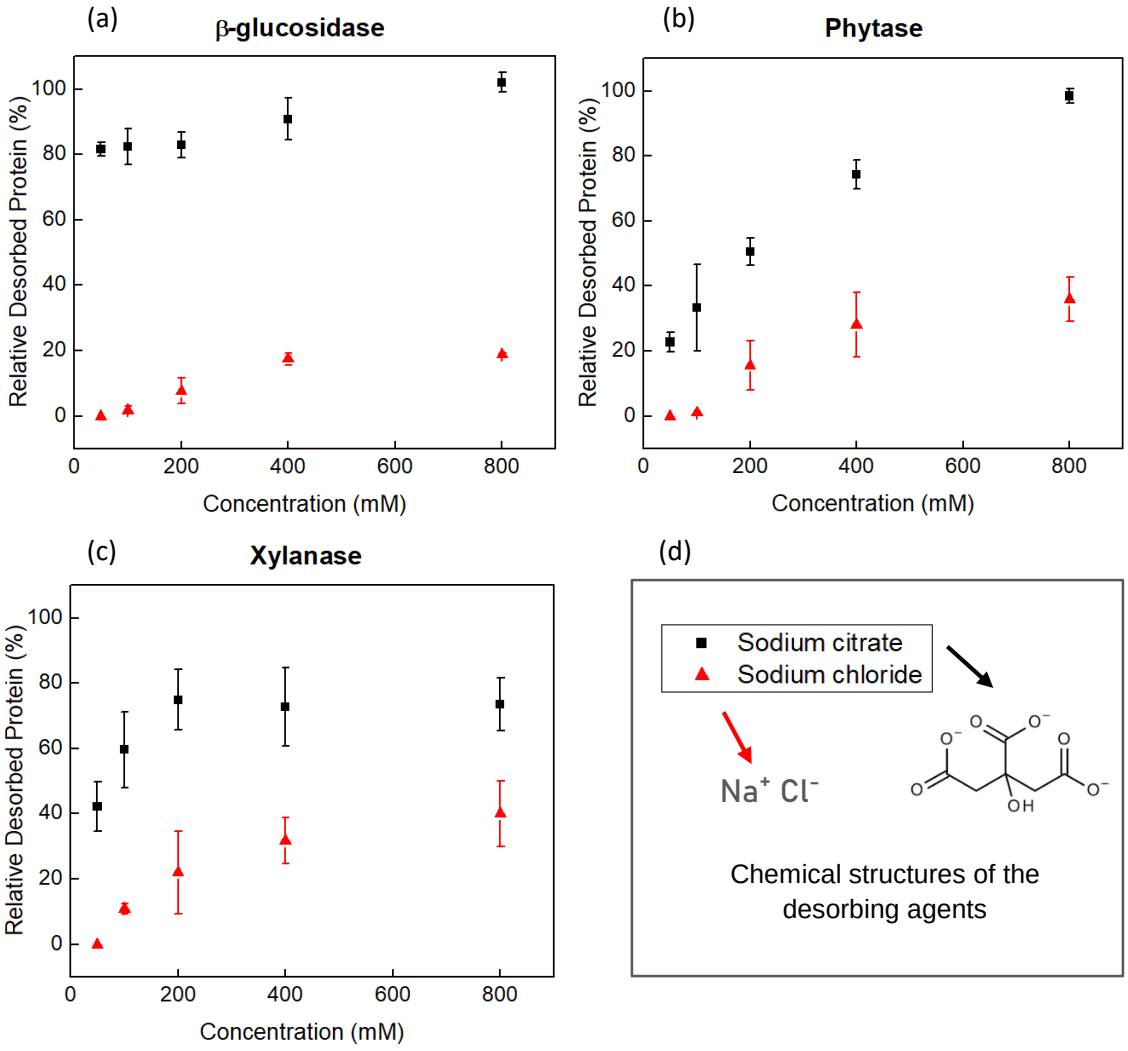

Fig 4 - Profiles of desorption of β-glucosidase (A) phytase (B) and xylanase (C) from HA:$CoFe_2O_4$ (2:1) nanoparticles incubated in different solutions (D) (all at pH 5) for 40 min. The enzyme was immobilized at pH 5.0 (20 mM), using an enzymatic loading of 5 mg protein/g support and a support concentration of 0.05 g/mL.

Another observation was that phytase and xylanase immobilized on the composite were slightly less resistant to the desorbent effect of sodium chlorite than β-glucosidase, which may evince that electrostatic interactions are more important in the immobilization process for these enzymes than for β-glucosidase. The general conclusions about the types of interaction of phytase and xylanase with HA:$CoFe_2O_4$ are that support metal chelation interactions occur with different amino acids that have electron donor pairs, complemented by electrostatic interactions (which can occur between positive support groups such as metals with enzyme negative groups, as well as between negative support groups such as phosphates with enzyme positive groups).

The general conclusions about the types of interaction of phytase and xylanase with HA:$CoFe_2O_4$ are that support metal chelation interactions occur with different amino acids that have electron donor pairs, complemented by electrostatic interactions (which can occur between positive support groups such as metals with enzyme negative groups, as well as between negative support groups such as phosphates with enzyme positive groups).

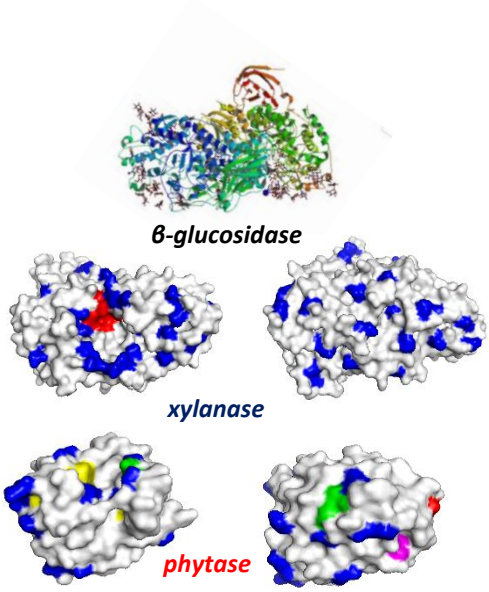

Fig. 5. Three-dimensional structure of phytase and xylanase, constructed using the PyMOL program (PyMOL Molecular Graphics System; Version 2.3.3 Schrödinger, LLC). For xylanse, the amino acid residues are as follows: red – His; blue – Glu and Asp; green – Arg; yellow – Trp; and magenta – Cys. For phytase the amino acid residues are as follows: red – His; blue – Glu and Asp; green – Arg; yellow – Trp; orange – Lys; magenta – Cys. The β-glucosiudase structure was constructed by Lima *et al.* (2013).

3.4 Activity profiles of derivatives at different pH and temperature

A set of enzymatic reaction experiments was carried out at different pH values and temperatures in order to determine the activity profiles of β-glucosidase, phytase and xylanase before and after the immobilization process (Fig. 6).

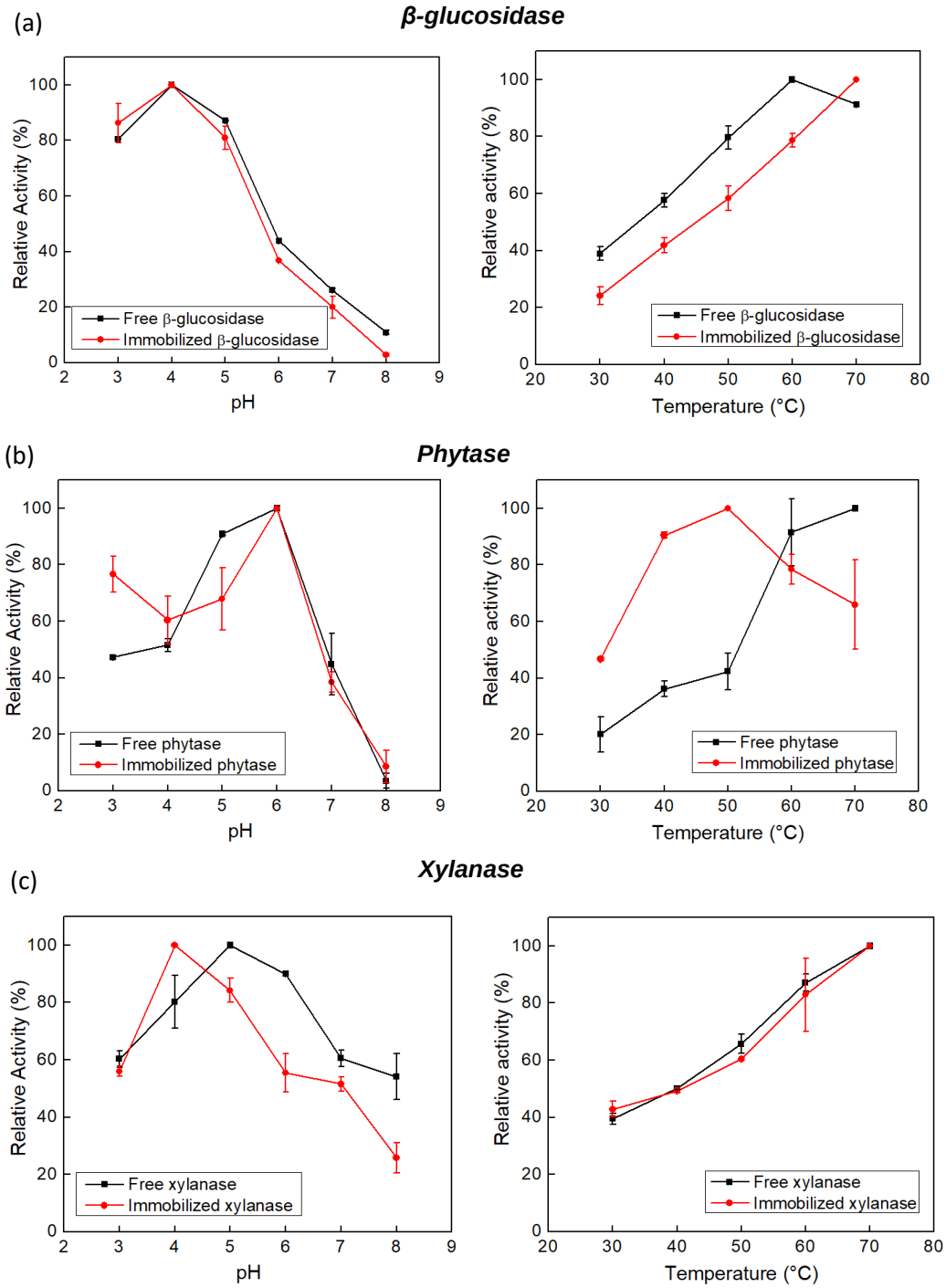

Fig. 6 – Profiles of the activities of (a) β-glucosidase, (b) xylanase and (c) phytase enzymes in form free and immobilized on HA:$CoFe_2O_4$, at different pHs and temperatures.

The β-glucosidase demonstrated the same activity profile at different pHs after its immobilization in the composite. On the other hand, phytase and xylanase immobilized on HA:$CoFe_2O_4$ showed some differences in the activity profile at different pH in relation to the free enzymes. These differences can be attributed to the electrostatic potential of the microenvironment of immobilized enzymes on composite (which contains the ionized functional groups Ca^{2+}, PO_4^{3-}, Co^{2+} and Fe^{2+}) that can affect the local concentration of H^+, influencing the behavior of the enzyme under different pH conditions. An interesting result to be highlighted is that both phytase and xylanase showed a better performance at acidic pH than the free enzyme, and this was also observed after its immobilization in pure HA (Coutinho *et al.* 2019; Coutinho *et al.*, 2020). The difference of the optimal pH of phytase free between studies is because Coutinho *et al.* (2019) utilized phosphate buffer for pH 6 impacting enzyme activity, while in this work acetate buffer was used.

Regarding the temperature profile, β-glucosidase and xylanase immobilized on the composite showed an activity profile similar to the free enzymes, while phytase immobilized showed higher activity profile at temperatures of 30 to 50 °C than free enzyme. The three enzymes (in free form) have the highest activity at a temperature of 70 °C. In general, the activity profiles at different temperatures of the three enzymes immobilized on the composite were similar to the activity profile of these enzymes immobilized on pure HA. These results suggest that enzyme immobilization by adsorption does not usually have any major impact on the activity profile, within this temperature range.

3.5 Thermostability studies

In order to investigate whether there was any improvement in the thermostability of the enzymes after being immobilized on the magnetic hydroxyapatite nanoparticles, the free and immobilized enzymes were kept at temperatures of 70 and 90 °C for 2 h, with periodic measurements of the activity (Fig. 7). Immobilized β-glucosidase showed an improvement in thermal stability at 70 °C compared to the free enzyme, maintaining around 60% of its activity after 1 h at 70 °C, while free enzyme retained only 15% of its initial activity. At 90 °C, a slight improvement in the thermal stability of immobilized β-glucosidase was also observed in relation to the free enzyme, although both forms of the enzyme maintained only about 15% of their initial activity after 2 h at 90 °C.

On the other hand, phytase and xylanase did not improve stability at either 70 or 90 °C after being immobilized on the composite. Such behavior is common for enzymes that are physically or ionically adsorbed on solid matrix, once high stabilization does not usually happen because of the reversibility of the bonds enzyme-support, in which the three-dimensional structure of the native enzyme is almost always preserved (Jesionowski *et al.*, 2014). Normally, covalent interactions that are able to improve the stiffness of the enzyme as demonstrated by Borges *et al.*

(2014) and Pal and Khanum (2011). Despite these associations, it is important to note that (Coutinho *et al.* (2019) have demonstrated an improvement on thermostability of phytase at 80 and 90 °C after being adsorbed on HA pure. Probably, the coordination interactions between phytase and pure HA were intense enough to cause an increase in enzyme stiffness, unlike the interactions of phytase with HA:$CoFe_2O_4$ composite demonstrated in this work.

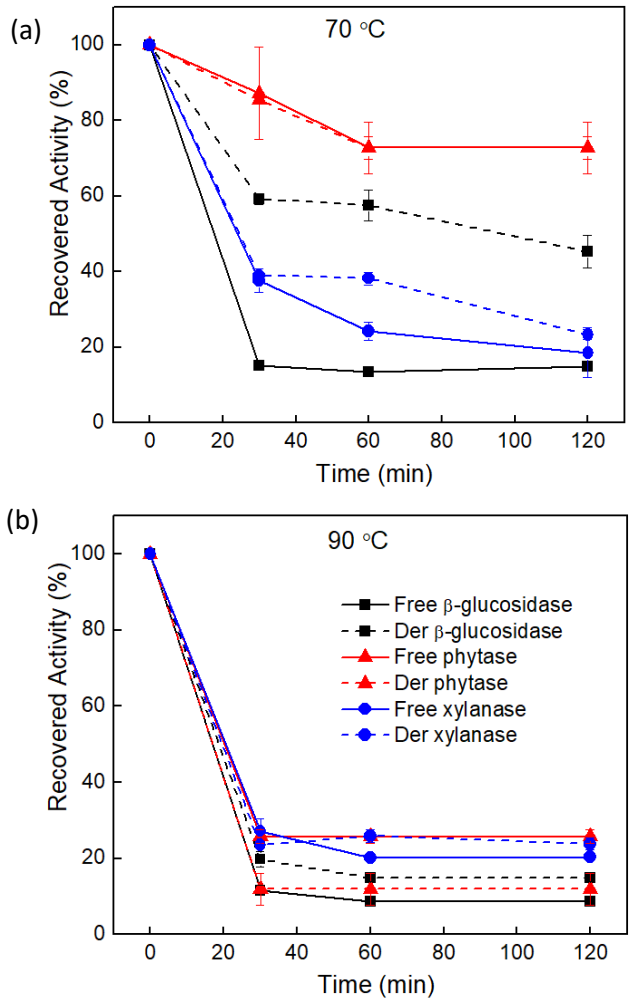

Fig. 7. Thermal inactivation profiles of β-glucosidase, xylanase and phytase enzymes in the forms free and immobilized on HA:$CoFe_2O_4$, at (a) 70 and (b) 90 °C. In the legend, "Der" is an abbreviation of Derivative.

3.6 Hydrolysis and reuse assays

The performance of each biocatalyst free and immobilized (β-glucosidase, phytase and xylanase) were evaluated in the hydrolysis of each specific substrate (cellobiose, phytate and xylan), by monitoring product released (glucose, phosphorus and xylose) into the reaction medium. The free and immobilized enzymes presented similar hydrolysis profiles yielding

glucose, phosphorus and xylose concentration of around 22, 160 and 30 µmol mL^{-1}, respectively, after 3h reaction (Fig. 8a).

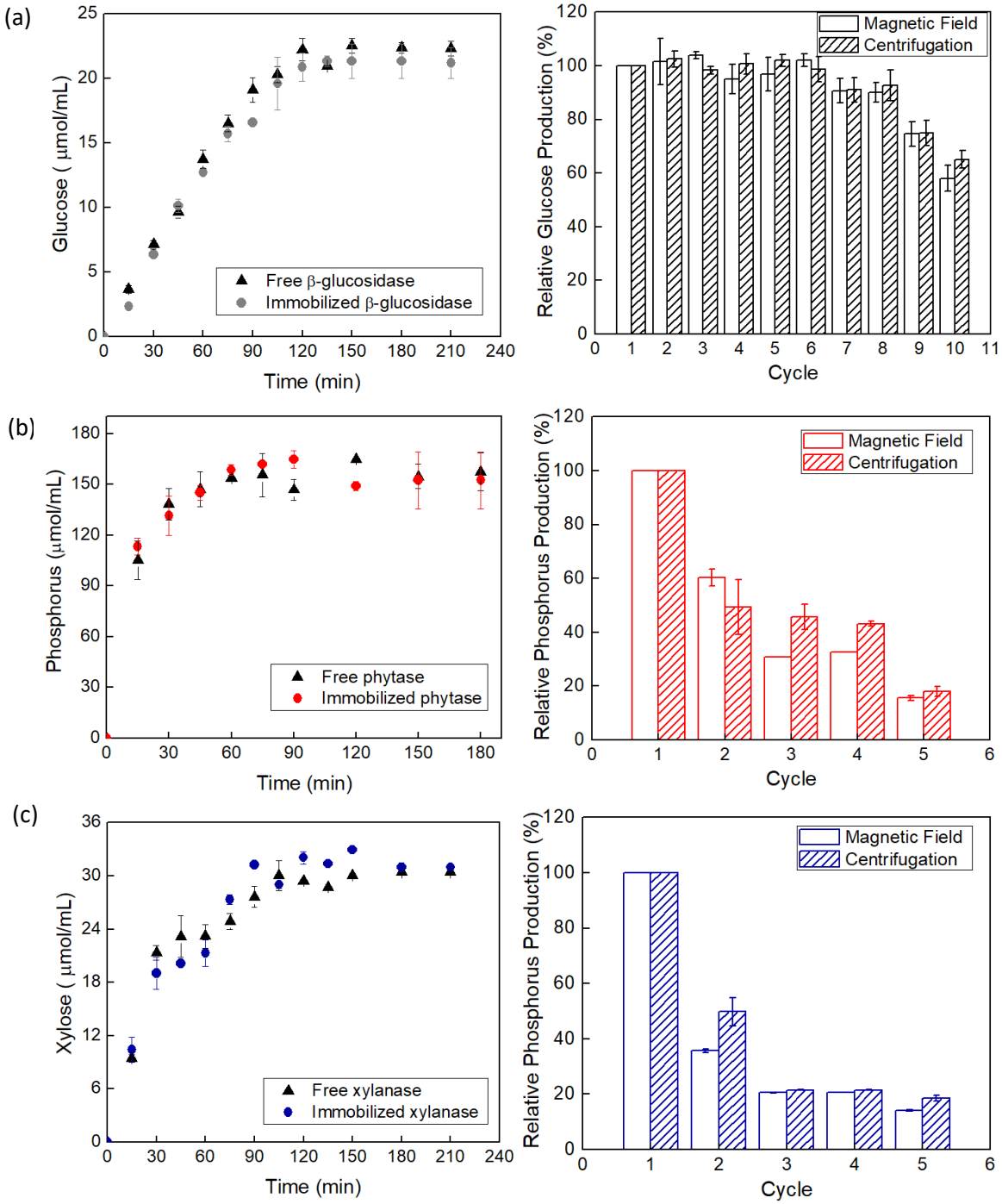

Fig. 8. (a) Cellobiose, (b) phytate and (c) xylan hydrolysis by free and immobilized β-glucosidase, xylanase and phytase, respectively. Reaction conditions: 40 U/g cellobiose, 15 g cellobiose/L and 50°C for β-glucosidase; 60 U/g xylan, 20 g xylan/L and 50 °C for xylanase; 150 U/g phytate, 30 g phytate/L and 37 °C for phytase. Reuse of immobilized enzymes in the hydrolysis of respective substrates. Conditions of each hydrolysis cycle were 2 h for β-glucosidase, 2 h for xylanase and 1 h for phytase.

These findings showed that under the conditions evaluated, there was no diffusional delay for the reactions catalyzed by the enzymes immobilized on the HA:$CoFe_2O_4$ supports. The HA composite matrix did not appear to affect the reaction kinetics, neither activating nor inhibiting the enzyme.

The reusability of β-glucosidase, phytase and xylanase can improve the profitability of different process in biorefineries and in the pharmaceutical, food, and beverage sectors. Depending on the process, the recovery of the biocatalyst by application of a magnetic field may facilitate the process of separating the immobilized enzyme from the reaction medium (Vaghari *et al.*, 2016). The results of the reuse experiment for the three immobilized enzymes (Fig. 8b) showed that there was no difference in the recovery efficiency between the application of a magnetic field and gravitational centrifugal force, indicating that the HA:$CoFe_2O_4$ matrix had efficient magnetic character for the recovery of biocatalysts in comparison to the centrifugation method.

For the β-glucosidase immobilized, the relative glucose production remained high up to the 10^{th} hydrolysis cycle, when the value was around 70% of the initial production. On the other hand, for phytase and xylanase derivatives, a decrease in phytate and xylan hydrolysis were observed in the second cycle, which continued to slowly decrease until the fifth cycle, after which the hydrolysis remained constant for the next 3 cycles (data not shown). The higher stability of β-glucosidase derivative in the reuse assays could be related to the previous findings related with the higher immobilization yield (Section 3.2.1) and higher affinity of this enzyme for HA:$CoFe_2O_4$ demonstrated by the faster adsorption, than phytase and xylanse enzymes (Section 3.2.2). These data indicate that the use of the HA:$CoFe_2O_4$ matrix resulted in the formation of chelates with β-glucosidase that were highly stable and able to complex more effectively with proteins, resulting in derivatives with optimal reusability. Therefore, the β-glucosidase/HA:$CoFe_2O_4$ derivative shows a great potential for applications in various industrial sectors.

4. Conclusions

The HA:$CoFe_2O_4$ magnetic nanoparticles were successfully prepared, and the composite with the highest cobalt ferrite content showed the best immobilization results of β-glucosidase, xylanase and phytase, favoring the enzyme recovery step from the reaction medium and consequently the enzyme reuse. The enzymes were efficiently immobilized onto HA:$CoFe_2O_4$ magnetic nanoparticles by means of a very simple and fast adsorption protocol, resulting in the formation of coordination bonds between HA:$CoFe_2O_4$ and enzymes, complemented by ionic bindings. The obtained derivatives could be easily recovered from the reaction medium by

applying a magnetic field, demonstrating promising applications of industrial interest, especially β-glucosidase that can be reused for at least 10 times while maintaining 70% of its initial activity.

5. References

Abdel-Hamid, Z., Rashad, M.M., Mahmoud, S.M., Kandil, A.T., 2017. Electrochemical hydroxyapatite-cobalt ferrite nanocomposite coatings as well hyperthermia treatment of cancer. Materials Science & Engineering C-Materials for Biological Applications 76, 827-838.

Alftren, J., Hobley, T., 2013. Covalent Immobilization of beta-Glucosidase on Magnetic Particles for Lignocellulose Hydrolysis. Applied Biochemistry and Biotechnology 169, 2076-2087.

Bailey, M.J., Biely, P., Poutanen, K., 1992. Interlaboratory testing of methods for assay of xylanase activity. Journal of Biotechnology 23, 257-270.

Bohara, R.A., Thorat, N.D., Pawar, S.H., 2016. Immobilization of cellulase on functionalized cobalt ferrite nanoparticles. Korean Journal of Chemical Engineering 33, 216-222.

Borges, D., Baraldo, A., Farinas, C., Giordano, R., Tardioli, P., 2014. Enhanced saccharification of sugarcane bagasse using soluble cellulase supplemented with immobilized beta-glucosidase. Bioresource Technology 167, 206-213.

Bresolin, I., Miranda, E., Bueno, S., 2009. Immobilized metal-ion affinity chromatography (imac) of biomolecules: fundamental aspects and technological applications. Quimica Nova 32, 1288-1296.

Coutinho, T.C., Rojas, M.J., Tardioli, P.W., Paris, E.C., Farinas, C.S., 2018. Nanoimmobilization of beta-glucosidase onto hydroxyapatite. International Journal of Biological Macromolecules 119, 1042-1051.

Coutinho, T.C., Tardioli, P.W., Farinas, C.S., Phytase Immobilization on Hydroxyapatite Nanoparticles Improves Its Properties for Use in Animal (2019). Applied Biochemistry and Biotechnology, 2.

Coutinho, T.C., Rojas, M.J., Tardioli, P.W., Paris, E.C., Farinas, C.S., 2020. Hydroxyapatite nanoparticles modified with metal ions forxylanase immobilization. International Journal of Biological Macromolecules 150, 344-353.

Farinas, C., Reis, P., Ferraz, H., Salim, V., Alves, T., 2007. Adsorption of myoglobin onto hydroxyapatite modified with metal ions. Adsorption Science & Technology 25, 717-727.

Foroughi, F., Hassanzadeh-Tabrizi, S.A., Amighian, J., 2015. Microemulsion synthesis and magnetic properties of hydroxyapatite-encapsulated nano CoFe2O4. Journal of Magnetism and Magnetic Materials 382, 182-187.

Gagnon, P., 2009. Monoclonal antibody purification with hydroxyapatite. New Biotechnology 25, 287-293.

Garcia-Embid, S., Di Renzo, F., De Matteis, L., Spreti, N., de la Fuente, J.M., 2018. Magnetic separation and high reusability of chloroperoxidase entrapped in multi polysaccharide micro-supports. Applied Catalysis a-General 560, 94-102.

GHOSE, T., 1987. Measurement of cellulase activities. pure and Applied Chemistry 59, 257-268.

Graebin, N.G., Schofer, J.D., de Andrades, D., Hertz, P.F., Ayub, M.A.Z., Rodrigues, R.C., 2016. Immobilization of Glycoside Hydrolase Families GH1, GH13, and GH70: State of the Art and Perspectives. Molecules 21, 38.

Harland, B.F., Harland, J., 1980. Fermentative reduction of phytate in rye, white, and whole wheat breads. Cereal Chemistry 57, 226-229.

Hench, L.L., WILSON, J., 1993. An introduction to bioceramics, First ed. World Scientific, Singapore.

Ivic, J., Dimitrijevic, A., Milosavic, N., Bezbradica, D., Drakulic, B., Jankulovic, M., Pavlovic, M., Rogniaux, H., Velickovic, D., 2016. Assessment of the interacting mechanism between Candida rugosa lipases and hydroxyapatite and identification of the hydroxyapatite-binding sequence through proteomics and molecular modelling. Rsc Advances 6, 34818-34824.

Jain, J., Sapna, Singh, B., 2016. Characteristics and biotechnological applications of bacterial phytases. Process Biochemistry 51, 159-169.

Jesionowski, T., Zdarta, J., Krajewska, B., 2014. Enzyme immobilization by adsorption: a review. Adsorption-Journal of the International Adsorption Society 20, 801-821.

Karthickraja, D., Karthi, S., Kumar, G.A., Sardar, D.K., Dannangoda, G.C., Martirosyan, K.S., Girija, E.K., 2019. Fabrication of core-shell CoFe2O4@HAp nanoparticles: a novel magnetic platform for biomedical applications. New Journal of Chemistry 43, 13584-13593.

Kojima, S., Nagata, F., Kugimiya, S., Kato, K., 2018. Synthesis of peptide-containing calcium phosphate nanoparticles exhibiting highly selective adsorption of various proteins. Applied Surface Science 458, 438-445.

Kollath, V., Van den Broeck, F., Feher, K., Martins, J., Luyten, J., Traina, K., Mullens, S., Cloots, R., 2015. A Modular Approach To Study Protein Adsorption on Surface Modified Hydroxyapatite. Chemistry-a European Journal 21, 10497-10505.

Kopp, W., Silva, F.A., Lima, L.N., Masunaga, S.H., Tardioli, P.W., Giordano, R.C., Araujo-Moreira, F.M., Giordano, R.L.C., 2015. Synthesis and characterization of robust magnetic carriers for bioprocess applications. Materials Science and Engineering B-Advanced Functional Solid-State Materials 193, 217-228.

Kumar, A., Galaev, I.Y., Mattiasson, B., 1998. Metal chelate affinity precipitation: a new approach to protein purification. Bioseparation 7, 185-194.

Lima, M., Oliveira-Neto, M., Kadowaki, M., Rosseto, F., Prates, E., Squina, F., Leme, A., Skaf, M., Polikarpov, I., 2013. Aspergillus niger beta-Glucosidase Has a Cellulase-like Tadpole Molecular Shape Insights into glycoside hydrolase family 3 (gh3) beta-glucosidase structure and function. Journal of Biological Chemistry 288, 32991-33005.

Liu, M.Q., Dai, X.J., Guan, R.F., Xu, X., 2014. Immobilization of Aspergillus niger xylanase A on Fe3O4-coated chitosan magnetic nanoparticles for xylooligosaccharide preparation. Catalysis Communications 55, 6-10.

Miller, G.L., 1959. Use of dinitrosalicylic acid reagent for determination of reducing sugar. Analytical Chemistry 31, 426-428.

Netto, C., Toma, H.E., Andrade, L.H., 2013. Superparamagnetic nanoparticles as versatile carriers and supporting materials for enzymes. Journal of Molecular Catalysis B-Enzymatic 85-86, 71-92.

Oakley, A.J., 2010. The structure of Aspergillus niger phytase PhyA in complex with a phytate mimetic. Biochemical and Biophysical Research Communications 397, 745-749.

Pal, A., Khanum, F., 2011. Covalent immobilization of xylanase on glutaraldehyde activated alginate beads using response surface methodology: Characterization of immobilized enzyme. Process Biochemistry 46, 1315-1322.

Polizeli, M., Rizzatti, A.C.S., Monti, R., Terenzi, H.F., Jorge, J.A., Amorim, D.S., 2005. Xylanases from fungi: properties and industrial applications. Applied Microbiology and Biotechnology 67, 577-591.

Qi, M.L., He, K., Huang, Z.N., Shahbazian-Yassar, R., Xiao, G.Y., Lu, Y.P., Shokuhfar, T., 2017. Hydroxyapatite Fibers: A Review of Synthesis Methods. Jom 69, 1354-1360.

Rychen, G., Aquilina, G., Azimonti, G., Bampidis, V., Bastos, M.D., Bories, G., Chesson, A., Flachowsky, G., Gropp, J., Kolar, B., Kouba, M., Lopez-Alonso, M., Puente, S.L., Mantovani, A., Mayo, B., Ramos, F., Saarela, M., Villa, R.E., Wallace, R.J., Wester, P., Brantom, P., Dierick, N.A., Glandorf, B., Herman, L., Karenlampi, S., Aguilera, J., Anguita, M., Cocconcelli, P.S., Subst, E.P.A.P., 2017. Safety and efficacy of Natuphos (R) E (6-phytase) as a feed additive for avian and porcine species. Efsa Journal 15, 3.

Sangeetha, K., Ashok, M., Girija, E.K., 2019. Development of multifunctional cobalt ferrite/hydroxyapatite nanocomposites by microwave assisted wet precipitation method: A promising platform for synergistic chemo-hyperthermia therapy. Ceramics International 45, 12860-12869.

Sheldon, R., van Pelt, S., 2013. Enzyme immobilisation in biocatalysis: why, what and how. Chemical Society Reviews 42, 6223-6235.

Taussky, H.H., Shorr, E., 1953. A microcolorimetric method for the determination of inorganic phosphorus. Journal of Biological Chemistry 202, 675-685.

Tohamy, K.M., Mabrouk, M., Soliman, I.E., Beherei, H.H., Aboelnasr, M.A., 2018. Novel alginate/hydroxyethyl cellulose/hydroxyapatite composite scaffold for bone regeneration: In vitro cell viability and proliferation of human mesenchymal stem cells. International Journal of Biological Macromolecules 112, 448-460.

Vaghari, H., Jafarizadeh-Malmiri, H., Mohammadlou, M., Berenjian, A., Anarjan, N., Jafari, N., Nasiri, S., 2016. Application of magnetic nanoparticles in smart enzyme immobilization. Biotechnology Letters 38, 223-233.

Wang, J.H., Li, K., He, Y.J., Wang, Y., Han, X.T., Yan, Y.J., 2019. Enhanced performance of lipase immobilized onto Co2+-chelated magnetic nanoparticles and its application in biodiesel production. Fuel 255, 8.

Xia, T.T., Liu, C.Z., Hu, J.H., Guo, C., 2016. Improved performance of immobilized laccase on amine-functioned magnetic Fe3O4 nanoparticles modified with polyethylenimine. Chemical Engineering Journal 295, 201-206.

Xie, W., Zang, X., 2017. Covalent immobilization of lipase onto aminopropyl-functionalized hydroxyapatite-encapsulated-gamma-Fe2O3 nanoparticles: A magnetic biocatalyst for interesterification of soybean oil. Food Chemistry 227, 397-403.

Yewle, J.N., Wei, Y.N., Puleo, D.A., Daunert, S., Bachas, L.G., 2012. Oriented Immobilization of Proteins on Hydroxyapatite Surface Using Bifunctional Bisphosphonates as Linkers. Biomacromolecules 13, 1742-1749.

Yu, X., Gao, Y.H., Chen, Z.F., 2004. Purification and characterization of an extracellular beta-glucosidase with high transglucosylation activity and stability from Aspergillus niger no. 5.1. Applied Biochemistry and Biotechnology 119, 229-240.

Zhang, W., Qiu, J., Feng, H., Zang, L., Sakai, E., 2015. Increase in stability of cellulase immobilized on functionalized magnetic nanospheres. Journal of Magnetism and Magnetic Materials 375, 117-123.

CHAPTER 6

"A alegria de ver e entender é o mais perfeito dom da natureza."
Albert Einsten

Overview of the developed research, Concluding remarks and Future perspectives

1. Overview of the developed research

In this topic it is presented in a succinct and chronological way what has been done throughout this work and the main results obtained, highlighting the conclusions of each stage.

The first part of the research consisted on the immobilization of the β-glucosidase enzyme in commercial hydroxyapatite (HA) nanoparticles, described in Chapter 2. For that, it was necessary to find the ideal physical-chemical conditions for enzymatic immobilization, such as pH, temperature, ionic strength, adsorption time and enzymatic load, in order to understand the biochemical behavior of the enzyme with nanoparticles under these different conditions. The results showed that the immobilization process was highly effective over a wide range of pH and ionic strength, resulting in Immobilization Yield (IY) and Recovered Activities (RA) up to 90%. It means that the adsorption process was not selective regarding the pH and ionic strength used. Besides, the adsorption was taken almost immediately after the first contact of the enzyme with the support, indicating the strong attraction for each other. The maximum enzyme load adsorbed was 32.5 mg protein/g support, which is considered a good value for enzymatic immobilization on nanoparticles.

Then, an investigative study was carried out on the type of interaction that prevailed in the process of immobilization of β-glucosidase on HA. For that, FT-IR analyzes, zeta potential measurements and desorption tests with different salts were conducted. The enzyme and support loads at different pHs and the strong and rapid desorption of the enzyme in the presence of citrate molecules indicated the formation of coordination bonds between Ca^{2+} sites of HA and COO^- of amino acids. These results suggested that the immobilization process took place by adsorption by chelation of the support metal with enzyme amino acids. The effective interaction of the enzyme by the support corroborated with the results of reuse, which showed that even after 10 cycles of reuse, the immobilized β-glucosidase retained about 70% of its initial activity, demonstrating the excellent operational stability of the immobilized enzyme. The results obtained in this first stage of the research indicated that β-glucosidase could be efficiently immobilized on HA nanoparticles

by means of a very simple adsorption protocol, offering a promising strategy for performing repeated enzymatic hydrolysis reactions in varied sectors of β-glucosidase industrial application.

Another important conclusion from the Chapter 2 was that HA showed to be a material with great potential for enzymatic immobilization, thus encouraging in testing this material as a matrix for other enzymes, such as phytase and xylanase. In this way, the Chapter 3 refered to the study of immobilization of phytase on HA nanoparticles, with emphasis on the application of the derivative obtained in animal feed and considering yet that HA may also to act as an inorganic source of calcium and phosphorus for the animal. The same structure and methodology as in Chapter 2 was followed, with the insertion of additional experiments regarding the application of the derivative in animal feed, such as thermal stability, *in vitro* simulation of gastro-intestinal conditions and degradation by proteases. As observed for β-glucosidase, phytase also demonstrated high affinity for the support, rapid adsorption (within 10 minutes) and IY close to 100%. However, the singularities observed were:

i) the maximum enzyme load for phytase adsorption was around 7 mg protein/g support, while for β-glucosidase it was around 32 mg protein/g support;

ii) the adsorption of phytase involved not only coordination interactions between the Ca^{2+} sites of HA and COO^- of the enzyme amino acids, but also electrostatic interactions that complemented the adsorption of the enzyme on the support.

iii) the RA of immobilized phytase showed to be above 100%, indicating that either the enzyme acquired a conformation that made the active site more available for biotransformation or the nanoparticles acted as a source of calcium cofactor for the enzyme, which do not occur with β-glucosidase.

iv) after immobilization, phytase showed a broader activity profile in relation to pH and temperature, while β-glucosidase showed the same activity profile as the free enzyme. These results suggest that changes in the phytase conformational state after anchoring to the support facilitated the reaction path under different pH and temperature conditions, while β-glucosidase was not significantly affected after its anchorage in HA.

After understanding the biochemical behavior of phytase in the presence of HA nanoparticles, experiments were carried out to evaluate the potential of phytase application in animal feed. These experiments showed that there was an improvement in the properties of phytase after its immobilization, since the enzyme showed to be more resistant to high temperatures (80 and 90 ° C), which implies greater stability during the pelletizing process of the feed. Besides, immobilized phytase showed to be as active as free phytase in simulated fish gastrointestinal conditions (hypothetically chosen). To complete, it was observed that the kinetics of phosphorus release from the phytate present in the soybean meal by the immobilized enzyme was similar to the kinetics obtained for the free enzyme, being the soybean meal an ingredient

widely used in animal feed. Therefore, the conclusions of this systematic study showed that phytase immobilized in HA has interesting properties, with great potential for application in animal feed.

Following the objective of the project in assessing the potential of HA to act as an enzyme matrix and in view of the promising results obtained for the immobilization of phytase and β-glucosidase, in the Chapter 4 it was carried out a study of enzymatic immobilization of xylanase in HA. However, in this work, the nanoparticles were modified with Cu^{2+} and Ni^{2+} metals, with the purpose of improving the enzyme/support interaction, since the literature showed that these metals formed more stable chelates with proteins. However, the method adopted in the previous chapters to obtain the physico-chemical conditions of immobilization (pH and ionic strength) required a considerable number of experiments, for this reason and considering that there were three supports (pure HA, HA-Cu^{2+} and HA-Ni^{2+}), in this stage of the project it was choose to use the Central Composite Rotational Design (CCRD), in order to optimize the search for these ideal immobilization conditions.

Again, a simple, fast and efficient immobilization protocol was established, but this time using an experimental design. As observed for phytase, xylanase adsorption occurred mainly by chelation, complemented by electrostatic interactions. The pH and temperature activity profile of the immobilized xylanase remained the same as that one of the free xylanase, indicating that enzyme did not undergo changes in its conformational state after immobilization, as also observed for β-glucosidase. The values obtained for the affinity constants during the construction of the adsorption isotherms indicated that the affinity of the xylanase was higher for the HA-Cu^{2+} support than for the HA and HA-Ni^{2+} supports, corroborating data in the literature that evidenced the strong chelating effect of copper compared to other metals. This fact became even more evident in the recycling experiments, in which the HA-Cu^{2+} derivative showed the best results, retaining up to 80% of the initial activity in the second hydrolysis cycle. The results demonstrated that xylanase derivatives could have promising applications for the industry, such as in the biofuels, pharmaceutical, paper and cellulose and food sectors.

Despite the excellent results of immobilization of these three enzymes in HA, we sought to improve the recoverability of these biocatalysts from the reaction medium using magnetic supports, which can be separated from the liquid medium by applying a magnetic field. Thus, in Chapter 5, an investigative study was carried out on the synthesis of HA magnetic nanoparticles and adsorption of these enzymes on them. The purpose of this research step was to obtain composites of HA:$CoFe_2O_4$ with different proportions of hydroxyapatite (HA) and cobalt ferrite ($CoFe_2O_4$) by the co-precipitation method, with the objective of obtaining effective matrices for immobilization of β-glucosidase, phytase and xylanase. The immobilization experiments in this step of the research were carried out with the immobilization conditions established in the previous work of immobilizing these enzymes in pure HA, that is, pH 5 and ionic strength of 20

mM. The results showed that the composite with the highest cobalt ferrite content (2:1) presented the best immobilization results for the three enzymes, besides being the composite with the largest surface area (revealed by the nitrogen adsorption method, BET). Therefore, in addition to offering the largest surface area for adsorption between composites, the 2:1 composite was also the support with the greatest magnetic character that could facilitate the recovery of biocatalysts from the reaction medium to be reused. Regarding the enzymatic loading during the immobilization process, it was noted a decrease in the adsorption capacity in the composites in relation to adsorption capacity in the HA nanoparticles (14.7; 6.9 and 4.5 mg protein/g support for β-glucosidase, phytase and xylanase, respectively, in the composite; and 32.5; 15 and 17 mg protein/g support for β-glucosidase, phytase and xylanase, respectively, in the HA), which probably occurred due to the decrease in the composite surface area in relation to that of pure HA. As well as the derivatives obtained with the HA nanoparticles, the derivatives obtained with the HA magnetic nanoparticles were obtained through a simple and fast protocol, by chelation interactions complemented by ionic interactions. These interactions occurred not only with the functional groups of HA, such as Ca^{2+} on the surface, but also with metals from cobalt ferrite, such as Fe^{2+} and Co^{2+}.

The last step of this research was to evaluate the enzymatic hydrolysis of the respective substrates (cellobiose, phytate and xylan) with the obtained magnetic derivatives, as well as their reuse capacity. The results demonstrated that the free and immobilized enzymes had a similar hydrolysis profile, indicating that the composite did not affect the reaction kinetics nor activated or inactivated the enzymes. Finally, the reuse experiments showed that there was no difference in the recovery efficiency of the immobilized enzymes between the centrifugation methods and the application of a magnetic field. The results indicated greater operational stability of β-glucosidase derivative in the reuse assays, since it could be reused up to 10 times with maintenance of about 70% of its initial activity (similar to the results obtained with HA pure), while the magnetic derivatives of phytase and xylanase could be reused up to 5 times with the maintenance of 20% of its initial activity. Although the β-glucosidase/HA:$CoFe_2O_4$ derivative demonstrated greater potential for application in industry, the reusability of phytase and xylanase can also improve the profitability of different industrial processes, that can be in the biorefineries, pharmaceutical processes, food production and others. In general, the main conclusion of this research is related to the potential of using HA nanoparticles to act as an enzyme matrix, which had a highly effective performance in both forms, free or in the form of magnetic composite.

2. Concluding remarks

A systematic study was developed on the immobilization process of the enzymes β-glucosidase, xylanase and phytase on hydroxyapatite nanoparticles, in both pure and magnetic

forms. It was established very simple, fast and efficient immobilization protocols, allowing to obtain derivatives by chelation, complemented by electrostatic interactions. The results demonstrated that derivatives obtained can have promising applications in the industry, such as in the biofuels, pharmaceutical, paper and cellulose and food sectors. In the case of β-glucosidase and xylanase derivatives, they can perform repeated enzymatic hydrolysis reactions in varied sectors in which these enzymes are used, contributing to more sustainable and profitable processes. In the case of phytase derivative, the improvement in the properties of enzyme after being immobilized in HA nanoparticles indicates promising application in animal feed. Given this context, the main conclusion of this research is related to the potential of using HA nanoparticles to act as an enzyme matrix, which had a highly effective performance in both forms, free or in the form of magnetic composite, thus encouraging in testing this material as a matrix for other enzymes. This strategy can offer a sustainable and lucrative way of applying derivatives in the agroindustry.

3. Future Perspectives

Although a complete and elaborate study had been developed of the immobilization of β-glucosidase, phytase and xylanase enzymes on HA nanoparticles, the results of this study represent opportunities for further research, especially with regard to the application of the derivatives obtained. Some future perspectives to be explored are described in the following paragraphs.

The first suggestion of future work is to investigate the production capacity of the derivatives (β-glucosidase, phytase and xylanase enzymes immobilized in HA, pure and magnetic) in a large scale, also evaluating the storage capacity of these derivatives, in order to verified if they will maintain their activities catalytic.

Another area to be studied is on the application of the derivatives obtained (β-glucosidase, phytase and xylanase) in different industrial sectors, including energy, pharmaceutical, pulp and cellulose, and food sectors. For this, it is suggested to investigate the biocatalytic performance of the derivatives using a reaction medium that simulates the condition used in the industry, which occur in bioreactors of different types, formats and sizes. The objective is to verify if there will be maintenance of the derivative's catalytic activity when acting in a higher volume of hydrolysis compared to the laboratory experiments, which will probably occur under adverse operating conditions, such as pH, ionic strength, density, temperature, pressure and agitation. In addition, it would be interesting to investigate the feasibility of recovering the immobilized enzymes from the bioreactor by different ways, that can be by filtration, by the use of membranes or by the application of a magnetic field (for the case of the magnetic derivative).

Some suggestions of specific areas of the derivatives performance to be investigated in a bioreactor are:

i) for β-glucosidase:
   a. 2G ethanol production;
   b. isoflavone derivatives production using soybean agroindustrial residues;
   c. production of aromatic molecules to improve flavor in beverages.

ii) for xylanase:
   a. 2G ethanol production;
   b. xylooligosaccharides production;
   c. beverages clarification, such as wines, teas and juices;
   d. pulp and cellulose production.

iii) for phytase:
   a. production of myo-inositol derivatives;

In addition to exploring the performance of derivatives obtained in industrial biocatalytic processes, there are also other possibilities. Regarding the phytase derivatives, it is suggested as future work to evaluate the production of animal feed with the immobilized enzyme on HA, in order to verify if there will be maintenance of the phytase catalytic activity after going through the feed manufacturing process (pelletization). Another interesting study would be on the *in vivo* application of the animal feed to confirm whether the use of immobilized phytase in the feed will not cause harmful effects for animals.

Regarding the derivatives obtained for xylanase, it is suggested to evaluate the immobilization of this enzyme together with β-glucosidase (in an enzymatic co-immobilization process) for potential application in the production of biofuels (such as 2G ethanol). It is also suggested as a future work to evaluate the immobilization of xylanase together with phytase (in another enzymatic co-immobilization process) for application in animal feed, since xylanase has also been widely applied as an animal feed supplement.

Finally, it is suggested to evaluate the potential of HA nanoparticles to act as a matrix for several other enzymes of industrial importance.

These suggestions of future work make evident the importance of the results obtained during this doctoral thesis, which leaves a range of possibilities to be explored in the scientific and industrial field about immobilization of enzymes in HA nanoparticles.

SUPPLEMENTARY MATERIAL

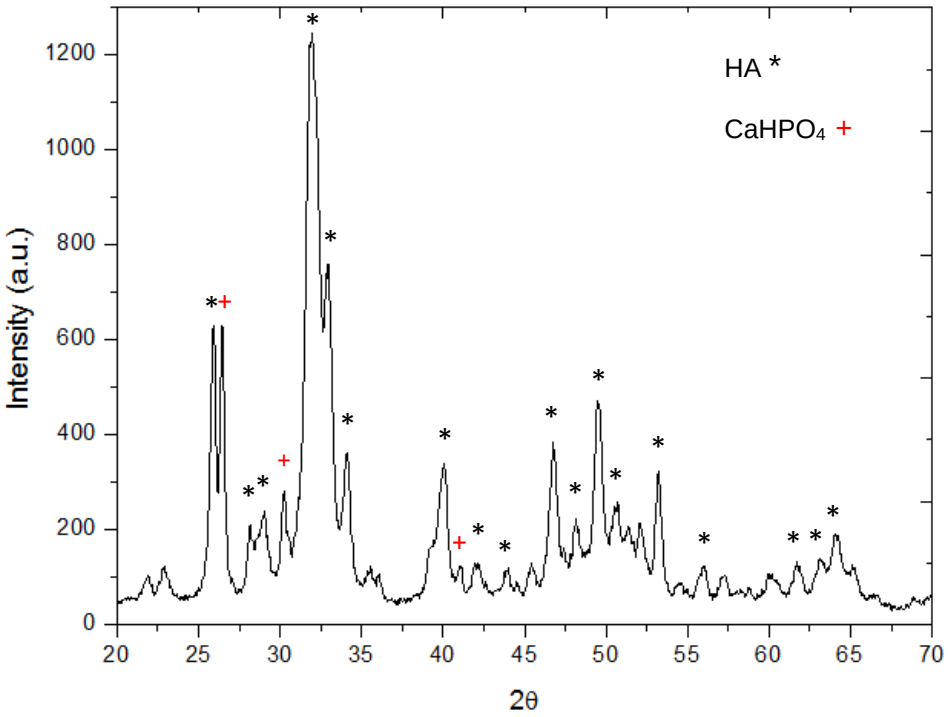

Fig. S1 X-ray diffractogram of hydroxyapatite.

Table S1. Characteristic peaks of HA and the calcium phosphate phase in the X-ray diffractograms, according to Joint Committee on Powder Diffraction Standards (JCPDS) card number 01-089-4405.

Phases			
HA $Ca_{10}(PO_4)_6(OH)_2$		Calcium phosphate $CaH(PO)_4$	
2Θ	Peaks	2Θ	Peaks
25.8°	002	26.4°	-102
28.0°	102	30.2°	120
29.0°	210	41.0°	-221
31.7°	211		
32.2°	112		
34.0°	202		
39.8°	310		
40.0°	130		
42.1°	131		
44.0°	113		
46.7°	222		
48.0°	132		
50.6°	321		
53.1°	004		
56.0°	322		
61.8°	124		
63.0°	502		
64.3°	332		

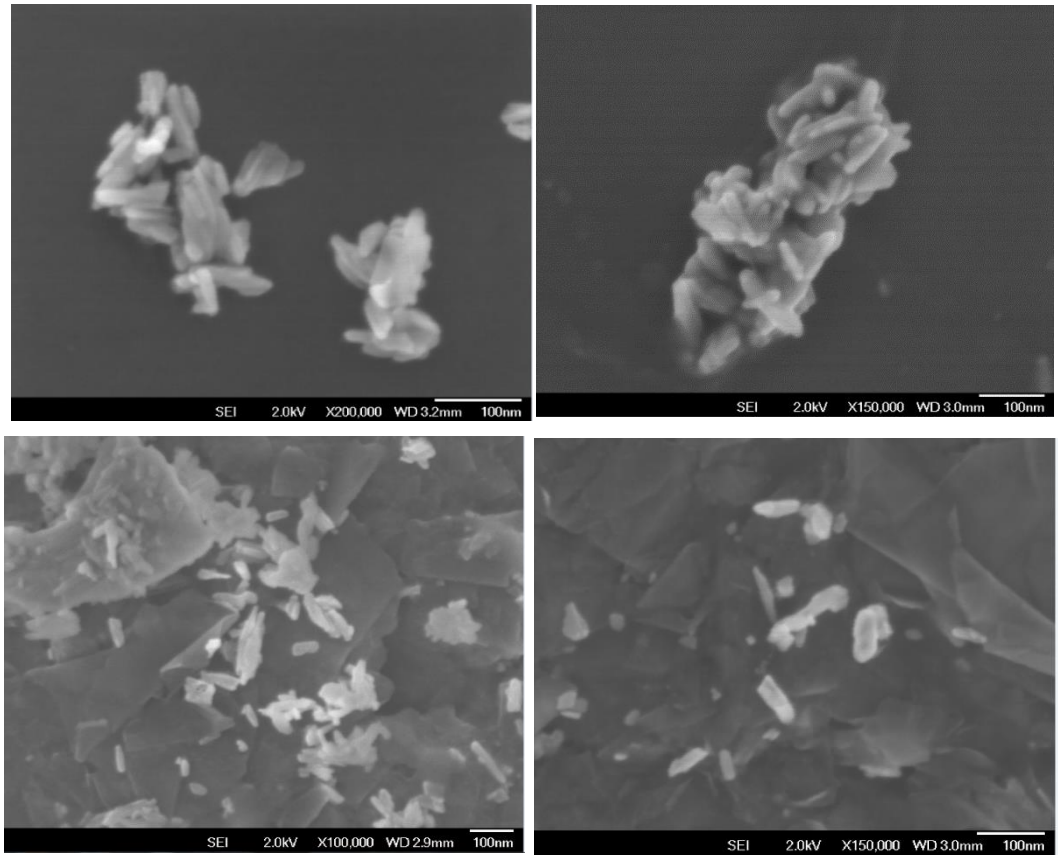

Fig. S2 - FEG-SEM images of hydroxyapatite nanoparticles. Samples analyzed using a JEOL Model JSM-6701F microscope operated at 2.0 kV, with 1.0 nm resolution.

(A)

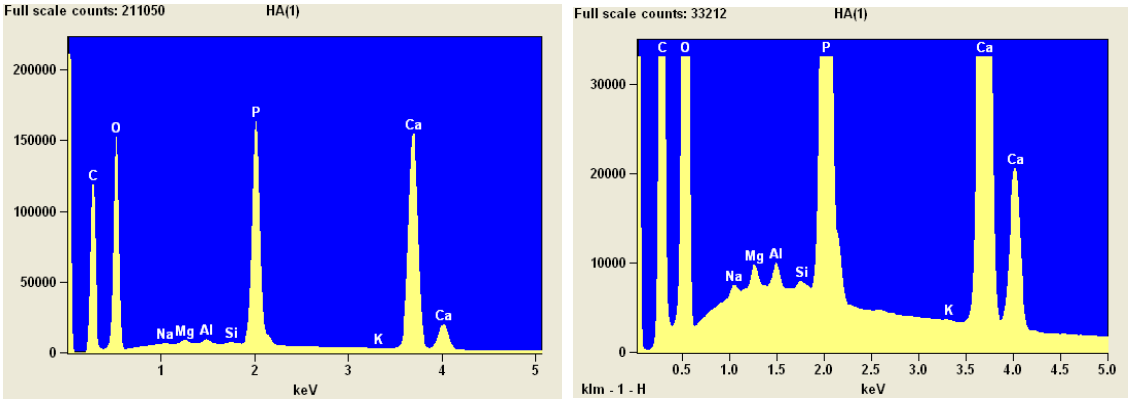

(B)

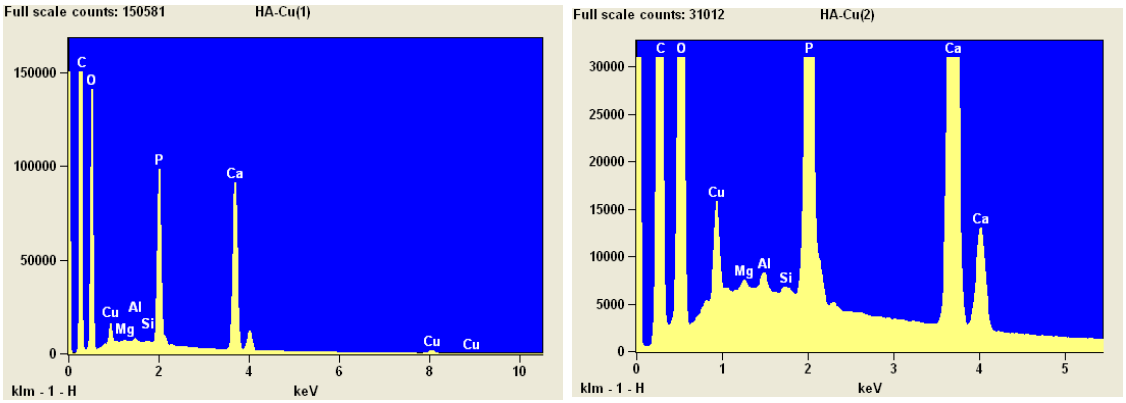

(C)

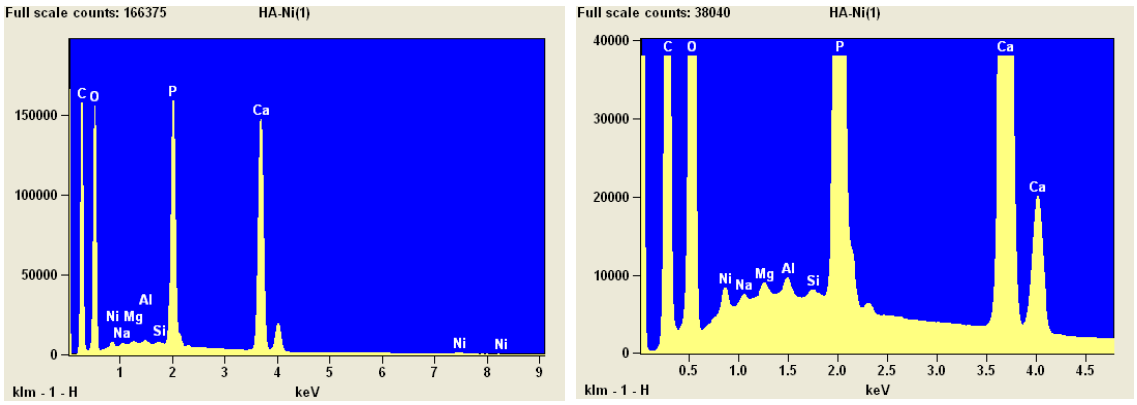

Fig. S3 – Energy dispersive X-ray spectroscopy (EDS spectra of (A) HA (B) HA-Cu^{2+} and (C) HA-Ni^{2+}.

Table S2 - Model Coefficients of CCRD.

	IY			IU/g support	
Support	pH (L)	pH (Q)	Ionic Strength (L/Q)	pH (L)	pH (Q)
HA	-140,049	8,209	---	-355,270	21,513
HA-Cu^{2+}	-175,217	10,633	$0{,}456^{L}$	-491,301	31,126
HA-Ni^{2+}	-177,781	11,325	$0{,}588^{L}/0{,}001^{Q}$	-599,917	36,735

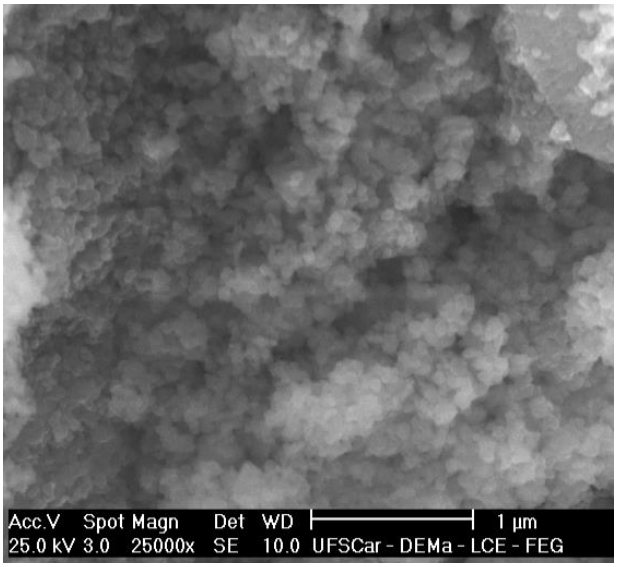

Fig. S4 - FEG-SEM images of magnetic hydroxyapatite nanoparticles (nanocomposites). Samples analyzed using a Phillips Model XL-30 microscope.

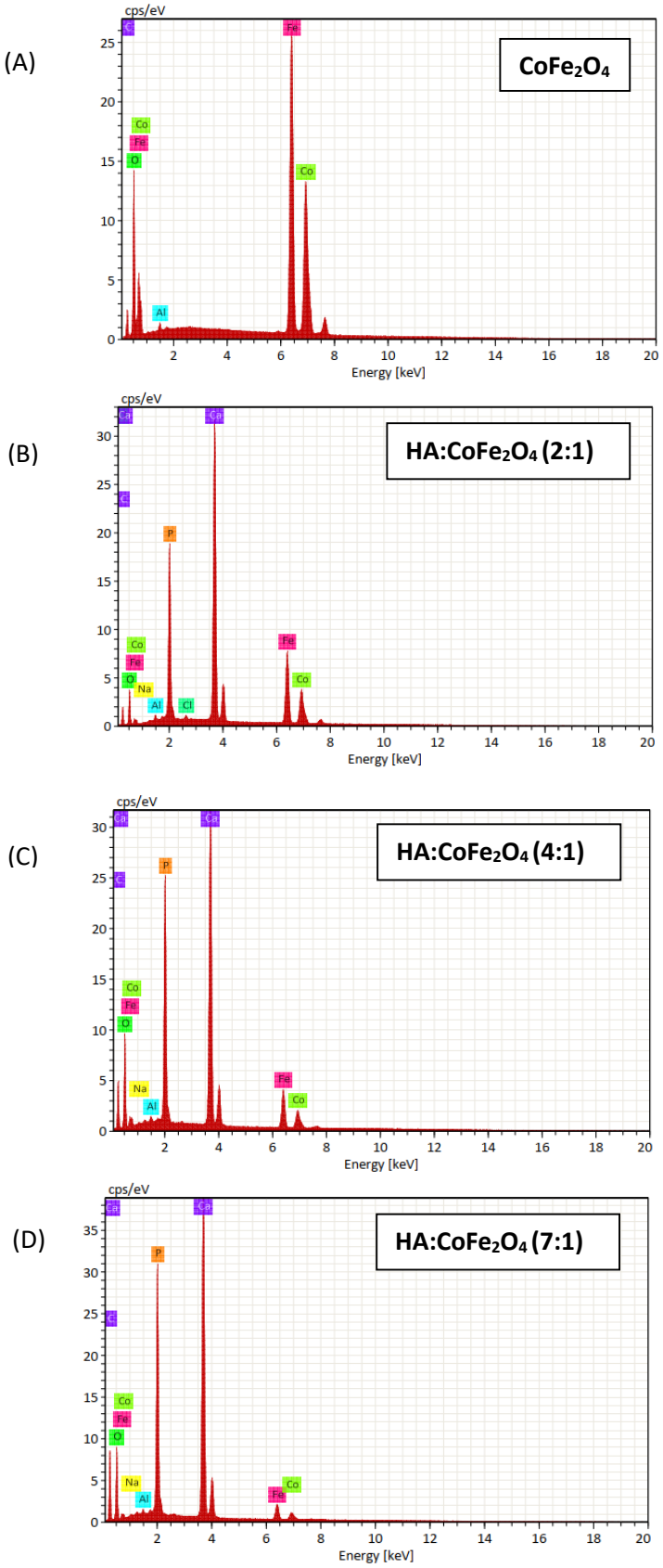

Fig. S5 – Energy dispersive X-ray spectroscopy (FEG-EDS) spectra of (A) $CoFe_2O_4$ (B) $HA:CoFe_2O_4$ (2:1) (C) $HA:CoFe_2O_4$ (4:1) and (D) $HA:CoFe_2O_4$ (7:1).

APPENDIX

APPENDIX 1.

Authorization to reuse the published articles on this thesis

- CHAPTER 2

- CHAPTER 3

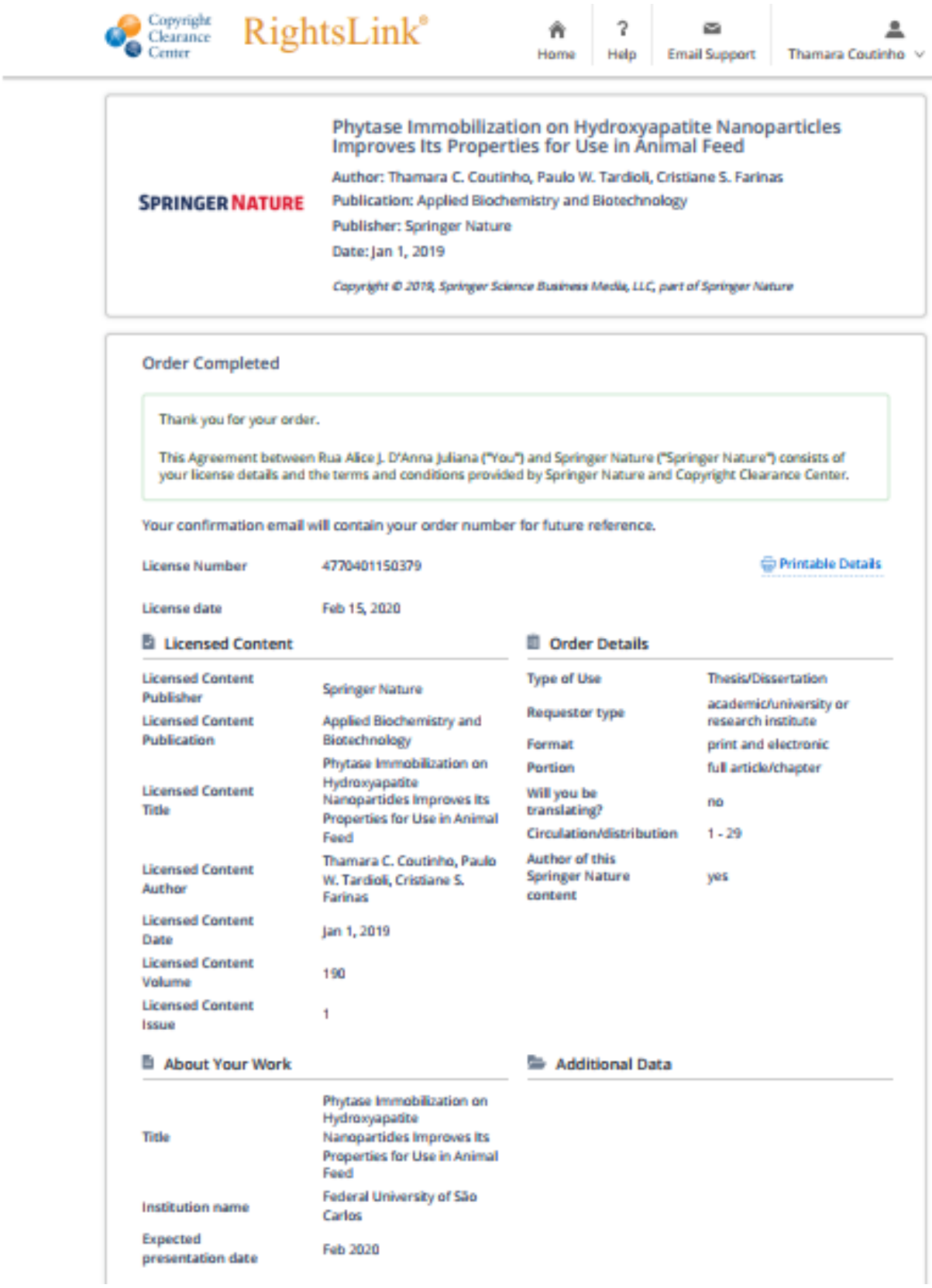

Copyright Clearance Center RightsLink®

Home | Help | Email Support | Thamara Coutinho

SPRINGER NATURE

Phytase Immobilization on Hydroxyapatite Nanoparticles Improves Its Properties for Use in Animal Feed

Author: Thamara C. Coutinho, Paulo W. Tardioli, Cristiane S. Farinas

Publication: Applied Biochemistry and Biotechnology

Publisher: Springer Nature

Date: Jan 1, 2019

Copyright © 2019, Springer Science Business Media, LLC, part of Springer Nature

Order Completed

Thank you for your order.

This Agreement between Rua Alice J. D'Anna Juliana ("You") and Springer Nature ("Springer Nature") consists of your license details and the terms and conditions provided by Springer Nature and Copyright Clearance Center.

Your confirmation email will contain your order number for future reference.

Printable Details

License Number	4770401150379
License date	Feb 15, 2020

Licensed Content

Licensed Content Publisher	Springer Nature
Licensed Content Publication	Applied Biochemistry and Biotechnology
Licensed Content Title	Phytase Immobilization on Hydroxyapatite Nanopartides Improves Its Properties for Use in Animal Feed
Licensed Content Author	Thamara C. Coutinho, Paulo W. Tardioli, Cristiane S. Farinas
Licensed Content Date	Jan 1, 2019
Licensed Content Volume	190
Licensed Content Issue	1

Order Details

Type of Use	Thesis/Dissertation
Requestor type	academic/university or research institute
Format	print and electronic
Portion	full article/chapter
Will you be translating?	no
Circulation/distribution	1 - 29
Author of this Springer Nature content	yes

About Your Work

Title	Phytase Immobilization on Hydroxyapatite Nanopartides Improves Its Properties for Use in Animal Feed
Institution name	Federal University of São Carlos
Expected presentation date	Feb 2020

Additional Data

- CHAPTER 4